Universität Hamburg
DER FORSCHUNG | DER LEHRE | DER BILDUNG

Heavy Quark Production in DIS

Mellin Moments of Coefficient Functions at NNLO

Dissertation

zur Erlangung des Doktorgrades
an der Fakultät für Mathematik, Informatik und Naturwissenschaften
Fachbereich Physik
der Universität Hamburg

vorgelegt von:

Marco Klann
aus Leer, Deutschland

Hamburg, 2026

Gutachter der Dissertation:	Prof. Dr Bernd Kniehl Prof. Dr Sven-Olaf Moch
Zusammensetzung der Prüfungskommission:	Prof. Dr Bernd Kniehl Prof. Dr Katerina Lipka Prof. Dr Sven-Olaf Moch Dr Pooja Mukherjee Prof. Dr Robin Santra
Vorsitzender der Prüfungskommission:	Prof. Dr Robin Santra
Datum der Disputation:	27.08.2026
Vorsitzender Fach-Promotionsausschuss PHYSIK:	Prof. Dr Johannes Haller
Leiter des Fachbereichs PHYSIK:	Prof. Dr Markus Drescher
Dekan der Fakultät MIN:	Prof. Dr-Ing. Norbert Ritter

Zusammenfassung

Diese Arbeit untersucht die Produktion schwerer Quarks in tiefinelastischer Streuung für neutrale, geladene und skalare Ströme. Da exakte Resultate mit vollständiger Massenabhängigkeit nur bis zur nächstführenden Ordnung vorliegen, werden stattdessen feste Mellin-Momente der massiven Koeffizientenfunktionen berechnet. Die harmonische Projektion der Vorwärts-Compton-Amplitude erlaubt es dabei, sämtliche Phasenraumintegrationen zu umgehen. Die auftretenden Schleifenintegrale werden in eine minimale Menge von Integralfamilien eingeteilt, mithilfe partieller Integration reduziert und über die Methode der Differentialgleichungen durch iterierte Integrale gelöst. In nächstführender Ordnung ergeben sich so die ersten elf geraden Momente des Vektor–Vektor-Beitrags zum neutralen Strom sowie die Axial–Axial- und Axial–Vektor-Beiträge, deren Abweichung sich auf die chirale Anomalie zurückführen lässt. Das Hauptresultat ist die Berechnung sämtlicher Dreischleifen-Integrale für den neutralen und den geladenen Strom sowie die erste exakte Bestimmung in nächstnächstführender Ordnung: das niedrigste gerade Moment der Strukturfunktionen des neutralen Stroms, in dem elliptische Strukturen des dreischleifigen Banana-Integrals auftreten. Diese Momente liefern Einschränkungen für die approximativen Koeffizientenfunktionen.

Summary

Heavy-quark production in deep-inelastic scattering is studied for neutral, charged and scalar currents. Since exact results with full mass dependence are available only up to next-to-leading order, fixed Mellin moments of the massive coefficient functions are computed instead. Harmonic projection of the forward Compton amplitude circumvents all phase-space integrations. The loop integrals encountered are organised into a minimal set of integral families, reduced by integration-by-parts identities, and solved with the method of differential equations in terms of iterated integrals. At next-to-leading order, this yields the first eleven even moments of the vector–vector contribution to the neutral current, together with the axial–axial and axial–vector contributions, whose deviation is traced to the chiral anomaly. The main result is the computation of all three-loop integrals for the neutral and charged currents, together with the first exact determination at next-to-next-to-leading order: the lowest even moment of the neutral current structure functions, in which elliptic structures of the three-loop banana integral appear. These moments provide model-independent constraints on the approximate coefficient functions.

(This page is intentionally left blank.)

Publication List

1. M. Klann, S.-O. Moch, K. Schönwald,
   Heavy-Quark Production in Deep-Inelastic Scattering: Mellin Moments of Structure Functions,
   Nucl. Phys. B (2026), 117572.

Acknowledgements

During the course of my PhD, I would like to express my sincere gratitude to *Sven-Olaf Moch* for his supervision, for answering numerous questions, for providing valuable references, and for offering me the opportunity to conduct my research in Hamburg. The many discussions we shared, including those beyond physics such as cycling, were much appreciated. I am especially grateful to *Kay Schönwald* for our collaboration on the project on which much of this thesis is based, for many insightful discussions, for constructive advice, and for guiding me into the world of heavy-quark physics. My thanks also go to *Bernd Kniehl* for acting as second referee for this thesis.

Regarding my colleagues, I would like to thank *Leonid Shumilov* and *Mrigank Chakraborty* for the many discussions we shared over the past three years, particularly during our weekly seminars and throughout our second year in Hamburg. Just as memorable were the experiences we had at various summer schools, from travel adventures ranging from earthquakes to questionable taxis, to our confusions over handbag graphs. My thanks also go to *Bakar Chargeishvili* for his support during my first year, especially for answering many organisational questions and for the excellent `FORM` tutorial at the CAPP School 2023. Thanks are due, too, to *Pooja Mukherjee* for our collaboration on related work, and to *Christoph Dlapa* for enlightening discussions on elliptic integrals. I am grateful to *Levente Fekasházy* and *Adam Kardos* for their advice on `Mathematica` and `FORM`, respectively, and to *Oliver Schnetz* for his excellent lectures on graphical functions. Finally, I thank my fellow PhD students *Tobias Bruschke*, *Tobias Porsche*, *Francesco Ventola* and *Lucas Cesinger* for their good company along the way.

Bien au-delà du cadre de ma thèse, je tiens également à remercier *Jessica* et *Alain*, avec qui je partage une passion commune pour les laits frappés et les glaces, ainsi que *Roger* et *Jeannette* pour l'intérêt qu'ils ont toujours porté à mon travail. Enfin, je remercie tout particulièrement ma femme *Anna*, dont la présence, le soutien et la patience m'ont accompagné tout au long de cette période, et bien au-delà, notamment lorsqu'il fallait supporter mes interminables conversations sur la physique et les hommes en lycra — autrement dit, les cyclistes professionnels.

Besonders möchte ich meiner Familie für ihre Unterstützung während meines Studiums, meiner Promotion und auch der Zeit davor herzlich danken. Mein besonderer Dank gilt meinem Vater, der nicht mehr unter uns ist, sowie meinen Großeltern für ihren prägenden Einfluss auf meinen Lebensweg.

Beyond all the humans, I finally thank that assistant who doesn't quite exist — answering to the names Claude Opus, Sonnet, and now Fable — for helping me proofread this work and for indulging some of my mildly obsessive formatting habits. Interesting times lie ahead…

(This page is intentionally left blank.)

Contents

"Begin at the beginning", the King said, very gravely, "and go on till you come to the end: then stop."

— *Alice's Adventures in Wonderland*, Lewis Carroll

Chapter 1

Introduction

1.1 Motivation

Deep-inelastic scattering (DIS) of leptons off nucleons has shaped the theory of the strong interaction like no other process. Approximate Bjorken scaling, observed in the SLAC-MIT experiments [1, 2] and anticipated in Ref. [3], revealed that at large momentum transfer the lepton scatters incoherently off point-like constituents of the proton [4]. These constituents were identified as spin-1/2 quarks by the Callan–Gross relation [5], confirmed by the data. Subsequently, the discovery of asymptotic freedom [6, 7] explained why a strongly coupled theory could nevertheless exhibit quasi-free behaviour at short distances and established quantum chromodynamics (QCD) as the underlying theory. Fifty years on, DIS remains the cleanest hard process in hadronic physics, with one identified hadron and one electroweak probe, and its structure functions form the backbone of every determination of the partonic content of the proton [8–12].

The process of interest is sketched in Fig. 1.1. Since the leptonic side of the interaction is known exactly, all sensitivity to the nucleon lies in the hadronic tensor, whose Lorentz decomposition defines the structure functions. For neutral currents (NC) two structure functions carry the bulk of the cross section. The dominant one measures the charge-weighted quark momentum distributions, whilst the longitudinal one vanishes in the naive parton model by the Callan–Gross relation and is generated first at order α_s, making it a direct probe of gluon radiation. A third, parity-violating structure function arises from Z exchange and from γZ interference and becomes relevant at large virtualities. Charged current (CC) scattering, in particular neutrino-nucleon scattering, involves in general five structure functions and is flavour selective. The additional structure functions arise from the absence of current conservation, which imposes fewer constraints on the tensor structure of the hadronic tensor. In practical applications, however, one often restricts attention to the same subset of structure functions as in the neutral current case.

Within the parton model, the structure functions depend on the Bjorken variable, $x_{\mathrm{B}} = -q^2/(2p \cdot q)$, alone, a property known as scaling. QCD refines this picture in a characteristic way. Quarks radiate gluons and gluons split into quark-antiquark pairs, so the parton content of the proton is not fixed but depends on how closely it is probed. In DIS the virtuality of the exchanged boson sets this resolution. As the resolution increases, radiation that was previously unresolved is revealed, and the parton distributions acquire a logarithmic dependence on the scale. These scaling violations

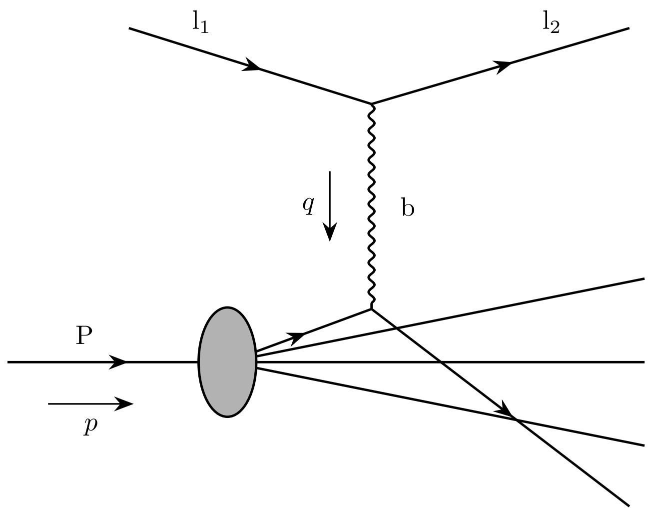

Figure 1.1: Kinematics of DIS: the incoming lepton l_1 scatters off a proton P (momentum p) via the exchange of a boson b with momentum q and virtuality $q^2 = -Q^2$, which couples to a parton inside the proton; the scattered lepton l_2 and the proton remnant emerge in the final state.

are governed by the DGLAP evolution equations [13–15], and their pattern is characteristic. At small values of the Bjorken variable the structure functions rise with the resolution scale, since gluon splitting feeds the quark sea, whilst at large values they fall, since radiation degrades the momenta of the valence quarks (see Fig. 1.2). Observed over many orders of magnitude, these violations rank amongst the most comprehensively verified predictions of QCD. They moreover determine quantities that are not directly measured. The gluon distribution, which drives the evolution at small Bjorken variable, is extracted precisely from this scale dependence, and scaling violations provide one of the classic determinations of the strong coupling constant.

This success rests on collinear factorisation [16]. Up to power corrections, structure functions decompose into universal, non-perturbative parton distribution functions (PDFs), convoluted with process-dependent but short-distance coefficient functions calculable order by order in the strong coupling [17, 18]. DIS thereby tests QCD twice over, since the coefficient functions probe the perturbative expansion whilst the scale dependence of the data probes the evolution. Once the perturbative input is sufficiently accurate, the same data determine the PDFs, which enter essentially every prediction at hadron colliders. PDF uncertainties are by now a limiting systematic for benchmark LHC measurements, from Higgs production in gluon fusion to the W-boson mass. This places the perturbative input to the DIS fits, the coefficient functions studied in this thesis amongst them, directly on the critical path of the collider programme [8–11].

Heavy quarks hold a special position in this programme, for two reasons. First, charm and bottom masses lie well above the QCD scale, so heavy-quark production is itself perturbative. Charm and bottom are not valence constituents, and at leading twist they are produced by the virtual boson off the gluon field of the proton, predominantly through photon–gluon fusion. Heavy-flavour structure functions are therefore a direct, theoretically clean probe of the gluon distribution, in particular at small

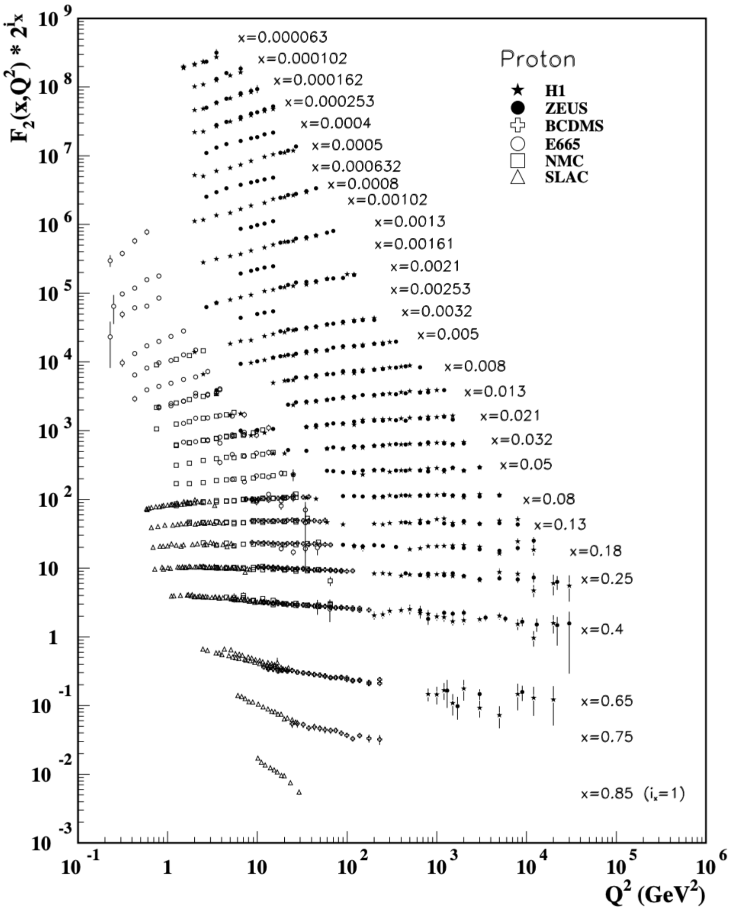

Figure 1.2: The proton structure function F_2^p measured in deep-inelastic scattering from HERA (ZEUS and H1) and fixed-target experiments (SLAC, BCDMS, E665, and NMC), shown as a function of Q^2 in fixed x_{B} bins. The plot is reproduced from Ref. [12] without modification.

Bjorken variable where the gluon dominates the proton wave function. Second, the quark mass introduces a genuine second hard scale next to the boson virtuality. Near the production threshold the mass suppresses the cross section and large threshold logarithms appear. At virtualities far above the mass, quasi-collinear logarithms of the scale ratio dominate and eventually require resummation into heavy-quark PDFs. In between, at virtualities comparable to the squared mass, no expansion applies and the full mass dependence is needed. The treatment of this interplay defines the general-mass variable flavour number schemes ACOT, TR and FONLL, whose differences at a given order measure the missing massive higher-order corrections and which are a standard source of spread amongst the global fits [19–23].

Experimentally, this sensitivity was exploited most prominently at HERA, to date the only electron-proton collider. The combined inclusive neutral- and charged current measurements of H1 and ZEUS [24] span six orders of magnitude in the kinematic variables and form the single most important data set in contemporary PDF fits, whilst the dedicated charm and beauty combination [25] isolates the heavy-flavour structure functions, yields competitive determinations of the heavy-quark masses, and directly tests the mass schemes described above. Since the charm contribution reaches up to roughly a quarter of the inclusive structure function at small Bjorken variable, the treatment of mass effects propagates straight into the extracted gluon distribution and into LHC benchmark cross sections [8,25]. The demands will sharpen at the Electron-Ion Collider (EIC) [26,27], which will revisit this physics with polarised beams, nuclear targets and luminosities two to three orders of magnitude beyond HERA. Projected uncertainties on neutral current observables, including heavy-flavour-tagged structure functions, reach the percent level and below, out of reach for next-to-leading-order (NLO[1]) theory with massive quarks, whilst Z exchange and parity-violating asymmetries promote the axial-vector and axial–axial contributions, so far of limited phenomenological relevance, to directly measurable quantities.

Charged current processes add motivation from the intensity frontier. The SHiP experiment at the CERN SPS [28,29], designed to search for feebly interacting hidden-sector particles, will dump 400 GeV protons on a dense target, of order 10^{20} over its initial running period, and the intense neutrino flux from charm decays turns its emulsion-based neutrino detector into a charged current DIS experiment of unprecedented statistics, including the first sizeable sample of tau neutrinos. Charm production in neutrino-nucleon scattering is the classic probe of the strange-quark sea, the two charged current structure functions that vanish for massless quarks become measurable in tau-neutrino interactions, and a similar physics case is emerging at the LHC forward neutrino experiments [30]. At the momentum transfers involved, of the order of the charm mass, neither the massless approximation nor an expansion around large virtualities is adequate, and full mass dependence is mandatory.

The common thread of these prospects is the demand for perturbative accuracy. For massless quarks DIS theory has long reached next-to-next-to-leading order (NNLO) and, in parts, the order beyond, whereas for massive quarks exact results end at NLO. Closing this gap, or constraining it by exact partial information where a full closure is out of reach, is the purpose of this thesis. The next section reviews the state of the art and locates our contribution.

1.2 State of the Art

In the fixed-flavour-number approach adopted here, the heavy-flavour structure functions are convolutions of the light-parton PDFs with massive coefficient functions, the heavy quarks arising only in the final state. This subsection reviews what is known about those coefficient functions, progressing from the massless case through the asymptotic regime to the exact mass dependence, and thereby situates the contribution of the present thesis.

For massless quarks the perturbative programme is essentially complete at the orders relevant here. The one-loop corrections date back to the late 1970s [17,18]. Two-loop coefficient functions followed [31], whilst the three-loop splitting functions [32,33] together with the third-order coefficient functions [34,35] completed the massless description at NNLO. Notably, these results were reached in stages. Exact fixed Mellin moments at two and three loops [36, 37], later extended in Ref. [38], preceded the complete results by a decade, served to validate them, and acted as anchors for ap-

[1]Throughout this thesis, we adopt the (non-standard) convention of identifying perturbative orders with the loop order of the corresponding forward amplitudes. Leading order corresponds to one loop, next-to-leading order to two loops, and so forth.

proximate parametrisations in the interim. This thesis transfers exactly that strategy to the massive case.

For massive quarks, complete higher-order results exist in the asymptotic regime of virtualities much larger than the squared quark mass. Here the massive coefficient functions factorise, up to power corrections in the mass-to-virtuality ratio, into process-independent massive operator matrix elements and the massless Wilson coefficients quoted above [39]. These operator matrix elements are matrix elements of the twist-two operators between partonic states and carry the entire mass dependence. Simultaneously, they furnish the matching conditions of the variable-flavour-number scheme [40, 41]. Blümlein and collaborators have carried this programme to three loops over the past two decades. The complete two-loop operator matrix elements [42–45] were followed by the first three-loop Mellin moments [46], obtained notably by the same fixed-moment techniques employed in this thesis, and by the asymptotic three-loop corrections to the longitudinal structure function [47]. Assembled contribution by contribution [48–54], the complete three-loop operator matrix elements culminated in the gluonic element, whose first-order-factorisable [55] and non-first-order-factorisable [56] parts were completed only recently. With all operator matrix elements available, the asymptotic corrections and the matching of the variable-flavour-number scheme are now complete [57, 58] at NNLO. Development of the polarised case has proceeded in parallel [59–63], and contributions with two distinct heavy-quark masses, relevant once charm and bottom act together, are known at the same level [64–68]. Beyond the asymptotic regime, only expansion limits are available at NLO, namely the threshold behaviour from soft-gluon resummation [69] and the leading high-energy behaviour from k_T-factorisation [70, 71]. Very recently, first exact analytic NLO results have appeared for the charged current non-singlet contribution [72], underlining that the field is moving, though the gluon channel, which dominates phenomenologically, remains untouched at this order.

Results with exact mass dependence are far more limited. Complete NLO corrections [73, 74], together with a fully differential treatment [75], exist only in semi-analytical form, with parts of the virtual and phase-space integrations performed numerically. For fit applications these results are encoded in the interpolation grids of Ref. [76], presumably accurate at the permille-to-percent level within their domains. The polarised case, including a public numerical implementation, has likewise been completed [77]. Fully analytic NLO expressions exist for the quark non-singlet and pure-singlet channels [78, 79], obtained by integrating over the final state in terms of iterated integrals. In the gluon channel, the dominant production mechanism, proceeding via photon–gluon fusion, exact analytic results remain confined to leading order (LO). They date back to the earliest days of perturbative QCD, heavy-quark electroproduction off gluons having been computed in the 1970s [80–85]. That five decades of effort have yielded no closed form beyond this order is itself informative, signalling the complexity of the problem.

1.3 Moments at Leading Order

Since exact knowledge in the gluon channel ends at LO, this section makes the boundary explicit by computing the coefficient function. This serves both as a worked example and as a reference point against which the Mellin moments of Ch. 4, there obtained by an entirely different method, may be compared.

For this purpose, the partonic subprocess $g\gamma^* \to q\bar{q}$, in which an off-shell photon interacts with a gluon to produce a quark-antiquark pair of mass m, is considered. Two Feynman graphs contribute to the corresponding matrix element. Denoting the momentum of the off-shell photon by q and the on-shell momenta of the gluon, quark, and antiquark by p, k, and $\bar{k}$ respectively, we define the Mandelstam variables as

$$s = (q+p)^2 = (k+\bar{k})^2\,, \tag{1.1}$$
$$t = (q-\bar{k})^2 = (p-k)^2\,, \tag{1.2}$$
$$u = (q-k)^2 = (p-\bar{k})^2\,. \tag{1.3}$$

Momentum conservation requires

$$q + p = k + \bar{k}\,, \tag{1.4}$$

so that only two of the three Mandelstam invariants are independent, the third being fixed by

$$s + t + u = 2m^2 + q^2\,. \tag{1.5}$$

Substituting the Feynman rules for the vertices and propagators, the matrix element takes the form

$$\mathcal{M}^{\mu\rho} = -ig_{\mathrm{s}} Q_{\mathrm{h}} T^a_{ij}\, \bar{v}(\bar{k}) \left[\gamma^\mu \left(\frac{\not{k} - \not{p} + m}{t - m^2}\right)\gamma^\rho + \gamma^\rho \left(\frac{\not{p} - \bar{\not{k}} + m}{u - m^2}\right)\gamma^\mu\right] u(k)\,, \tag{1.6}$$

where Q_{h} denotes the electromagnetic charge of the heavy quark and T^a_{ij} the colour generator in the fundamental representation of $\mathrm{SU}(N_F)$. Squaring the amplitude, averaging over the spins and colours of the incoming gluon, summing over those of the outgoing quark-antiquark pair, applying the photon projectors, and re-expressing the result in terms of the Mandelstam invariants, we obtain

$$\begin{aligned} g_{\mu\nu}\mathcal{M}^{\mu\rho}\mathcal{M}^{*\ \nu}_{\ \rho} = -4T_F Q_{\mathrm{h}}^2 g_{\mathrm{s}}^2 \Bigg[&\frac{2\left(2m^4 + m^2\left(-2q^2 + t + u\right) + q^2\left(-q^2 + t + u\right)\right)}{\left(t - m^2\right)\left(u - m^2\right)} \\ &+ \frac{\left(m^4 + m^2\left(2q^2 + 3t + u\right) - tu\right)}{\left(t - m^2\right)^2} \\ &+ \frac{\left(m^4 + m^2\left(2q^2 + t + 3u\right) - tu\right)}{\left(u - m^2\right)^2}\Bigg]\,, \end{aligned} \tag{1.7}$$

$$p_\mu p_\nu \mathcal{M}^{\mu\rho}\mathcal{M}^{*\ \nu}_{\ \rho} = 4T_F(Q_{\mathrm{h}}^2 g_{\mathrm{s}}^2)\left[\frac{m^2\left(u - m^2\right)}{t - m^2} + \frac{m^2\left(t - m^2\right)}{u - m^2} - \left(q^2 - t - u\right)\right]. \tag{1.8}$$

Because the amplitude is a tree-level quantity, it is free of ultraviolet divergences. Infrared singularities are likewise absent, as the quark mass m regulates all collinear divergences, and no regularisation is therefore required. As a first step, the two-particle phase-space integral is written in the form

$$\begin{aligned} \Phi_2 &= \int \frac{\mathrm{d}^4 k}{(2\pi)^3} \int \frac{\mathrm{d}^4 \bar{k}}{(2\pi)^3} (2\pi)^4 \delta^{(4)}\left(q + p - k - \bar{k}\right)\delta_+\left(k^2 - m^2\right)\delta_+\left(\bar{k}^2 - m^2\right) \\ &= \int \frac{\mathrm{d}^4 k}{(2\pi)^2} \delta_+\left(k^2 - m^2\right)\delta_+\left(\left(q + p - k\right)^2 - m^2\right)\,, \end{aligned} \tag{1.9}$$

with the kinematics evaluated in the centre-of-mass frame. In this frame, imposing the delta function associated with the antiquark together with momentum conservation fixes the energy of the quark,

$$\begin{aligned} 0 &= \bar{k}^2 - m^2 \\ &= s - 2\sqrt{s}\,k_0 \quad \Longrightarrow \quad k_0 = \frac{\sqrt{s}}{2}\,. \end{aligned} \tag{1.10}$$

Performing the k_0 integration against the delta function, the phase-space measure reads

$$\begin{aligned} \Phi_2 &= \frac{1}{4\pi^2}\frac{1}{2\sqrt{s}}\theta(\sqrt{s}-2m^2)\int \mathrm{d}^3k\;\delta_+\left(k^2-m^2\right) \\ &= \frac{1}{4\pi^2}\frac{1}{2\sqrt{s}}\theta(\sqrt{s}-2m^2)\int \mathrm{d}\Omega_k \int \mathrm{d}|\boldsymbol{k}|\;|\boldsymbol{k}|^2\,\delta_+\left(k^2-m^2\right)\,. \end{aligned} \tag{1.11}$$

The remaining delta function, together with the constraints already imposed, then fixes the magnitude of the three-momentum,

$$\begin{aligned} 0 &= k^2 - m^2 \\ &= \frac{s}{4} - |\boldsymbol{k}|^2 - m^2 \quad \Longrightarrow \quad |\boldsymbol{k}| = \frac{1}{2}\sqrt{s-4m^2}\,. \end{aligned} \tag{1.12}$$

Performing the $|\boldsymbol{k}|$ integration against the delta function leaves a purely angular integral,

$$\Phi_2 = \frac{1}{32\pi^2}\theta(\sqrt{s}-2m^2)\theta(\sqrt{s})\sqrt{1-\frac{4m^2}{s}}\int \mathrm{d}\Omega_k\,. \tag{1.13}$$

To integrate the squared matrix element, we express the Mandelstam variables in terms of the angular coordinates and impose the constraints enforced by the delta functions. The t- and u-channel invariants then take the form

$$t = m^2 - \frac{1}{2}\left(s-q^2\right)\left(1-\eta\cos\vartheta_k\right), \tag{1.14}$$

$$u = m^2 - \frac{1}{2}\left(s-q^2\right)\left(1+\eta\cos\vartheta_k\right), \tag{1.15}$$

where ϑ_k denotes the polar angle of the outgoing quark in the centre-of-mass frame, and

$$\eta = \sqrt{1-\frac{4m^2}{s}} \tag{1.16}$$

is the centre-of-mass speed of the produced quarks. Since the matrix element is independent of the azimuthal angle φ_k, that integration is trivial, and the phase-space measure reduces to

$$\Phi_2 = \frac{\eta}{16\pi}\theta(\sqrt{s}-2m^2)\theta(\sqrt{s})\int_{-1}^{+1}\mathrm{d}\cos\vartheta_k\,. \tag{1.17}$$

Performing the remaining angular integral, we obtain

$$\begin{aligned} \Phi_2\left[p_\mu p_\nu \mathcal{M}^{\mu\rho}\mathcal{M}^{*}{}_{\rho}{}^{\nu}\right] = -2(\alpha_s Q_{\mathrm{h}}^2)T_F\eta\theta(\sqrt{s}-2m^2)\theta(\sqrt{s})\Bigg[s \\ + \frac{2m^2}{\eta}\ln\left(\frac{1-\eta}{1+\eta}\right)\Bigg]\,, \end{aligned} \tag{1.18}$$

$$\Phi_2\left[g_{\mu\nu}\mathcal{M}^{\mu\rho}\mathcal{M}^{*}{}_{\rho}{}^{\nu}\right] = -4(\alpha_s Q_{\mathrm{h}}^2)T_F\frac{\eta\theta(\sqrt{s}-2m^2)\theta(\sqrt{s})}{(q^2-s)^2}\Bigg[s\left(4m^2+s\right)+(q^2)^2 \\ +\frac{\left(8m^4+4m^2\left(q^2-s\right)-(q^2)^2-s^2\right)}{\eta}\ln\left(\frac{1-\eta}{1+\eta}\right)\Bigg]. \tag{1.19}$$

In the deep-inelastic scattering regime the momentum transfer is space-like, $q^2 < 0$. Defining the photon virtuality $Q^2 = -q^2 > 0$ and the mass ratio $\xi = m^2/Q^2$, we parametrise the partonic centre-of-mass energy through the momentum fraction $\hat{z}$ and the production threshold through a, given by

$$s = \frac{Q^2(1-\hat{z})}{\hat{z}}\,, \tag{1.20}$$

$$a = \frac{1}{1+4\xi}\,. \tag{1.21}$$

The momentum fraction $\hat{z}$ takes values in $(0, 1)$, with any collinear singularities in the limit $\hat{z} \to 1$ regulated by the production threshold a. At LO, the heavy-quark contributions to the structure functions then take the form

$$\begin{aligned} H_{L,g}^{(1)}(\hat{z},\xi) &= \frac{8\hat{z}^2}{Q^2}\Phi_2\left[p_\mu p_\nu\mathcal{M}^{\mu\rho}\mathcal{M}^{*}{}_{\rho}{}^{\nu}\right] \\ &= 16(\alpha_s Q_{\mathrm{h}}^2)T_F\theta\left(a-\hat{z}\right)\theta(\hat{z})\left[\eta\hat{z}(1-\hat{z})+2\xi\hat{z}^2\ln\left(\frac{1-\eta}{1+\eta}\right)\right], \end{aligned} \tag{1.22}$$

$$\begin{aligned} H_{2,g}^{(1)}(\hat{z},\xi) &= \frac{24\hat{z}^2}{3Q^2}\Phi_2\left[p_\mu p_\nu\mathcal{M}^{\mu\rho}\mathcal{M}^{*}{}_{\rho}{}^{\nu}\right]-\Phi_2\left[g_{\mu\nu}\mathcal{M}^{\mu\rho}\mathcal{M}^{*}{}_{\rho}{}^{\nu}\right] \\ &= 8(\alpha_s Q_{\mathrm{h}}^2)T_F\theta\left(a-\hat{z}\right)\theta(\hat{z})\Bigg\{\eta\left[-\frac{1}{2}+4\hat{z}(1-\hat{z})-2\xi\hat{z}(1-\hat{z})\right] \\ &\quad +\left[-\frac{1}{2}+\hat{z}-\hat{z}^2+2\xi\hat{z}(3\hat{z}-1)+4\xi^2\hat{z}^2\right]\ln\left(\frac{1-\eta}{1+\eta}\right)\Bigg\}. \end{aligned} \tag{1.23}$$

Due to crossing symmetry, only the even Mellin moments are non-trivial, as the odd moments vanish (see Subsec. 2.1.4). The even moments may be obtained by integrating against the momentum fraction,

$$H_{i,g}^{N,(n)}(\xi) = \int_0^\infty \mathrm{d}\hat{z}\,\hat{z}^{N-1}H_{i,g}^{(n)}(\hat{z},\xi)\,. \tag{1.24}$$

Direct integration yields

$$\begin{aligned} H_{L,g}^{2,(1)}(\upsilon) = (\alpha_s Q_{\mathrm{h}}^2)T_F\Bigg[&\frac{4}{3(\upsilon+1)^4}\left(\upsilon^4+9\upsilon^3+10\upsilon^2+9\upsilon+1\right)-\frac{8\upsilon\ln(\upsilon)}{(\upsilon-1)(\upsilon+1)^5} \\ &\times\left(\upsilon^4+2\upsilon^3+4\upsilon^2+2\upsilon+1\right)\Bigg], \end{aligned} \tag{1.25}$$

$$\begin{aligned} H_{L,g}^{4,(1)}(\upsilon) = (\alpha_s Q_{\mathrm{h}}^2)T_F\Bigg[&\frac{4}{45(\upsilon+1)^8}\Big(6\upsilon^8+125\upsilon^7+356\upsilon^6+925\upsilon^5+956\upsilon^4 \\ &+925\upsilon^3+356\upsilon^2+125\upsilon+6\Big)-\frac{16\upsilon\ln(\upsilon)}{3(\upsilon-1)(\upsilon+1)^9}\Big(\upsilon^8+4\upsilon^7+16\upsilon^6 \\ &+24\upsilon^5+36\upsilon^4+24\upsilon^3+16\upsilon^2+4\upsilon+1\Big)\Bigg], \end{aligned} \tag{1.26}$$

$$H_{2,g}^{2,(1)}(\upsilon) = (\alpha_s Q_{\mathrm{h}}^2) T_F \Bigg[- \frac{1}{(\upsilon+1)^2} \Big(\upsilon^2 - 4\upsilon + 1 \Big) + \frac{4\ln(\upsilon)}{3(\upsilon-1)(\upsilon+1)^3} \Big(\upsilon^4 - 3\upsilon^3 + \upsilon^2 - 3\upsilon + 1 \Big) \Bigg] , \tag{1.27}$$

$$H_{2,g}^{4,(1)}(\upsilon) = (\alpha_s Q_{\mathrm{h}}^2) T_F \Bigg[- \frac{1}{180(\upsilon+1)^6} \Big(133\upsilon^6 - 66\upsilon^5 + 887\upsilon^4 - 228\upsilon^3 + 887\upsilon^2 - 66\upsilon + 133 \Big) + \frac{\ln(\upsilon)}{30(\upsilon-1)(\upsilon+1)^7} \Big(11\upsilon^8 - 6\upsilon^7 + 158\upsilon^6 - 54\upsilon^5 + 342\upsilon^4 - 54\upsilon^3 + 158\upsilon^2 - 6\upsilon + 11 \Big) \Bigg] , \tag{1.28}$$

where we have rationalised the square roots arising in the integration by introducing the variable

$$\xi = \frac{\upsilon}{(1-\upsilon)^2} . \tag{1.29}$$

In the Mellin moments, the denominator follows a simple pattern, acquiring an additional factor $(\upsilon+1)^{-4}$ for each step from N to $N+2$, whereas the numerator polynomials grow considerably more intricate. It is already apparent that an analytic reconstruction in the Mellin variable N lies beyond reach, as the number of moments required to constrain an ansatz would be prohibitively large. The Mellin moments in Eqs. (1.25)–(1.28) are the simplest instances of the central objects of this thesis. Here, the Mellin moments are obtained by direct integration of the coefficient functions, which requires evaluating all phase-space integrals. In Ch. 4, the Mellin moments are instead obtained through harmonic projection, effectively circumventing the need to perform the phase-space integrations.

1.4 Approximate Coefficient Functions

Beyond LO the direct phase-space approach becomes challenging once virtual corrections, mass renormalisation and multi-particle final states enter. Phenomenology therefore relies on approximate coefficient functions built from the known expansions, most importantly the asymptotic one, together with an estimate of the residual uncertainty [86]. These constructions underpin global PDF fits and have recently been extended to approximate NNLO accuracy for PDF determination [87]. Figure 1.3 illustrates the situation at two loops, where such constructions can still be tested against the exact result. The approximation works well in the threshold and asymptotic regions but its uncertainty band widens where the boson virtuality is comparable to the squared quark mass, precisely the region populated by the HERA charm data and the projected EIC measurements. At three loops no exact benchmark exists at all. The residual uncertainty propagates into the gluon PDF and the charm-mass determinations and has been identified as one of the dominant theory systematics of the corresponding NNLO fits [87, 88].

Exact information, even if partial, is therefore of direct value, all the more so since complete NNLO results with full mass dependence may well remain out of reach for some time. This motivates the computation of fixed Mellin moments, which constrain approximations of this type over the full kinematic range.

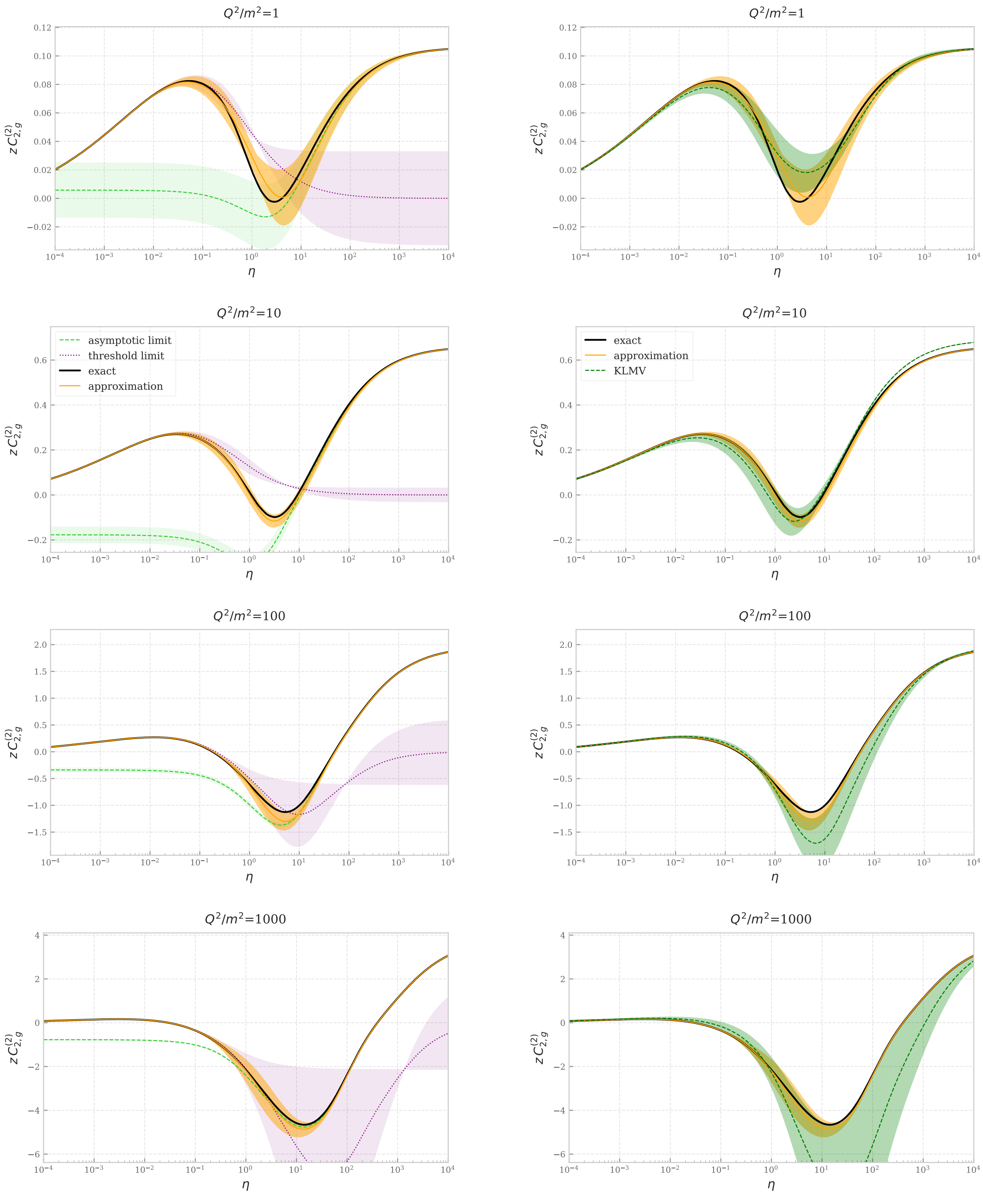

Figure 1.3: The two-loop massive gluon coefficient function. The exact semi-analytical result is compared, left, to its threshold and asymptotic limits and to the interpolated approximation with its uncertainty band, and, right, to the earlier approximation of Ref. [86], for several ratios of the boson virtuality to the squared quark mass, increasing from top to bottom. The plot is reproduced from Ref. [87] without modification. The bands widen in the intermediate region populated by the heavy-flavour data. Exact Mellin moments with full mass dependence provide model-independent integral constraints on precisely these bands. At three loops, where no exact benchmark exists, they are the only ones available.

1.5 Thesis Outline

The structure of this thesis is motivated by a quotation from one of the standard references on perturbative QCD [89]:

> **Mental health warning:** *There are no fixed conventions for the normalizations of many of the objects discussed in this section. The objects concerned range from the definitions even of basic mathematical quantities, like $\epsilon_{\kappa\lambda\mu\nu}$, through the definitions of various kinds of spin vector, to the definitions of structure functions and parton densities. Quantities of the same name and symbol change their normalizations between different papers, even by the same authors. If one needs to make numerical results, it is important to check all conventions very carefully.*

Far from being limited to the specific section from which it is taken, this warning extends to essentially all of perturbative QCD, and in particular to DIS. A persistent feature of the field as a whole is the lack of universally agreed conventions and normalisations, which in fact motivates the structure of this work. Accordingly, an explicit, if inevitably imperfect, effort is made to render all conventions fully transparent, so that all signs and factors are fixed here, and no *magic numbers* are required in order to reproduce the results presented.

The field-theoretic framework is developed in Ch. 2. Starting from the hadronic tensor and its decomposition into structure functions, we derive the relation to the forward Compton amplitude via the optical theorem and set up the operator product expansion that yields the Mellin moments. Since conventions vary considerably across the literature, renormalisation and the mixing of the twist-two operators between the quark non-singlet, quark singlet and gluon sectors are treated in detail. Closing the chapter is the flavour decomposition of the neutral- and charged current structure functions, including the electroweak couplings and a systematic discussion of flavour structures mixing light and heavy quarks, which fixes the complete set of vector–vector (VV), axial–vector (AV) and axial–axial (AA) contributions computed later.

Multi-loop technology required for the computation is assembled in Ch. 3, covering parametric representations [90, 91] and their symmetries, dimensional regularisation [92, 93], and the reduction to master integrals through integration–by–parts (IBP) identities [94–96]. Its main part develops the method of differential equations [97–99], ε-factorised bases [100], boundary conditions obtained from expansion by subgraphs [101, 102], and the iterated integrals [103] in which the solutions are expressed. Particular emphasis is placed on the representation of Feynman integrals, as it is later used to study the factorisation of integrals, a result that, surprisingly, does not appear in the literature, and to optimise integral families. How individual integrals are computed is not reviewed in detail, since more complicated integrals typically require case-by-case treatment; instead, we consider explicitly the integrals encountered in the computation of the Mellin moments in the following chapter.

Both chapters serve a common purpose: to render the notation fully unambiguous. Normalisation constants are derived from first principles and renormalisation constants are listed explicitly, so that every sign and factor is fixed and no magic numbers are needed to reproduce the results. Neither chapter, however, claims to be self-contained. For a comprehensive treatment, the reader is referred to the extensive literature on quantum field theory [104–109] and the rapidly growing literature on Feynman integrals [110–113].

In Ch. 4 the computation of the Mellin moments itself is carried out. It extends the fixed-moment method of Refs. [37, 38] to the massive case. The harmonic projection extracts fixed Mellin moments from the forward amplitudes, which are computed using Feynman graphs. Furthermore, we identify symmetries of the amplitudes that are not captured by graph automorphisms alone (see Subsec. 4.2.3 and Subsec. 4.2.4). To organise the loop integrals, we do not assign arbitrary integral families to the integrals but rather find a minimal set by solving a set covering problem. Its solution guarantees the smallest possible number of independent integral families, making IBP reductions more tractable. The master integrals are then classified and solved, with the two- and three-loop banana subtopologies introducing the elliptic structures of the charged- and neutral current cases, respectively.

Finally, Ch. 5 presents the results of this work. As a validation of the results, the Mellin moments of the vector–vector neutral current structure functions at NLO are compared against the parametrisations of Refs. [76, 77], with which they agree at the level of the quoted accuracy, and are further checked against the known asymptotic limits [43]. Next, the axial–axial and axial–vector contributions are presented, whose deviation from the vector–vector case beyond leading order is traced back to the chiral anomaly. Complementing these, the scalar-current results serve as a consistency check on our computational setup, since in this case both gauge invariance and renormalisation constitute non-trivial tests [114]. The chapter culminates in the first exact result at NNLO, the lowest even Mellin moment of the neutral current structure functions, before closing with conclusions and an outlook.

Supplementary material is collected in the appendices. These comprise lists of master integrals for the neutral- and charged current families, technical material on the two- and three-loop banana integrals that define the elliptic structures encountered, a description of the accompanying data files, and a summary of our conventions, including Feynman rules and colour algebra. The data files contain the majority of the results, most of which resist being printed in any reasonable number of pages, or indeed font size.

(This page is intentionally left blank.)

"Curiouser and curiouser!" cried Alice (she was so much surprised, that for the moment she quite forgot how to speak good English).

— *Alice's Adventures in Wonderland*, Lewis Carroll

Chapter 2

Deep Inelastic Scattering

This chapter reviews the notation required for the calculation of Mellin moments in deep-inelastic scattering. Although the underlying formalism is well established, conventions vary considerably across the literature, with different choices of normalisation, overall signs, and numerical prefactors leading to results that appear superficially inconsistent. Our principal aim here is to fix these conventions unambiguously, so that the expressions and numerical results presented in the remainder of this thesis are fully reproducible.

The hadronic tensor and its decomposition into structure functions are first introduced, followed by their relation to the forward scattering amplitude through the optical theorem. An operator product expansion then connects the moments of the structure functions to matrix elements of local twist-two operators, weighted by the corresponding Wilson coefficients. Since these operators mix under renormalisation [115], we outline the renormalisation procedure and the resulting mixing structure in some detail, paying particular attention to the interplay between the quark non-singlet, quark singlet, and gluon sectors.

Finally, we discuss the flavour factors that arise when coupling the electroweak currents to both light and heavy quarks. In doing so, we extend the standard treatment by including a systematic discussion of flavour structures involving the mixing between light and heavy quark flavours, which, to the best of our knowledge, is not available in the literature in this form. Careful bookkeeping of these factors is essential, as they determine the precise combinations of coefficient functions contributing to a given structure function and, ultimately, the mapping between our perturbative results and physical cross sections.

2.1 Hadronic Tensor

2.1.1 Hadronic Tensor

In this section, we establish the framework for computing fixed-order moments of the coefficient functions. Our focus now falls on the hadronic sector of lepton hadron scattering, which encompasses both light quark fields ψ_{l} and heavy quark fields ψ_{h} of mass m. These fields couple to external vector and axial-vector sources, specifically the electroweak gauge bosons, through a conserved current,

$$J_\mu(z) = \bar{\psi}_{\mathrm{l}}(z)\big(Q_{\mathrm{l}}^{\mathrm{v}} + Q_{\mathrm{l}}^{\mathrm{a}}\gamma_5\big)\gamma_\mu\psi_{\mathrm{l}}(z) + \bar{\psi}_{\mathrm{h}}(z)\big(Q_{\mathrm{h}}^{\mathrm{v}} + Q_{\mathrm{h}}^{\mathrm{a}}\gamma_5\big)\gamma_\mu\psi_{\mathrm{h}}(z)\,, \tag{2.1}$$

where Q_l^v, Q_l^a, Q_h^v, and Q_h^a denote the vector and axial-vector charge matrices for the light and heavy quark flavours, respectively.

While the current, Eq. (2.1), is of direct physical relevance, it proves equally instructive to consider a scalar source coupled to gluons and heavy quarks. Representing the gluon field through the field strength tensor G^a, we describe such an interaction by a scalar current of the form,

$$J(z) = g_\mathrm{s} G^a{}_{\mu\nu}(z) G^{a,\mu\nu}(z) + m\bar{\psi}_\mathrm{h}\psi_\mathrm{h}\,, \tag{2.2}$$

with g_s denoting the scalar coupling constant. The scalar current, Eq. (2.2), is closely related to the Weyl anomaly [116], and the Yukawa coupling is required for its renormalisation [114]. Although such a scalar current does not appear in the Standard Model Lagrangian, it is useful for extracting quantities such as anomalous dimensions and coefficient functions from lower-order calculations in the strong coupling. Unlike processes induced by an external quark, processes induced by gluons receive no tree-level contributions from the electroweak gauge bosons. The scalar current circumvents this limitation by generating tree-level contributions, thereby providing access to gluonic quantities at lower orders in perturbation theory [38].

In the context of deep-inelastic scattering, we typically consider unpolarised states $|P, s\rangle$ with time-like four-momentum P and spin s, representing massive particles such as the proton. The spin-averaged hadronic matrix element of a product of vector and axial-vector currents is defined as

$$\langle \mathrm{P}| J^\dagger{}_\mu(z) J_\nu(0) |\mathrm{P}\rangle \equiv \frac{1}{|\mathcal{S}|}\sum_{s\in\mathcal{S}} \langle p, s| J^\dagger{}_\mu(z) J_\nu(0) |p, s\rangle\ , \tag{2.3}$$

with an analogous definition applying to the product of scalar currents. Here, $\mathcal{S}$ denotes the set of all spin states of the hadron under consideration. Our attention now turns to the product of vector currents, with analogous arguments extending to products of scalar currents. The hadronic tensor is then given by the Fourier transform of the spin-averaged matrix element, Eq. (2.3),

$$W_{\mu\nu}(p, q) = \frac{1}{4\pi}\int \mathrm{d}^4 z\, e^{iq\cdot z} \langle \mathrm{P}| J^\dagger{}_\mu(z) J_\nu(0) |\mathrm{P}\rangle\ . \tag{2.4}$$

The hadronic tensor, Eq. (2.4), depends additionally on the heavy quark mass m and the strong coupling α_s. By convention, however, we suppress functional dependencies arising from parameters in the Lagrangian unless they are essential to the discussion.

As a rank-two tensor, the hadronic tensor admits a natural decomposition into symmetric and antisymmetric parts,

$$W_{\mu\nu}(p, q) = W^\mathrm{S}{}_{\mu\nu}(p, q) + W^\mathrm{A}{}_{\mu\nu}(p, q)\,, \tag{2.5}$$

where $W^\mathrm{S}{}_{\mu\nu}$ is symmetric and $W^\mathrm{A}{}_{\mu\nu}$ antisymmetric. Lorentz symmetry fixes the symmetric part to its most general decomposition in terms of the available momenta and the metric tensor,

$$W^\mathrm{S}{}_{\mu\nu}(p, q) = g_{\mu\nu} W_1(p, q) + p_\mu p_\nu W_2(p, q) + q_\mu q_\nu W_3(p, q) + \big(p_\mu q_\nu + q_\mu p_\nu\big) W_4(p, q)\,. \tag{2.6}$$

In general, the coefficients W_i depend on all Lorentz-invariant scalar products formed from the hadronic momentum p and the bosonic momentum transfer q. Current conservation imposes a transversality condition on the hadronic tensor, Eq. (2.4), and consequently on its symmetric part, Eq. (2.6),

$$q^\mu W^{\mathrm{S}}{}_{\mu\nu}(p,q) = \big(W_1(p,q) + q^2\, W_3(p,q) + p\cdot q\, W_4(p,q)\big) q_\nu + \big(p\cdot q\, W_2(p,q) \\ + q^2 W_4(p,q)\big) p_\nu = 0\,. \tag{2.7}$$

Because q is space-like and p time-like, the two four-vectors must be linearly independent, and their respective coefficients must vanish separately. Hence, Eq. (2.7) implies a system of equations that fixes two of the four unknown coefficients. Normalising the remaining coefficients to be dimensionless, we can express the symmetric part of the hadronic tensor, Eq. (2.6), as

$$W^{\mathrm{S}}{}_{\mu\nu}(p,q) = e_{\mu\nu}\tilde{W}_1(p,q) + d_{\mu\nu}\tilde{W}_2(p,q)\,, \tag{2.8}$$

with the tensors

$$e_{\mu\nu} = g_{\mu\nu} - \frac{q_\mu q_\nu}{q^2}\,, \tag{2.9}$$

$$d_{\mu\nu} = -\frac{2x_{\mathrm{B}}}{q^2}(p_\mu q_\nu + q_\mu p_\nu) - \frac{4x_{\mathrm{B}}^2}{q^2} p_\mu p_\nu - g_{\mu\nu}\,. \tag{2.10}$$

For the antisymmetric tensor, the general form follows directly, as only one independent way exists to construct an antisymmetric combination of p and q,

$$W^{\mathrm{A}}{}_{\mu\nu}(p,q) = \epsilon_{\mu\nu\alpha\beta}\frac{p^\alpha q^\beta}{p\cdot q}\tilde{W}_3(p,q)\,. \tag{2.11}$$

Due to the total antisymmetry of the Levi-Civita tensor, this contribution automatically satisfies the transversality condition and remains consistent with current conservation.

The hadronic tensor thus emerges in its most general form upon adding the symmetric and antisymmetric parts, Eqs. (2.8) and (2.11),

$$W_{\mu\nu}(p,q) = e_{\mu\nu}\tilde{W}_1(p,q) + d_{\mu\nu}\tilde{W}_2(p,q) + \epsilon_{\mu\nu\alpha\beta}\frac{p^\alpha q^\beta}{p\cdot q}\tilde{W}_3(p,q)\,. \tag{2.12}$$

Following standard convention in the literature [18], we normalise the coefficients to coincide with structure functions such that tree-level contributions are real and equal to unity. The hadronic tensor reads

$$W_{\mu\nu}(p,q) = \frac{1}{2x_{\mathrm{B}}} e_{\mu\nu} F_L(p,q) + \frac{1}{2x_{\mathrm{B}}} d_{\mu\nu} F_2(p,q) + i\epsilon_{\mu\nu\alpha\beta}\frac{p^\alpha q^\beta}{p\cdot q} F_3(p,q)\,. \tag{2.13}$$

Here, F_L denotes the longitudinal structure function. For completeness, we introduce the transverse structure function,

$$F_T(p,q) = F_2(p,q) - F_L(p,q)\,. \tag{2.14}$$

2.1.2 Light-Cone Dominance

In the deep-inelastic scattering limit, where the momentum transfer is strongly space-like, the exponential factor in the hadronic tensor, (2.4), becomes highly oscillatory.

The Riemann–Lebesgue lemma ensures that the dominant contributions to the integral originate from regions where the phase remains finite. Such behaviour occurs on the light cone, allowing us to approximate the hadronic tensor in the large momentum transfer limit as

$$\lim_{q^2\to-\infty} W_{\mu\nu}(p,q) = \frac{1}{4\pi}\int_{\{z|z^2=0\}} \mathrm{d}^4z\, e^{iq\cdot z} \langle \mathrm{P}| \, J^\dagger{}_\mu(z) J_\nu(0) \, |\mathrm{P}\rangle \; . \tag{2.15}$$

While this expression becomes exact only in the strict limit, in practice it remains an approximation, as such large momentum transfers cannot be realised experimentally.

To assess the validity of the limit in Eq. (2.15), we rewrite the hadronic tensor by adding a term that vanishes identically,

$$W_{\mu\nu}(p,q) = \frac{1}{4\pi}\int \mathrm{d}^4z\, e^{iq\cdot z} \langle \mathrm{P}| \left[J^\dagger{}_\mu(z), J_\nu(0)\right] + J_\nu(0) J^\dagger{}_\mu(z) \, |\mathrm{P}\rangle \; . \tag{2.16}$$

Focusing on the second term, we insert a complete set of states between the currents, and exploit translational invariance to remove the explicit position dependence,

$$\begin{aligned}
\int \mathrm{d}^4z\, e^{iq\cdot z} \langle \mathrm{P}| \, J_\nu(0) J^\dagger{}_\mu(z) \, |\mathrm{P}\rangle &= \sum_X \int \mathrm{d}^4z\, e^{iq\cdot z} \langle \mathrm{P}| \, J_\nu(0) \, |X\rangle \langle X| \, J^\dagger{}_\mu(z) \, |\mathrm{P}\rangle \\
&= \sum_X \int \mathrm{d}^4z\, e^{i(q-p+p_X)\cdot z} \\
&\qquad \times \langle \mathrm{P}| \, J_\nu(0) \, |X\rangle \langle X| \, J^\dagger{}_\mu(0) \, |\mathrm{P}\rangle \\
&= \sum_X (2\pi)^4 \delta^{(4)}(q-p+p_X) \\
&\qquad \times \langle \mathrm{P}| \, J_\nu(0) \, |X\rangle \langle X| \, J^\dagger{}_\mu(0) \, |\mathrm{P}\rangle \; .
\end{aligned} \tag{2.17}$$

At this stage, we may ask whether the delta function in Eq. (2.17) can be satisfied for a physical configuration with q space-like and p time-like, both future-directed. If so, the momenta would obey

$$q - p + p_X = 0 \, . \tag{2.18}$$

For time-like p, it is convenient to work in the hadron rest frame, $p = (M_\mathrm{P}, \mathbf{0})$, where M_P denotes the hadron mass. In this reference frame, the boson energy is

$$p_X^2 = (p-q)^2 = M_\mathrm{P}^2 - 2M_\mathrm{P} q_0 + q^2 \, , \quad \Rightarrow \quad q_0 = \frac{M_\mathrm{P}^2 + q^2 - p_X^2}{2M_\mathrm{P}} \, . \tag{2.19}$$

In the physical region, the intermediate state mass is bounded below by M_P, which renders the numerator strictly negative and implies $q^0 < 0$. The delta function therefore has no support, causing the second term to vanish. As a result, we can write the hadronic tensor, Eq. (2.4), alternatively as

$$W_{\mu\nu}(p,q) = \frac{1}{4\pi}\int \mathrm{d}^4z\, e^{iq\cdot z} \langle \mathrm{P}| \left[J^\dagger{}_\mu(z), J_\nu(0)\right] |\mathrm{P}\rangle \; . \tag{2.20}$$

The integration domain is restricted to the support of the commutator, as causality enforces vanishing commutators at space-like separation. Consequently, the momentum transfer q is either time-like or light-like.

With the momentum transfer being real-valued, the phase of the exponential is likewise real. By the Riemann–Lebesgue lemma [117], the dominant contributions to the integral originate from regions where the phase varies slowly and remains finite. Expanding the phase in powers of the energy transfer then yields

$$\begin{aligned} q \cdot z &= q_0 z_0 - |\boldsymbol{q}||\boldsymbol{z}|\cos\theta \\ &= q_0 \left(z_0 - \sqrt{1 - \frac{q^2}{q_0^2}} |\boldsymbol{z}|\cos\theta \right) \\ &= q_0(z_0 - |\boldsymbol{z}|\cos\theta) + \frac{q^2}{2q_0}|\boldsymbol{z}|\cos\theta + \mathcal{O}\left(\frac{1}{q_0^2}\right), \end{aligned} \tag{2.21}$$

where θ denotes the angle between the vectors $\boldsymbol{z}$ and $\boldsymbol{q}$. For the phase to remain finite for large but finite q_0, its absolute value must be bounded from above by some positive constant δ. Applying the triangle inequality yields

$$\begin{aligned} |q \cdot z| &= |q_0(z_0 - |\boldsymbol{z}|\cos\theta) - M_{\mathrm{P}} x_{\mathrm{B}} |\boldsymbol{z}|\cos\theta| \\ &\leq |q_0(z_0 - |\boldsymbol{z}|\cos\theta)| + |M_{\mathrm{P}} x_{\mathrm{B}} |\boldsymbol{z}|\cos\theta| \\ &\leq \delta\,. \end{aligned} \tag{2.22}$$

Because Eq. (2.22) is the sum of two non-negative terms, each must be bounded for the sum to remain finite. Without loss of generality, both terms may be bounded by a constant, and taking the larger of the two bounds and denoting it by $\delta/2$ yields the inequalities,

$$q_0|z_0 - |\boldsymbol{z}|\cos\theta| \leq \frac{\delta}{2}\,, \tag{2.23}$$

$$\frac{x_{\mathrm{B}}||\boldsymbol{z}|\cos\theta|}{M_{\mathrm{P}}} \leq \frac{\delta}{2}\,. \tag{2.24}$$

Then, by imposing both inequalities, Eqs.(2.23) and (2.24), we obtain the constraint

$$\begin{aligned} z_0^2 &\leq \left(|\boldsymbol{z}|\cos\theta \pm \frac{\delta}{2q_0} \right)^2 \\ &\leq (|\boldsymbol{z}|\cos\theta)^2 + \frac{|\boldsymbol{z}|}{q_0}\cos\theta\delta + \mathcal{O}(\delta^2) \\ &\leq |\boldsymbol{z}|^2 + \frac{M_{\mathrm{P}}}{2x_{\mathrm{B}} q_0}\delta + \mathcal{O}(\delta^2) \\ &= |\boldsymbol{z}|^2 + \mathcal{O}(\delta)\,. \end{aligned} \tag{2.25}$$

Hence, from Eq. (2.25), we find that in the limit $\delta \to 0$, the separation z becomes either time-like or light-like. Since the integrand vanishes at space-like separations, the dominant contributions arise from the light cone, a phenomenon known as light-cone dominance [118].

Despite light-cone dominance, an operator product expansion of the hadronic tensor is not immediately justified. Although the integral is dominated by contributions near the light cone, the corresponding space-time separations need not be small, as the Lorentzian inner product is not positive definite. Moreover, an operator product expansion requires a time-ordered product of operators, which is absent. To address this flaw, we rewrite the hadronic tensor by inserting a complete set of states and invoking translational invariance,

$$
\begin{aligned}
W_{\mu\nu}(p,q) = \frac{1}{4\pi}\sum_X \bigg[& (2\pi)^4 \delta^{(4)}(q+p-p_X) \langle \mathrm{P}| J^\dagger{}_\mu(0) |X\rangle \langle X| J_\nu(0) |\mathrm{P}\rangle \\
& - (2\pi)^4 \delta^{(4)}(q-p+p_X) \langle \mathrm{P}| J_\nu(0) |X\rangle \langle X| J^\dagger{}_\mu(0) |\mathrm{P}\rangle \bigg] .
\end{aligned}
\tag{2.26}
$$

The energy delta distribution admits a representation as a sequence of Cauchy distributions centred at zero,

$$
\delta(E) = -\frac{1}{2\pi i}\lim_{\eta\to 0}\left(\frac{1}{E+i\eta} - \frac{1}{E-i\eta}\right) , \tag{2.27}
$$

which can be verified by direct integration against a well-behaved test function, for both vanishing and non-vanishing energies. Substituting the nascent delta distribution, Eq. (2.27), into Eq. (2.26), gives

$$
\begin{aligned}
W_{\mu\nu}(p,q) = \frac{1}{4\pi i}\sum_X \lim_{\eta\to 0} \bigg[& - (2\pi)^3 \delta^{(3)}(\boldsymbol{q}+\boldsymbol{p}-\boldsymbol{p}_X) \langle \mathrm{P}| J^\dagger{}_\mu(0) |X\rangle \langle X| J_\nu(0) |\mathrm{P}\rangle \\
& \times \left(\frac{1}{q_0+p_0-p_{X,0}+i\eta} - \frac{1}{q_0-p_0+p_{X,0}-i\eta} \right) \\
& + (2\pi)^3 \delta^{(3)}(\boldsymbol{q}-\boldsymbol{p}+\boldsymbol{p}_X) \langle \mathrm{P}| J_\nu(0) |X\rangle \langle X| J^\dagger{}_\mu(0) |\mathrm{P}\rangle \\
& \times \left(\frac{1}{q_0-p_0+p_{X,0}+i\eta} - \frac{1}{q_0-p_0+p_{X,0}-i\eta} \right) \bigg] .
\end{aligned}
\tag{2.28}
$$

Here, the expressions in round parentheses are precisely the discontinuity of the corresponding energy denominators,

$$
\mathrm{Disc}\left(\frac{1}{E}\right) = \lim_{\eta\to 0}\left(\frac{1}{E+i\eta} - \frac{1}{E-i\eta}\right). \tag{2.29}
$$

Substituting the discontinuity of the energy propagators, Eq. (2.29), into Eq. (2.28) yields

$$
\begin{aligned}
W_{\mu\nu}(p,q) = \frac{1}{4\pi i}\sum_X \mathrm{Disc}\bigg[& - \frac{(2\pi)^3 \delta^{(3)}(\boldsymbol{q}+\boldsymbol{p}-\boldsymbol{p}_X) \langle \mathrm{P}| J^\dagger{}_\mu(0) |X\rangle \langle X| J_\nu(0) |\mathrm{P}\rangle}{q_0+p_0-p_{X,0}} \\
& + \frac{(2\pi)^3 \delta^{(3)}(\boldsymbol{q}-\boldsymbol{p}+\boldsymbol{p}_X) \langle \mathrm{P}| J_\nu(0) |X\rangle \langle X| J^\dagger{}_\mu(0) |\mathrm{P}\rangle}{q_0-p_0+p_{X,0}} \bigg] .
\end{aligned}
\tag{2.30}
$$

To relate the hadronic tensor to a time-ordered product, we must reinstate the step functions. Recall that energies are taken to be real with an infinitesimal negative imaginary part, in accordance with the Feynman prescription. At this point, we introduce a factor of unity of the form

$$\begin{aligned}
\pm\frac{i}{E-i\eta} &= \frac{1}{i}\int_{-\infty}^{+\infty}\mathrm{d}s\,\frac{\delta(\mp E+s)}{s-i\eta} \\
&= \frac{1}{2\pi i}\int_{-\infty}^{+\infty}\mathrm{d}s\,\frac{1}{s-i\eta}\int_{-\infty}^{+\infty}\mathrm{d}t\,e^{it(\mp E+s)} \\
&= \int_{-\infty}^{+\infty}\mathrm{d}t\,e^{its}\frac{1}{2\pi i}\int_{-\infty}^{+\infty}\mathrm{d}s\,\frac{e^{\mp itE}}{s-i\eta} \\
&= \int_{-\infty}^{+\infty}\mathrm{d}t\,e^{itE}\theta(\pm t)\,,
\end{aligned} \tag{2.31}$$

where the final line follows from integrating along the real s-axis and closing the contour with a semicircle at infinity in the upper half-plane. Since the energies are real, the contribution from the arc at infinity vanishes owing to exponential damping, and the step function arises via the residue theorem.

Upon substitution of Eq. (2.31) into Eq. (2.30), we obtain the desired time-ordered product of currents,

$$\begin{aligned}
W_{\mu\nu}(p,q) &= \frac{1}{4\pi i}\sum_X \mathrm{Disc}\Bigg[\int \mathrm{d}^4z\,e^{iz\cdot(q+p-p_X)}\theta(z_0)\,\langle\mathrm{P}|\,J^\dagger_\mu(0)\,|X\rangle\,\langle X|\,J_\nu(0)\,|\mathrm{P}\rangle \\
&\quad + \int \mathrm{d}^4z\,e^{iz\cdot(q-p+p_X)}\theta(-z_0)\,\langle\mathrm{P}|\,J_\nu(0)\,|X\rangle\,\langle X|\,J^\dagger_\mu(0)\,|\mathrm{P}\rangle\Bigg] \\
&= \frac{1}{4\pi i}\mathrm{Disc}\Bigg[i\int \mathrm{d}^4z\,e^{iz\cdot q}\,\langle\mathrm{P}|\,\theta(z_0)J^\dagger_\mu(z)J_\nu(0) \\
&\quad + \theta(-z_0)J_\nu(0)J^\dagger_\mu(z)\,|\mathrm{P}\rangle\Bigg] \\
&= \frac{1}{4\pi i}\mathrm{Disc}\Bigg[i\int \mathrm{d}^4z\,e^{iz\cdot q}\,\langle\mathrm{P}|\,\mathcal{T}\left\{J^\dagger_\mu(z)J_\nu(0)\right\}|\mathrm{P}\rangle\Bigg]\,,
\end{aligned} \tag{2.32}$$

with the time-ordering operator,

$$\mathcal{T}\left\{O(z_1)O(z_2)\right\} \equiv \theta(z_{1,0}-z_{2,0})O(z_1)O(z_2) + \theta(z_{2,0}-z_{1,0})O(z_2)O(z_1)\,. \tag{2.33}$$

An analogous calculation carries over to the product of scalar currents, since the derivation does not rely on the currents being vector currents.

2.1.3 Forward Scattering

In the preceding section, we expressed the hadronic tensor in terms of the discontinuity, Eq. (2.32), of the forward scattering amplitude,

$$T_{\mu\nu} = i\int \mathrm{d}^4z\;e^{iq\cdot z}\,\langle\mathrm{P}|\,\mathcal{T}\{J^\dagger_\mu(z)J_\nu(0)\}\,|\mathrm{P}\rangle\;. \tag{2.34}$$

Under the assumption that the forward scattering amplitude is analytic away from its singularities and real-valued on the real axis, the Schwarz reflection principle [117] relates its discontinuity to its imaginary part,

$$W_{\mu\nu} = \frac{1}{2\pi}\,\mathrm{Im}\,T_{\mu\nu}\,. \tag{2.35}$$

Through this relation, the hadronic tensor connects directly to the operator product expansion of the forward scattering amplitude.

At leading twist, and setting aside for the moment the question of its physical validity, the forward amplitude admits an operator product expansion [119, 120],

$$T_{\mu\nu} = \sum_{N\in\mathbb{N}}\sum_{k\in\mathbb{S}_a}\left(\frac{1}{-q^2}\right)^N {t^N}_{\mu\nu,\lambda_1\lambda_2} q_{\lambda_3}\dots q_{\lambda_N} {O_k}^{\{\lambda_1\dots\lambda_N\}}\,, \tag{2.36}$$

where braces denote symmetrisation over the enclosed Lorentz indices with all traces subtracted, and t^N denotes a family of tensors whose components are, in general, dimensionless functions of the coupling and renormalisation scale. In Eq. (2.36), the outer sum runs over all operator spins, whilst the inner sum runs over all local, symmetric, traceless twist-two operators, labelled by the set $\mathbb{S}_a = \{\,a\,\}\cup\mathbb{S}$ with $\mathbb{S} = \{\,\mathrm{q},\mathrm{g}\,\}$, where q, g and a label quark-singlet, gluon and quark non-singlet, respectively. The operators are classified into quark non-singlet, quark singlet, and gluon operators,

$$\begin{aligned} {O_a}^{\{\mu_1\dots\mu_N\}} &= i^{N-1}\bar{\psi}_{\mathrm{l}}\lambda^a_{\mathrm{l}}\gamma^{\{\mu_1}D^{\mu_2}\cdots D^{\mu_N\}}\psi_{\mathrm{l}}\,, &(2.37)\\ {O_{\mathrm{q}}}^{\{\mu_1\dots\mu_N\}} &= i^{N-1}\bar{\psi}_{\mathrm{l}}\gamma^{\{\mu_1}D^{\mu_2}\cdots D^{\mu_N\}}\psi_{\mathrm{l}}\,, &(2.38)\\ {O_{\mathrm{g}}}^{\{\mu_1\dots\mu_N\}} &= i^{N-2}G^{\{\lambda\mu_1}D^{\mu_2}\cdots D^{\mu_{N-1}}G^{\mu_N\lambda\}}\,, &(2.39) \end{aligned}$$

where in the non-singlet case λ^a_{l} denotes the generators of the light-flavour symmetry group. In the parton model, hadrons are described in terms of massless partonic degrees of freedom. Within the fixed-flavour number scheme adopted here, the operator basis is restricted to the light-quark sector, with heavy-quark contributions treated as perturbative corrections to the coefficient functions.

As with the hadronic tensor in Subsec. 2.1.1, we can decompose the undetermined rank-four tensors in Eq. (2.36) into symmetric and antisymmetric parts,

$${t^N}_{k,\mu\nu,\lambda_1\lambda_2}(q) = {t^{\mathrm{S},N}}_{k,\mu\nu,\lambda_1\lambda_2}(q) + {t^{\mathrm{A},N}}_{k,\mu\nu,\lambda_1\lambda_2}(q)\,. \tag{2.40}$$

The symmetric part is constrained by Lorentz symmetry to a form in which all coefficients can be chosen to be dimensionless,

$$\begin{aligned} {t^{\mathrm{S},N}}_{k,\mu\nu,\lambda_1\lambda_2}(q) = {}& g_{\mu\nu}q_{\lambda_1}q_{\lambda_2}t^{\mathrm{S},N}_{k,1}(q) + \frac{q_\mu q_\nu}{q^2}q_{\lambda_1}q_{\lambda_2}t^{\mathrm{S},N}_{k,2}(q) + g_{\mu\lambda_2}q_\nu q_{\lambda_1}t^{\mathrm{S},N}_{k,3}(q)\\ &+ g_{\lambda_1\nu}q_\mu q_{\lambda_2}t^{\mathrm{S},N}_{k,4}(q) + g_{\mu\lambda_2}g_{\lambda_1\nu}q^2t^{\mathrm{S},N}_{k,5}(q) + g_{\mu\nu}g_{\lambda_1\lambda_2}q^2t^{\mathrm{S},N}_{k,6}(q)\\ &+ g_{\lambda_1\lambda_2}q_\mu q_\nu t^{\mathrm{S},N}_{k,7}(q)\quad. \end{aligned} \tag{2.41}$$

Because this tensor contracts with traceless operators, the sixth and seventh terms do not contribute to the forward scattering amplitude at leading twist and may therefore be set to zero. Moreover, the complete symmetry of the operators forces the coefficients of the third and fourth terms to be equal. The ansatz for the symmetric part, Eq. (2.41), then reduces to

$$\begin{aligned} {t^{\mathrm{S},N}}_{k,\mu\nu,\lambda_1\lambda_2}(q) = {}& g_{\mu\nu}q_{\lambda_1}q_{\lambda_2}t^{\mathrm{S},N}_{k,1}(q) + q_\mu q_\nu q_{\lambda_1}q_{\lambda_2}t^{\mathrm{S},N}_{k,2}(q) + \Big(g_{\mu\lambda_2}q_\nu q_{\lambda_1}\\ &+ g_{\lambda_1\nu}q_\mu q_{\lambda_2}\Big)t^{\mathrm{S},N}_{k,3}(q) + g_{\mu\lambda_2}g_{\lambda_1\nu}t^{\mathrm{S},N}_{k,5}(q)\,, \end{aligned} \tag{2.42}$$

leaving only four unknown coefficients. Current conservation imposes again a transversality condition on the forward scattering amplitude, which implies that

$$
\begin{aligned}
q^\mu t^{\mathrm{S},N}{}_{k,\mu\nu,\lambda_1\lambda_2}(q) &= q^2 g_{\nu\lambda_1} q_{\lambda_2}\Big(t^{\mathrm{S},N}_{k,3}(q) + t^{\mathrm{S},N}_{k,5}(q)\Big) \\
&\quad + q_\nu q_{\lambda_1} q_{\lambda_2}\Big(t^{\mathrm{S},N}_{k,1}(q) + t^{\mathrm{S},N}_{k,2}(q) + t^{\mathrm{S},N}_{k,3}(q)\Big) = 0\,.
\end{aligned}
\tag{2.43}
$$

Since the two tensor structures are linearly independent on dimensional grounds, their coefficients must vanish separately, yielding a system of equations. Solving this system, we find

$$
\begin{aligned}
t^{\mathrm{S},N}{}_{k,\mu\nu,\lambda_1\lambda_2}(q) = &\left(g_{\mu\lambda_2} q_{\lambda_1} q_\nu + g_{\lambda_1\nu} q_\mu q_{\lambda_2} - g_{\mu\nu} g_{\lambda_1\lambda_2} q^2 - g_{\lambda_1\lambda_2} q_\mu q_\nu\right) C^N_{2,k}(q) \\
&+ \left(g_{\mu\nu} - \frac{q_\mu q_\nu}{q^2}\right) q_{\lambda_1} q_{\lambda_2} C^N_{L,k}(q)\,,
\end{aligned}
\tag{2.44}
$$

where the coefficient functions have been redefined such that the associated tensor structures are manifestly transverse.

For the antisymmetric part, only a single contribution arises, since the Levi-Civita tensor can contract non-trivially with the same vector at most once. By virtue of its total antisymmetry, this tensor structure automatically satisfies the transversality condition. With a conventional normalisation chosen to ensure a real coefficient function, we may therefore write it as

$$
t^{\mathrm{A},N}{}_{k,\mu\nu,\lambda_1\lambda_2}(q) = i\epsilon_{\mu\nu\lambda_1\lambda} q^\lambda q_{\lambda_2} C^N_{3,k}(q)\,.
\tag{2.45}
$$

Combining the symmetric and antisymmetric parts, Eqs. (2.44) and (2.45), the forward scattering amplitude becomes

$$
\begin{aligned}
T_{\mu\nu} = \sum_{N\in\mathbb{N}} \sum_{k\in\mathbb{S}_a} \left(\frac{1}{-q^2}\right)^N \Bigg[&\left(g_{\mu\nu} - \frac{q_\mu q_\nu}{q^2}\right) q_{\lambda_1} q_{\lambda_2} C^N_{L,k}(q) \\
&+ \left(g_{\mu\lambda_2} q_{\lambda_1} q_\nu + g_{\lambda_1\nu} q_\mu q_{\lambda_2} - g_{\mu\nu} g_{\lambda_1\lambda_2} q^2 - g_{\lambda_1\lambda_2} q_\mu q_\nu\right) C^N_{2,k}(q) \\
&+ i\epsilon_{\mu\nu\lambda_1\lambda} q^\lambda q_{\lambda_2} C^N_{3,k}(q)\Bigg] q_{\lambda_3}\dots q_{\lambda_N} \langle \mathrm{P}|\, O_k{}^{\{\lambda_1\dots\lambda_N\}}\, |\mathrm{P}\rangle\,.
\end{aligned}
\tag{2.46}
$$

In the regime of large virtualities relative to the squared hadronic mass, hadronic mass effects in the operator matrix elements are suppressed. Within the leading-twist approximation, we then find

$$
\begin{aligned}
\langle \mathrm{P}|\, O_k{}^{\{\lambda_1\dots\lambda_N\}}\, |\mathrm{P}\rangle &= p^{\{\lambda_1}\dots p^{\lambda_N\}} A^N_{k,\mathrm{P}}(p) \\
&= p^{\ \lambda_1}\dots p^{\ \lambda_N} A^N_{k,\mathrm{P}}(p) + \mathcal{O}\big(p^2\big)\,,
\end{aligned}
\tag{2.47}
$$

where these operator matrix elements are inaccessible within perturbative QCD. This circumstance poses no fundamental difficulty, since the primary focus lies on the coefficient functions in the operator product expansion of the forward scattering amplitude. Because the expansion holds at the operator level, the coefficient functions are universal and independent of the external states. A more detailed discussion is deferred to the following section on renormalisation (see Subsec. 2.2.1).

Upon inserting the operator matrix elements, Eq. (2.47), into the operator product expansion, Eq. (2.46), and performing subsequent algebraic manipulations, we obtain

$$\begin{aligned} T_{\mu\nu} = \sum_{N\in\mathbb{N}} \sum_{k\in\mathbb{S}_a} \left(\frac{1}{2x_\mathrm{B}}\right)^N A^N_{k,\mathrm{P}}(p) \Bigg[& e_{\mu\nu} C^N_{L,k}(q) + d_{\mu\nu} C^N_{2,k}(q) \\ & + i\epsilon_{\mu\nu\alpha\beta} \frac{p^\alpha q^\beta}{p\cdot q} C^N_{3,k}(q) \Bigg] + \mathcal{O}\big(p^2\big) \,, \end{aligned} \tag{2.48}$$

where the tensors $e_{\mu\nu}$ and $d_{\mu\nu}$, defined in Eqs. (2.9) and (2.10), are the same tensor structures that appear in Eq. (2.13) for the hadronic tensor.

To extract the coefficient functions, we introduce a set of suitable projectors, constructed in direct analogy with the decomposition of both the hadronic tensor and the forward scattering amplitude. These projectors are designed to isolate the symmetric and antisymmetric components, each parametrised by yet undetermined coefficients. Their most general decomposition reads

$$\begin{aligned} {\mathcal{P}_{\mathrm{S},i}}^{\mu\nu}(p,q) = {} & g^{\mu\nu} c^{\mathrm{S}}_{i,1}(p,q) + p^\mu p^\nu c^{\mathrm{S}}_{i,2}(p,q) + q^\mu q^\nu c^{\mathrm{S}}_{i,3}(p,q) + q^\mu p^\nu c^{\mathrm{S}}_{i,4}(p,q) \\ & + p^\mu q^\nu c^{\mathrm{S}}_{i,5}(p,q) \,, \qquad i \in \{\, L, 2 \,\} \,, \end{aligned} \tag{2.49}$$

$${\mathcal{P}_{\mathrm{A},3}}^{\mu\nu}(p,q) = \epsilon_{\mu\nu\alpha\beta} p^\alpha q^\beta c^{\mathrm{A}}_{3,1}(p,q) \,. \tag{2.50}$$

Since $e_{\mu\nu}$ and $d_{\mu\nu}$ are manifestly transverse, the tensors multiplying $c^{\mathrm{S}}_{k,3}$, $c^{\mathrm{S}}_{k,4}$ and $c^{\mathrm{S}}_{k,5}$ vanish under projection. These three coefficients thus remain arbitrary, and we may as well set them to zero without loss of generality. What remains are two symmetric tensors, each carrying two undetermined coefficients, which are constrained by the orthogonality conditions,

$$\begin{cases} \mathcal{P}^{\mu\nu}_{\mathrm{S,L}}(p,q) e_{\mu\nu} = 1 \,, \\ \mathcal{P}^{\mu\nu}_{\mathrm{S,L}}(p,q) d_{\mu\nu} = 0 \,, \end{cases} \tag{2.51}$$

$$\begin{cases} \mathcal{P}^{\mu\nu}_{\mathrm{S},2}(p,q) e_{\mu\nu} = 0 \,, \\ \mathcal{P}^{\mu\nu}_{\mathrm{S},2}(p,q) d_{\mu\nu} = 1 \,. \end{cases} \tag{2.52}$$

In addition, both symmetric tensors of Eq. (2.49) are trivially orthogonal to the antisymmetric one in Eq. (2.50). For the antisymmetric case, a single undetermined coefficient uniquely fixes the normalisation,

$$\mathcal{P}^{\mu\nu}_{\mathrm{A},3} \left(i\epsilon_{\mu\nu\alpha\beta} \frac{p^\alpha q^\beta}{p\cdot q} \right) = 1 \,. \tag{2.53}$$

Placing each projector ansatz into the corresponding orthogonality condition, Eqs. (2.51)–(2.53), yields a system of equations that follows from the linear independence of the tensor structures. Its solution gives the projectors

$$\mathcal{P}^{\mu\nu}_{\mathrm{S},L}(p,q) = -\frac{q^2}{(p\cdot q)^2} p^\mu p^\nu \,, \tag{2.54}$$

$$\mathcal{P}^{\mu\nu}_{\mathrm{S},2}(p,q) = -\frac{(D-1)}{(D-2)} \frac{q^2}{(p\cdot q)^2} p^\mu p^\nu - \frac{1}{(D-2)} g^{\mu\nu} \,, \tag{2.55}$$

$$\mathcal{P}_{\mathrm{A},3}^{\mu\nu}(p,q) = \frac{i}{(D-2)(D-3)}\epsilon_{\mu\nu\alpha\beta}\frac{p^\alpha q^\beta}{p\cdot q}\,. \tag{2.56}$$

These projectors let us decompose the forward scattering amplitude in direct analogy with the hadronic tensor, Eq. (2.13), the hadronic invariants now playing the role of the structure functions. At leading twist, we find the decomposition

$$T_{\mu\nu}(p,q) = e_{\mu\nu}T_L(p,q) + d_{\mu\nu}T_2(p,q) + i\epsilon_{\mu\nu\alpha\beta}\frac{p^\alpha q^\beta}{p\cdot q}T_3(p,q) + \mathcal{O}(p^2)\,, \tag{2.57}$$

with the hadronic invariants

$$T_i(p,q) = \mathcal{P}_{\mathrm{S},i}{}^{\mu\nu}T_{\mu\nu}(p,q)\,, \qquad i\in\{\,L,2\,\}\,, \tag{2.58}$$
$$T_3(p,q) = \mathcal{P}_{\mathrm{A},3}{}^{\mu\nu}T_{\mu\nu}(p,q)\,. \tag{2.59}$$

Having expressed the forward scattering amplitude, Eq. (2.34), in terms of the same tensor structures as the hadronic tensor, Eq. (2.4), we arrive via the optical theorem, Eq. (2.35), at a direct relation between the hadronic invariants and the structure functions,

$$\frac{1}{2\pi}\,\mathrm{Im}\,T_i(p,q) = \frac{1}{2x_\mathrm{B}}F_i(p,q)\,, \qquad i\in\{\,L,2\,\}\,, \tag{2.60}$$
$$\frac{1}{2\pi}\,\mathrm{Im}\,T_3(p,q) = F_3(p,q)\,. \tag{2.61}$$

2.1.4 Mellin Moments

The operator product expansion, Eq. (2.48), recasts the hadronic invariants, Eqs. (2.60) and (2.61), as a series in inverse powers of x_B. For convenience, we define $\omega = 1/x_\mathrm{B}$ to label these powers. Working in ω is natural because the limit $x_\mathrm{B}\to\infty$ translates to the limit $\omega\to 0$. In this variable, the series then reads

$$T_i(p,q) = \sum_{N\in\mathbb{N}}\sum_{k\in\mathbb{S}_a}\left(\frac{\omega}{2}\right)^N A^N_{k,\mathrm{P}}C^N_{i,k}(q)\,, \qquad i\in\{\,L,2,3\,\}\,. \tag{2.62}$$

To connect the hadronic invariants to the structure functions, we multiply this expression by ω^{-M-1} and integrate along a contour γ encircling the origin (see Fig. 2.1a). By Cauchy's theorem, we obtain

$$\begin{aligned}\frac{1}{2\pi i}\int_\gamma \mathrm{d}\omega\,\frac{T_i(p,q)}{\omega^{M+1}} &= \sum_{N\in\mathbb{N}}\sum_{k\in\mathbb{S}_a}\frac{1}{2^N}A^N_{k,\mathrm{P}}(p)C^N_{i,k}(q)\left(\frac{1}{2\pi i}\int_\gamma\frac{\mathrm{d}\omega}{\omega^{M-N+1}}\right)\\ &= \sum_{N\in\mathbb{N}}\sum_{k\in\mathbb{S}_a}\frac{\delta_{N,M}}{2^N}A^N_{k,\mathrm{P}}(p)C^N_{i,k}(q)\\ &= \sum_{k\in\mathbb{S}_a}\frac{A^N_{k,\mathrm{P}}(p)C^N_{i,k}(q)}{2^M}\,, \qquad i\in\{\,L,2,3\,\}\,.\end{aligned} \tag{2.63}$$

Alternatively, rather than evaluating the integral directly, we may invoke the optical theorem. Since we assume the forward scattering amplitude to be analytic away

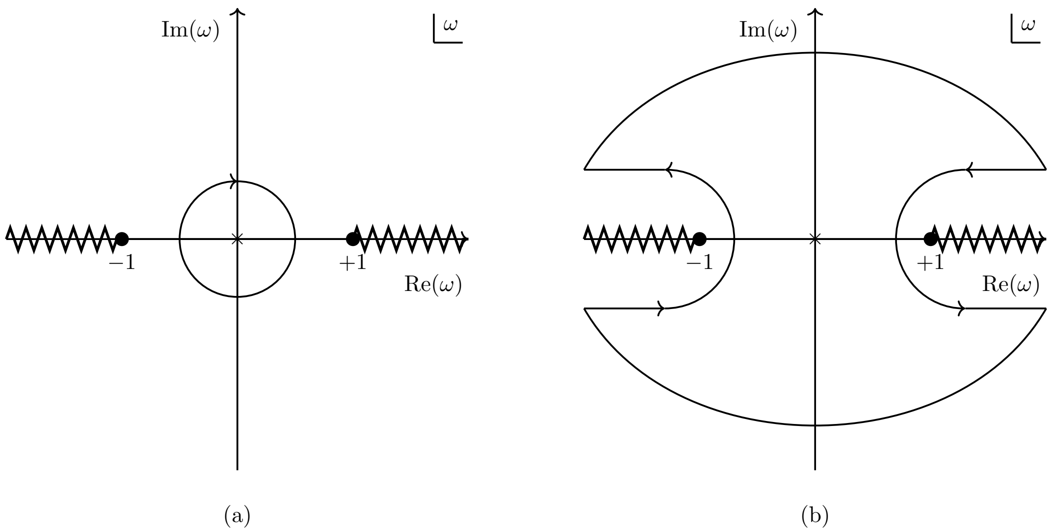

Figure 2.1: The figure displays the branch points, indicated by bold dots, and the branch cuts along the real axis, shown as zigzag lines, with the origin marked by a cross. Panel (a) shows the contour encircling the origin, whilst panel (b) depicts the deformed contour running along the branch cuts, with semicircles closing at infinity.

from its branch cuts, we can deform the contour to enclose the cuts with two semicircles closing at infinity (see Fig. 2.1b). The integral reduces to an integral over the discontinuities of the integrand along the cuts,

$$\frac{1}{2\pi i}\int_\gamma \mathrm{d}\omega\,\frac{T_i(p,q)}{\omega^{M+1}} = \frac{1}{2\pi i}\left(\int_1^\infty \mathrm{d}\omega\,\frac{\mathrm{Disc}(T_i(p,q))}{\omega^{M+1}} + \int_{-\infty}^{-1} \mathrm{d}\omega\,\frac{\mathrm{Disc}(T_i(p,q))}{\omega^{M+1}}\right) \qquad i \in \{\,L,2,3\,\}\,. \tag{2.64}$$

To combine the integrals in Eq. (2.64), we note that the forward scattering amplitude, Eq. (2.34), decomposes into vector–vector, axial–axial and mixed contributions,

$$T_{\mu\nu}\,(p,q) = T_{\mathrm{vv},\mu\nu}\,(p,q) + T_{\mathrm{aa},\mu\nu}\,(p,q) + T_{\mathrm{va},\mu\nu}\,(p,q) + T_{\mathrm{av},\mu\nu}\,(p,q)\,, \tag{2.65}$$

induced by the decomposition of the currents, Eq. (2.1). Outside this section we omit the vector and axial-vector subscripts, since the context makes their meaning clear. Depending on the type of the bosons, the individual terms of the forward scattering amplitude transform under charge conjugation

$$T_{\mathrm{b}_1\mathrm{b}_2,\mu\nu}\,(p,q) = (-1)^{1+\delta_{\mathrm{b}_1\mathrm{b}_2}}\,T_{\mathrm{b}_1\mathrm{b}_2,\nu\mu}\,(p,-q)\,, \qquad \mathrm{b}_1,\mathrm{b}_2 \in \{\,\mathrm{v},\mathrm{a}\,\}\,. \tag{2.66}$$

Since the forward scattering amplitude is decomposed into tensor structures that are even in both momenta, Eq. (2.57), parity transformations leave it invariant. Only the hadronic invariants are affected. Taking the forward scattering amplitude to be invariant under crossing of the external bosons [121], we find

$$
\begin{aligned}
T_{\mathrm{b}_1\mathrm{b}_2,\mu\nu}(p,q) &= T_{\mathrm{b}_1\mathrm{b}_2,\nu\mu}(p,-q) \\
&= e_{\nu\mu}T_{\mathrm{b}_1\mathrm{b}_2,L}(p,-q) + d_{\nu\mu}T_{\mathrm{b}_1\mathrm{b}_2,2}(p,-q) \\
&\qquad i\epsilon_{\nu\mu\alpha\beta}\frac{p^\alpha q^\beta}{p\cdot q}T_{\mathrm{b}_1\mathrm{b}_2,3}(p,-q) \\
&= (-1)^{1+\delta_{\mathrm{b}_1\mathrm{b}_2}}\Big[e_{\nu\mu}T_{\mathrm{b}_1\mathrm{b}_2,L}(p,-q) + d_{\nu\mu}T_{\mathrm{b}_1\mathrm{b}_2,2}(p,-q) \\
&\qquad + i\epsilon_{\nu\mu\alpha\beta}\frac{p^\alpha q^\beta}{p\cdot q}T_{\mathrm{b}_1\mathrm{b}_2,3}(p,-q)\Big] \\
&= (-1)^{1+\delta_{\mathrm{b}_1\mathrm{b}_2}}\Big[e_{\mu\nu}T_{\mathrm{b}_1\mathrm{b}_2,L}(p,-q) + d_{\mu\nu}T_{\mathrm{b}_1\mathrm{b}_2,2}(p,-q) \\
&\qquad - i\epsilon_{\mu\nu\alpha\beta}\frac{p^\alpha q^\beta}{p\cdot q}T_{\mathrm{b}_1\mathrm{b}_2,3}(p,-q)\Big] .
\end{aligned}
\tag{2.67}
$$

Comparing the charge conjugation relation, Eq. (2.66), with the crossing relation, Eq. (2.67), we read off

$$
T_{\mathrm{b}_1\mathrm{b}_2,i}(p,q) = (-1)^{1+\delta_{\mathrm{b}_1\mathrm{b}_2}}T_{\mathrm{b}_1\mathrm{b}_2,i}(p,-q)\,, \qquad i\in\{\,L,2\,\}\,, \tag{2.68}
$$

$$
T_{\mathrm{b}_1\mathrm{b}_2,3}(p,q) = (-1)^{\delta_{\mathrm{b}_1\mathrm{b}_2}}T_{\mathrm{b}_1\mathrm{b}_2,3}(p,-q)\,. \tag{2.69}
$$

The hadronic invariants are thus either even or odd functions of the momentum q. Because they depend only on scalar products of p and q, with both p^2 and q^2 invariant under parity, the invariants must in fact be even or odd in x_B and consequently in ω.

Returning to the integral, Eq. (2.64), we exploit (anti)symmetry of the hadronic invariant, Eq. (2.68), together with the optical theorem, Eqs. (2.60) and (2.61), to express the integral in terms of the Mellin moments of the structure functions.

$$
\frac{1}{2\pi i}\int_\gamma \mathrm{d}\omega\,\frac{T_{\mathrm{b}_1\mathrm{b}_2,i}(p,q)}{\omega^{M+1}} = \begin{cases} 2\displaystyle\int_1^\infty \mathrm{d}\omega\,\frac{F_{\mathrm{b}_1\mathrm{b}_2,i}(p,q)}{\omega^M}\,, & i\in\{\,L,2\,\}\,, \\ 4\displaystyle\int_1^\infty \mathrm{d}\omega\,\frac{F_{\mathrm{b}_1\mathrm{b}_2,3}(p,q)}{\omega^{M+1}}\,. \end{cases} \tag{2.70}
$$

Reverting from ω to the original variable $x_\mathrm{B} = 1/\omega$, with $\mathrm{d}\omega = -\,\mathrm{d}x_\mathrm{B}\,/x_\mathrm{B}^2$, and reversing the integration limits accordingly, we arrive at

$$
\frac{1}{2\pi i}\int_\gamma \mathrm{d}\omega\,\frac{T_{\mathrm{b}_1\mathrm{b}_2,i}(p,q)}{\omega^{M+1}} = \begin{cases} 2\displaystyle\int_0^1 \mathrm{d}x_\mathrm{B}\,x_\mathrm{B}^{M-2}F_{\mathrm{b}_1\mathrm{b}_2,i}(p,q)\,, & i\in\{\,L,2\,\}\,, \\ 4\displaystyle\int_0^1 \mathrm{d}x_\mathrm{B}\,x_\mathrm{B}^{M-1}F_{\mathrm{b}_1\mathrm{b}_2,3}(p,q)\,. \end{cases} \tag{2.71}
$$

Finally, combining these results, Eqs. (2.63) and (2.70), we obtain a relation between products of the hadronic operator matrix elements and coefficient functions on one side, and Mellin moments of the structure functions on the other,

$$
\int_0^1 \mathrm{d}x_\mathrm{B}\,x_\mathrm{B}^{N-2}F_{\mathrm{b}_1\mathrm{b}_2,i}(p,q) = \sum_{k\in\mathbb{S}_a}\frac{A^N_{k,\mathrm{P}}(p)C^N_{\mathrm{b}_1\mathrm{b}_2,i,k}(q)}{2^{N+1}}\,, \qquad i\in\{\,L,2\,\}\,, \tag{2.72}
$$

$$
\int_0^1 \mathrm{d}x_\mathrm{B}\,x_\mathrm{B}^{N-1}F_{\mathrm{b}_1\mathrm{b}_2,3}(p,q) = \sum_{k\in\mathbb{S}_a}\frac{A^N_{k,\mathrm{P}}(p)C^N_{\mathrm{b}_1\mathrm{b}_2,3,k}(q)}{2^{N+1}}\,. \tag{2.73}
$$

Only the even or odd moments of the structure functions are constrained, depending on whether the corresponding hadronic invariants are even or odd in x_{B}. Such behaviour arises because the derivation relies on each invariant having a definite parity in x_{B}, so that the opposite contributions cancel.

2.2 Renormalisation

2.2.1 Operator Mixing

In determining the fixed-order moments of the coefficient functions from the hadronic invariants, one obstacle remains, namely the hadronic operator matrix elements. The operator product expansion of the forward scattering amplitude holds at the operator level, so the coefficient functions do not depend on the choice of external states and all hadronic information resides in the matrix elements alone. Therefore, we may replace the hadronic states by partonic ones carrying momentum p, the partons now taken to be massless, unlike the hadrons.

The relevant partonic states comprise non-singlet and singlet quark configurations together with gluons, the corresponding operator matrix elements being given by

$$\langle \mathrm{p}| \, {O_k}^{\{\lambda_1 \ldots \lambda_N\}} \, |\mathrm{p}\rangle = p^{\{\lambda_1} \ldots p^{\lambda_N\}} A^N_{k,\mathrm{p}}(p) \,, \tag{2.74}$$

which are in general divergent and require renormalisation. To regularise these divergences, we work in dimensional regularisation [92, 93] and consider all observables at $D = 4-2\varepsilon$ space-time dimensions, as discussed in Sec. 3.2. The bare singlet operators are then related to the renormalised ones through

$${O_l}^{\{\lambda_1 \ldots \lambda_N\}} = \sum_{k \in \{\mathrm{q},\mathrm{g}\}} Z_{kl} {O_{k,\mathrm{ren}}}^{\{\lambda_1 \ldots \lambda_N\}} \,, \tag{2.75}$$

where the renormalisation constants Z_{kl} generally mix operators within the singlet sector. Because the renormalised operators acquire a dependence on the renormalisation scale μ^2 through this procedure, their evolution is governed by a renormalisation group equation. To derive it, we use that the bare operators carry no such dependence,

$$\begin{aligned}
0 &= \frac{\mathrm{d}}{\mathrm{d}\log\mu^2} O_l^{\{\lambda_1 \ldots \lambda_N\}} \\
&= \frac{\mathrm{d}}{\mathrm{d}\log\mu^2} \sum_{k \in \mathbb{S}} \left(Z^{-1}\right)_{lk} O_{k,\mathrm{ren}}^{\{\lambda_1 \ldots \lambda_N\}} \\
&= \sum_{k \in \mathbb{S}} \left[\frac{\mathrm{d}\left(Z^{-1}\right)_{lk}}{\mathrm{d}\log\mu^2} O_{k,\mathrm{ren}}^{\{\lambda_1 \ldots \lambda_N\}} + \left(Z^{-1}\right)_{lk} \frac{\mathrm{d}O_{k,\mathrm{ren}}^{\{\lambda_1 \ldots \lambda_N\}}}{\mathrm{d}\log\mu^2} \right] \\
&= \sum_{j,k \in \mathbb{S}} \frac{\mathrm{d}Z_{lj}}{\mathrm{d}\log\mu^2} \left(Z^{-1}\right)_{jk} O_{k,\mathrm{ren}}^{\{\lambda_1 \ldots \lambda_N\}} + \delta_{lk} \frac{\mathrm{d}O_{k,\mathrm{ren}}^{\{\lambda_1 \ldots \lambda_N\}}}{\mathrm{d}\log\mu^2} \\
&\equiv - \sum_{k \in \mathbb{S}} \gamma_{lk} O_{k,\mathrm{ren}}^{\{\lambda_1 \ldots \lambda_N\}} + \frac{\mathrm{d}O_{l,\mathrm{ren}}^{\{\lambda_1 \ldots \lambda_N\}}}{\mathrm{d}\log\mu^2} \,.
\end{aligned} \tag{2.76}$$

In Eq. (2.76), we have implicitly defined the matrix valued anomalous dimensions γ and used that the bare operators are independent of the renormalisation scale, together with the identity,

$$\delta_{lk} = \sum_{j\in\mathbb{S}} Z_{lj} \left(Z^{-1}\right)_{jk} \Rightarrow\ 0 = \sum_{j\in\mathbb{S}} Z_{lj} \frac{\mathrm{d}\left(Z^{-1}\right)_{jk}}{\mathrm{d}\log\mu^2} + \sum_{j\in\mathbb{S}} \frac{\mathrm{d}Z_{lj}}{\mathrm{d}\log\mu^2} \left(Z^{-1}\right)_{jk} . \tag{2.77}$$

Since the renormalisation constants depend on the renormalisation scale μ^2 only implicitly through the renormalised coupling $a_{s,\mathrm{ren}}$, the chain rule gives

$$\gamma_{lk} = -\sum_{j\in\mathbb{S}} \frac{\mathrm{d}a_{s,\mathrm{ren}}}{\mathrm{d}\log\mu^2} \frac{\partial Z_{lj}}{\partial a_{s,\mathrm{ren}}} \left(Z^{-1}\right)_{jk} , \tag{2.78}$$

where we have written the coupling in the rescaled form

$$a_{s,\mathrm{ren}} = \frac{\alpha_{s,\mathrm{ren}}}{4\pi} . \tag{2.79}$$

To evaluate the derivative with respect to the renormalised coupling in Eq. (2.78), we use the fact that the bare coupling a_s is multiplicatively renormalised,

$$a_s = Z_{a_s}\, a_{s,\mathrm{ren}} , \tag{2.80}$$

with a renormalisation constant that admits a Laurent expansion in inverse powers of the dimensional regulator,

$$Z_{a_s} = 1 + \sum_{n\in\mathbb{N}^*} \frac{Z_{a_s}^{(n)}}{\varepsilon^n} . \tag{2.81}$$

Because the dimensionful bare coupling $a_s\mu^{2\varepsilon}$ is independent of the renormalisation scale, its total derivative vanishes,

$$\frac{\mathrm{d}a_s\mu^{2\varepsilon}}{\mathrm{d}\log\mu^2} = \varepsilon\mu^{2\varepsilon} Z_{a_s} a_{s,\mathrm{ren}} + \mu^{2\varepsilon} \frac{\mathrm{d}a_{s,\mathrm{ren}}}{\mathrm{d}\log\mu^2} \left(a_{s,\mathrm{ren}} \frac{\partial Z_{a_s}}{\partial a_{s,\mathrm{ren}}} + Z_{a_s} \right) = 0 . \tag{2.82}$$

The renormalised coupling is finite, so its running carries no poles in the regulator. Substituting the Laurent expansion of Z_{a_s} then yields

$$\begin{aligned} \frac{\mathrm{d}a_{s,\mathrm{ren}}}{\mathrm{d}\log\mu^2} &= -\frac{\varepsilon a_{s,\mathrm{ren}}}{\frac{\partial \log Z_{a_s}}{\partial \log a_{s,\mathrm{ren}}} + 1} \\ &= -\varepsilon a_{s,\mathrm{ren}} + a_{s,\mathrm{ren}}^2 \frac{\partial Z_{a_s}^{(1)}}{\partial a_{s,\mathrm{ren}}} + \mathcal{O}\left(\varepsilon^{-1}\right) \\ &= -\varepsilon a_{s,\mathrm{ren}} + \beta . \end{aligned} \tag{2.83}$$

Finiteness of the left-hand side of Eq. (2.83) forces the poles on the right-hand side to cancel. This running is the D-dimensional beta function, whilst the β on the right is its four-dimensional counterpart, both in a theory with $n_\mathrm{l} + n_\mathrm{h}$ active quark flavours. With the beta function identified, the anomalous dimensions take the form

$$\gamma_{lk} = -\sum_{j\in\mathbb{S}} \left(-\varepsilon a_{s,\mathrm{ren}} + \beta\right) \frac{\partial Z_{lj}}{\partial a_{s,\mathrm{ren}}} \left(Z^{-1}\right)_{jk} . \tag{2.84}$$

The renormalisation constants, anomalous dimensions and beta function each admit a power-series expansion in the renormalised strong coupling. Of these, the first two may, in addition, be expanded in the dimensional regulator. However,we assume that no positive powers of the regulator appear in either expansion, since such terms would amount to finite renormalisations. This assumption is equivalent to working in the modified minimal-subtraction scheme [17, 122]. Because the anomalous dimensions are finite, the scheme reduces their expansion to a pure power series in the coupling. The expansions read

$$Z_{ij} = \sum_{m=0}^{\infty} \sum_{n=1}^{m} Z_{ij}^{(m,n)} \frac{a_{s,\text{ren}}^m}{\varepsilon^n} , \tag{2.85}$$

$$\gamma_{ij} = \sum_{m=1}^{\infty} \gamma_{ij}^{(m-1)} a_{s,\text{ren}}^m , \tag{2.86}$$

$$\beta = -\sum_{m=2}^{\infty} \beta_{m-2} a_{s,\text{ren}}^m . \tag{2.87}$$

For our calculation, we require the Mellin moments of the anomalous dimensions only up to two loops [35, 37, 38, 120, 123]. Likewise, only the two-loop coefficients of the beta function are needed [124–126], although results at higher loop orders are available [127–130].

At zeroth order in the coupling, the operators are finite and do not mix, so no renormalisation is required. Therefore, we may take the Z-factors to be diagonal and normalised such that

$$Z_{ij} = \delta_{ij} + \mathcal{O}(a_{s,\text{ren}}) . \tag{2.88}$$

This normalisation fixes the renormalisation constants entirely through the anomalous dimensions and the beta-function coefficients, allowing a recursive solution order by order in the strong coupling and the dimensional regulator,

$i = j \neq k \quad :$

$$Z_{ij}^{(0,0)} = 1 , \tag{2.89}$$

$$Z_{ij}^{(1,1)} = \gamma_{ij}^{(0)} , \tag{2.90}$$

$$Z_{ij}^{(2,2)} = -\frac{1}{2}\beta_0 \gamma_{ij}^{(0)} + \frac{1}{2} \sum_{m\in\mathbb{S}} \gamma_{im}^{(0)} \gamma_{mj}^{(0)} , \tag{2.91}$$

$$Z_{ij}^{(2,1)} = \frac{1}{2}\gamma_{ij}^{(0)} , \tag{2.92}$$

$$Z_{ij}^{(3,3)} = \frac{1}{3}\beta_0^2 \gamma_{ij}^{(0)} - \frac{1}{2}\beta_0 \sum_{m\in\mathbb{S}} \gamma_{im}^{(0)} \gamma_{mj}^{(0)} + \frac{1}{6} \sum_{m,n\in\mathbb{S}} \gamma_{im}^{(0)} \gamma_{mn}^{(0)} \gamma_{mj}^{(0)} , \tag{2.93}$$

$$Z_{ij}^{(3,2)} = -\frac{1}{3}\beta_1 \gamma_{ij}^{(0)} - \frac{1}{3}\beta_0 \gamma_{ij}^{(1)} + \frac{1}{2} \sum_{m\in\mathbb{S}} \gamma_{im}^{(0)} \gamma_{mj}^{(1)} + \frac{1}{3}\gamma_{ik}^{(1)} \gamma_{kj}^{(0)} - \frac{1}{3}\gamma_{ik}^{(0)} \gamma_{kj}^{(1)} , \tag{2.94}$$

$$Z_{ij}^{(3,1)} = \frac{1}{3}\gamma_{ij}^{(0)} , \tag{2.95}$$

$i = j :$

$$Z_{ij}^{(0,0)} = 0\,, \tag{2.96}$$

$$Z_{ij}^{(1,1)} = \gamma_{ij}^{(0)}\,, \tag{2.97}$$

$$Z_{ij}^{(2,2)} = -\frac{1}{2}\beta_0\gamma_{ij}^{(0)} + \frac{1}{2}\sum_{m\in\mathbb{S}}\gamma_{im}^{(0)}\gamma_{mj}^{(0)}\,, \tag{2.98}$$

$$Z_{ij}^{(2,1)} = \frac{1}{2}\gamma_{ij}^{(0)}\,, \tag{2.99}$$

$$Z_{ij}^{(3,3)} = \frac{1}{3}\beta_0^2\gamma_{ij}^{(0)} - \frac{1}{2}\beta_0\sum_{m\in\mathbb{S}}\gamma_{im}^{(0)}\gamma_{mj}^{(0)} + \frac{1}{6}\sum_{m,n\in\mathbb{S}}\gamma_{im}^{(0)}\gamma_{mn}^{(0)}\gamma_{mj}^{(0)}\,, \tag{2.100}$$

$$Z_{ij}^{(3,2)} = -\frac{1}{3}\beta_1\gamma_{ij}^{(0)} - \frac{1}{3}\beta_0\gamma_{ij}^{(1)} + \frac{1}{3}\sum_{m\in\mathbb{S}}\gamma_{im}^{(1)}\gamma_{mj}^{(0)} + \frac{1}{6}\sum_{m\in\mathbb{S}}\gamma_{im}^{(0)}\gamma_{mj}^{(1)}\,, \tag{2.101}$$

$$Z_{ij}^{(3,1)} = \frac{1}{3}\gamma_{ij}^{(0)}\,. \tag{2.102}$$

To complete the renormalisation of the operator product expansion, the bare operators must be replaced by their renormalised counterparts and, correspondingly, the bare matrix elements by the renormalised ones. In the leading-twist approximation, this yields the renormalised partonic invariants,

$$T_{i,\mathrm{p}}^{\mathrm{ren}}(p,q) = \sum_{N\in\mathbb{N}}\left(\frac{1}{2x_{\mathrm{B}}}\right)^N \sum_{j,k\in\mathbb{S}} C_{i,j}^N(q) Z_{jk} A_{k,\mathrm{p}}^{N,\mathrm{ren}}(p)\,. \tag{2.103}$$

2.2.2 Mass Factorisation

With the formalism now complete, we are ready to set up the calculation. To extract the Mellin moments of the coefficient functions, we employ a derivative operator $\mathcal{P}_N$,

$$\mathcal{P}_N(T_i(p,q)) = (-1)^N \sum_{j\in\mathbb{S}} A_{j,\mathrm{P}}^N(p) C_{i,j}^N(q)\bigg|_{p=0} \equiv T_{i,\mathrm{P}}^N(q)\,, \tag{2.104}$$

that projects onto the N-th Mellin moment of the partonic invariants. This operator is the harmonic projection, whose construction and properties are discussed in Sec. 4.1.

As a derivative operator, the harmonic projection acts on the Mellin moments regardless of whether the states are hadronic or partonic, so the partonic invariants may be used in place of the hadronic ones. Being a derivative with respect to the now partonic momentum, it commutes with the renormalisation of the forward amplitude. The renormalised N-th Mellin moment of the coefficient functions reads

$$T_{i,\mathrm{p}}^{N,\mathrm{ren}}(p,q) = (-1)^N \sum_{j,k\in\mathbb{S}} C_{i,j}^N(q) Z_{jk} A_{k,\mathrm{p}}^{N,\mathrm{ren}}(p)\bigg|_{p=0}\,, \qquad i\in\{\,L,2,3,S\,\}\,. \tag{2.105}$$

Nullifying the partonic momentum affects only the operator matrix element. In a theory with light flavours alone, this matrix element contributes solely at tree level once p has been nullified, since all higher orders in the coupling reduce to scaleless loop integrals, which vanish in dimensional regularisation. Heavy flavours change this; the heavy-quark mass provides a physical scale that gives rise to non-vanishing massive bubble integrals,

$$A_{k,\mathrm{p}}^{N,\mathrm{ren}}(p)\bigg|_{p=0} = \sum_{n=0}^{\infty} a_{s,\mathrm{ren}}^{n} A_{k,\mathrm{p}}^{N,\mathrm{ren},(n)}(p)\bigg|_{p=0}\,, \tag{2.106}$$

Since our aim is to apply the harmonic projection to the forward scattering amplitude directly and thereby extract the coefficient functions, Eq. (2.106) implies that the coefficient functions mix with the operator matrix elements in the perturbative expansion, so that their extraction requires full knowledge of the latter.

To circumvent the mixing, we evaluate the operator matrix elements in a kinematic renormalisation scheme in which the finite contributions from the massive vacuum integrals are absorbed into a finite renormalisation. Within such a scheme

$$\begin{aligned} A_{k,\mathrm{p}}^{N,\mathrm{ren}}(p)\bigg|_{p=0} &= A_{k,\mathrm{p}}^{N,\mathrm{ren},(0)}(p)\bigg|_{p=0} \delta_{k,\mathrm{p}} \\ &\equiv a_k^N \delta_{k,\mathrm{p}}\,. \end{aligned} \tag{2.107}$$

the matrix element is rendered independent of the external momentum, although it retains its dependence on the dimensional regulator and the operator spin. The Kronecker delta in Eq. (2.107) reflects the absence of tree-level contributions to the off-diagonal elements, which therefore vanish once the partonic momentum is set to zero. These operator matrix elements can be drawn with the inserted vertex shown as a labelled circle, as

$A_{\mathrm{q,q}}^{N,\mathrm{ren}}(p)\Big|_{p=0} =$ 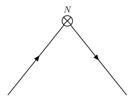 $\Big|_{p=0} +$ 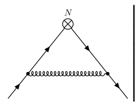 $\Big|_{p=0} + \mathcal{O}(a_s^2)$

$\equiv (a_{\mathrm{q}}^N)^{-1}\,,$ (2.108)

$A_{\mathrm{g,q}}^{N,\mathrm{ren}}(p)\Big|_{p=0} =$ 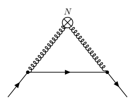 $\Big|_{p=0} + \mathcal{O}(a_s^2)$

$= 0\,,$ (2.109)

$A_{\mathrm{g,g}}^{N,\mathrm{ren}}(p)\Big|_{p=0} =$ 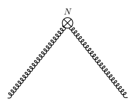 $\Big|_{p=0} +$ 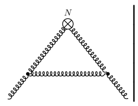 $\Big|_{p=0} + \mathcal{O}(a_s^2)$

$\equiv (a_{\mathrm{g}}^N)^{-1}\,,$ (2.110)

$A_{\mathrm{q,g}}^{N,\mathrm{ren}}(p)\Big|_{p=0} =$ 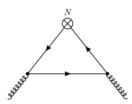 $\Big|_{p=0} + \mathcal{O}(a_s^2)$

$= 0\,.$ (2.111)

From this representation it is clear that nullifying the momentum, that is amputating the external edges carrying partonic momentum, reduces these operator matrix elements to vacuum graphs.

Replacing the operator matrix elements in Eq. (2.105) by their tree-level contribution simplifies the moments of the forward scattering amplitude to

$$T^{N,\text{ren}}_{i,\text{p}}(q) = (-1)^N \sum_{j\in\mathbb{S}} C^N_{i,j}(q) Z_{j\text{p}} A^{N,\text{ren},(0)}_{\text{p},\text{p}}(p)\bigg|_{p=0} , \qquad i \in \{\, L, 2, 3, S \,\} . \tag{2.112}$$

Finally, to extract the finite coefficient functions, we assume that they admit an expansion in both the renormalised coupling and the dimensional regulator,

$$C^N_{i,j}(q) = \sum_{m=0}^{\infty}\sum_{n=0}^{\infty} c^{N,(m,n)}_{i,\text{p}}(q) a^m_{s,\text{ren}} \varepsilon^n , \qquad i \in \{\, L, 2, 3, S \,\} . \tag{2.113}$$

For convenience, we normalise the partonic invariants by their tree-level contribution (see Subsec. 2.2.1), thereby fixing the non-vanishing tree-level coefficients. The partonic invariants likewise admit an expansion in the strong coupling constant,

$$T^{N,\text{ren}}_{i,k}(q) = \sum_{m=0}^{\infty} T^{N,\text{ren},(m)}_{i,k} a^m_{s,\text{ren}} , \qquad i \in \{\, L, 2, 3, S \,\} . \tag{2.114}$$

Together with the renormalisation constants of Eq. (2.85), these expansions relate the Mellin moments of the coefficient functions to those of the partonic invariants, Eq. (2.112). Matching the two sides order by order in the coupling and the regulator then determines the finite coefficient functions. Carrying this out explicitly, and suppressing all functional dependence for brevity, we obtain,

$$T^{N,\text{ren},(0)}_{i,\text{p}} = \delta_{\text{qp}} , \tag{2.115}$$

$$T^{N,\text{ren},(1)}_{i,\text{p}} = \varepsilon^{-1}\gamma^{N,(0)}_{\text{qp}} + c^{N,(1,0)}_{i,\text{p}} + \varepsilon c^{N,(1,1)}_{i,\text{p}} + \varepsilon^2 c^{N,(1,2)}_{i,\text{p}} , \tag{2.116}$$

$$\begin{aligned} T^{N,\text{ren},(2)}_{i,\text{p}} &= \varepsilon^{-2}\left[\frac{1}{2}\sum_{m\in\mathbb{S}}\left(\gamma^{N,(0)}_{\text{q}m} - \beta_0\delta_{\text{q}m}\right)\gamma^{N,(0)}_{m\text{q}}\right] + \varepsilon^{-1}\left[\frac{1}{2}\gamma^{N,(1)}_{\text{qp}} + \sum_{m\in\mathbb{S}}\gamma^{N,(0)}_{m\text{p}} c^{N,(1,0)}_{i,m}\right] \\ &\quad + c^{N,(2,0)}_{i,\text{p}} + \sum_{m\in\mathbb{S}}\gamma^{N,(0)}_{m\text{p}} c^{N,(1,1)}_{i,m} + \varepsilon\left[c^{N,(2,1)}_{i,\text{p}} + \sum_{m\in\mathbb{S}}\gamma^{N,(0)}_{m\text{p}} c^{N,(1,2)}_{i,m}\right] \end{aligned} \tag{2.117}$$

$$\begin{aligned} T^{N,\text{ren},(3)}_{i,\text{p}} &= \varepsilon^{-3}\left[\frac{1}{6}\sum_{m,n\in\mathbb{S}}\gamma^{N,(0)}_{\text{q}m}\gamma^{N,(0)}_{mn}\gamma^{N,(0)}_{n\text{p}} + \frac{1}{3}\sum_{m\in\mathbb{S}}\beta_0^2\gamma^{N,(0)}_{\text{qp}} - \frac{1}{2}\sum_{m\in\mathbb{S}}\beta_0\gamma^{N,(0)}_{\text{q}m}\gamma^{N,(0)}_{m\text{p}}\right] , \\ &\quad + \varepsilon^{-2}\bigg[-\frac{1}{3}\beta_0\gamma^{N,(1)}_{\text{qp}} - \frac{1}{3}\beta_1\gamma^{N,(0)}_{\text{qp}} + \frac{1}{6}\sum_{m\in\mathbb{S}}\gamma^{N,(0)}_{\text{q}m}\gamma^{N,(1)}_{m\text{p}} + \frac{1}{3}\sum_{m\in\mathbb{S}}\gamma^{N,(1)}_{\text{q}m}\gamma^{N,(0)}_{m\text{p}} \\ &\qquad + \frac{1}{2}\sum_{m,n\in\mathbb{S}} c^{N,(1,0)}_{i,m}\left(\gamma^{N,(0)}_{mn} - \beta_0\delta_{mn}\right)\gamma^{N,(0)}_{n\text{p}}\bigg] \\ &\quad + \varepsilon^{-1}\bigg[\frac{1}{3}\gamma^{N,(2)}_{\text{qp}} + \frac{1}{2}\sum_{m\in\mathbb{S}} c^{N,(1,0)}_{i,m}\gamma^{N,(1)}_{m\text{p}} + \sum_{m\in\mathbb{S}} c^{N,(2,0)}_{i,m}\gamma^{N,(0)}_{m\text{p}} + \frac{1}{2}\sum_{m,n\in\mathbb{S}} c^{N,(1,1)}_{i,m} \\ &\qquad \times\left(\gamma^{N,(0)}_{mn} - \beta_0\,\delta_{mn}\right)\gamma^{N,(0)}_{n\text{p}}\bigg] \\ &\quad + c^{N,(3,0)}_{i,\text{p}} + \frac{1}{2}\sum_{m\in\mathbb{S}} c^{N,(1,1)}_{i,m}\gamma^{N,(1)}_{m\text{p}} + \sum_{m\in\mathbb{S}} c^{N,(2,1)}_{i,m}\gamma^{N,(0)}_{m\text{p}} + \frac{1}{2}\sum_{m,n\in\mathbb{S}} c^{N,(2,2)}_{i,m}\bigg(\gamma^{N,(0)}_{mn} \end{aligned}$$

$$- \beta_0 \, \delta_{mn} \Big) \,, \tag{2.118}$$

$$T_{S,\mathrm{p}}^{N,\mathrm{ren},(0)} = \delta_{\mathrm{gp}} \,, \tag{2.119}$$

$$T_{S,\mathrm{p}}^{N,\mathrm{ren},(1)} = \varepsilon^{-1} \gamma_{\mathrm{gp}}^{N,(0)} + c_{S,\mathrm{p}}^{N,(1,0)} + \varepsilon c_{S,\mathrm{p}}^{N,(1,1)} + \varepsilon^2 c_{S,\mathrm{p}}^{N,(1,2)} \,, \tag{2.120}$$

$$\begin{aligned} T_{S,\mathrm{p}}^{N,\mathrm{ren},(2)} &= \varepsilon^{-2} \left[\frac{1}{2} \sum_{m \in \mathbb{S}} \left(\gamma_{\mathrm{g}m}^{N,(0)} - \beta_0 \delta_{\mathrm{g}m} \right) \gamma_{m\mathrm{g}}^{N,(0)} \right] + \varepsilon^{-1} \left[\frac{1}{2} \gamma_{\mathrm{gp}}^{N,(1)} + \sum_{m \in \mathbb{S}} \gamma_{m\mathrm{p}}^{N,(0)} c_{S,m}^{N,(1,0)} \right] \\ &\quad + c_{S,\mathrm{p}}^{N,(2,0)} + \sum_{m \in \mathbb{S}} \gamma_{m\mathrm{p}}^{N,(0)} c_{S,m}^{N,(1,1)} + \varepsilon \left[c_{S,\mathrm{p}}^{N,(2,1)} + \sum_{m \in \mathbb{S}} \gamma_{m\mathrm{p}}^{N,(0)} c_{S,m}^{N,(1,2)} \right] , \end{aligned} \tag{2.121}$$

$$\begin{aligned} T_{S,\mathrm{p}}^{N,\mathrm{ren},(3)} &= \varepsilon^{-3} \left[\frac{1}{6} \sum_{m,n \in \mathbb{S}} \gamma_{\mathrm{g}m}^{N,(0)} \gamma_{mn}^{N,(0)} \gamma_{n\mathrm{p}}^{N,(0)} + \frac{1}{3} \sum_{m \in \mathbb{S}} \beta_0^2 \gamma_{\mathrm{gp}}^{N,(0)} - \frac{1}{2} \sum_{m \in \mathbb{S}} \beta_0 \gamma_{\mathrm{g}m}^{N,(0)} \gamma_{m\mathrm{p}}^{N,(0)} \right] \\ &\quad + \varepsilon^{-2} \bigg[- \frac{1}{3} \beta_0 \gamma_{\mathrm{gp}}^{N,(1)} - \frac{1}{3} \beta_1 \gamma_{\mathrm{gp}}^{N,(0)} + \frac{1}{6} \sum_{m \in \mathbb{S}} \gamma_{\mathrm{g}m}^{N,(0)} \gamma_{m\mathrm{p}}^{N,(1)} + \frac{1}{3} \sum_{m \in \mathbb{S}} \gamma_{\mathrm{g}m}^{N,(1)} \gamma_{m\mathrm{p}}^{N,(0)} \\ &\quad + \frac{1}{2} \sum_{m,n \in \mathbb{S}} c_{S,m}^{N,(1,0)} \left(\gamma_{mn}^{N,(0)} - \beta_0 \delta_{mn} \right) \gamma_{n\mathrm{p}}^{N,(0)} \bigg] \\ &\quad + \varepsilon^{-1} \bigg[\frac{1}{3} \gamma_{\mathrm{gp}}^{N,(2)} + \frac{1}{2} \sum_{m \in \mathbb{S}} c_{S,m}^{N,(1,0)} \gamma_{m\mathrm{p}}^{N,(1)} + \sum_{m \in \mathbb{S}} c_{S,m}^{N,(2,0)} \gamma_{m\mathrm{p}}^{N,(0)} + \frac{1}{2} \sum_{m,n \in \mathbb{S}} c_{S,m}^{N,(1,1)} \\ &\quad \times \Big(\gamma_{mn}^{N,(0)} - \beta_0 \, \delta_{mn} \Big) \gamma_{n\mathrm{p}}^{N,(0)} \bigg] \\ &\quad + c_{S,\mathrm{p}}^{N,(3,0)} + \frac{1}{2} \sum_{m \in \mathbb{S}} c_{S,m}^{N,(1,1)} \gamma_{m\mathrm{p}}^{N,(1)} + \sum_{m \in \mathbb{S}} c_{S,m}^{N,(2,1)} \gamma_{m\mathrm{p}}^{N,(0)} + \frac{1}{2} \sum_{m,n \in \mathbb{S}} c_{S,m}^{N,(2,2)} \Big(\gamma_{mn}^{N,(0)} \\ &\quad - \beta_0 \, \delta_{mn} \Big) \,, \end{aligned} \tag{2.122}$$

$$T_{L,\mathrm{p}}^{N,\mathrm{ren},(0)} = 0 \,, \tag{2.123}$$

$$T_{L,\mathrm{p}}^{N,\mathrm{ren},(1)} = c_{L,\mathrm{p}}^{N,(1,0)} + \varepsilon c_{L,\mathrm{p}}^{N,(1,1)} + \varepsilon^2 c_{L,\mathrm{p}}^{N,(1,2)} \,, \tag{2.124}$$

$$\begin{aligned} T_{L,\mathrm{p}}^{N,\mathrm{ren},(2)} &= \varepsilon^{-1} \left[\sum_{m \in \mathbb{S}} \gamma_{m\mathrm{p}}^{N,(0)} c_{L,m}^{N,(1,0)} \right] + c_{L,\mathrm{p}}^{N,(2,0)} + \sum_{m \in \mathbb{S}} \gamma_{m\mathrm{p}}^{N,(0)} c_{L,m}^{N,(1,1)} + \varepsilon \bigg[c_{L,\mathrm{p}}^{N,(2,1)} + \sum_{m \in \mathbb{S}} \gamma_{m\mathrm{p}}^{N,(0)} \\ &\quad \times c_{L,m}^{N,(1,2)} \bigg] \end{aligned} \tag{2.125}$$

$$\begin{aligned} T_{L,\mathrm{p}}^{N,\mathrm{ren},(3)} &= \varepsilon^{-2} \left[\frac{1}{2} \sum_{m,n \in \mathbb{S}} c_{L,m}^{N,(1,0)} \left(\gamma_{mn}^{N,(0)} - \beta_0 \delta_{mn} \right) \gamma_{n\mathrm{p}}^{N,(0)} \right] \\ &\quad + \varepsilon^{-1} \bigg[\frac{1}{2} \sum_{m \in \mathbb{S}} c_{L,m}^{N,(1,0)} \gamma_{m\mathrm{p}}^{N,(1)} + \sum_{m \in \mathbb{S}} c_{L,m}^{N,(2,0)} \gamma_{m\mathrm{p}}^{N,(0)} + \frac{1}{2} \sum_{m,n \in \mathbb{S}} c_{L,m}^{N,(1,1)} \Big(\gamma_{mn}^{N,(0)} \\ &\quad - \beta_0 \, \delta_{mn} \Big) \gamma_{n\mathrm{p}}^{N,(0)} \bigg] \end{aligned}$$

$$+ c_{L,\mathrm{p}}^{N,(3,0)} + \frac{1}{2}\sum_{m\in\mathbb{S}} c_{L,m}^{N,(1,1)}\gamma_{m\mathrm{p}}^{N,(1)} + \sum_{m\in\mathbb{S}} c_{L,m}^{N,(2,1)}\gamma_{m\mathrm{p}}^{N,(0)} + \frac{1}{2}\sum_{m,n\in\mathbb{S}} c_{L,m}^{N,(2,2)}\Big(\gamma_{mn}^{N,(0)} - \beta_0\,\delta_{mn}\Big)\,. \tag{2.126}$$

Computing the partonic invariants for both the vector- and scalar-current cases makes it possible to extract all anomalous dimensions and coefficient functions at once, and in principle the beta-function coefficients too, though this route is highly inefficient. In the present setup, these quantities are therefore not inputs but results, computed here as a consistency check on the calculation.

2.2.3 Renormalisation Constants

The renormalisation of the forward scattering amplitude has been kept brief so far. Extracting the coefficient functions, however, requires computing the amplitude directly from Feynman graphs, which themselves require renormalisation. In what follows, we adopt the minimal-subtraction scheme and list for completeness all constants needed to renormalise to NNLO. For notational convenience, we define the renormalisation constants as follows:

$$Z_k = 1 + \sum_{n=1}^{\infty} Z_k^{(n)}\big(a_{s,\mathrm{ren}}^{(n_\mathrm{f})}\big)^n\,, \tag{2.127}$$

where $a_{s,\mathrm{ren}}^{(n_\mathrm{f})}$ denotes the renormalised strong coupling in a theory with $n_\mathrm{f} = n_\mathrm{l} + n_\mathrm{h}$ active flavours. The renormalisation is implemented multiplicatively,

$$a_s = Z_a a_{s,\mathrm{ren}}^{(n_\mathrm{f})}\,, \tag{2.128}$$

with renormalisation constant,

$$Z_a^{(1)} = \varepsilon^{-1}\Big[-\frac{11}{3}C_A + \frac{4}{3}T_F n_\mathrm{f}\Big]\,, \tag{2.129}$$

$$Z_a^{(2)} = \varepsilon^{-2}\Big[\frac{121}{9}C_A^2 + \frac{16}{9}T_F^2 n_\mathrm{f} - \frac{88}{9}C_A T_F n_\mathrm{f}^2\Big] + \varepsilon^{-1}\Big[\frac{10}{3}C_A T_F n_\mathrm{f} - \frac{17}{3}C_A^2 + 2C_F T_F n_\mathrm{f}\Big]\,. \tag{2.130}$$

However, since the mass factorisation, Eqs. (2.115) to (2.126), was performed with only n_l active light flavours, the n_h heavy flavours must be decoupled through a decoupling relation [114, 131], shown here for conciseness only for $\mu^2 = m^2$,

$$a_{s,\mathrm{ren}}^{(n_\mathrm{f})} = a_{s,\mathrm{ren}}\Big\{1 + a_{s,\mathrm{ren}} T_F n_\mathrm{h}\Big[\frac{2}{3}\zeta_2\varepsilon - \frac{4}{9}\zeta_3\varepsilon^2 + \mathcal{O}(\varepsilon^3)\Big] + a_{s,\mathrm{ren}}^2\Big[-\frac{32}{9}C_A T_F n_\mathrm{h} + 15 C_F T_F n_\mathrm{h} + \varepsilon\Big(C_A T_F n_\mathrm{h}\Big(\frac{10}{3}\zeta_2 + \frac{172}{27}\Big) + C_F T_F n_\mathrm{h}\Big(2\zeta_2 + \frac{31}{2}\Big)\Big) + \mathcal{O}(\varepsilon^2)\Big] + \mathcal{O}(a_{s,\mathrm{ren}}^3)\Big\}\,. \tag{2.131}$$

For the field renormalisation, we note that the vector-boson and scalar wave functions require no renormalisation, since QCD corrections to their propagators appear only at NLO in the respective couplings and are therefore neglected at LO,

$$Z_{\mathrm{v}} = 1 + \mathcal{O}\big(g_{\mathrm{v}}^2, g_{\mathrm{v}} g_{\mathrm{a}}, g_{\mathrm{a}}^2\big)\,, \tag{2.132}$$

$$Z_{\mathrm{a}} = 1 + \mathcal{O}\big(g_{\mathrm{v}}^2, g_{\mathrm{v}} g_{\mathrm{a}}, g_{\mathrm{a}}^2\big)\,, \tag{2.133}$$

$$Z_{\mathrm{s}} = 1 + \mathcal{O}\big(g_{\mathrm{s}}^2\big)\,. \tag{2.134}$$

In contrast, the gluon and light-quark propagators receive QCD corrections from heavy-quark loops, at one-loop level for gluons and at two-loop level for light quarks, necessitating their wave-function renormalisation [46, 132, 133],

$$Z_2^{(1)} = 0 \tag{2.135}$$

$$Z_2^{(2)} = C_F T_F n_{\mathrm{h}} \left[\varepsilon^{-1} - \frac{5}{6} + \varepsilon\left(\frac{89}{36} + \zeta_2\right) + \mathcal{O}(\varepsilon^2)\right] \tag{2.136}$$

$$\begin{aligned}
Z_2^{(3)} = \varepsilon^{-2}&\left[C_A C_F T_F n_{\mathrm{h}}\left(-\frac{56}{9}\right) + C_F^2 T_F\left(\frac{2}{3}\right) n_{\mathrm{h}} + C_F T_F^2 n_{\mathrm{h}}^2\left(\frac{8}{9}\right) + C_F T_F^2 n_{\mathrm{h}} n_{\mathrm{l}}\left(\frac{16}{9}\right)\right] \\
&+ \varepsilon^{-1}\left[C_A C_F T_F n_{\mathrm{h}}\left(\frac{1}{2}\zeta_2 + \frac{392}{27}\right) + C_F^2 T_F n_{\mathrm{h}}\Big(-1\Big) + C_F T_F^2 n_{\mathrm{h}}^2\left(-\frac{20}{27}\right)\right. \\
&\qquad \left. + C_F T_F^2 n_{\mathrm{h}} n_{\mathrm{l}}\left(-\frac{40}{27}\right)\right] \\
&+ \left[C_A C_F T_F n_{\mathrm{h}}\left(-\frac{17}{3}\zeta_2 - \frac{17}{3}\zeta_3 - \frac{2408}{81}\right) + C_F^2 T_F n_{\mathrm{h}}\left(\zeta_2 + 8\zeta_3 + \frac{443}{18}\right)\right. \\
&\qquad \left. + C_F T_F^2 n_{\mathrm{h}} n_{\mathrm{l}}\left(\frac{4}{3}\zeta_2 - \frac{140}{81}\right) + C_F T_F^2 n_{\mathrm{h}}^2\left(-\frac{70}{81}\right)\right] + \mathcal{O}(\varepsilon)
\end{aligned} \tag{2.137}$$

$$Z_3^{(1)} = T_F n_{\mathrm{h}}\left[-\frac{4}{3}\varepsilon^{-1} - \frac{2}{3}\zeta_2\varepsilon + \frac{4}{9}\zeta_3\varepsilon^2 + \mathcal{O}\big(\varepsilon^3\big)\right] \tag{2.138}$$

$$\begin{aligned}
Z_3^{(2)} = \varepsilon^{-2}&\left[C_A T_F n_{\mathrm{h}}\left(\frac{35}{9}\right) + T_F^2 n_{\mathrm{h}} n_{\mathrm{l}}\left(-\frac{16}{9}\right)\right] \\
&+ \varepsilon^{-1}\left[C_A T_F n_{\mathrm{h}}\left(-\frac{5}{2}\right) + C_F T_F n_{\mathrm{h}}\Big(-2\Big)\right] \\
&+ \left[C_A T_F n_{\mathrm{h}}\left(\frac{13}{9}\zeta_2 + \frac{13}{12}\right) + C_F T_F n_{\mathrm{h}}\Big(-15\Big) + T_F^2 n_{\mathrm{h}}^2\left(\frac{8}{9}\zeta_2\right)\right. \\
&\qquad \left. + C_F T_F n_{\mathrm{h}} n_{\mathrm{l}}\left(-\frac{8}{9}\zeta_2\right)\right] \\
&+ \varepsilon\left[C_A T_F n_{\mathrm{h}}\left(-\frac{5}{2}\zeta_2 - \frac{26}{27}\zeta_3 - \frac{169}{72}\right) + C_F T_F n_{\mathrm{h}}\left(-2\zeta_2 - \frac{31}{2}\right)\right. \\
&\qquad \left. + T_F^2 n_{\mathrm{h}} n_{\mathrm{l}}\left(\frac{16}{27}\zeta_3\right) + + T_F^2 n_{\mathrm{h}}^2\left(-\frac{16}{27}\zeta_3\right)\right] + \mathcal{O}\big(\varepsilon^2\big)\,.
\end{aligned} \tag{2.139}$$

It should be noted that the external ghost propagators would receive corrections at two loops. Since the leading ghost contributions for the VV and AA currents are already two-loop, however, these corrections do not enter at three loops, which is the aim of this work. Were the scalar currents to be computed at three loops, the ghost wave-function renormalisation would have to be accounted for, as there are indeed contributions.

Because internal quarks may be massive, we renormalise their mass m through the insertion of counterterms [134],

$$Z_m^{(1)} = C_F\Big[-3\varepsilon^{-1} - 4 - \varepsilon\Big(8 + \frac{3}{2}\zeta_2\Big) + \varepsilon^2\Big(-2\zeta_2 + \zeta_3 - 16\Big) + \mathcal{O}\big(\varepsilon^3\big)\Big] \tag{2.140}$$

$$\begin{aligned} Z_m^{(2)} = \varepsilon^{-2}&\Big[C_F C_A\Big(\frac{11}{2}\Big) + C_F^2\Big(\frac{9}{2}\Big) + C_F T_F n_\mathrm{f}\Big(-2\Big)\Big] \\ &+ \varepsilon^{-1}\Big[C_A C_F\Big(-\frac{97}{12}\Big) + C_F^2\Big(\frac{45}{4}\Big) + C_F T_F n_\mathrm{f}\Big(\frac{5}{3}\Big)\Big] \\ &+ \Big[C_A C_F\Big(8\zeta_2 + 6\zeta_3 - 24\zeta_2\log(2) - \frac{1111}{24}\Big) + C_F^2\Big(-\frac{51}{2}\zeta_2 - 12\zeta_3 \\ &\quad + \frac{199}{8}\Big) + C_F T_F n_\mathrm{h}\Big(\frac{143}{6} - 16\zeta_2\Big) + C_F T_F n_\mathrm{l}\Big(8\zeta_2 + \frac{71}{6}\Big)\Big)\Big] \\ &+ \varepsilon\Big[C_A C_F\Big(96\mathrm{Li}_4\Big(\frac{1}{2}\Big) + \frac{271}{12}\zeta_2 + 52\zeta_3 - 126\zeta_4 + 48\zeta_2\log^2(2) - 144\zeta_2\log(2) \\ &\quad - \frac{8581}{48} + 4\log^4(2)\Big) + C_F^2\Big(-192\mathrm{Li}_4\Big(\frac{1}{2}\Big) - \frac{615}{4}\zeta_2 - 135\zeta_3 + 252\zeta_4 \\ &\quad - 96\zeta_2\log^2(2) + 288\zeta_2\log(2) + \frac{677}{16} - 8\log^4(2)\Big) + C_F T_F n_\mathrm{h}\Big(-\frac{227}{3}\zeta_2 \\ &\quad - 56\zeta_3 + 96\zeta_2\log(2) + \frac{1133}{12}\Big) + C_F T_F n_\mathrm{l})\Big(\frac{97}{3}\zeta_2 + 16\zeta_3 + \frac{581}{12}\Big)\Big] \\ &\quad + \mathcal{O}\big(\varepsilon^2\big)\,. \end{aligned} \tag{2.141}$$

This concludes the renormalisation of the vector currents. For the axial-vector currents, the amplitudes contain γ_5, which requires special treatment in dimensional regularisation. Adopting the Larin scheme [135], we handle this through the substitution

$$\gamma_\mu\gamma_5 = \frac{i}{6}\varepsilon_{\mu\rho\sigma\tau}\gamma^\rho\gamma^\sigma\gamma^\tau\,. \tag{2.142}$$

Employing the Larin scheme proves useful only for the antisymmetric AV and symmetric AA contributions to the Mellin moments of the coefficient functions, where an even number of Levi-Civita tensors appears. Such even products can be expressed entirely in terms of metric tensors,

$$\varepsilon^{\alpha_1\alpha_2\alpha_3\alpha_4}\varepsilon_{\beta_1\beta_2\beta_3\beta_4} = \begin{vmatrix} \delta^{\alpha_1}{}_{\beta_1} & \delta^{\alpha_1}{}_{\beta_2} & \delta^{\alpha_1}{}_{\beta_3} & \delta^{\alpha_1}{}_{\beta_4} \\ \delta^{\alpha_2}{}_{\beta_1} & \delta^{\alpha_2}{}_{\beta_2} & \delta^{\alpha_2}{}_{\beta_3} & \delta^{\alpha_2}{}_{\beta_4} \\ \delta^{\alpha_3}{}_{\beta_1} & \delta^{\alpha_3}{}_{\beta_2} & \delta^{\alpha_3}{}_{\beta_3} & \delta^{\alpha_3}{}_{\beta_4} \\ \delta^{\alpha_4}{}_{\beta_1} & \delta^{\alpha_4}{}_{\beta_2} & \delta^{\alpha_4}{}_{\beta_3} & \delta^{\alpha_4}{}_{\beta_4} \end{vmatrix}\,. \tag{2.143}$$

Conversely, no such reduction is possible when an odd number of Levi-Civita tensors is present. All such amplitudes vanish, however, owing to the forward kinematics.

The naive use of the Larin scheme in dimensional regularisation violates the axial Ward identity. To restore it, we introduce additional renormalisation constants [136]

$$Z_A^{(1)} = 0\,, \tag{2.144}$$

$$Z_A^{(2)} = \varepsilon^{-1}\left[\frac{22}{3}C_AC_F - \frac{8}{3}C_FT_Fn_\mathrm{f}\right], \tag{2.145}$$

$$\begin{aligned} Z_A^{(3)} &= \varepsilon^{-2}\left[\frac{3578}{81}C_A^2C_F - \frac{308}{9}C_AC_F^2 - \frac{1664}{81}C_AC_FT_Fn_\mathrm{f} + \frac{64}{9}C_F^2T_Fn_\mathrm{f} + \frac{32}{81}C_FT_F^2n_\mathrm{f}^2\right] \\ &\quad + \varepsilon^{-1}\left[-\frac{484}{27}C_A^2C_F + \frac{352}{27}C_AC_FT_Fn_\mathrm{f} + \frac{352}{27}C_FT_F^2n_\mathrm{f}^2\right], \end{aligned} \tag{2.146}$$

$$Z_5^{(1)} = 4C_F\,, \tag{2.147}$$

$$Z_5^{(2)} = \frac{107}{9}C_AC_F - 22C_F - \frac{4}{9}C_FT_Fn_\mathrm{f}\,, \tag{2.148}$$

$$\begin{aligned} Z_5^{(3)} &= C_A^2C_F\left(\frac{2147}{27} - 56\zeta_3\right) + C_AC_F^2\left(-\frac{5834}{27} - 160\zeta_3\right) + C_F^3\left(\frac{370}{3} - 96\zeta_3\right) \\ &\quad + C_AC_FT_Fn_\mathrm{f}\left(-\frac{712}{81} - \frac{64}{3}\zeta_3\right) + C_F^2T_Fn_\mathrm{f}\left(-\frac{124}{27} - \frac{64}{3}\zeta_3\right) \\ &\quad + n_\mathrm{f}^2\left(-\frac{208}{81}C_FT_F^2\right), \end{aligned} \tag{2.149}$$

the latter being a finite renormalisation constant relating the renormalisation of vector and axial-vector currents through the R-operation,

$$(R\gamma^\mu)\gamma_5 = Z_5R(\gamma_5\gamma^\mu)\,. \tag{2.150}$$

The renormalisation of the scalar current is more intricate, as it requires a Yukawa-type coupling between the scalar source and the quarks [114], with the quark mass playing the role of the coupling constant. No such renormalisation is therefore needed in the absence of heavy quarks, leaving

$$Z_\mathrm{gs} = 1 + \beta\,, \tag{2.151}$$

$$Z_\mathrm{qs} = Z_m\,, \tag{2.152}$$

with coefficients of the beta function, Eq. (2.87),

$$\beta_0 = \frac{11}{3}C_A - \frac{4}{3}T_Fn_\mathrm{f}\,, \tag{2.153}$$

$$\beta_1 = \frac{34}{3}C_A^2 - \frac{20}{3}C_AT_Fn_\mathrm{f} - 4C_FT_Fn_\mathrm{f}\,. \tag{2.154}$$

2.2.4 Normalisation Constants

To conclude this section, we discuss the various normalisations in place. The constants arising from the tree-level operator matrix elements, Eq. (2.107), may be computed explicitly. At LO in the strong coupling, the singlet operators, Eqs. (2.38) and (2.39), read

$$O_\mathrm{q}{}^{\{\mu_1\ldots\mu_N\}} = i^{N-1}\bar{\psi}_1\gamma^{\{\mu_1}\partial^{\mu_2}\cdots\partial^{\mu_N\}}\psi_1 + \mathcal{O}(g_s)\,, \tag{2.155}$$

$$O_\mathrm{g}{}^{\{\mu_1\ldots\mu_N\}} = i^{N-2}G^{\{\mu_1\lambda}\partial^{\mu_2}\cdots\partial^{\mu_{N-1}}G^{\mu_N}{}_{\lambda\}} + \mathcal{O}(g_s)\,, \tag{2.156}$$

with the gluon field strength tensor

$$G^{\mu\nu} = \partial^\mu A^\nu - \partial^\nu A^\mu + \mathcal{O}(g_s)\,. \tag{2.157}$$

Contracting both sides of Eqs. (2.155) and (2.156) with a light-like vector Δ^μ satisfying $\Delta^2 = 0$ removes all trace terms,

$$\Delta_{\mu_1} \dots \Delta_{\mu_N} \langle k| \, O_k^{\{\mu_1 \dots \mu_N\}} \, |k\rangle = (\Delta \cdot p)^N \, A^N_{k,k}(p)\,, \qquad k \in \mathbb{S}\,. \tag{2.158}$$

Take first the gluonic operator matrix element. The two field strengths are Wick-contracted against the external gluon states, and their Lorentz indices are traced over. Each external field is replaced by a plane wave,

$$A^\mu(z) \sim e^{-iz\cdot p}\,, \tag{2.159}$$

$$A^\mu(z) \sim e^{+iz\cdot p}\,, \tag{2.160}$$

for the annihilated and created field respectively, so that each field-strength contraction gives

$$\Delta_\rho G^{\rho\lambda} \longrightarrow \pm i\big[(\Delta \cdot p)\, g^{\mu\lambda} - p^\mu \Delta^\lambda\big]\,, \tag{2.161}$$

where the upper or lower sign corresponds to the created or annihilated gluon, and μ is the external gluon index, traced over in the matrix element. Inserting both contractions then gives

$$\begin{aligned}\Delta_{\mu_1} \dots \Delta_{\mu_N} \langle \mathrm{g}| \, O_\mathrm{g}^{\{\mu_1 \dots \mu_N\}} \, |\mathrm{g}\rangle &= (\Delta \cdot p)^{N-2} \left[(\Delta \cdot p)\, g^{\mu\lambda} - p^\mu \Delta^\lambda\right] \\ &\quad \times \left[(\Delta \cdot p)\, g_{\mu\lambda} - p_\mu \Delta_\lambda\right] \\ &= (\Delta \cdot p)^N \,(D-2)\,.\end{aligned} \tag{2.162}$$

Comparing Eqs. (2.158) and (2.162), the operator matrix element can be read off directly. The quark operator matrix element follows in the same way. Each external field is replaced by a plane wave,

$$\psi(z) \sim e^{-iz\cdot p}\,, \tag{2.163}$$

$$\psi(z) \sim e^{+iz\cdot p}\,, \tag{2.164}$$

for the annihilated and created quark respectively, so that tracing over the external Dirac indices gives

$$\begin{aligned}\Delta_{\mu_1} \dots \Delta_{\mu_N} \langle \mathrm{q}| \, O_\mathrm{q}^{\{\mu_1 \dots \mu_N\}} \, |\mathrm{q}\rangle &= (\Delta{\cdot}p)^{N-1}\, \mathrm{Tr}\Big[\not{\Delta}\, \not{p}\Big] \\ &= 4\,(\Delta{\cdot}p)^N\,.\end{aligned} \tag{2.165}$$

As for the gluon, comparison of Eqs. (2.158) and (2.165) allows the operator matrix element to be extracted. The normalisation constants therefore read,

$$a^N_\mathrm{q} = \frac{1}{4}\,, \tag{2.166}$$

$$a^N_\mathrm{g} = \frac{1}{D-2}\,. \tag{2.167}$$

A second set of constants is fixed by normalising each partonic invariant to its tree-level contribution. Fixing them requires four independent processes, namely VV, AV, AA and SS (see Fig. 2.2). For the quark-initiated processes, we find

$$\begin{aligned} T_{i,\mathrm{q}}^{\mathrm{ren}} &= N_{\mathrm{b}_1\mathrm{b}_2}(p\cdot q)\left[\frac{1}{(p-q)^2} - (-1)^{1+\delta_{\mathrm{b}_1\mathrm{b}_2}}\frac{1}{(p+q)^2}\right] + \mathcal{O}(a_{s,\mathrm{ren}}) \\ &= N_{\mathrm{b}_1\mathrm{b}_2}\frac{2(p\cdot q)}{q^2}\sum_{N=0}^{\infty}\left(\frac{-2p\cdot q}{q^2}\right)^{2N+\delta_{\mathrm{b}_1\mathrm{b}_2}} + \mathcal{O}(a_{s,\mathrm{ren}}) \\ &= -N_{\mathrm{b}_1\mathrm{b}_2}\sum_{N=0}^{\infty} x_{\mathrm{B}}^{2N+\delta_{\mathrm{b}_1\mathrm{b}_2}+1} + \mathcal{O}(a_{s,\mathrm{ren}})\,, \qquad \mathrm{b}_1\mathrm{b}_2 \in \{\,\mathrm{v},\mathrm{a}\,\}\,, \end{aligned} \tag{2.168}$$

where $N_{\mathrm{b}_1\mathrm{b}_2}$ denotes the numerical prefactor arising from the Dirac traces. The N-th Mellin moment is therefore given by

$$T_{i,\mathrm{q}}^{N,\mathrm{ren},(0)} = -2^N N_{\mathrm{b}_1\mathrm{b}_2}\,. \tag{2.169}$$

As anticipated from Eqs. (2.63) and (2.70), the AV term contributes only at odd moments, whereas the VV and AA terms survive only at even moments. For the gluon-initiated processes, an analogous calculation yields

$$\begin{aligned} T_{S,\mathrm{g}}^{\mathrm{ren}} &= N_{\mathrm{ss}}(p\cdot q)^2\left[\frac{1}{(p-q)^2} + \frac{1}{(p+q)^2}\right] + \mathcal{O}(a_{s,\mathrm{ren}}) \\ &= N_{\mathrm{ss}}\frac{q^2}{2}\sum_{N=0}^{\infty} x_{\mathrm{B}}^{2N+2} + \mathcal{O}(a_{s,\mathrm{ren}})\,, \end{aligned} \tag{2.170}$$

where, in accordance with crossing symmetry, only even moments contribute. The corresponding moment then reads

$$T_{S,\mathrm{g}}^{N,\mathrm{ren},(0)} = 2^{N-1}q^2 N_{\mathrm{ss}}\,. \tag{2.171}$$

Imposing the tree-level normalisation (see also Ref. [137]) therefore amounts to multiplying each Mellin moment by

$$\hat{N}_{\mathrm{vv}} = \frac{1}{2^{N+2}}\,, \tag{2.172}$$

$$\hat{N}_{\mathrm{av}} = \frac{1}{2^{N+2}}\,, \tag{2.173}$$

$$\hat{N}_{\mathrm{aa}} = \frac{3}{2^{N+1}(D-6)(D-3)(D-1)}\,, \tag{2.174}$$

$$\hat{N}_{\mathrm{ss}} = \frac{1}{2^{N-1}(D-2)q^2}\,, \tag{2.175}$$

where all traces were evaluated with FORM [138, 139]. Whilst each partonic invariant may in principle be normalised independently, any calculation of a physical observable involving a sum of several currents must employ a consistent normalisation throughout, since it combines vector and axial-vector contributions.

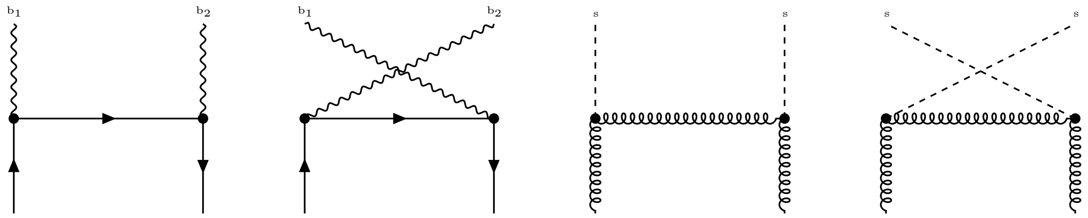

Figure 2.2: Tree-level contributions to the partonic forward scattering amplitude for the quark-initiated and gluon-initiated processes.

2.3 Flavours

2.3.1 Flavour Factors

So far we have ignored the physical processes to which the external bosons correspond, in particular the vector and axial-vector currents. These split into two types, neutral currents (NC) and charged currents (CC), the former preserving flavour along the quark lines and the latter changing it. Each type generates a different combination of electroweak couplings, which we refer to as a flavour structure.

To classify these flavour structures, we proceed graphically, considering processes with two external vector bosons, at most two closed quark loops and at most one open light-quark line. Neutral currents preserve flavour and give *mass-preserving* vertices, whereas charged currents permit up-to-down and light-to-heavy transitions, giving *mass-changing* vertices (as shown in Fig. 2.3). Since QCD also preserves flavour, its vertices are mass-preserving too.

By systematically constructing every graph in which each of the two external bosons, whether vector or axial-vector, attaches to quark lines that may be light or heavy, we arrive at fifteen distinct flavour structures for the neutral current, collected in Fig. 2.4. The construction for the charged current is analogous but gives rise, as shown in Fig. 2.4, to five additional structures with mixed light-heavy quark lines. Importantly, since QCD is flavour-preserving, an even number of mass-changing bosons must attach to each fermion loop. For our two-boson setup this means that the initial- and final-state bosons must attach to the same line.

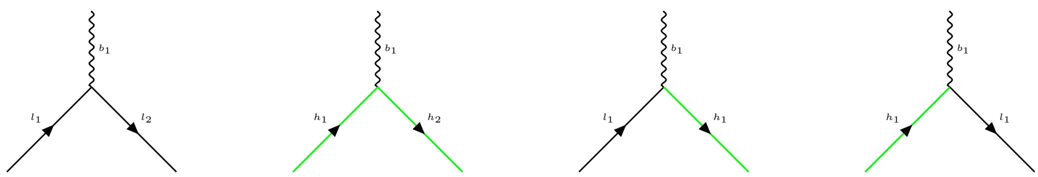

Figure 2.3: Mass-preserving and mass-changing quark-boson vertices. Light quarks l_i are drawn in black, heavy quarks h_i in green, and bosons are labelled b_i.

2.3.2 Notation

To place the preceding analysis on a precise footing, we examine the flavour structures admitted by the global flavour symmetry groups, beginning with the flavour-diagonal case. Specifically, we consider n_l light and n_h heavy quark flavours, associated with the symmetry groups $\mathrm{SU}(n_\mathrm{l})$ and $\mathrm{SU}(n_\mathrm{h})$, with respective generators λ_l^a and λ_h^a. Both light and heavy flavours are then combined into a single flavour vector defined on an enlarged flavour space,

$$\mathbf{f} = \big(\mathrm{l}_1, \ldots, \mathrm{l}_{n_\mathrm{l}}, \mathrm{h}_1, \ldots, \mathrm{h}_{n_\mathrm{h}}\big) \,. \tag{2.176}$$

In this representation, the flavour-group generators become direct sums, padded with zero blocks so that they act on the whole enlarged flavour space,

$$\hat{\lambda}_\mathrm{l}^a = \lambda_\mathrm{l}^a \oplus 0_{n_\mathrm{h}\times n_\mathrm{h}} \,, \tag{2.177}$$

$$\hat{\lambda}_\mathrm{h}^a = 0_{n_\mathrm{l}\times n_\mathrm{l}} \oplus \lambda_\mathrm{h}^a \,. \tag{2.178}$$

Throughout, a circumflex marks an embedding into the enlarged space. The charge matrices $Q_{i,\mathrm{l}}$ and $Q_{i,\mathrm{h}}$ encode the couplings of the vector bosons to the light and heavy quarks. For neutral currents they are diagonal, as required by flavour conservation. Each charge matrix is embedded into the enlarged space as

$$\hat{Q}_{i,\mathrm{l}} = Q_{i,\mathrm{l}} \oplus 0_{n_\mathrm{h}\times n_\mathrm{h}} \,, \qquad i \in \{\,\mathrm{a}, \mathrm{v}\,\} \;, \tag{2.179}$$

$$\hat{Q}_{i,\mathrm{h}} = 0_{n_\mathrm{l}\times n_\mathrm{l}} \oplus Q_{i,\mathrm{h}} \,, \qquad i \in \{\,\mathrm{a}, \mathrm{v}\,\} \;. \tag{2.180}$$

The total charge matrices then follow by summing the embedded light- and heavy-flavour contributions, Eqs. (2.179) and (2.180),

$$Q_i = \hat{Q}_{i,\mathrm{l}} + \hat{Q}_{i,\mathrm{h}} \,, \qquad i \in \{\,\mathrm{a}, \mathrm{v}\,\} \;. \tag{2.181}$$

For later convenience, we likewise introduce the embedded light- and heavy-flavour unit matrices,

$$\hat{1}_\mathrm{l} = 1_{n_\mathrm{l}\times n_\mathrm{l}} \oplus 0_{n_\mathrm{h}\times n_\mathrm{h}} \,, \tag{2.182}$$

$$\hat{1}_\mathrm{h} = 0_{n_\mathrm{l}\times n_\mathrm{l}} \oplus 1_{n_\mathrm{h}\times n_\mathrm{h}} \,. \tag{2.183}$$

In direct analogy with the total charge matrix, Eq. (2.181), we define the total unit matrix as the sum of the two embedded unit matrices, Eqs. (2.182) and (2.183),

$$1_\mathrm{f} = \hat{1}_\mathrm{l} + \hat{1}_\mathrm{h} \,. \tag{2.184}$$

With this notation in place, we may analyse the flavour structures that arise in processes with two external vector bosons mediated by neutral currents. To identify every such structure, we systematically examine the combinatorics of multiplying charge and unit matrices and taking the corresponding traces. For this purpose, we introduce a shorthand for traces over quark lines carrying either a vector or an axial-vector boson. Overlined symbols denote external quark lines and unbarred symbols internal ones,

$$f_B \equiv \mathrm{tr}\left(\prod_{i\in B} Q_{i,f}\right) \,, \qquad B \subseteq \{\,\mathrm{v}, \mathrm{a}\,\} \,, \qquad f \in \{\,\mathrm{l}, \mathrm{h}\,\} \,, \tag{2.185}$$

$$\bar{f}^a_{\bar{B}} \equiv \frac{1}{T_{R,f}} \operatorname{tr}\left(\prod_{i\in\bar{B}} Q_{i,f}\lambda^a_f\right)\hat{\lambda}^a_f\,, \qquad \bar{B}\subseteq\{\,\mathrm{v},\mathrm{a}\,\}\,, \qquad f\in\{\,\mathrm{l},\mathrm{h}\,\}\,, \tag{2.186}$$

$$\bar{f}_{\bar{B}} \equiv \frac{1}{n_f} \operatorname{tr}\left(\prod_{i\in\bar{B}} Q_{i,f}\right)\hat{1}_f\,, \qquad \bar{B}\subseteq\{\,\mathrm{v},\mathrm{a}\,\}\,, \qquad f\in\{\,\mathrm{l},\mathrm{h}\,\}\,, \tag{2.187}$$

where $T_{R,f}$ denotes the trace normalisation of the $\mathrm{SU}(n_f)$ generators. The subscript records which bosons are attached to the quark line. Because the charge matrices are diagonal, and therefore commute, each trace is insensitive to the order in which these bosons appear, so the subscript may be regarded as an unordered set. To collect several such traces, we introduce a list notation,

$$\langle x_1,\ldots,x_n\rangle^{\mathrm{g}} \equiv \prod_{i=1}^{n} x_i\,, \tag{2.188}$$

$$\langle x_1,\ldots,x_n\rangle^{\mathrm{q}} \equiv 1_{\mathrm{f}}\prod_{i=1}^{n} x_i\,, \tag{2.189}$$

where both variants differ only by the total unit matrix (2.184) inserted in the second. Their entries may be placed in any order because, for the single open quark line of interest here, the product is fully commutative.

For products of matrices that remain untraced, we use that any complex $n_\mathrm{f}\times n_\mathrm{f}$ matrix can be expanded in the generators of $\mathrm{SU}(n_\mathrm{f})$, an expansion that carries over directly to matrices embedded in the enlarged space,

$$\begin{aligned}
\prod_{i\in B}\hat{Q}_{i,f} &= \frac{1}{n_f}\operatorname{tr}\left(\prod_{i\in B}\hat{Q}_{i,f}\right)\hat{1}_f + \frac{1}{T_{R,f}}\sum_a \operatorname{tr}\left(\prod_{i\in B}\hat{Q}_{i,f}\hat{\lambda}^a_f\right)\hat{\lambda}^a_f \\
&= \frac{1}{n_f}\operatorname{tr}\left(\prod_{i\in B} Q_{i,f}\right)\hat{1}_f + \frac{1}{T_{R,f}}\sum_a \operatorname{tr}\left(\prod_{i\in B} Q_{i,f}\lambda^a_f\right)\hat{\lambda}^a_f \\
&= \bar{f}_{\bar{B}} + \bar{f}^a_{\bar{B}}\,, \qquad \bar{B}\subseteq\{\,\mathrm{v},\mathrm{a}\,\}\,, \qquad f\in\{\,\mathrm{l},\mathrm{h}\,\}\,.
\end{aligned} \tag{2.190}$$

2.3.3 Neutral Current

To analyse the admissible flavour factors, we begin with the neutral current, whose vertices are mass-preserving. Here the simplest factors are flavour factors composed entirely of traces, free of any accompanying matrices. The first of these is the trace of a product of two quark charge matrices, written in the list notation of Eq. (2.188),

$$\begin{aligned}
\langle \mathrm{f}_{\{\,i,j\,\}}\rangle^{\mathrm{g}} &\equiv \operatorname{tr}(Q_iQ_j) \\
&= \langle \mathrm{l}_{\{\,i,j\,\}}\rangle^{\mathrm{g}} + \langle \mathrm{h}_{\{\,i,j\,\}}\rangle^{\mathrm{g}}\,.
\end{aligned} \tag{2.191}$$

In deriving this, we have used that the charge matrices are diagonal by assumption and split into light and heavy blocks as in Eq. (2.181). Since diagonal matrices commute, this flavour factor is symmetric in i and j. It corresponds to Figs. 2.4.1 and 2.4.2, in which both vector bosons attach to the same closed quark line.

The next factor arises from the product of traces of individual quark charge matrices,

$$\begin{aligned}\langle \mathrm{f}_{\{i\}}\mathrm{f}_{\{j\}}\rangle^{\mathrm{g}} &\equiv \mathrm{tr}(Q_i)\,\mathrm{tr}(Q_j) \\ &= \langle \mathrm{l}_{\{i\}}\mathrm{l}_{\{j\}}\rangle^{\mathrm{g}} + \langle \mathrm{l}_{\{i\}}\mathrm{h}_{\{j\}}\rangle^{\mathrm{g}} + \langle \mathrm{h}_{\{i\}}\mathrm{l}_{\{j\}}\rangle^{\mathrm{g}} + \langle \mathrm{h}_{\{i\}}\mathrm{h}_{\{j\}}\rangle^{\mathrm{g}} .\end{aligned} \tag{2.192}$$

Here the resulting flavour factors are symmetric in i and j only when the corresponding quark lines are of the same type, since the charge matrices may differ between the light and heavy quark flavours. These factors correspond to Figs. 2.4.3 to 2.4.6, in which the two vector bosons attach to separate closed quark lines. Both of the above flavour factors arise exclusively in processes with external gluons or ghosts.

Analogous flavour factors emerge for external quarks, now multiplied by the flavour unit matrix, Eq. (2.184), to account for the external quark flavour. The first is the trace of a product of quark charge matrices, multiplied by the flavour unit matrix,

$$\begin{aligned}\langle \mathrm{f}_{\{i,j\}}\rangle^{\mathrm{q}} &\equiv \mathrm{tr}(Q_iQ_j)\,1_{\mathrm{f}} \\ &= \langle \mathrm{l}_{\{i,j\}}\rangle^{\mathrm{q}} + \langle \mathrm{h}_{\{i,j\}}\rangle^{\mathrm{q}} .\end{aligned} \tag{2.193}$$

These flavour factors correspond to Figs. 2.4.7 and 2.4.8, which feature an open quark line together with both vector bosons attached to the same closed quark loop. The second is the product of traces of the individual quark charge matrices, multiplied by the unit matrix,

$$\begin{aligned}\langle \mathrm{f}_{\{i\}}\mathrm{f}_{\{j\}}\rangle^{\mathrm{q}} &\equiv \mathrm{tr}(Q_i)\,\mathrm{tr}(Q_j)\,1_{\mathrm{f}} \\ &= \langle \mathrm{l}_{\{i\}}\mathrm{l}_{\{j\}}\rangle^{\mathrm{q}} + \langle \mathrm{l}_{\{i\}}\mathrm{h}_{\{j\}}\rangle^{\mathrm{q}} + \langle \mathrm{h}_{\{i\}}\mathrm{l}_{\{j\}}\rangle^{\mathrm{q}} + \langle \mathrm{h}_{\{i\}}\mathrm{h}_{\{j\}}\rangle^{\mathrm{q}} .\end{aligned} \tag{2.194}$$

Realising these flavour factors, Figs. 2.4.9 to 2.4.12 feature an open quark line together with the two vector bosons attached to separate closed quark lines.

Further flavour factors arise by tracing over only a subset of the quark charge matrices. For a product of two charge matrices with no trace taken, we find

$$\begin{aligned}\langle \bar{\mathrm{f}}_{\{i,j\}}\rangle^{\mathrm{q}} &\equiv Q_iQ_j \\ &= \langle \bar{\mathrm{l}}^{a}_{\{i,j\}}\rangle^{\mathrm{q}} + \langle \bar{\mathrm{l}}_{\{i,j\}}\rangle^{\mathrm{q}} + \langle \bar{\mathrm{h}}^{a}_{\{i,j\}}\rangle^{\mathrm{q}} + \langle \bar{\mathrm{h}}_{\{i,j\}}\rangle^{\mathrm{q}} ,\end{aligned} \tag{2.195}$$

where we have applied the decomposition of the quark charge matrices in Eq. (2.190). The commutativity of diagonal matrices again renders this flavour factor symmetric in i and j. It corresponds to Fig. 2.4.13, in which both vector bosons attach to the same open quark line.

Lastly, a flavour factor emerges from taking a trace over only a single charge matrix,

$$\begin{aligned}\langle \bar{\mathrm{f}}_{\{i\}}\mathrm{f}_{\{j\}}\rangle^{\mathrm{q}} &\equiv Q_i\,\mathrm{tr}\left(Q_j\right) \\ &= \langle \bar{\mathrm{l}}^{a}_{\{i\}}\mathrm{l}_{\{j\}}\rangle^{\mathrm{q}} + \langle \bar{\mathrm{l}}_{\{i\}}\mathrm{l}_{\{j\}}\rangle^{\mathrm{q}} + \langle \bar{\mathrm{l}}^{a}_{\{i\}}\mathrm{h}_{\{j\}}\rangle^{\mathrm{q}} + \langle \bar{\mathrm{l}}_{\{i\}}\mathrm{h}_{\{j\}}\rangle^{\mathrm{q}} \\ &\quad + \langle \bar{\mathrm{h}}^{a}_{\{i\}}\mathrm{h}_{\{j\}}\rangle^{\mathrm{q}} + \langle \bar{\mathrm{h}}_{\{i\}}\mathrm{h}_{\{j\}}\rangle^{\mathrm{q}} + \langle \bar{\mathrm{h}}^{a}_{\{i\}}\mathrm{l}_{\{j\}}\rangle^{\mathrm{q}} + \langle \bar{\mathrm{h}}_{\{i\}}\mathrm{l}_{\{j\}}\rangle^{\mathrm{q}} ,\end{aligned} \tag{2.196}$$

where we have again decomposed the matrices as in the previous case. By construction, this flavour factor is not symmetric. It corresponds to Figs. 2.4.14 and 2.4.15, in which the two vector bosons attach respectively to a closed quark line and to an open quark line. Flavour factors involving external quark lines receive contributions

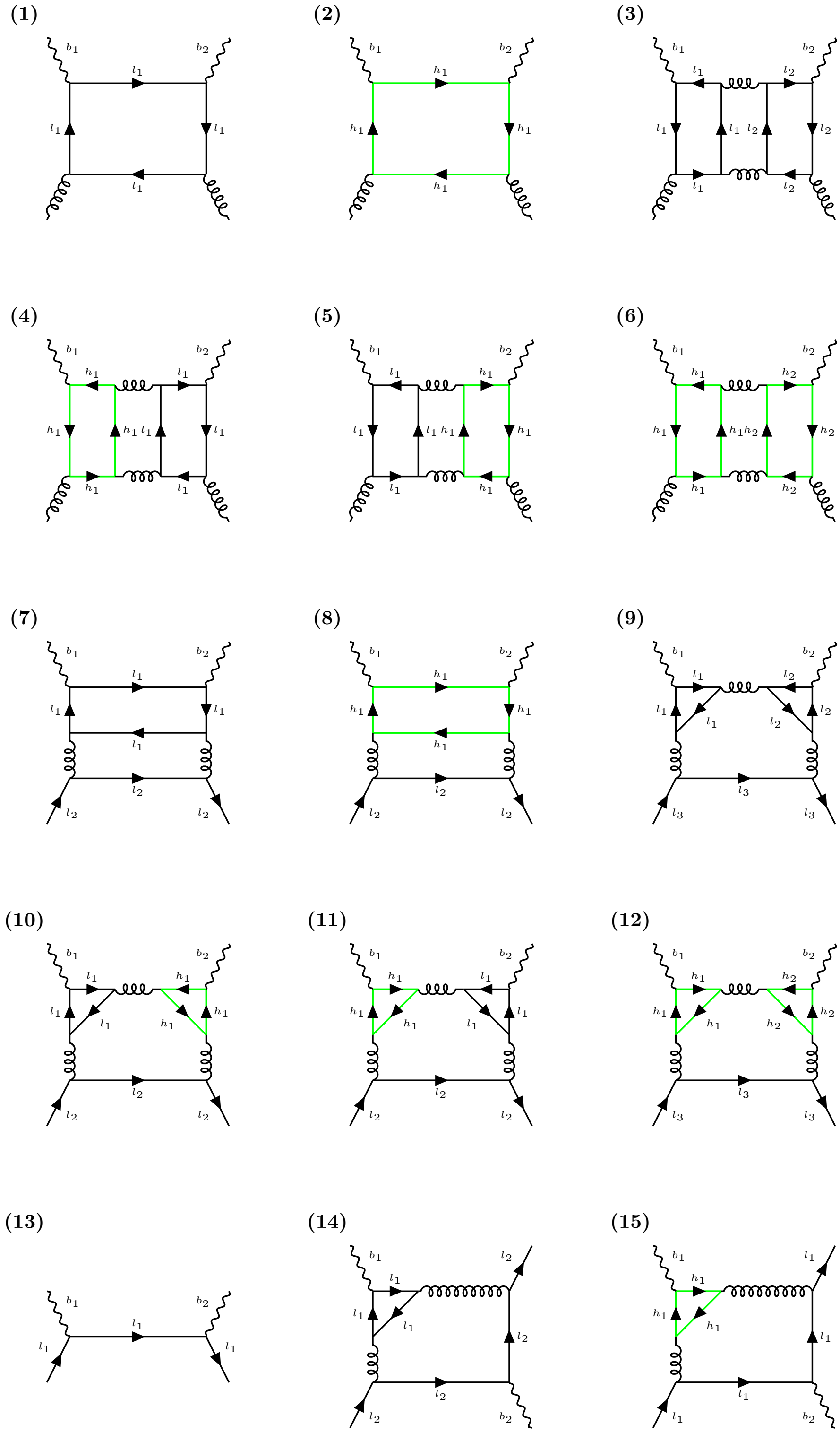

Figure 2.4: Representative Feynman graphs illustrating the flavour factors that arise in neutral current forward-scattering amplitudes. Light quarks l_i are drawn as solid black lines, heavy quarks h_i as solid green lines, and vector bosons are labelled b_i.

from both light and heavy flavours. Since we restrict our attention to external light quarks, we project onto the corresponding subspace by multiplying with the embedded light-flavour unit matrix, Eq. (2.182).

The flavour factors obtained through combinatorial analysis of the trace factors and from the graph-theoretic classification (see Subsec. 2.3.1) agree, providing a consistency check that indeed all flavour factors have been accounted for.

2.3.4 Charged Current

Conceptual problems arise if we work within the full electroweak theory at leading order in the weak coupling. Within this setting, the assumption of n_{l} light and n_{h} heavy quark flavours becomes inconsistent. Before electroweak symmetry breaking there are $n_{\mathrm{l}} + n_{\mathrm{h}}$ massless quark flavours in total.

After symmetry breaking, the transition from the flavour basis to the mass basis ceases to be well defined, because under our assumption the mass matrices are already diagonal, with zeros and a single mass m along the diagonal. Ordering the flavours so that the light ones come first and the heavy ones second renders the mass matrix block-diagonal, with a null block and a block proportional to the identity. Any unitary transformation of the flavour basis then preserves the diagonality of both blocks. The CKM matrix [140, 141], however, is defined as the product of the transformations diagonalising the up- and down-type mass matrices, and therefore fails to be uniquely determined under these assumptions. Introducing an external current that represents only the flavour-changing charged current weak interaction resolves the non-uniqueness; its coupling constants are precisely the ordinary CKM matrix elements or their complex conjugates.

To define the charge matrices, we denote the set of flavours by $\mathscr{F}$. These flavours decompose simultaneously along two orthogonal axes, into light and heavy flavours on the one hand and into up-type and down-type flavours on the other. The first decomposition reads

$$\mathscr{F} = \mathscr{F}_{\mathrm{l}} \sqcup \mathscr{F}_{\mathrm{h}} \,, \tag{2.197}$$
$$\mathscr{U} = \mathscr{U}_{\mathrm{l}} \sqcup \mathscr{U}_{\mathrm{h}} \,, \tag{2.198}$$
$$\mathscr{D} = \mathscr{D}_{\mathrm{l}} \sqcup \mathscr{D}_{\mathrm{h}} \,, \tag{2.199}$$

whilst the second gives

$$\mathscr{F}_{\mathrm{l}} = \mathscr{U}_{\mathrm{l}} \sqcup \mathscr{D}_{\mathrm{l}} \,, \tag{2.200}$$
$$\mathscr{F}_{\mathrm{h}} = \mathscr{U}_{\mathrm{h}} \sqcup \mathscr{D}_{\mathrm{h}} \,. \tag{2.201}$$

Unlike the neutral current case, the sizes of these sets are no longer unconstrained once flavour-changing transitions are admitted. In particular, there must be equal numbers of up- and down-type quarks, which forces the total number of flavours to be even,

$$|\mathscr{U}| = |\mathscr{D}| \quad \to \quad |\mathscr{F}| = 2m, \qquad m \in \mathbb{N} \,. \tag{2.202}$$

For the flavour-changing transitions, we let V_{ij} denote a CKM matrix element, which is in general complex. Unitarity of the CKM matrix then implies

$$\sum_{k \in \mathscr{X}} V_{i,k} V^*_{k,j} = \delta_{i,j} \,, \quad i,j \in \mathscr{F} - \mathscr{X} \,, \quad \mathscr{X} \in \{ \mathscr{U}, \mathscr{D} \} \,. \tag{2.203}$$

Because quarks cannot transition from up-type to up-type, nor from down-type to down-type, we define the charge matrix through

$$Q_{ij} = 0\,, \quad i,j \in \mathscr{U}\,, \quad i,j \in \mathscr{D}\,. \tag{2.204}$$

Next we compute the product of two charge matrices from which the flavour factors are built,

$$\begin{aligned}\sum_{f\in\mathscr{F}} Q_{if}Q_{fj} &= \sum_{u\in\mathscr{U}} Q_{iu}Q_{uj} + \sum_{d\in\mathscr{D}} Q_{id}Q_{dj}\\ &= \begin{cases}\sum_{u\in\mathscr{U}} V^*_{ui}V_{uj}, & i,j\in\mathscr{D}\,,\\ 0, & (i\in\mathscr{D}\wedge j\in\mathscr{U})\vee(j\in\mathscr{D}\wedge i\in\mathscr{U})\,,\\ \sum_{d\in\mathscr{D}} V_{di}V^*_{dj}, & i,j\in\mathscr{U}\,,\end{cases}\\ &= \delta_{i,j}\,, \quad i,j\in\mathscr{F}\,.\end{aligned} \tag{2.205}$$

Here we have used the unitarity of the CKM matrix, Eq. (2.203), which implies that the charge matrix is involutory. Naively, we might conclude from this that the flavour factors become trivial for charged currents. This is not the case, however, since the flavour factors are weighted by matrix elements that differ between the massive and the massless flavours.

As in the neutral current, we need a decomposition of the flavour factors. First we observe that traces of a single charge matrix vanish, since the diagonal entries are zero by construction, Eq. (2.204),

$$\operatorname{tr} Q = 0\,. \tag{2.206}$$

For the product of two charge matrices, the flavour factors require modification, since transitions between light and heavy quarks are not captured by our previous notation. In general, the charge matrix admits the block decomposition

$$Q = \begin{pmatrix} Q_{\mathrm{l}} & Q_{[\mathrm{lh}]}\\ Q_{[\mathrm{hl}]} & Q_{\mathrm{h}}\end{pmatrix}\,, \tag{2.207}$$

where $Q_{[\mathrm{lh}]}$ and $Q_{[\mathrm{hl}]}$ are rectangular matrices of size $n_{\mathrm{l}}\times n_{\mathrm{h}}$ and $n_{\mathrm{h}}\times n_{\mathrm{l}}$ respectively, encoding the off-diagonal couplings. Accordingly, we must allow for mixed quark lines [lh] and [hl], denoting transitions from a light to a heavy flavour and vice versa. With this notation at hand, we decompose the charge matrix as

$$Q = \hat{Q}_{\mathrm{l}} + \hat{Q}_{\mathrm{h}} + \hat{Q}_{[\mathrm{hl}]} + \hat{Q}_{[\mathrm{lh}]}\,, \tag{2.208}$$

where $\hat{Q}_{\mathrm{l}}$ and $\hat{Q}_{\mathrm{h}}$ are embeddings of the light and heavy diagonal blocks, whilst $\hat{Q}_{[\mathrm{lh}]}$ and $\hat{Q}_{[\mathrm{hl}]}$ are embeddings of the off-diagonal blocks.

To evaluate traces of products of charge matrices, we exploit a simple structural property. Any matrix that splits into a block-diagonal part D and a block-anti-diagonal part A satisfies

$$Q = D + A \quad\Longrightarrow\quad Q^2 = D^2 + A^2 + DA + AD\,, \tag{2.209}$$

whose components evaluate to

$$\left(D^2\right)_{ij} = \sum_k D_{ik}D_{kj} = D^2_{ii}\,\delta_{ij}\,, \tag{2.210}$$

$$\big(A^2\big)_{ij} = \sum_k A_{ik} A_{kj} = A_{i,n+1-i}\, A_{n+1-i,j}\, \delta_{ij}\,, \tag{2.211}$$

$$\big(DA\big)_{ij} = D_{ii} A_{ij}\,, \tag{2.212}$$

$$\big(AD\big)_{ij} = A_{ij} D_{jj}\,. \tag{2.213}$$

Hence D^2 and A^2 are diagonal, whereas DA and AD remain anti-diagonal and therefore drop out under the trace, leaving

$$\mathrm{tr}\big(Q^2\big) = \mathrm{tr}\big(D^2\big) + \mathrm{tr}\big(A^2\big)\,. \tag{2.214}$$

Applying Eq. (2.214) to the charge matrix, with $\hat{Q}_\mathrm{l}$ and $\hat{Q}_\mathrm{h}$ forming the block-diagonal part and $\hat{Q}_{[\mathrm{lh}]}$ and $\hat{Q}_{[\mathrm{hl}]}$ forming the block-off-diagonal part, we obtain for closed fermion lines

$$\mathrm{tr}(Q_i Q_j) = \mathrm{tr}\big(\hat{Q}_{\mathrm{l},i}\hat{Q}_{\mathrm{l},j}\big) + \mathrm{tr}\big(\hat{Q}_{\mathrm{h},i}\hat{Q}_{\mathrm{h},j}\big) + \mathrm{tr}\big(\hat{Q}_{[\mathrm{lh}],i}\hat{Q}_{[\mathrm{hl}],j}\big) + \mathrm{tr}\big(\hat{Q}_{[\mathrm{hl}],i}\hat{Q}_{[\mathrm{lh}],j}\big)\,. \tag{2.215}$$

From Eq. (2.215) we can directly read off the flavour factors for the gluon-initiated processes, that is, those without an open quark line, in which the two vector bosons couple to the same closed quark loop. The first two terms give rise to diagonal flavour factors analogous to those already obtained for the neutral current. By contrast, the remaining two terms define genuinely new flavour factors, which we denote by

$$\langle[\mathrm{lh}]\rangle^{\mathrm{g}}_{\{\,i,j\,\}} \equiv \mathrm{tr}\big(\hat{Q}_{[\mathrm{lh}],i}\hat{Q}_{[\mathrm{hl}],j}\big)\,, \tag{2.216}$$

$$\langle[\mathrm{hl}]\rangle^{\mathrm{g}}_{\{\,i,j\,\}} \equiv \mathrm{tr}\big(\hat{Q}_{[\mathrm{hl}],i}\hat{Q}_{[\mathrm{lh}],j}\big)\,. \tag{2.217}$$

Similarly, for quark-initiated processes in which the two vector bosons couple to a closed quark loop, we find

$$\langle[\mathrm{lh}]\rangle^{\mathrm{q}}_{\{\,i,j\,\}} \equiv \mathrm{tr}\big(\hat{Q}_{[\mathrm{lh}],i}\hat{Q}_{[\mathrm{hl}],j}\big)1_\mathrm{f}\,, \tag{2.218}$$

$$\langle[\mathrm{hl}]\rangle^{\mathrm{q}}_{\{\,i,j\,\}} \equiv \mathrm{tr}\big(\hat{Q}_{[\mathrm{hl}],i}\hat{Q}_{[\mathrm{lh}],j}\big)1_\mathrm{f}\,. \tag{2.219}$$

All of the flavour factors in Eqs. (2.216)–(2.219) correspond to Figs. 2.5.16 to 2.5.19, with one closed fermion line to which both external currents are attached.

The case of open quark lines, as in Fig. 2.5.20, requires more care. Since we are computing the forward-scattering amplitude, the flavours of the incoming and outgoing external quarks must coincide. For purely kinematic reasons, transitions from a heavy to a light quark on an open line are therefore excluded,

$$p^2 = 0 \quad \not\Leftrightarrow \quad p^2 = m^2 \quad \forall\, m \neq 0 \in \mathbb{C}\,. \tag{2.220}$$

Forming the product of two charge matrices and projecting onto the diagonal part, we obtain

$$\mathrm{Diag}(Q_i Q_j) = \Big[\hat{Q}_{\mathrm{l},i}\hat{Q}_{\mathrm{l},j}\hat{1}_\mathrm{l} + \hat{Q}_{\mathrm{h},i}\hat{Q}_{\mathrm{h},j}\hat{1}_\mathrm{h}\Big] + \Big[\hat{Q}_{[\mathrm{lh}],i}\hat{Q}_{[\mathrm{hl}],j}\hat{1}_\mathrm{l} + \hat{Q}_{[\mathrm{hl}],i}\hat{Q}_{[\mathrm{lh}],j}\hat{1}_\mathrm{h}\Big]\,. \tag{2.221}$$

As before, the first two terms are analogous to the neutral current contributions, whilst the remaining two capture the new structures that arise from the mass-changing transitions. Focusing on the new contributions, which are respectively $n_\mathrm{l} \times n_\mathrm{l}$ and $n_\mathrm{h} \times n_\mathrm{h}$ dimensional matrices, we find that they admit the decomposition

$$\hat{Q}_{[\mathrm{lh}],i}\hat{Q}_{[\mathrm{hl}],j}\hat{1}_\mathrm{l} = \langle\overline{[\mathrm{lh}]}^{a}_{\{\,i,j\,\}}\rangle^{\mathrm{q}} + \langle\widetilde{[\mathrm{lh}]}_{\{\,i,j\,\}}\rangle^{\mathrm{q}}\,, \tag{2.222}$$

$$\hat{Q}_{[\mathrm{hl}],i}\hat{Q}_{[\mathrm{lh}],j}\hat{1}_{\mathrm{h}} = \langle\overline{[\mathrm{hl}]}^{a}_{\{\,i,j\,\}}\rangle^{\mathrm{q}} + \langle\overline{[\mathrm{hl}]}^{a}_{\{\,i,j\,\}}\rangle^{\mathrm{q}}\,. \tag{2.223}$$

In the non-singlet contribution, as for the neutral current, only the diagonal generators play a role, since the forward-scattering kinematics conserves flavour along each open line. Once again we take the external lines to be light, thereby projecting out the heavy-quark contributions.

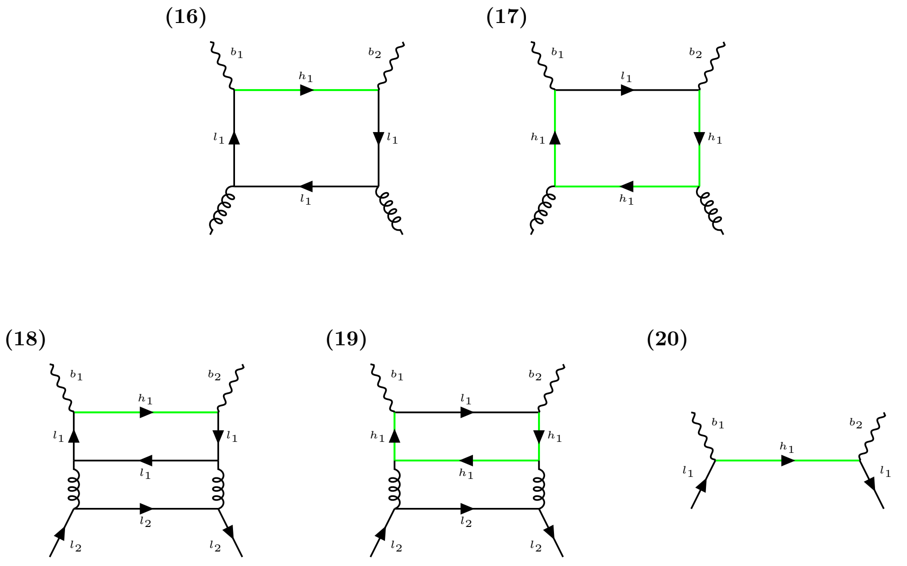

Figure 2.5: Representative Feynman graphs illustrating the flavour factors that exclusively arise in charged current forward-scattering amplitudes. Light quarks l_i are drawn as solid black lines, heavy quarks h_i as solid green lines, and vector bosons are labelled b_i.

2.3.5 Flavour Decomposition

Next we analyse the flavour factors involving traces over flavour-group generators. Quarks, whether light or heavy, are partially characterised by their quantum numbers, namely their electric charges and weak isospins. As already mentioned, these quantum numbers partition the flavour space into up-type and down-type sectors, thereby decomposing any set of flavours $\mathscr{F}$ into the subsets $\mathscr{U}$ and $\mathscr{D}$. For a matrix in flavour space, we define the trace as

$$\mathrm{tr}_{\mathscr{F}}(\lambda) = \sum_{f\in\mathscr{F}} \lambda_{ff}\,, \tag{2.224}$$

where λ is an arbitrary flavour matrix. This definition coincides with the standard trace over flavour matrices, but has the advantage that the summation can be readily restricted to a subset of flavours.

With this notation at hand, we now prove the following lemma, which allows us to re-express traces over the full flavour space, involving products of charge matrices and flavour generators, in terms of traces over the up-type flavours alone.

Lemma: *Let $\mathscr{F}$ be the disjoint union of the finite sets $\mathscr{U}$ and $\mathscr{D}$, and let λ be a traceless matrix,* $\mathrm{tr}_{\mathscr{F}}(\lambda) = 0$. *Then*

$$\sum_{\mathrm{f}\in\mathscr{F}} c_{\mathrm{f}}\lambda_{\mathrm{ff}} = (c_{\mathscr{U}} - c_{\mathscr{D}})\,\mathrm{tr}_{\mathscr{U}}(\lambda) \quad \text{if} \quad c_{\mathrm{f}} = \begin{cases} c_{\mathscr{U}}, & \text{if} \quad \mathrm{f}\in\mathscr{U}\,, \\ c_{\mathscr{D}}, & \text{if} \quad \mathrm{f}\in\mathscr{D}\,. \end{cases} \tag{2.225}$$

Proof. To establish the identity, we proceed by direct computation, splitting the index set of the sum into the disjoint subsets $\mathscr{U}$ and $\mathscr{D}$,

$$\begin{aligned} \sum_{f\in\mathscr{F}} c_f\lambda_{ff} &= \sum_{f\in\mathscr{U}} c_{\mathscr{U}}\lambda_{ff} + \sum_{f\in\mathscr{D}} c_{\mathscr{D}}\lambda_{ff} \\ &= \sum_{f\in\mathscr{U}} \big((c_{\mathscr{U}} - c_{\mathscr{D}}) + c_{\mathscr{D}}\big)\lambda_{ff} + \sum_{f\in\mathscr{D}} c_{\mathscr{D}}\lambda_{ff} \\ &= (c_{\mathscr{U}} - c_{\mathscr{D}}) \sum_{f\in\mathscr{U}} \lambda_{ff} + c_{\mathscr{D}} \sum_{f\in\mathscr{D}\sqcup\mathscr{U}} \lambda_{ff} \\ &= (c_{\mathscr{U}} - c_{\mathscr{D}}) \sum_{f\in\mathscr{U}} \lambda_{ff} + c_{\mathscr{D}} \sum_{f\in\mathscr{F}} \lambda_{ff} \\ &= (c_{\mathscr{U}} - c_{\mathscr{D}})\,\mathrm{tr}_{\mathscr{U}}(\lambda) + c_{\mathscr{D}}\,\mathrm{tr}_{\mathscr{F}}(\lambda) \\ &= (c_{\mathscr{U}} - c_{\mathscr{D}})\,\mathrm{tr}_{\mathscr{U}}(\lambda) \end{aligned}$$

where the last step uses the tracelessness. An analogous identity, differing only by an overall sign, holds for the complementary subset upon interchanging $\mathscr{U}$ and $\mathscr{D}$. $\square$

The preceding analysis of the flavour factors, and in particular Eq. (2.190), shows that the partonic invariants naturally decompose into non-singlet and pure-singlet contributions. In the case of external quarks, the partonic invariants take the form

$$T_{i,\mathrm{q}}(p,q) = \sum_a T^a_{i,\mathrm{q}}(p,q)\hat{\lambda}^a_l + T^{\mathrm{ps}}_{i,\mathrm{q}}(p,q)\hat{1}_l\,, \quad i\in\{\,L,2,3\,\} \tag{2.226}$$

whilst for external gluons and ghosts, no such decomposition is needed, since only the pure-singlet part survives.

The non-singlet component is isolated by inserting a light-flavour generator and tracing the product, whereas the pure-singlet component follows from the trace alone. Explicitly, the two components are defined by

$$\begin{aligned} T^{\mathrm{ns}}_{i,\mathrm{q}}(p,q) &\equiv \sum_a \frac{1}{T_{R,\mathrm{l}}}\,\mathrm{tr}\left(T_{i,\mathrm{q}}(p,q)\hat{\lambda}^a_{\mathrm{l}}\right) \\ &= \sum_N \left(\frac{1}{2x_{\mathrm{B}}}\right)^N \sum_a \frac{A^N_{a,\mathrm{q}}(p)C^N_{i,a}(q)}{T_{R,\mathrm{l}}}\,, \quad i\in\{\,L,2,3\,\}\,, \\ T^{\mathrm{ps}}_{i,\mathrm{q}}(p,q) &\equiv \frac{1}{n_{\mathrm{l}}}\,\mathrm{tr}\left(T_{i,\mathrm{q}}(p,q)\right) \\ &= \sum_N \left(\frac{1}{2x_{\mathrm{B}}}\right)^N \sum_{k\in\mathbb{S}} \frac{A^N_{k,\mathrm{q}}(p)C^N_{i,k}(q)}{n_{\mathrm{l}}}\,, \quad i\in\{\,L,2,3\,\}\,. \end{aligned} \tag{2.227}$$

In the non-singlet case, each coefficient function is a single monomial in the flavour factors. With $\mathscr{F}_a$ denoting the set of all non-singlet flavour factors, it follows that

$$
\begin{aligned}
T^{\mathrm{ns}}_{i,\mathrm{q}}(p,q) &= \sum_N \left(\frac{1}{2x_\mathrm{B}}\right)^N \sum_a \frac{A^N_{a,\mathrm{q}}(p) C^N_{i,a}(q)}{T_{R,\mathrm{l}}} \\
&= \sum_N \left(\frac{1}{2x_\mathrm{B}}\right)^N \sum_a \sum_{F_a \in \mathscr{F}_a} \frac{A^N_{a,\mathrm{q}}(p) F_a}{T_{R,\mathrm{l}}} \frac{\mathrm{d}C^N_{i,a}(q)}{\mathrm{d}F_a} \\
&= \sum_N \left(\frac{1}{2x_\mathrm{B}}\right)^N \left(\sum_a \frac{\mathrm{tr}_{\mathscr{U}}(\hat{\lambda}^a_\mathrm{l})}{T_{R,\mathrm{l}}} A^N_{a,\mathrm{q}}(p)\right) \left(\sum_{F_a \in \mathscr{F}_a} \frac{F_a}{\mathrm{tr}_{\mathscr{U}}(\hat{\lambda}^a_\mathrm{l})} \frac{\mathrm{d}C^N_{i,a}(q)}{\mathrm{d}F_a}\right) \\
&\equiv \sum_N \left(\frac{1}{2x_\mathrm{B}}\right)^N A^N_{\mathrm{ns}} C^N_{i,\mathrm{ns}}(q)\,, \quad i \in \{\, L, 2, 3 \,\}\ .
\end{aligned}
\tag{2.228}
$$

Here we have used the fact that both the derivatives of the coefficient functions and the ratios of flavour factors are independent of the flavour generators. As a consequence, the non-singlet coefficient functions carry no dependence on the flavour index a, since all traces over the light-flavour generators cancel [36].

For the calculation of the Mellin moments of the coefficient functions, the flavour factors enter only as overall multiplicative prefactors. There is therefore no need to compute the pure-singlet and non-singlet contributions separately, since both follow from the singlet result upon substituting the appropriate flavour factors. In what follows, we accordingly confine our attention to the singlet case.

This factorisation, Eq. (2.228), holds for all flavour factors, and in principle we are free to extract any one flavour factor and absorb it into the operator matrix element. A common convention extracts the flavour factor whenever it is a trace over two charge matrices. This normalisation works for the VV and AV structures but not the AA case, where the non-singlet flavour factor vanishes for physical processes. In the pure-singlet sector, extracting flavour factors would impose an artificial asymmetry between the light and heavy internal flavours, so we refrain from it here. Conversion to the standard conventions is nevertheless straightforward, as the differences amount only to overall multiplicative factors.

Treating the partonic invariants as formal monomials in the flavour factors, that is, disregarding the process-dependent values these factors take, we obtain the following relation between the charged- and neutral current cases,

$$
\begin{aligned}
T^{\mathrm{NC}}_{i,\mathrm{p}} = \sum_{\mathrm{b}_1,\mathrm{b}_2 \in \{\,\mathrm{a},\mathrm{v}\,\}} \Bigg(& 1 - \langle[\mathrm{hl}]\rangle^{\mathrm{p}}_{\{\,\mathrm{b}_1,\mathrm{b}_2\,\}} \frac{\partial}{\partial\langle[\mathrm{hl}]\rangle^{\mathrm{p}}_{\{\,\mathrm{b}_1,\mathrm{b}_2\,\}}} - \langle[\mathrm{lh}]\rangle^{\mathrm{p}}_{\{\,\mathrm{b}_1,\mathrm{b}_2\,\}} \frac{\partial}{\partial\langle[\mathrm{lh}]\rangle^{\mathrm{p}}_{\{\,\mathrm{b}_1,\mathrm{b}_2\,\}}} \\
&- \delta_{\mathrm{qp}} \sum_a \langle\overline{[\mathrm{lh}]}\rangle^a_{\{\,\mathrm{b}_1,\mathrm{b}_2\,\}} \frac{\partial}{\partial\langle\overline{[\mathrm{lh}]}^a\rangle^{\mathrm{q}}_{\{\,\mathrm{b}_1,\mathrm{b}_2\,\}}} \Bigg) T^{\mathrm{CC}}_{i,\mathrm{p}}\,, \quad i \in \{\, L, 2, 3 \,\}\,, \quad \mathrm{p} \in \mathbb{S}\,.
\end{aligned}
\tag{2.229}
$$

Consequently, the charged current case requires only the additional evaluation of amplitudes with mass-changing currents, the remainder being inherited directly from the neutral current computation.

2.3.6 Coupling Constants

At this point, the calculation connects to physical observables. The objects considered so far, namely arbitrary vector and axial-vector currents, acquire physical meaning only once specific flavour factors are supplied. This is what lets us compute the coefficient functions independently for each combination of vector and axial-vector currents, since the physical result is always assembled from them. Moreover, as shown earlier, the pure-singlet and non-singlet contributions need not be separated, since all of this information is absorbed into the flavour factors.

Here we focus on the neutral current case, since the charged current contributions are fixed entirely by the CKM matrix. It remains to give the explicit values of the relevant flavour factors. Within the electroweak theory, the charge-matrix entries are set by the electromagnetic charge q_f, the weak isospin $T_{3,f}$, and the electroweak mixing angle θ_W [142, 143]. The first two quantities split the quark flavours into up-type and down-type sectors, which is the decomposition introduced earlier. With this split, the charge matrices take the form

$$Q_{\gamma_\mathrm{v},\mathrm{b}_1\mathrm{b}_2} = q_f \delta_{\mathrm{b}_1\mathrm{b}_2} \qquad \mathrm{b}_1, \mathrm{b}_2 \in \{\,\mathrm{v}, \mathrm{a}\,\}\,, \tag{2.230}$$

$$Q_{\gamma_\mathrm{a},\mathrm{b}_1\mathrm{b}_2} = 0 \qquad \mathrm{b}_1, \mathrm{b}_2 \in \{\,\mathrm{v}, \mathrm{a}\,\}\,, \tag{2.231}$$

$$Q_{\mathrm{Z}_\mathrm{v},\mathrm{b}_1\mathrm{b}_2} = \Big(\frac{1}{2}T_{3,f} - q_f \sin^2\theta_\mathrm{W}\Big)\delta_{\mathrm{b}_1\mathrm{b}_2} \qquad \mathrm{b}_1, \mathrm{b}_2 \in \{\,\mathrm{v}, \mathrm{a}\,\}\,, \tag{2.232}$$

$$Q_{\mathrm{Z}_\mathrm{a},\mathrm{b}_1\mathrm{b}_2} = T_{3,f}\delta_{\mathrm{b}_1\mathrm{b}_2} \qquad \mathrm{b}_1, \mathrm{b}_2 \in \{\,\mathrm{v}, \mathrm{a}\,\}\,. \tag{2.233}$$

The photon couplings follow from the Z-boson expressions for suitable values of the weak mixing angle and weak isospin. It therefore suffices to treat the Z-boson case, for which the traces entering the pure-singlet coefficient functions read

$$\mathrm{tr}(Q_{\mathrm{Z}_\mathrm{a}}) = \sum_{f\in\mathscr{F}} T_{3,f}\,, \tag{2.234}$$

$$\mathrm{tr}(Q_{\mathrm{Z}_\mathrm{v}}) = \sum_{f\in\mathscr{F}} \Big(\frac{1}{2}T_{3,f} - q_f \sin^2\theta_\mathrm{W}\Big)\,, \tag{2.235}$$

$$\mathrm{tr}(Q_{\mathrm{Z}_\mathrm{v}}Q_{\mathrm{Z}_\mathrm{v}}) = \sum_{f\in\mathscr{F}} \Big(\frac{1}{2}T_{3,f} - q_f \sin^2\theta_\mathrm{W}\Big)^2\,, \tag{2.236}$$

$$\mathrm{tr}(Q_{\mathrm{Z}_\mathrm{a}}Q_{\mathrm{Z}_\mathrm{a}}) = \sum_{f\in\mathscr{F}} T_{3,f}^2\,, \tag{2.237}$$

$$\mathrm{tr}(Q_{\mathrm{Z}_\mathrm{a}}Q_{\mathrm{Z}_\mathrm{v}}) = \sum_{f\in\mathscr{F}} T_{3,f}\Big(\frac{1}{2}T_{3,f} - q_f \sin^2\theta_\mathrm{W}\Big)\,. \tag{2.238}$$

By the lemma, the corresponding traces entering the non-singlet coefficient functions read, where the subscripts $\mathscr{U}$ and $\mathscr{D}$ denote the up- and down-type values respectively,

$$\mathrm{tr}(Q_{\mathrm{Z}_\mathrm{a}}\lambda^a) = \frac{1}{2}\Big(T_{3,\mathscr{U}} - T_{3,\mathscr{D}}\big)\,\mathrm{tr}_\mathscr{U}(\lambda^a\Big)\,, \tag{2.239}$$

$$\mathrm{tr}(Q_{\mathrm{Z}_\mathrm{v}}\lambda^a) = \Big(\frac{1}{2}(T_{3,\mathscr{U}} - T_{3,\mathscr{D}}) - (q_\mathscr{U} - q_\mathscr{D})\sin^2\theta_\mathrm{W}\Big)\,\mathrm{tr}_\mathscr{U}(\lambda^a)\,, \tag{2.240}$$

$$\begin{aligned}\mathrm{tr}(Q_{\mathrm{Z}_\mathrm{v}}Q_{\mathrm{Z}_\mathrm{v}}\lambda^a) = \Big(&(q_\mathscr{U}^2 - q_\mathscr{D}^2)\sin^4\theta_\mathrm{W} \\ &- (T_{3,\mathscr{U}}q_\mathscr{U} - T_{3,\mathscr{D}}q_\mathscr{D})\sin^2\theta_\mathrm{W}\Big)\,\mathrm{tr}_\mathscr{U}(\lambda^a)\,,\end{aligned} \tag{2.241}$$

$$\mathrm{tr}(Q_{\mathrm{Z}_\mathrm{a}}Q_{\mathrm{Z}_\mathrm{a}}\lambda^a) = 0\,, \tag{2.242}$$

$$\mathrm{tr}(Q_{\mathrm{Z}_\mathrm{a}}Q_{\mathrm{Z}_\mathrm{v}}\lambda^a) = \Big(-(T_{3,\mathscr{U}}q_\mathscr{U} - T_{3,\mathscr{D}}q_\mathscr{D})\sin^2\theta_\mathrm{W}\Big)\,\mathrm{tr}_\mathscr{U}(\lambda^a)\,. \tag{2.243}$$

(This page is intentionally left blank.)

Down, down, down. Would the fall never come to an end!

"I wonder how many miles I've fallen by this time?" she said aloud. "I must be getting somewhere near the centre of the earth. Let me see: that would be four thousand miles down, I think–"

(for, you see, Alice had learnt several things of this sort in her lessons in the schoolroom, and though this was not a very good opportunity for showing off her knowledge, as there was no one to listen to her, still it was good practice to say it over)

"–yes, that's about the right distance–but then I wonder what Latitude or Longitude I've got to?"

(Alice had no idea what Latitude was, or Longitude either, but thought they were nice grand words to say.)

— *Alice's Adventures in Wonderland*, Lewis Carroll

Chapter 3

Feynman Integrals

This chapter lays the computational groundwork for the calculation of heavy-quark coefficient functions at higher loop orders, forming a substantial part of the present work. Rather than aiming for mathematical completeness, a task well beyond the scope of a thesis in phenomenology, the presentation prioritises clarity and practical utility, with definitions accompanied throughout by worked examples. Standard references for parts of the material discussed in this chapter are [110–112], where the computation of Feynman integrals is discussed in great detail.

Three topics are covered in turn. The first concerns the integral representation of Feynman integrals, examined in detail as it forms the foundation for the symmetry analysis and the optimisation of integral families. Within this framework, criteria for identifying factorisable integrals are derived, drawing on a connection between factorisation and the structure of graph polynomials that appears not to have been treated systematically in the literature. Moreover, the combinatorial complexity of analysing symmetries of Feynman integrals via the Lee–Pomeransky polynomial is assessed, a result that is, to the best of our knowledge, new.

Next, dimensional regularisation and integration by parts are introduced, establishing the framework for the reduction of Feynman integrals to master integrals.

The computation of the master integrals via differential equations forms the third topic, covering dimensional shift relations, the construction of an ε-factorised basis, the determination of boundary values through expansion by subgraphs, and the integration of the resulting systems in terms of iterated integrals. Conciseness is a necessity here, as the sheer complexity of the calculations of the following chapter precludes explicit illustration, with the focus lying on establishing the notation and conventions employed throughout.

3.1 Integral Representations

3.1.1 Momentum-Space Representation

Throughout this section, we restrict attention to Feynman integrals that admit a graphical representation, in contrast to the general case in which the number of propagators is left unconstrained. This restriction imposes an upper bound on the number of propagators, dictated by the topological constraints encoded in the Euler characteristic. Henceforth, Γ denotes a graph with C connected components, E internal edges, N external edges, V vertices, and L independent loops. These quantities are related by

$$L = E - V + C\,. \tag{3.1}$$

The independence of the loops is essential, since a graph may contain additional cycles, not all of which are fundamental in the sense of algebraic topology. To each independent loop we assign an internal momentum k_l, and to each external edge an external momentum p_n. The external edges are oriented such that all momenta are incoming, subject to overall momentum conservation,

$$\sum_{n=1}^{N} p_n = 0\,. \tag{3.2}$$

Each internal edge carries a mass m_i and an edge momentum q_e, the latter being defined such that the momenta at every vertex sum to zero. The Feynman propagator reads

$$D_{\mathrm{F}}(q_e, m_e) = \frac{1}{q_e^2 - m_e^2 + i\eta_e}\,, \tag{3.3}$$

where η_e is an infinitesimal positive constant, in general different for each internal edge, encoding the Feynman pole prescription and thereby enforcing causality. Edge momenta are linear combinations of the internal and external momenta,

$$q_e = \sum_{l=1}^{L} \omega_{k,el} k_l + \sum_{n=1}^{N-1} \omega_{p,en} p_n\,, \tag{3.4}$$

where the second sum runs over only $N-1$ of the external momenta, since the remaining one is fixed by momentum conservation, Eq. (3.2). The coefficients $\omega_{k,el}$ and $\omega_{p,en}$ take values in $\mathbb{C}$ in full generality, though without much loss of generality their values may be restricted to the *incidence set*

$$\mathscr{X} = \{\, -1, 0, 1 \,\}\,. \tag{3.5}$$

With this notation in place, we assign to each propagator a weight $\hat{\nu}_e$, and the *Feynman integral of the graph* Γ is formally defined in D space-time dimensions as

$$\hat{I}_{\hat{\nu}_1 \ldots \hat{\nu}_E}(\Gamma; D, p, m) = C_{L,D} \int \prod_{l=1}^{L} \frac{\mathrm{d}^D k_l}{i\pi^{D/2}} \prod_{e=1}^{E} [D_{\mathrm{F}}(q_e, m_e)]^{\hat{\nu}_e} \mathcal{N}(\boldsymbol{k}, \boldsymbol{p}, \boldsymbol{m})\,. \tag{3.6}$$

Here $C_{L,D}$ is a normalisation constant left unspecified for the time being, $\mathcal{N}$ denotes a numerator function regular in all its arguments, and the symbols $\boldsymbol{k}$, $\boldsymbol{p}$, $\boldsymbol{m}$ stand for vectors collecting the loop momenta, external momenta, and masses respectively.

At first sight, the Feynman integral depends on a large number of parameters, though not all are independent owing to the constraints already established. Momentum conservation reduces the number of independent external momenta by one, and Lorentz symmetry further dictates that the integral may depend only on scalar invariants. The latter consist of the masses associated with each internal edge, together with the scalar products formed from the external momenta. Products of a momentum with itself are referred to as *scales*, whilst those involving two distinct momenta are called *angles*. Accounting for momentum conservation, the total number of independent invariants is

$$S_{\mathrm{ext}} = \frac{N(N-1)}{2} + E\,. \tag{3.7}$$

For convenience, we collect all invariants, comprising the masses, scales, and angles, into a single vector $\boldsymbol{x}$. The Feynman integral in Eq. (3.6) then takes the form

$$I_{\hat{\nu}_1\ldots\hat{\nu}_E}(\Gamma; D, \boldsymbol{x}) = C_{L,D} \int \prod_{l=1}^{L} \frac{\mathrm{d}^D k_l}{i\pi^{D/2}} \prod_{e=1}^{E} [D_{\mathrm{F}}(q_e(\boldsymbol{x}), m_e)]^{\hat{\nu}_e} \mathcal{N}(\boldsymbol{k}, \boldsymbol{x}) \,. \tag{3.8}$$

Henceforth, we take the numerator to be a scalar function. This entails no loss of generality, since by linearity and Lorentz symmetry any tensor-valued numerator decomposes into a linear combination of tensors constructed from the metric tensor g, the totally antisymmetric tensor ϵ, and the external momenta p_n, with coefficients that are functions of the scalar products involving internal and external momenta as well as the space-time dimension [144].

Our aim is to express the numerator in terms of the propagators, thereby allowing us to write the full integral as a linear combination of integrals with different weights. To this end, we first observe that the number of independent scalar products that may be formed from the internal and external momenta is

$$S_{\mathrm{int}} = \frac{L(L+1)}{2} + L(N-1) \,. \tag{3.9}$$

Collecting all such scalar products into a vector $\boldsymbol{s}$, this number generally exceeds the number of propagators, so that a bijection between the two sets need not exist. The set of propagators appearing in a Feynman integral is henceforth referred to as a *family*. Neglecting the infinitesimal constants, the inverse propagators are affine functions of the form

$$\frac{1}{D_{\mathrm{F}}(q_e, m_e)} = \sum_{i=1}^{S_{\mathrm{int}}} c_{\mathrm{int},e,i} s_i + \sum_{i=1}^{S_{\mathrm{ext}}} c_{\mathrm{ext},e,i} x_i \,. \tag{3.10}$$

Whenever the coefficient matrix $c_{\mathrm{int},e,i}$ does not have full rank, the family is said to be *incomplete*. Such a family may be completed by iteratively adjoining *auxiliary propagators*, each addition raising the rank of the matrix, until full rank is reached, at which point the family is termed *complete*. Given a complete family F, we denote the corresponding integral by

$$F_{\nu_1\ldots\nu_{S_{\mathrm{int}}}}(D, \boldsymbol{x}) = C_{L,D} \int \prod_{l=1}^{L} \frac{\mathrm{d}^D k_l}{i\pi^{D/2}} \prod_{e=1}^{E} [D_{\mathrm{F}}(q_e(\boldsymbol{x}), m_e)]^{\nu_e} \prod_{e=E+1}^{S_{\mathrm{int}}} [D_{\mathrm{F}}(q_e(\boldsymbol{x}), m_e)]^{\nu_e} \,, \tag{3.11}$$

where the first product runs over the original propagators of the graph and the second over the auxiliary ones, the latter factor being absent whenever no auxiliary propagators are required. The embedding of the original propagators into a complete family is not unique, since different choices of auxiliary propagators give rise to distinct families. By linearity of the integral, any such integral may be expressed as a finite linear combination

$$I_{\hat{\nu}_1\ldots\hat{\nu}_E}(\Gamma; D, \boldsymbol{x}) = \sum_{i\in\mathbb{N}} c_i(\boldsymbol{x}) F_{\nu_{i,1}\ldots\nu_{i,S_{\mathrm{int}}}}(D, \boldsymbol{x}) \,, \tag{3.12}$$

with all but finitely many coefficients c_i vanishing. In particular, the embedding of a given integral into a family need not be unique, and different choices of auxiliary propagators may yield distinct but equivalent representations.

Example 1: *Consider the one-loop family $F_{B,\nu_1\nu_2}$, defined by a single external momentum q, two massive propagators with masses m_1 and m_2, edge momenta $q_1 = k_1$ and $q_2 = k_1 + q$, and weights ν_1 and ν_2,*

$$F_{B,\nu_1\nu_2}(D, \boldsymbol{x}_B) = C_{1,D} \int \frac{\mathrm{d}^D k_1}{i\pi^{D/2}} \frac{1}{\left[k^2 - m_1^2 + i\eta_1\right]^{\nu_1} \left[(k+q)^2 - m_2^2 + i\eta_2\right]^{\nu_2}} \,. \tag{3.13}$$

This family is complete, since the two propagators span all scalar products involving the internal momentum k.

As a consequence of the foregoing discussion, any Feynman integral, including those with tensor numerators, may be expressed as a linear combination of scalar integrals. Partial fractioning further extends the applicability of this strategy beyond the topological constraints. Indeed, for $m_{e,1} \neq m_{e,2}$, a product of propagators sharing the same momentum decomposes as

$$D_\mathrm{F}(q_e, m_{e,1}) D_\mathrm{F}(q_e, m_{e,2}) = \frac{1}{m_{e,1}^2 - m_{e,2}^2} \left[D_\mathrm{F}(q_e, m_{e,1}) - D_\mathrm{F}(q_e, m_{e,2})\right] \,, \tag{3.14}$$

and repeated application allows any number of masses associated with a given edge momentum q_e to be reduced to the case of a single mass. In a similar vein, partial fraction decomposition permits us to consider integrands corresponding to integrals with more propagators than available edges, even when the resulting terms no longer admit a graphical interpretation. Such integrands are then replaced by ones obtained via partial fractioning, for which several algorithmic approaches exist, including those based on Gröbner bases [145] and the Leinartas decomposition [146, 147]. Further details are omitted, since the calculations considered in this thesis involve only a single external momentum, for which such a decomposition is not needed.

3.1.2 Schwinger Representation

As defined, Feynman integrals are purely formal objects, and whether they carry a well-defined meaning is not clear a priori. Two potential issues arise. First, the propagators should be properly regarded as tempered distributions [148], so their pointwise product is in general ill-defined [149]. Treating the pole-prescription parameters η_e as finite regulators circumvents this difficulty [150]. Second, the integral may diverge in the ultraviolet, as $k_l \to \infty$, or in the infrared, as $k_l \to 0$.

An alternative representation is therefore needed in order to regularise these integrals and endow them with a precise meaning. Assuming for the moment that all weights ν_e are strictly positive, such a representation is obtained by substituting for each propagator

$$\frac{1}{\left[q_e^2(\boldsymbol{x}) - m_e^2\right]^{\nu_e}} = \frac{1}{\Gamma(\nu_e)} \int_{\mathbb{R}_+} \mathrm{d}a_e \, a_e^{\nu_e - 1} e^{-a_e (q_e^2(\boldsymbol{x}) - m_e^2)} \,. \tag{3.15}$$

Repeated application of this identity transforms the Feynman integral, Eq. (3.11), into a Gaussian integral [151],

$$\begin{aligned} F_{\nu_1 \ldots \nu_{S_\mathrm{int}}}(D, \boldsymbol{x}) = C_{L,D} &\frac{1}{\prod_{e=1}^{S_\mathrm{int}} \Gamma(\nu_e)} \int_{\mathbb{R}_+^{S_\mathrm{int}}} \mathrm{d}^{S_\mathrm{int}} a \prod_{e=1}^{S_\mathrm{int}} a_e^{\nu_e - 1} \\ &\times \int \prod_{l=1}^{L} \frac{\mathrm{d}^D k_i}{i\pi^{D/2}} \exp\left(-\sum_{e=1}^{S_\mathrm{int}} a_e (q_e^2(\boldsymbol{x}) - m_e^2)\right) \,. \end{aligned} \tag{3.16}$$

The exponent in Eq. (3.16) is a quadratic polynomial in the internal momenta k_l, and is therefore determined by a matrix M, a vector V, and a scalar S,

$$-\sum_{e=1}^{S_{\text{int}}} a_e(q_e^2 - m_e^2) = -\sum_{i=1}^{L}\sum_{j=1}^{L} k_i M_{ij}(\boldsymbol{a}) k_j + 2\sum_{i=1}^{L} V_i(\boldsymbol{a}) k_i + S(\boldsymbol{a}, \boldsymbol{x})\,. \tag{3.17}$$

By virtue of the integration domain of the a_e parameters, the matrix M is symmetric and positive definite. Wick rotating the energy components of the internal momenta, $k_{l,0} \mapsto ik_{l,0}$, then allows all internal momenta to be integrated out through the standard Gaussian integral [152],

$$\int_{\mathbb{R}^{LD}} \mathrm{d}^{LD}y \exp\bigl(-y^T M y + 2Vy + S\bigr) = \pi^{LD/2}\,[\det M]^{-1/2} \exp\bigl(V^T M^{-1} V + S\bigr)\,, \tag{3.18}$$

yielding

$$F_{\nu_1\ldots\nu_{S_{\text{int}}}}(D, \boldsymbol{x}) = \frac{C_{L,D}}{\prod_{e=1}^{S_{\text{int}}}\Gamma(\nu_e)} \int_{\mathbb{R}_+^{S_{\text{int}}}} \mathrm{d}^{S_{\text{int}}}a \prod_{e=1}^{S_{\text{int}}} a_e^{\nu_e - 1}\,[\mathcal{U}(\boldsymbol{a})]^{-D/2} \exp\left(-\frac{\mathcal{F}(\boldsymbol{a}, \boldsymbol{x})}{\mathcal{U}(\boldsymbol{a})}\right)\,. \tag{3.19}$$

Here we have introduced the *first* and *second graph polynomials* [90, 91], defined respectively by

$$\mathcal{U}(\boldsymbol{a}) = \det(M)\,, \tag{3.20}$$

$$\mathcal{F}(\boldsymbol{a}, \boldsymbol{x}) = \det(M)(V^T M^{-1} V + S)\,. \tag{3.21}$$

For integrals admitting a graphical representation, an equivalent topological definition exists in terms of spanning trees and forests, making no reference to the momenta. The present definition is more straightforward to implement, whereas the topological one is of greater structural interest by virtue of its recursive nature [153].

Although not immediately apparent from their definitions in Eqs. (3.20) and (3.21), the graph polynomials are in fact independent of the momentum routing, that is, they are invariant under shifts and rotations of the internal momenta,

$$k \mapsto Rk + Q(\boldsymbol{x}) \quad \text{with} \quad \det(R) = \pm 1\,, \tag{3.22}$$

where R is an $L \times L$ matrix and Q is an L-dimensional vector. Such transformations leave the measure invariant, yet the quadratic polynomial in Eq. (3.17) transforms non-trivially,

$$M' = R^T M R\,, \tag{3.23}$$

$$V' = R^T V - R^T Q M\,, \tag{3.24}$$

$$S' = S + 2VQ - Q^T M Q\,. \tag{3.25}$$

Inserting Eqs. (3.23) to (3.25) into Eqs. (3.20) and (3.21), we confirm by an elementary calculation that indeed

$$\mathcal{U}'(\boldsymbol{a}) = \mathcal{U}(\boldsymbol{a})\,, \tag{3.26}$$

$$\mathcal{F}'(\boldsymbol{a}, \boldsymbol{x}) = \mathcal{F}(\boldsymbol{a}, \boldsymbol{x})\,. \tag{3.27}$$

The graph polynomials are therefore invariant under momentum re-routing. Furthermore, they are homogeneous polynomials of degrees L and $L+1$ respectively.

Example 2: *For the family F_{B,ν_1,ν_2} (see Ex. 1), we readily determine the quadratic polynomial in the exponent,*

$$-a_1 q_1^2 - a_2 q_2^2 = -a_1\left(k^2 - m_1^2\right) - a_2\left(k^2 + 2k\cdot q + q^2 - m_2^2\right) . \tag{3.28}$$

Reading off the coefficients, and noting that all three are scalars for a one-loop integral, gives

$$M = a_1 + a_2\,, \tag{3.29}$$
$$V = -a_2 q\,, \tag{3.30}$$
$$S = -a_1 m_1^2 - a_2(q^2 - m_2^2)\,. \tag{3.31}$$

A straightforward calculation then yields the first and second graph polynomials,

$$\mathcal{U}(\boldsymbol{a}) = a_1 + a_2\,, \tag{3.32}$$
$$\mathcal{F}(\boldsymbol{a}) = a_1 a_2 q^2 + a_1 m_1^2 + a_2 m_2^2\,. \tag{3.33}$$

The first graph polynomial provides a readily verifiable criterion for whether a Feynman integral factorises into integrals involving fewer internal momenta. In momentum space, an integral factorises whenever the internal momenta admit a partition into two disjoint sets such that each edge momentum q_e depends on the internal momenta in only one of the two sets. Repeated application extends this criterion to factorisations into arbitrarily many factors. When such a partition exists, the integration over each set of internal momenta may be performed separately.

Verifying this directly is, however, not straightforward, since it requires identifying the appropriate transformation. Passing to the parametric representation, the factorisation of a Feynman integral implies a partition of the parameters a_e into disjoint sets A_1 and A_2 and amounts to

$$\mathcal{U}(\boldsymbol{a}) = \mathcal{U}_1(\boldsymbol{a}_1)\mathcal{U}_2(\boldsymbol{a}_2) \quad \text{with} \quad a_e \in A_i \Leftrightarrow a_e \notin A_j \quad \forall i \neq j\,. \tag{3.34}$$

Here, $\boldsymbol{a}_i$ denotes the vector of edge parameters belonging to the set A_i. This condition implies that the matrix M must be block diagonal, since we require not only that the determinant factorise, but also that each factor depends on a distinct set of parameters A_i, a requirement that would be violated by the presence of off-diagonal blocks,

$$M = M_1 \oplus M_2\,. \tag{3.35}$$

Such a block-diagonal structure naturally partitions the internal momenta, with both the vector and scalar terms in the quadratic polynomial splitting accordingly. It should be noted, however, that the second graph polynomial need not factorise simply because the first does.

Example 3: *Consider four edge momenta $q_1 = k_1$, $q_2 = k_1 + q$, $q_3 = k_2$, $q_4 = k_2 + q$ and vanishing masses. Taking all propagators into account simultaneously, the graph polynomials read*

$$\mathcal{U}(\boldsymbol{a}) = a_1 a_3 + a_1 a_4 + a_2 a_3 + a_2 a_4\,, \tag{3.36}$$
$$\mathcal{F}(\boldsymbol{a}, \boldsymbol{x}) = q^2(a_1 a_2 a_3 + a_1 a_2 a_4 + a_1 a_3 a_4 + a_2 a_3 a_4)\,. \tag{3.37}$$

Restricting instead to each pair of propagators sharing a common internal momentum, we find

$$\mathcal{U}(\boldsymbol{a}_1) = a_1 + a_2\,, \tag{3.38}$$
$$\mathcal{F}(\boldsymbol{a}_1, \boldsymbol{x}) = q^2(a_1 a_2)\,, \tag{3.39}$$
$$\mathcal{U}(\boldsymbol{a}_2) = a_3 + a_4\,, \tag{3.40}$$
$$\mathcal{F}(\boldsymbol{a}_2, \boldsymbol{x}) = q^2(a_3 a_4)\,. \tag{3.41}$$

The first graph polynomial factorises as $\mathcal{U}(\boldsymbol{a}) = \mathcal{U}(\boldsymbol{a}_1)\cdot\mathcal{U}(\boldsymbol{a}_2)$, yet the second does not.

Returning to the parametric representation of the Feynman integral in Eq. (3.19), we may simplify it by inserting the identity

$$1 = \int_{\mathbb{R}_+} \mathrm{d}t\, \delta\left(t - \sum_{e=1}^{S_{\text{int}}} a_e\right), \tag{3.42}$$

which is valid since all $\hat{a}_e$ are strictly positive. Upon substituting this factor, rescaling $a_e \mapsto \alpha_e t$, and exploiting the fact that $\mathcal{F}$ and $\mathcal{U}$ are homogeneous polynomials of degrees $L+1$ and L respectively, we obtain

$$\begin{aligned} F_{\nu_1\ldots\nu_{S_{\text{int}}}}(D, \boldsymbol{x}) = \frac{C_{L,D}}{\prod_{e=1}^{S_{\text{int}}}\Gamma(\nu_e)} &\int_{\mathbb{R}_+^{S_{\text{int}}}} \mathrm{d}^{S_{\text{int}}}a\, \delta\left(1 - \sum_{e=1}^{S_{\text{int}}} \alpha_e\right) \prod_{e=1}^{S_{\text{int}}} \alpha_e^{\nu_e - 1}\, [\mathcal{U}(\boldsymbol{\alpha})]^{-D/2} \\ \times &\int_{\mathbb{R}_+} \mathrm{d}t\, t^{\nu - LD/2 - 1} \exp\left(-\frac{\mathcal{F}(\boldsymbol{\alpha}, \boldsymbol{x})}{\mathcal{U}(\boldsymbol{\alpha})} t\right). \end{aligned} \tag{3.43}$$

The remaining t-integral is recognised as a Gamma function under the substitution $t \mapsto \mathcal{U}(\boldsymbol{\alpha})/\mathcal{F}(\boldsymbol{\alpha}, \boldsymbol{x}) \cdot t$. This yields the *Schwinger representation*, where $\nu = \sum_{e=1}^{S_{\text{int}}} \nu_e$ denotes the total weight,

$$\begin{aligned} F_{\nu_1\ldots\nu_{S_{\text{int}}}}(D, \boldsymbol{x}) = C_{L,D} \frac{\Gamma(\nu - LD/2)}{\prod_{e=1}^{S_{\text{int}}}\Gamma(\nu_e)} &\int_{\mathbb{R}_+^{S_{\text{int}}}} \mathrm{d}^{S_{\text{int}}}\alpha\, \delta\left(1 - \sum_{e=1}^{S_{\text{int}}} \alpha_e\right) \\ \times \prod_{e=1}^{S_{\text{int}}} &\alpha_e^{\nu_e - 1} \frac{[\mathcal{U}(\boldsymbol{\alpha})]^{\nu - (L+1)D/2}}{[\mathcal{F}(\boldsymbol{\alpha}, \boldsymbol{x})]^{\nu - LD/2}}. \end{aligned} \tag{3.44}$$

As it stands, the Schwinger representation applies only to integrals with strictly positive propagator weights. In order to extend its range of validity and accommodate propagators that are either absent or appear in the numerator, we note that for non-positive weights the substitution instead reads

$$\frac{1}{\left[q_e^2(\boldsymbol{x}) - m_e^2\right]^{\nu_e}} = (-1)^{\nu_e} \frac{\partial^{-\nu_e}}{\partial \alpha_e^{-\nu_e}} e^{-\alpha_e (q_e^2(\boldsymbol{x}) - m_e^2)}\Big|_{\alpha_e = 0}. \tag{3.45}$$

To unify both cases, we introduce the shorthand

$$\mathrm{d}(\alpha_e, \nu_e) = \begin{cases} \mathrm{d}\alpha_e\, \dfrac{\alpha_e^{\nu_e - 1}}{\Gamma(\nu_e)}\,, & 0 < \nu_e\,, \\ \mathrm{d}\alpha_e\, (-1)^{\nu_e} \dfrac{\partial^{-\nu_e}}{\partial \alpha_e^{-\nu_e}} \delta(\alpha_e)\,, & \nu_e \leq 0\,. \end{cases} \tag{3.46}$$

Both expressions scale identically under $\alpha_e \mapsto \lambda\alpha_e$. The Schwinger representation, Eq. (3.19) thereby generalises to

$$\begin{aligned} F_{\nu_1\dots\nu_{S_{\mathrm{int}}}}(D,\boldsymbol{x}) = C_{L,D}\Gamma(\nu - LD/2) \int_{\mathbb{R}_+^{S_{\mathrm{int}}}} \prod_{e=1}^{S_{\mathrm{int}}} \mathrm{d}(\alpha_e,\nu_e) \\ \times\,\delta\Big(1-\sum_{e=1}^{S_{\mathrm{int}}}\alpha_e\Big)\frac{[\mathcal{U}(\boldsymbol{\alpha})]^{\nu-(L+1)D/2}}{[\mathcal{F}(\boldsymbol{\alpha},\boldsymbol{x})]^{\nu-LD/2}}\,, \end{aligned} \tag{3.47}$$

where the right-hand side, initially defined for integer weights ν_e, admits an analytic continuation to complex-valued weights. A notable distinction between the momentum-space representation, Eq. (3.11), and the Schwinger representation, Eq. (3.47), is that the former is an integral *in* D space-time dimensions, whilst the latter is an integral *at* D space-time dimensions, since the dimensionality enters only as a parameter.

3.1.3 Lee–Pomeransky Representation

Yet another representation, particularly useful for identifying integral symmetries and vanishing integrals, is obtained by replacing the Gamma function in Eq. (3.47) with the Euler beta function,

$$\Gamma(\nu - LD/2) = \frac{\Gamma(D/2)}{\Gamma((L+1)D/2-\nu)}\int_{\mathbb{R}_+}\mathrm{d}t\, t^{\nu-LD/2-1}(1+t)^{-D/2}\,, \tag{3.48}$$

which under the substitution $t \mapsto \mathcal{F}(\boldsymbol{\alpha})/\mathcal{U}(\boldsymbol{\alpha},\boldsymbol{x})\cdot t$ becomes

$$\begin{aligned} \Gamma(\nu - LD/2) = \frac{\Gamma(D/2)}{\Gamma((L+1)D/2-\nu)}\int_{\mathbb{R}_+}\mathrm{d}t\, t^{\nu-LD/2-1}(\mathcal{U}(\boldsymbol{\alpha})+\mathcal{F}(\boldsymbol{\alpha},\boldsymbol{x})t)^{-LD/2} \\ \times\,\frac{[\mathcal{F}(\boldsymbol{\alpha},\boldsymbol{x})]^{\nu-LD/2}}{[\mathcal{U}(\boldsymbol{\alpha})]^{\nu-(L+1)D/2}}\,. \end{aligned} \tag{3.49}$$

Inserting this formula for the Gamma function, Eq. (3.49), into the Schwinger representation, Eq. (3.47), gives

$$\begin{aligned} F_{\nu_1\dots\nu_{S_{\mathrm{int}}}}(D,\boldsymbol{x}) = C_{L,D}\frac{\Gamma(D/2)}{\Gamma((L+1)D/2-\nu)}\int_{\mathbb{R}_+}\mathrm{d}t\, t^{\nu-LD/2-1}\int_{\mathbb{R}_+^{S_{\mathrm{int}}}}\prod_{e=1}^{S_{\mathrm{int}}}\mathrm{d}(\alpha_e,\nu_e) \\ \times\,(\mathcal{U}(\boldsymbol{\alpha})+\mathcal{F}(\boldsymbol{\alpha},\boldsymbol{x})t)^{-D/2}\delta\Big(1-\textstyle\sum_{e=1}^{S_{\mathrm{int}}}\alpha_e\Big)\,. \end{aligned} \tag{3.50}$$

Changing variables $\alpha_e \mapsto u_e/t$, exploiting the homogeneity of the graph polynomials to collect powers of t, and rescaling the delta distribution accordingly, we obtain

$$\begin{aligned} F_{\nu_1\dots\nu_{S_{\mathrm{int}}}}(D,\boldsymbol{x}) = C_{L,D}\frac{\Gamma(D/2)}{\Gamma((L+1)D/2-\nu)}\int_{\mathbb{R}_+}\mathrm{d}t\int_{\mathbb{R}_+^{S_{\mathrm{int}}}}\prod_{e=1}^{S_{\mathrm{int}}}\mathrm{d}(u_e,\nu_e) \\ \times\,(\mathcal{U}(\boldsymbol{u})+\mathcal{F}(\boldsymbol{u},\boldsymbol{x}))^{-D/2}\delta\Big(t-\textstyle\sum_{e=1}^{S_{\mathrm{int}}}u_e\Big)\,. \end{aligned} \tag{3.51}$$

Since the integrals are understood in the formal sense, the order of integration may be interchanged. Performing the t-integration then yields the *Lee–Pomeransky representation*,

$$F_{\nu_1 \ldots \nu_{S_\text{int}}}(D, \boldsymbol{x}) = C_{L,D} \frac{\Gamma(D/2)}{\Gamma((L+1)D/2 - \nu)} \int_{\mathbb{R}_+^{S_\text{int}}} \prod_{e=1}^{S_\text{int}} \mathrm{d}(u_e, \nu_e) \left(\mathcal{G}(\boldsymbol{u}, \boldsymbol{x})\right)^{-D/2}, \quad (3.52)$$

with the *Lee–Pomeransky polynomial* [154],

$$\mathcal{G}(\boldsymbol{u}, \boldsymbol{x}) = \mathcal{U}(\boldsymbol{u}) + \mathcal{F}(\boldsymbol{u}, \boldsymbol{x}) \,. \quad (3.53)$$

In this representation, the first and second graph polynomials appear on equal footing, entering only through their sum rather than as a ratio.

To establish a criterion for an integral to vanish [155, 156], consider a *corner integral*, that is, one for which each ν_e is either unity or zero,

$$F_{\nu_1 \ldots \nu_{S_\text{int}}}(D, \boldsymbol{x}) = C_{L,D} \frac{\Gamma(D/2)}{\Gamma((L+1)D/2 - \nu)} \int_{\mathbb{R}_+^{S_\text{int}}} \prod_{e=1}^{S_\text{int}} \mathrm{d}(u_e, \nu_e) \left(\mathcal{G}(\boldsymbol{u}, \boldsymbol{x})\right)^{-D/2}. \quad (3.54)$$

Scaleless integrals are those that acquire non-trivial factors under a rescaling of the internal momenta, or equivalently of the Lee–Pomeransky parameters,

$$u_e \mapsto u_e' = (1 + c_e \delta) u_e \,, \quad (3.55)$$

for an infinitesimal δ and constants c_e. Under the rescaling, Eq. (3.55), the corner integral, Eq. (3.54) transforms as

$$F_{\nu_1 \ldots \nu_{S_\text{int}}}(D, \boldsymbol{x}) = \left[1 + \delta \left(\sum_{e=1}^{S_\text{int}} c_e - \frac{D}{2}\right)\right] F_{\nu_1 \ldots \nu_{S_\text{int}}}(D, \boldsymbol{x}) + \mathcal{O}\big(\delta^2\big) \,. \quad (3.56)$$

Whenever the coefficient of the corner integral is non-zero, the integral is scaleless. Suppose instead that $\mathcal{G}$ transforms non-trivially under such a rescaling. On the one hand, this requires

$$\mathcal{G}(\boldsymbol{u}', \boldsymbol{x}) = (1 + \delta) \mathcal{G}(\boldsymbol{u}, \boldsymbol{x}) \,, \quad (3.57)$$

whilst on the other hand, an infinitesimal expansion of the left-hand side gives explicitly

$$\mathcal{G}(\boldsymbol{u}', \boldsymbol{x}) = \mathcal{G}(\boldsymbol{u}, \boldsymbol{x}) + \delta \sum_{e=1}^{S_\text{int}} c_e \frac{\partial}{\partial u_e} \mathcal{G}(\boldsymbol{u}, \boldsymbol{x}) + \mathcal{O}\big(\delta^2\big) \,. \quad (3.58)$$

Equating Eqs. (3.57) and (3.58) and taking a small but finite δ, we arrive at the *zero sector criterion*

$$0 = \left[1 - \sum_{e=1}^{S_\text{int}} c_e u_e \frac{\partial}{\partial u_e}\right] \mathcal{G}(\boldsymbol{u}, \boldsymbol{x}) \,. \quad (3.59)$$

For this to hold, the coefficient of each monomial in the u_e, including those encoding the kinematic invariants, must vanish identically. A priori, these conditions yield an overdetermined system of linear equations for the constants c_e, which may be solved straightforwardly with computer algebra. The integral is scaleless if and only if this system admits a constant solution.

In order to extend this reasoning to the full *sector*, that is, the set of Feynman integrals sharing the same pattern of positive indices, we observe that propagators with non-positive weights may be treated by repeated integration by parts. This shifts the power to which the Lee–Pomeransky polynomial is raised and generates numerator polynomials. Once the relevant derivatives have been applied, the cases of non-positive and negative integer weights become structurally analogous. The resulting numerator polynomials introduce only an additional scaling factor, leaving the argument unchanged. Hence, if the corner integral vanishes, so do all integrals in its sector [155], and such a sector is referred to as a *zero sector*.

Example 4: *For the family F_{B,ν_1,ν_2} (see Ex. 1) with $m_1^2 = m^2$ and $m_2^2 = 0$, the Lee–Pomeransky polynomial is given by*

$$\mathcal{G}(\boldsymbol{u}, \boldsymbol{x}) = u_1 + u_2 + u_1 u_2 q^2 + u_1^2 m^2 + u_1 u_2 m^2 \,. \tag{3.60}$$

When $\nu_1, \nu_2 \leq 0$, the zero-sector criterion, Eq. (3.59), is trivially satisfied, and hence all integrals are zero. In the mixed-sign cases $\nu_1 \leq 0 < \nu_2$ and $\nu_2 \leq 0 < \nu_1$, the corresponding conditions are

$$0 = (1 - c_2) u_2 \,, \tag{3.61}$$

$$0 = (1 - c_1) u_1 + (1 - 2c_1) u_1^2 m^2 \,, \tag{3.62}$$

respectively. While Eq. (3.61) admits a solution, Eq. (3.62) does not. It follows that integrals with $\nu_1 \leq 0 < \nu_2$ are zero, whereas those with $\nu_2 \leq 0 < \nu_1$ are non-zero. If both weights are strictly positive, the criterion takes the form

$$0 = (1 - c_1) u_1 + (1 - c_2) u_2 + (1 - 2c_1) u_1^2 m^2 + (1 - c_1 - c_2) u_1 u_2 (m^2 + q^2), \tag{3.63}$$

and admits no solution. As a consequence, all integrals with $0 < \nu_1, \nu_2$ are non-zero.

The example suggests that, in practice, not all corner integrals need to be checked explicitly. Indeed, a sector with fewer positive weights being zero may already imply that sectors with a larger number of positive weights are also zero. It is therefore sufficient to proceed in a bottom-up manner, considering sectors in order of increasing numbers of positive weights. At each stage, we check whether the current sector contains a zero-sector.

3.1.4 Sector Symmetries

A further application of the Lee–Pomeransky polynomial, Eq. (3.53) is the identification of symmetries amongst Feynman integrals. To this end, we note that the Lee–Pomeransky polynomial may in full generality be written as

$$\mathcal{G}(\boldsymbol{u}, \boldsymbol{x}) = \sum_{(k_1,\ldots,k_{S_\text{int}}) \in \mathbb{N}^{S_\text{int}}} c_{k_1,\ldots,k_{S_\text{int}}}(\boldsymbol{x}) \prod_{i=1}^{S_\text{int}} u_i^{k_i} \,, \tag{3.64}$$

where almost all coefficients $c_{k_1,\ldots,k_{S_\text{int}}}$ either vanish or depend on kinematic invariants. The coefficients are furthermore assumed to be at most linear in the kinematic invariants, with each depending on at most one invariant,

$$\frac{\partial^2 c_{k_1,\ldots,k_{S_\text{int}}}(\boldsymbol{x})}{\partial x_i \, \partial x_j} = 0 \,, \qquad \forall\, i, j \leq S_\text{ext}, \tag{3.65}$$

$$\frac{\partial c_{k_1,\ldots,k_{S_\mathrm{int}}}(\boldsymbol{x})}{\partial x_i} \neq 0 \implies \frac{\partial c_{k_1,\ldots,k_{S_\mathrm{int}}}(\boldsymbol{x})}{\partial x_j} = 0\,, \qquad \forall\, j \neq i,\ j \leq S_\mathrm{ext}. \tag{3.66}$$

From the coefficients of $\mathcal{G}$, the coloured bipartite graph $\mathrm{B}[\mathcal{G}]$ is built by assigning a vertex $v_{k_1,\ldots,k_{S_\mathrm{int}}}$ to each non-zero coefficient $c_{k_1,\ldots,k_{S_\mathrm{int}}}$ and a vertex to each variable u_e, with vertex and edge sets

$$\mathcal{V}_{B[\mathcal{G}]} = \left[\bigsqcup_{e=1}^{S_\mathrm{int}} \{\, u_e \,\}\right] \sqcup \left[\bigsqcup_{(k_1,\ldots,k_{S_\mathrm{int}})\in\mathbb{N}^{S_\mathrm{int}}\,:\,0\neq c_{k_1,\ldots,k_{S_\mathrm{int}}}} \left\{ v_{k_1,\ldots,k_{S_\mathrm{int}}} \right\}\right], \tag{3.67}$$

$$\mathcal{E}_{B[\mathcal{G}]} = \bigsqcup_{(k_1,\ldots,k_{S_\mathrm{int}})\in\mathbb{N}^{S_\mathrm{int}}\,:\,0\neq c_{k_1,\ldots,k_{S_\mathrm{int}}}} \ \bigsqcup_{e\leq S_\mathrm{int}:k_e\neq 0} \left\{ v_{k_1,\ldots,k_{S_\mathrm{int}}}, u_e \right\}, \tag{3.68}$$

where the edges are coloured by the kinematic invariant appearing in the corresponding monomial. Automorphisms of this graph then correspond to symmetries of the integrand. In practice, identifying integral symmetries reduces to computing graph automorphisms, for which efficient implementations are readily available. One such implementation is, for instance, `Feynson` [157].

Example 5: *For the family $F_{B,\nu_1\nu_2}$ with non-degenerate masses $m_1^2 \neq m_2^2$, the Lee–Pomeransky polynomial reads*

$$\mathcal{G}(\boldsymbol{u},\boldsymbol{x}) = u_1 + u_2 + q^2 u_1 u_2 + (m_1^2 u_1 + m_2^2 u_2)(u_1 + u_2)\,. \tag{3.69}$$

Compared to the original two vertices and two edges, the associated bipartite graph has nine vertices and twelve edges, with multiple edges indicated by a dot,

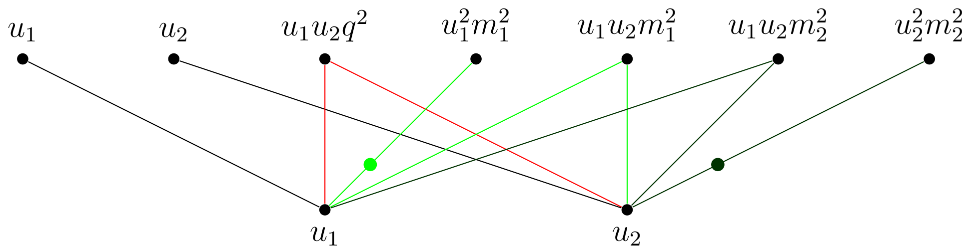

and admits no non-trivial automorphism. When $m_1^2 = m_2^2 = m^2$, the bipartite graph

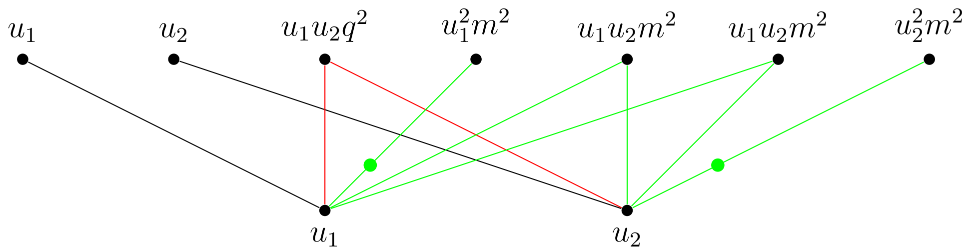

acquires a non-trivial automorphism corresponding to the exchange $u_1 \leftrightarrow u_2$. This symmetry reflects the shift $k \mapsto k - q$ of the loop momentum, under which each propagator picks up a sign that drops out, since the edge momentum appears only squared.

One common source of confusion deserves mention here. The strategy outlined above does not capture all symmetries of a Feynman integral, since not every integral symmetry manifests as a symmetry of the integrand. In particular, the method detects only symmetries within a given integral family, remaining insensitive to the propagator weights and to external symmetries acting on the kinematic invariants.

For factorised graphs, the product of the Lee–Pomeransky polynomials of each factor need not agree with that of the whole graph, so the corresponding bipartite graphs may have vertex sets of differing degrees, precluding any automorphism between them. What the method provides, therefore, are symmetries of sectors rather than of the integral itself.

Example 6: *To illustrate how integral symmetries need not manifest as symmetries of the integrand, consider a massless integral with edge momenta $q_1 = k_1$ and $q_2 = k_1 + q$, and weights $\nu_1 = 1$ and $\nu_2 = 2$. The Lee–Pomeransky polynomial reads*

$$\mathcal{G}_2(\boldsymbol{u}, \boldsymbol{x}) = u_1 + u_2 + q^2 u_1 u_2 \,. \tag{3.70}$$

Instead, the same integral can be written by introducing a degenerate edge momentum $q_3 = q_2$ with the adjusted weights $\nu_2 = \nu_3 = 1$. The corresponding Lee–Pomeransky polynomial reads

$$\mathcal{G}_3(\boldsymbol{u}, \boldsymbol{x}) = u_1 + u_2 + u_3 q^2 (u_1 u_2 + u_1 u_3) \,. \tag{3.71}$$

Although the two representations are equivalent, the polynomials are not isomorphic, as is already evident from their dependence on different numbers of variables, and the automorphism-based method therefore fails to identify the symmetry.

The translation of graph polynomials into bipartite graphs and the subsequent computation of graph automorphisms are both computationally expensive. Even though Feynman graphs typically have few vertices by the standards of modern graph theory, the associated bipartite graphs may contain orders of magnitude more vertices and edges. For the integrals considered in this work, which all admit a graphical representation, it therefore proves advantageous to work directly with the Feynman graph and bypass the bipartite construction entirely. The scaling behaviour of both approaches is examined below.

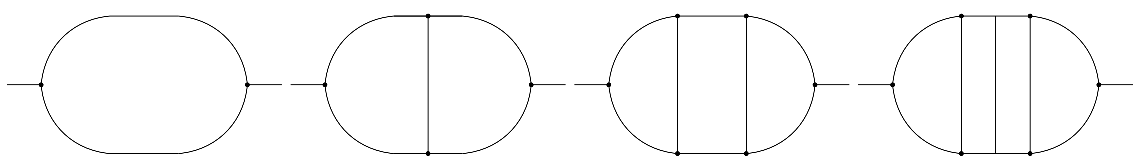

Figure 3.1: Ladder graphs at one-, two-, three-, and four-loop order, respectively.

To illustrate this growth, consider the massless *ladder graph* family shown in Fig. 3.1, which has

$$V = 2L \,, \tag{3.72}$$
$$E = 3L - 1 \tag{3.73}$$

vertices and edges respectively. The numbers of terms in the graph polynomials follow the recursively defined sequences A001353 [158] and A317405 [159],

$$N_{\mathcal{U}}(L) = \hat{N}_{\mathcal{U}}(L), \qquad \text{with} \qquad \hat{N}_{\mathcal{U}}(0) = 0, \qquad \hat{N}_{\mathcal{U}}(1) = 2 \,, \tag{3.74}$$

$$N_{\mathcal{F}}(L) = L\,\hat{N}_{\mathcal{F}}(L), \qquad \text{with} \qquad \hat{N}_{\mathcal{F}}(0) = 0, \qquad \hat{N}_{\mathcal{F}}(1) = 1\,, \tag{3.75}$$

where

$$\hat{N}_i(L) = 4\,\hat{N}_i(L-1) - \hat{N}_i(L-2)\,. \tag{3.76}$$

Recalling that the first and second graph polynomials are of degrees L and $L+1$ respectively, the vertex and edge counts of the bipartite graph read

$$V_{\mathrm{B}[\mathcal{G}]} = N_{\mathcal{U}}(L) + N_{\mathcal{F}}(L) + E\,, \tag{3.77}$$
$$E_{\mathrm{B}[\mathcal{G}]} = L\,N_{\mathcal{U}}(L) + (L+1)N_{\mathcal{F}}(L)\,, \tag{3.78}$$

where multi-edges are included. Both sequences grow exponentially with the loop order. To determine the asymptotic behaviour for large L, the characteristic equation method assumes a solution of the form

$$\hat{N}_i(L) = C_i \hat{N}_{i,0}^{L+1}\,, \tag{3.79}$$

with C_i a constant of proportionality. Inserting this ansatz into the recurrence relation gives

$$\hat{N}_{i,0}^{L+1} - 4\hat{N}_{i,0}^{L} + \hat{N}_{i,0}^{L-1} = 0 \qquad \Longrightarrow \qquad \hat{N}_{i,0} = 2 + \sqrt{3}\,. \tag{3.80}$$

As an immediate consequence, the leading asymptotic behaviour of both sequences reads

$$\hat{N}_i(L) \sim c_i \hat{N}_0^{L+1}\,, \tag{3.81}$$

where the constants C_i are fixed so as to compensate for the slow convergence at low loop order,

$$c_{\mathcal{U}} = \frac{8}{\hat{N}_{\mathcal{U},0}}\,, \tag{3.82}$$
$$c_{\mathcal{F}} = \frac{4}{\hat{N}_{\mathcal{F},0}}\,. \tag{3.83}$$

In Tab. 3.1, this approximation is already in excellent agreement with the exact combinatorics at low loop orders. The vertex and edge counts of the bipartite graph are therefore governed by exponential growth modulated by a polynomial prefactor, with the two sequences differing only in their initial values.

These estimates apply to a particularly simple class of graphs, and more complex topologies yield even less favourable combinatorics. In practice, however, graph automorphism remains tractable thanks to highly efficient implementations, of which `nauty` and `Traces` [160] are the most widely used.

L	1	2	3	4	5	6
$\hat{N}_{\mathcal{U}}(L)$	2.1436	8.0000	29.856	111.43	415.85	1552.0
$N_{\mathcal{U}}(L)$	2	8	30	112	418	1560
$\hat{N}_{\mathcal{F}}(L)$	1.0718	4.0000	14.928	55.713	207.92	775.98
$N_{\mathcal{F}}(L)$	1	4	15	56	209	780

Table 3.1: Comparison of the asymptotic approximation with the exact values for the number of terms in the graph polynomials.

3.2 Dimensional Regularisation

In general, Feynman integrals are not well defined as ordinary integrals, exhibiting *ultraviolet* singularities when the internal momenta become large and *infrared* singularities when they vanish. Passing to renormalised integrands removes the ultraviolet divergences [150, 161–163], and in sufficiently high space-time dimension the resulting integrals are infrared finite as well.

Once rendered finite, these integrals admit a rigorous definition through the parametric representation [164], in which the space-time dimension enters only as a parameter and may be analytically continued to complex values, whilst the physical space-time itself remains integer-dimensional throughout [165, 166]. The parametric framework is particularly well suited to this construction, since the graph polynomials are inherently compatible with the contraction and deletion of edges and subgraphs, and thus with the procedure of renormalisation.

Concretely, the space-time dimension is written as $D = D_0 - 2\varepsilon$, with $D_0 \in \mathbb{N}$ the integer part and ε the dimensional regulator [93], so that Feynman integrals are understood not as ordinary integrals but as operators assigning a Laurent series in ε to an integrand. In practice, it is often preferable to work in momentum space, where the dimensionally regularised integral is defined axiomatically as a linear operator [92, 115],

$$\int \frac{\mathrm{d}^D k}{\pi^{D/2}} \left[c_1 \Phi_1(k) + c_2 \Phi_2(k)\right] = c_1 \int \frac{\mathrm{d}^D k}{\pi^{D/2}} \Phi_1(k) + c_2 \int \frac{\mathrm{d}^D k}{\pi^{D/2}} \Phi_2(k)\,, \tag{3.84}$$

for any complex constants c_1, c_2 and any integrands Φ_1, Φ_2. The remaining axioms require invariance under translations by a vector p, invariance under rescaling by a complex constant λ, and normalisation to unity on the Gaussian integrand,

$$\int \frac{\mathrm{d}^D k}{\pi^{D/2}} \Phi(k+p) = \int \frac{\mathrm{d}^D k}{\pi^{D/2}} \Phi(k)\,, \tag{3.85}$$

$$\int \frac{\mathrm{d}^D k}{\pi^{D/2}} \Phi(\lambda k) = \frac{1}{\lambda^D} \int \frac{\mathrm{d}^D k}{\pi^{D/2}} \Phi(k)\,, \tag{3.86}$$

$$\int \frac{\mathrm{d}^D k}{\pi^{D/2}} e^{-k^2} = 1\,. \tag{3.87}$$

Seemingly innocuous, these axioms give rise to non-trivial relations amongst integrals. Expanding Eqs. (3.85) and (3.86) to first order in ϵ under the infinitesimal translation $k \mapsto k + \epsilon p$ and the infinitesimal rescaling $k \mapsto (1+\epsilon)k$, respectively, and applying integration by parts to the result, we obtain

$$\begin{aligned} \int \frac{\mathrm{d}^D k}{\pi^{D/2}} \Phi(k) &= \int \frac{\mathrm{d}^D k}{\pi^{D/2}} \Phi(k + \epsilon p) \\ &= \int \frac{\mathrm{d}^D k}{\pi^{D/2}} \Phi(k) + \epsilon p^\mu \int \frac{\mathrm{d}^D k}{\pi^{D/2}} \frac{\partial \Phi(k)}{\partial k^\mu} + \mathcal{O}(\epsilon^2)\,, \end{aligned} \tag{3.88}$$

$$\begin{aligned} \int \frac{\mathrm{d}^D k}{\pi^{D/2}} \Phi(k) &= (1+\epsilon)^D \int \frac{\mathrm{d}^D k}{\pi^{D/2}} \Phi((1+\epsilon)k) \\ &= \int \frac{\mathrm{d}^D k}{\pi^{D/2}} \Phi(k) + \epsilon \int \frac{\mathrm{d}^D k}{\pi^{D/2}} \frac{\partial}{\partial k^\mu} \left[k^\mu \Phi(k)\right] + \mathcal{O}(\epsilon^2)\,, \end{aligned} \tag{3.89}$$

from which it follows that

$$0 = \int \frac{\mathrm{d}^D k}{\pi^{D/2}} \frac{\partial}{\partial k^\mu} \left[p^\mu \Phi(k) \right] , \tag{3.90}$$

$$0 = \int \frac{\mathrm{d}^D k}{\pi^{D/2}} \frac{\partial}{\partial k^\mu} \left[k^\mu \Phi(k) \right] . \tag{3.91}$$

Both (3.90) and (3.91) hold for any linear combination of internal and external momenta q_{IBP}, giving rise to *IBP identities* [94–96],

$$0 = \int \frac{\mathrm{d}^D k}{\pi^{D/2}} \frac{\partial}{\partial k^\mu} \left[{q_{\mathrm{IBP}}}^\mu \Phi(k) \right] . \tag{3.92}$$

These identities connect integrals within the same family but with different weights, enabling systematic raising or lowering of individual propagator powers.

3.3 Master Integrals

3.3.1 Integration by Parts

Through IBP identities, Eq. (3.92), any integral in a family may be expressed as a linear combination of a finite set of linearly independent integrals [154, 167], called *master integrals*. To facilitate the reduction, a handful of bookkeeping parameters are associated to each integral embedded in a family,

$$t[F_{\nu_i \ldots \nu_{S_{\mathrm{int}}}}(D, \boldsymbol{x})] = \sum_{e=1}^{S_{\mathrm{int}}} \theta(\nu_e - 1/2) , \tag{3.93}$$

$$n[F_{\nu_i \ldots \nu_{S_{\mathrm{int}}}}(D, \boldsymbol{x})] = \sum_{e=1}^{S_{\mathrm{int}}} \theta(\nu_e - 1/2) 2^{e-1} , \tag{3.94}$$

$$s[F_{\nu_i \ldots \nu_{S_{\mathrm{int}}}}(D, \boldsymbol{x})] = \sum_{e=1}^{S_{\mathrm{int}}} \theta(\nu_e - 1/2) \nu_e , \tag{3.95}$$

$$r[F_{\nu_i \ldots \nu_{S_{\mathrm{int}}}}(D, \boldsymbol{x})] = \sum_{e=1}^{S_{\mathrm{int}}} \theta(1/2 - \nu_e)(-\nu_e) , \tag{3.96}$$

$$d[F_{\nu_i \ldots \nu_{S_{\mathrm{int}}}}(D, \boldsymbol{x})] = \sum_{e=1}^{S_{\mathrm{int}}} \theta(\nu_e - 3/2)(\nu_e - 1) , \tag{3.97}$$

where t denotes the number of propagators with strictly positive weights, n the sector, s the combined weight of all positive powers, r the number of numerator propagators, and d the total excess power above unity (also called *dots*). Subsequently, integrals are assumed to be ordered lexicographically by

$$t > n > r > d > s . \tag{3.98}$$

The ordering, Eq. (3.98), is common but a priori arbitrary. Indeed, there is no reason to expect that integrals with few numerator propagators yield simpler IBP identities than those with few dots.

More motivated alternatives, such as ordering first by sector and subsequently by properties of the underlying geometry, arise naturally in the context of twisted cohomology [168–170]. At the time of writing, however, such orderings have not been explored enough to find widespread use in practice.

Example 7: *Consider the family F_{B,ν_1,ν_2} (see Ex. 1) with equal masses $m_1^2 = m_2^2 = m^2$ and $p^2 \neq 0$, and strictly positive weights $\nu_1, \nu_2 > 0$. Taking $q_{\text{IBP}} = k$ and $q_{\text{IBP}} = q$ in Eq.* (3.92) *yields two IBP identities,*

$$\begin{aligned} 0 &= (D - \nu_1 - 2\nu_2) F_{B,\nu_1\nu_2}(D, \boldsymbol{x}) - \nu_2(2m^2 - q^2) F_{B,\nu_1(\nu_2+1)}(D, \boldsymbol{x}) \\ &\quad - \nu_2 F_{B,(\nu_1-1)(\nu_2+1)}(D, \boldsymbol{x}) - 2\nu_1 m^2 F_{B,(\nu_1+1)\nu_2}(D, \boldsymbol{x}) \,, \end{aligned} \tag{3.99}$$

$$\begin{aligned} 0 &= (\nu_1 - \nu_2) F_{B,\nu_1\nu_2}(D, \boldsymbol{x}) - \nu_2 q^2 F_{B,\nu_1(\nu_2+1)} + \nu_2 F_{B,(\nu_1-1)(\nu_2+1)}(D, \boldsymbol{x}) \\ &\quad + \nu_1 q^2 F_{B,(\nu_1+1)\nu_2}(D, \boldsymbol{x}) - \nu_1 F_{B,(\nu_1+1)(\nu_2-1)}(D, \boldsymbol{x}) \,. \end{aligned} \tag{3.100}$$

Through a suitable linear combination of Eqs. (3.99) *and* (3.100) *another, more useful, identity is found*

$$\begin{aligned} \nu_2 q^2 (4m^2 - q^2) F_{B,\nu_1(\nu_2+1)}(D, \boldsymbol{x}) &= \big(D q^2 + 2\nu_1(m^2 - q^2) - \nu_2(2m^2 + q^2)\big) F_{B,\nu_1\nu_2}(D, \boldsymbol{x}) \\ &\quad + \nu_2(2m^2 - q^2) F_{B,(\nu_1-1)(\nu_2+1)}(D, \boldsymbol{x}) - 2\nu_1 m^2 F_{B,(\nu_1+1)(\nu_2-1)}(D, \boldsymbol{x}) \,. \end{aligned} \tag{3.101}$$

Using this identity repeatedly, each application reduces the total weight by one, since the left-hand side carries weight $\nu_1+\nu_2+1$ whilst the right-hand side has weight $\nu_1+\nu_2$.

Lifting the constraint $0 < \nu_1$ and setting $\nu_2 = 0$ with $q_{\text{IBP}} = k$ yields a further identity

$$0 = (D - 2\nu_1) F_{B,\nu_1,0}(D, \boldsymbol{x}) - 2\nu_1 m^2 F_{B,(\nu_1+1),0}(D, \boldsymbol{x}) \,, \tag{3.102}$$

which upon repeated application reduces ν_1 to unity. By symmetry, the analogous reduction holds when $\nu_1 = 0$ and $0 < \nu_2$. Every integral within the family may therefore be expressed as a linear combination of precisely two master integrals,

$$F_{B,\nu_1\nu_2}(D, \boldsymbol{x}) = c_{11,\nu_1\nu_2}(D, \boldsymbol{x}) F_{B,11}(D, \boldsymbol{x}) + c_{10,\nu_1\nu_2}(D, \boldsymbol{x}) F_{B,10}(D, \boldsymbol{x}) \,. \tag{3.103}$$

Symbolic IBP reductions are implemented in `Forcer` [171], `Mincer` [172, 173] and `Matad` [174], which are written in FORM [175], and in `LiteRed` [156], which interfaces with MATHEMATICA. Generally, a closed-form solution to the identities is not available, and the method is typically restricted to problems with few loops or a single kinematic invariant such as in the context of massive vacuum graphs or massless two-point functions. In all cases the strategy proceeds sector by sector, generating and solving IBP identities, applying symmetry relations, and discarding integrals in zero sectors, until each sector is expressed in terms of master integrals and contributions from lower sectors. This procedure is repeated recursively until every integral in the family has been reduced to a master integral.

When the number of loops or scales renders a symbolic approach intractable, the *Laporta algorithm* [176] becomes the method of choice. Rather than solving the identities in closed form, explicit integer values are substituted for the propagator weights, generating a large linear system whose coefficients are rational functions of the kinematic invariants and the space-time dimension. Gaussian elimination then expresses harder integrals, ranked by the ordering defined above, in terms of simpler ones. Iterating this across all sectors either reduces every integral to a master integral or establishes that it vanishes. The reduction is guaranteed to terminate for any fixed set of weight values with no need for a closed-form solution, which is precisely what renders the approach superior to symbolic methods. The algorithm finds various implementations such as `Kira` [177–179], `Fire` [180–182] and `Reduze` [183, 184].

Both approaches share a common subtlety in that the choice of ordering determines which integrals are identified as master integrals, and different choices can yield reductions of vastly different complexity. In particular, certain orderings produce reductions whose rational coefficients have denominators that do not factorise into separate functions of the kinematic scales and the space-time dimension, a situation referred to as *bad denominators* [185, 186]. Such denominators significantly complicate subsequent manipulations, and a judicious choice of ordering is therefore essential for a tractable reduction.

3.3.2 Dimensional Shifts

Feynman integrals in different space-time dimensions are related by *dimensional shift relations* [187, 188], which connect integrals at dimension D to those at dimension $D \pm 2$. Such relations prove particularly useful when the integrand simplifies in a shifted dimension, or when combined with IBP identities. Two families of operators formalise this connection. The first is the *dimensional shift operator* $\mathbf{D}^{\pm}$, defined by

$$\mathbf{D}^{\pm} F_{\nu_1,\ldots\nu_{S_{\text{int}}}}(D,\boldsymbol{x}) = F_{\nu_1,\ldots\nu_{S_{\text{int}}}}(D \pm 2,\boldsymbol{x})\,, \tag{3.104}$$

and the second consists of the *raising operators* $\mathbf{R}_e^+$, which increase the weight of the e-th propagator by one unit,

$$\mathbf{R}_j^+ F_{\nu_1,\ldots\nu_j\ldots\nu_{S_{\text{int}}}}(D,\boldsymbol{x}) = \nu_j F_{\nu_1,\ldots(\nu_j+1)\ldots\nu_{S_{\text{int}}}}(D,\boldsymbol{x})\,. \tag{3.105}$$

The action of these operators on a Feynman integral is most transparently verified by means of the Schwinger representation, Eq. (3.47),

$$\mathbf{D}^+ F_{\nu_1,\ldots\nu_j\ldots\nu_{S_{\text{int}}}}(D,\boldsymbol{x}) = C_{L,D}\int_{\mathbb{R}_+^E}\prod_{e=1}^{S_{\text{int}}}\mathrm{d}(\alpha_e,\nu_e)\exp\left(-\frac{\mathcal{F}(\boldsymbol{\alpha},\boldsymbol{x})}{\mathcal{U}(\boldsymbol{\alpha})}\right)[\mathcal{U}(\boldsymbol{\alpha})]^{-(D+2)/2}\,, \tag{3.106}$$

$$\mathbf{R}_j^+ F_{\nu_1,\ldots\nu_j\ldots\nu_{S_{\text{int}}}}(D,\boldsymbol{x}) = C_{L,D}\int_{\mathbb{R}_+^E}\prod_{e=1}^{S_{\text{int}}}\mathrm{d}(\alpha_e,\nu_e)\exp\left(-\frac{\mathcal{F}(\boldsymbol{\alpha},\boldsymbol{x})}{\mathcal{U}(a)}\right)\alpha_j\,[\mathcal{U}(\boldsymbol{\alpha})]^{-D/2}\,, \tag{3.107}$$

where we have used $\Gamma(\nu_j+1) = \nu_j\Gamma(\nu_j)$. Combining Eqs. (3.106) and (3.107) yields the commutation relations

$$\left[\mathbf{R}_i^+, \mathbf{R}_j^+\right] = 0\,, \tag{3.108}$$

$$\left[\mathbf{R}_j^+, \mathbf{D}^{\pm}\right] = 0\,. \tag{3.109}$$

To each Schwinger parameter, we may associate a raising operator via the map satisfying

$$R^+(\alpha_j) = \mathbf{R}_j^+\,, \tag{3.110}$$

and derive the *dimensional shift relation*,

$$\begin{aligned} F_{\nu_1,\ldots\nu_j\ldots\nu_{S_{\text{int}}}}(D,\boldsymbol{x}) &= C_{L,D}\int_{\mathbb{R}_+^E}\prod_{e=1}^{S_{\text{int}}}\mathrm{d}(\alpha_e,\nu_e)\exp\left(-\frac{\mathcal{F}(\boldsymbol{\alpha}.\boldsymbol{x})}{\mathcal{U}(\boldsymbol{\alpha})}\right)[\mathcal{U}(\boldsymbol{\alpha})]^{-D/2} \\ &= \mathcal{U}(R^+(\boldsymbol{\alpha}))\,\mathbf{D}^+ F_{\nu_1,\ldots\nu_j\ldots\nu_{S_{\text{int}}}}(D,\boldsymbol{x})\,, \end{aligned} \tag{3.111}$$

a relation between integrals in D and $D+2$ dimensions. Taking the master integrals as a basis $\mathbf{F}$ and reducing the raised-index integrals on the right-hand side by means of IBP identities, we arrive at the matrix equation

$$I(D,\boldsymbol{x}) = S(D,\boldsymbol{x})\, I(D+2,\boldsymbol{x})\,, \tag{3.112}$$

where S is a matrix whose entries are rational functions of the space-time dimension and of the kinematic invariants, and whose invertibility follows immediately from the observation,

$$\mathbf{D}^{\pm}\mathbf{D}^{\mp} = \mathrm{id}\,. \tag{3.113}$$

Example 8: *Consider the family F_{B,ν_1,ν_2} with equal masses and master integrals chosen as in Ex. 7. Direct application of the dimensional shift relation, Eq.* (3.111), *leads to*

$$F_{B,\nu_1\nu_2}(D,\boldsymbol{x}) = \mathcal{U}_B(\mathbf{1}^+,\mathbf{2}^+) F_{B,\nu_1\nu_2}(D+2,\boldsymbol{x})\,. \tag{3.114}$$

Employing the raising operators together with the symmetries of the family then yields

$$\begin{bmatrix} F_{B,1,0} \\ F_{B,1,1} \end{bmatrix} (D,\boldsymbol{x}) = \begin{bmatrix} F_{B,2,0} \\ 2F_{B,2,1} \end{bmatrix} (D+2,\boldsymbol{x})\,. \tag{3.115}$$

Reducing the right-hand side to the master basis via Eqs. (3.99)–(3.102) *gives the dimensional shift matrix*

$$\begin{bmatrix} F_{B,1,0} \\ F_{B,1,1} \end{bmatrix} (D,\boldsymbol{x}) = \underbrace{\begin{bmatrix} \frac{D}{2m^2} & 0 \\ \frac{D}{m^2(4m^2-q^2)} & \frac{2(D-1)}{4m^2-q^2} \end{bmatrix}}_{S_B(D,\boldsymbol{x})} \begin{bmatrix} F_{B,1,0} \\ F_{B,1,1} \end{bmatrix} (D+2,\boldsymbol{x})\,, \tag{3.116}$$

which is invertible for all space-time dimensions except at $D=0$ and $D=1$, two cases of no physical interest.

3.3.3 Differential Equations

To evaluate the master integrals, we employ the method of differential equations [97–99], though their derivation does not always proceed by direct differentiation. Since the second graph polynomial is linear in all kinematic invariants and scales, it satisfies the Euler relation

$$\mathcal{F}(\boldsymbol{\alpha},\boldsymbol{x}) = \sum_{j=1}^{S_{\mathrm{int}}} \frac{\partial \mathcal{F}(\boldsymbol{\alpha},\boldsymbol{x})}{\partial x_j} x_j\,. \tag{3.117}$$

Differentiating the Schwinger representation, Eq. (3.47), with respect to x_j and using Eq. (3.117) gives

$$\frac{\partial}{\partial x_j} F_{\nu_1,\ldots\nu_{S_{\mathrm{int}}}}(D,\boldsymbol{x}) = C_{L,D} \int_{\mathbb{R}_+^E} \prod_{e=1}^{S_{\mathrm{int}}} \mathrm{d}(\alpha_e,\nu_e)\, \frac{1}{[\mathcal{U}(\boldsymbol{\alpha})]^{-D/2}} \frac{\partial \mathcal{F}(\boldsymbol{\alpha},\boldsymbol{x})}{\partial x_j} \exp\left(-\frac{\mathcal{F}(\boldsymbol{\alpha},\boldsymbol{x})}{\mathcal{U}(\boldsymbol{\alpha})}\right), \tag{3.118}$$

where the derivative acts only on the exponent through the second graph polynomial, leaving the measure unchanged. Comparing with the definitions of the dimensional shift and raising operators, Eqs. (3.104) and (3.105), the partial derivative may be written as

$$\frac{\partial}{\partial x_j} F_{\nu_1,\ldots\nu_{S_{\rm int}}}(D,\boldsymbol{x}) = -\frac{\partial \mathcal{F}(R^+(\boldsymbol{\alpha}),\boldsymbol{x}))}{\partial x_j}\mathbf{D}^+ F_{\nu_1,\ldots\nu_{S_{\rm int}}}(D,\boldsymbol{x})\,. \tag{3.119}$$

Consequently, Eq. (3.119), allows derivatives with respect to the kinematic invariants to be computed without introducing the Gram determinants that would otherwise arise [156].

For a basis of master integrals $\boldsymbol{F}$, differentiating with respect to an invariant x_j, applying dimensional shift relations, and reducing via IBP yields a system of differential equations,

$$\partial_{x_j}\mathbf{F}(D,\boldsymbol{x}) = A_{x_j}(D,\boldsymbol{x})\mathbf{F}(D,\boldsymbol{x})\,, \tag{3.120}$$

where A_{x_j} is a matrix of rational functions of the space-time dimension and the kinematic invariants. Repeating this for all invariants and assembling the result into a total differential,

$$\mathrm{d}\mathbf{F}(D,\boldsymbol{x}) = A(D,\boldsymbol{x})\mathbf{F}(D,\boldsymbol{x})\,, \tag{3.121}$$

with the total differential of the master integrals and the *connection matrix* defined respectively by

$$\mathrm{d}\mathbf{F}(D,\boldsymbol{x}) = \sum_{j=1}^{S_{\rm ext}} \frac{\partial}{\partial x_j}\mathbf{F}(D,\boldsymbol{x})\,\mathrm{d}x_j\ , \tag{3.122}$$

$$A(D,\boldsymbol{x}) = \sum_{j=1}^{S_{\rm int}} A_{x_j}(D,\boldsymbol{x})\,\mathrm{d}x_j\ . \tag{3.123}$$

Although deriving the differential equations via the second graph polynomial is conceptually straightforward, it is computationally expensive, since the total propagator weight is shifted by the degree of the second graph polynomial, rendering the subsequent IBP reductions significantly more costly.

At times it proves more efficient to differentiate directly with respect to the kinematic invariants. For masses this is straightforward, but for momentum invariants it is less immediate [189]. In the case of a two-point function, for instance, we find

$$\frac{\partial}{\partial q^2} = \frac{q^\mu}{2q^2}\frac{\partial}{\partial q^\mu}\,, \tag{3.124}$$

whereas for more general scalar products the momenta depend implicitly on the invariants, and naive differentiation gives rise to Gram determinants, since each kinematic invariant is formally a function of the external momenta, or rather their components.

Example 9: *Consider the family F_{B,ν_1,ν_2} with equal masses and master integrals chosen as in Ex. 7. Application of the dimensional shift relation, Eq.* (3.116)*, and IBP identities, Eqs.* (3.99) *to* (3.102)*, yields the differential equations,*

$$\begin{aligned}\partial_{m^2}\begin{bmatrix} F_{B,10} \\ F_{B,11}\end{bmatrix}(D,\boldsymbol{x}) &= \begin{bmatrix} -2F_{B,30} \\ -4F_{B,31}-2F_{B,22}\end{bmatrix}(D,\boldsymbol{x}) \\ &= \begin{bmatrix} \frac{D-2}{2m^2} & 0 \\ \frac{2-D}{m^2(4m^2-q^2)} & \frac{2(D-3)}{4m^2-q^2}\end{bmatrix}\begin{bmatrix} F_{B,10} \\ F_{B,11}\end{bmatrix}(D,\boldsymbol{x})\,,\end{aligned} \tag{3.125}$$

$$
\begin{aligned}
\partial_{q^2}\begin{bmatrix} F_{B,10} \\ F_{B,11} \end{bmatrix}(D,\boldsymbol{x}) &= \begin{bmatrix} 0 \\ 2F_{B,22} \end{bmatrix}(D,\boldsymbol{x}) \\
&= \begin{bmatrix} 0 & 0 \\ \frac{2-D}{q^2(q^2-4m^2)} & \frac{(D-4)q^2+4m^2}{2q^2(q^2-4m^2)} \end{bmatrix}\begin{bmatrix} F_{B,10} \\ F_{B,11} \end{bmatrix}(D,\boldsymbol{x}) \,.
\end{aligned}
\tag{3.126}
$$

To derive the differential equations, it suffices to compute the graph polynomials once for the top sector of a complete integral family, since all subsectors follow from it. Subsectors correspond to integrals with some propagator weights set to zero, so any raising operator acting on a vanishing propagator contributes nothing. The graph polynomial of a subsector is therefore recovered from that of the top sector by setting the corresponding Schwinger parameters to zero, which is precisely the same operation.

Consistency of the differential equation requires the *integrability condition*, which follows from the equality of mixed partial derivatives and reads

$$
\mathrm{d}A(D,\boldsymbol{x}) = A(D,\boldsymbol{x}) \wedge A(D,\boldsymbol{x}) \,. \tag{3.127}
$$

This is, however, a trivial check whenever the differential equation involves only a single variable. A more meaningful consistency condition arises from the *scaling relation*, obtained by exploiting the linearity of the second graph polynomial in the kinematic invariants,

$$
\sum_{j=1}^{S_{\mathrm{ext}}} x_j \frac{\partial}{\partial x_j} F_{\nu_1,\ldots\nu_j\ldots\nu_{S_{\mathrm{int}}}}(D,\boldsymbol{x}) = \left(\frac{LD}{2} - \nu\right) F_{\nu_1,\ldots\nu_j\ldots\nu_{S_{\mathrm{int}}}}(D,\boldsymbol{x}) \,. \tag{3.128}
$$

Example 10: *Both consistency checks are demonstrated through Ex. 9. Direct computation confirms the integrability condition,*

$$
\begin{aligned}
A(D,\boldsymbol{x}) \wedge A(D,\boldsymbol{x}) &= \left(A_{m^2}(D,\boldsymbol{x})A_{q^2}(D,\boldsymbol{x}) - A_{q^2}(D,\boldsymbol{x})A_{m^2}(D,\boldsymbol{x})\right)\mathrm{d}q^2 \wedge \mathrm{d}m^2 \\
&= \begin{bmatrix} 0 & 0 \\ \frac{2-D}{q^2m^2(4m^2-q^2)} & 0 \end{bmatrix} \mathrm{d}q^2 \wedge \mathrm{d}m^2 \,,
\end{aligned}
\tag{3.129}
$$

$$
\begin{aligned}
\mathrm{d}A(D,\boldsymbol{x}) &= \left(\partial_{q^2}A_{m^2}(D,\boldsymbol{x}) - \partial_{m^2}A_{q^2}(D,\boldsymbol{x})\right)\mathrm{d}q^2 \wedge \mathrm{d}m^2 \\
&= \begin{bmatrix} 0 & 0 \\ \frac{2-D}{q^2m^2(4m^2-q^2)} & 0 \end{bmatrix} \mathrm{d}q^2 \wedge \mathrm{d}m^2 \,.
\end{aligned}
\tag{3.130}
$$

Hence the integrability condition is satisfied. For a generic integral in the family with arbitrary weights, the scaling relation reads

$$
\left(q^2\partial_{q^2} + m^2\partial_{m^2}\right) F_{B,\nu_1\nu_2}(D,\boldsymbol{x}) = \left(\frac{D}{2} - \nu_1 - \nu_2\right) F_{B,\nu_1\nu_2}(D,\boldsymbol{x}) \,, \tag{3.131}
$$

which, upon specialising to the master integrals $F_{B,10}$ and $F_{B,11}$, gives the scaling relation

$$
\left(q^2\partial_{q^2} + m^2\partial_{m^2}\right) \begin{bmatrix} F_{B,10} \\ F_{B,11} \end{bmatrix}(D,\boldsymbol{x}) = \begin{bmatrix} -\varepsilon & 0 \\ 0 & -\varepsilon - 1 \end{bmatrix} \begin{bmatrix} F_{B,10} \\ F_{B,11} \end{bmatrix}(D,\boldsymbol{x}) \,. \tag{3.132}
$$

A further consequence of the linearity of the second graph polynomial in the kinematic invariants is that any scale x_i may be factored out, leaving a rescaled set of invariants $\boldsymbol{x}' = \boldsymbol{x}/x_i$, such that

$$F_{\nu_1,\ldots\nu_j\ldots\nu_{S_{\rm int}}}(D,\boldsymbol{x}) = (x_i^2)^{LD/2-\nu} F_{\nu_1,\ldots\nu_j\ldots\nu_{S_{\rm int}}}(D,\boldsymbol{x}')\,. \tag{3.133}$$

Hence any one scale x_i may be set to unity without loss of generality, since the scaling relation, Eq. (3.133), allows it to be restored at any point. This reduces the number of independent scales by one, greatly simplifying the multivariate system of differential equations. For problems involving only two scales, the system reduces entirely to a univariate differential equation, though this normalisation renders the scaling relation trivial and hence ineffective as a consistency check.

Example 11: *Returning to Ex. 9, setting $m^2 = 1$ reduces the differential equation, Eq. (3.126), to a univariate differential equation in $x = q^2/m^2$, and with $D = 4-2\varepsilon$,*

$$\partial_x \begin{bmatrix} F_{B,10} \\ F_{B,11} \end{bmatrix} (D,x) = \left\{ \begin{bmatrix} 0 & 0 \\ -\frac{2}{(x-4)x} & \frac{2}{(x-4)x} \end{bmatrix} + \varepsilon \begin{bmatrix} 0 & 0 \\ \frac{2}{(x-4)x} & -\frac{1}{x-4} \end{bmatrix} \right\} \begin{bmatrix} F_{B,10} \\ F_{B,11} \end{bmatrix} (D,x)\,. \tag{3.134}$$

If a row of the connection matrix is identically zero, the corresponding master integral has a vanishing derivative with respect to the kinematic invariant and is therefore constant. Such an integral, fully determined by its boundary conditions and requiring no further integration, is said to be a *boundary integral*.

3.3.4 Factorisation

Direct integration of the differential equation for the master integrals is in general not feasible. The choice of basis is, however, not unique, and a well-chosen transformation can render the equation much more tractable [100]. Given an invertible matrix R, a new basis is obtained by

$$\mathbf{F}(\varepsilon,\boldsymbol{x}) = R(\varepsilon,\boldsymbol{x})\mathbf{F}'(\varepsilon,\boldsymbol{x})\,. \tag{3.135}$$

Differentiating both sides and substituting the original differential equation, the new basis is found to satisfy

$$\mathrm{d}\mathbf{F}'(\varepsilon,\boldsymbol{x}) = A'(\varepsilon,\boldsymbol{x})\,\mathbf{F}'(\varepsilon,\boldsymbol{x})\,, \tag{3.136}$$

with the transformed connection matrix

$$A'(\varepsilon,\boldsymbol{x}) = R^{-1}(\varepsilon,\boldsymbol{x})A(\varepsilon,\boldsymbol{x})R(\varepsilon,\boldsymbol{x}) - R^{-1}(\varepsilon,\boldsymbol{x})\mathrm{d}R(\varepsilon,\boldsymbol{x})\,. \tag{3.137}$$

Dimensional shifts and IBP identities are themselves particular instances of such basis rotations, and an appropriate choice of R allows *some* integrals defined in one space-time dimension to be rotated into a basis of integrals in another, a technique that proves very convenient in later chapters. At the level of the differential equation, this amounts to substituting the appropriate value of the space-time dimension into both the connection matrix and the master integrals. Since the differential equation couples the integrals to one another, consistency requires the full basis to be transformed simultaneously, as applying the substitution to individual integrals in isolation yields an incorrect result.

Given that the connection matrix generically depends on both ε and the kinematic invariants in a complicated way, direct integration is impractical. The goal is therefore to find a transformation bringing the differential equation into the *ε-factorised form* [190],

$$\mathrm{d}\mathbf{F}'(\varepsilon, \boldsymbol{x}) = \varepsilon B(\boldsymbol{x})\mathbf{F}'(\varepsilon, \boldsymbol{x})\,, \tag{3.138}$$

in which the dependence on the dimensional regulator is entirely factored out. Expanding the rotated master integrals, $\boldsymbol{F}'$, as a Laurent series in ε,

$$\mathbf{F}'(\varepsilon, \boldsymbol{x}) = \sum_{n=0}^{\infty} \varepsilon^n \mathbf{F}'^{(n)}(\boldsymbol{x})\,. \tag{3.139}$$

The series is truncated from below by the maximal pole order, determined by the ultraviolet and infrared structure of the integrals. Without loss of generality, an overall rescaling of the basis ensures the series begins at constant order. The solution at each order is obtained by integrating the previous one, so each successive term adds one layer of iterated integration [191]. Assigning *transcendental weight* one to each integration and weight minus one to ε, the solution at any given order is a linear combination of iterated integrals of uniform weight.

This simplification does not hold in a generic basis, where functions of different weights would mix. The recursion is solved by repeated integration starting from the boundary values

$$\mathbf{F}'(\varepsilon, \boldsymbol{x}_0) = \sum_{n=0}^{\infty} \varepsilon^n \mathbf{F}'^{(n)}(\boldsymbol{x}_0)\,, \tag{3.140}$$

specified at a given point $\boldsymbol{x}_0$. Note that if the rotated boundary values themselves are not of uniform weight, the uniform-weight structure of the iterated integrals is broken, and the simplification no longer applies.

Computing the master integrals therefore reduces to three tasks, namely constructing a basis that brings the system into ε-factorised form, integrating the resulting equation order by order, and determining the boundary values.

Example 12: *Returning to the univariate differential equation of Ex. 11, Eq.* (3.134)*, two successive rotations bring it into ε-factorised form. First, a dimensional shift from $D = 4 - 2\varepsilon$ to $D = 2 - 2\varepsilon$ via Eq.* (3.116) *gives*

$$A'(\varepsilon, x) = \left\{ \begin{bmatrix} 0 & 0 \\ 0 & \frac{2-x}{(x-4)x} \end{bmatrix} + \varepsilon \begin{bmatrix} 0 & 0 \\ \frac{2}{(x-4)x} & -\frac{1}{x-4} \end{bmatrix} \right\}. \tag{3.141}$$

Second, for the rotation matrix, the ansatz

$$R(\varepsilon, x) = \begin{bmatrix} 1 & 0 \\ 0 & r(x) \end{bmatrix} \tag{3.142}$$

is adopted. Transforming Eq. (3.141) *and demanding that all $\mathcal{O}(\varepsilon^0)$ terms vanish determines the unknown function,*

$$r(x) = \sqrt{x(4-x)}\,, \tag{3.143}$$

and the ε-factorised connection matrix reads

$$B(x) = \begin{bmatrix} 0 & 0 \\ -\frac{2}{r(x)} & \frac{1}{4-x} \end{bmatrix}. \tag{3.144}$$

3.3.5 Boundary Values

Boundary values of the master integrals are extracted by evaluating them in a suitable asymptotic limit. A naive term-by-term expansion of the integrand is insufficient, as individual terms may develop spurious divergences absent from the full integral, which cancel only in the complete sum. Systematic control is provided by the method of *expansion by subgraphs* [101,102], which reorganises the expansion so that every term is individually well-defined as a Feynman integral. Here, the *large mass expansion* is employed, in which one mass is taken much larger than all remaining scales.

The internal edges of a graph Γ fall into two types. *Heavy lines* carry the large mass m, whilst *light lines* carry any smaller mass or are massless. A subgraph γ is called *asymptotically irreducible* when it meets two conditions. First, it must contain every heavy line of Γ. Second, each connected component must be two-edge-connected with respect to the light lines, so that no single light edge can be removed without disconnecting that component. To each such subgraph we associate a *co-graph* Γ/γ, obtained by contracting γ to a point and retaining only the light edges. In dimensional regularisation, the asymptotically irreducible subgraphs are equivalently those containing no cut composed solely of light edges [192]. This cut criterion is simple to verify, and any contribution whose co-graph is scaleless is discarded.

With these definitions in place, the large-mass expansion of a Feynman integral takes the form

$$I_\Gamma = \sum_{\gamma \in \mathrm{AI}(\Gamma)} I_{\Gamma/\gamma} \circ \mathcal{M}_\gamma \, I_\gamma \,, \tag{3.145}$$

where the sum runs over all asymptotically irreducible subgraphs, including Γ itself.

Acting on the subgraph integrand, the Taylor operator $\mathcal{M}_\gamma$ expands it in the external momenta of the subgraph, which together with the small masses constitute the small scales of the problem. Each resulting numerator is inserted into the co-graph integrand via the composition $\circ$, and the two integrals are evaluated independently. To facilitate the expansion in several small momenta, we make use of the standard result

$$f(\boldsymbol{z}) = \sum_{n=0}^{\infty} \frac{1}{n!} \left(\boldsymbol{z} \cdot \nabla_{\boldsymbol{z}'}\right)^n f(\boldsymbol{z}')\bigg|_{\boldsymbol{z}'=\boldsymbol{0}} = \sum_{n=0}^{\infty} \frac{\delta^n}{n!} \frac{\mathrm{d}^n f(\delta' \boldsymbol{z})}{\mathrm{d}\delta'^n}\bigg|_{\delta'=0}\bigg|_{\delta=1} = f(\delta \boldsymbol{z})\big|_{\delta=1} \,, \tag{3.146}$$

which trades the multivariable expansion in $z_1, z_2, \ldots$ for a univariate expansion in a bookkeeping parameter [193], formally around zero and ultimately evaluated at one.

Example 13: *Returning to Ex. 12, the first master integral is a vacuum bubble carrying no external momentum, and its large-mass expansion is therefore trivial. The second integral is a massive bubble with a single asymptotically irreducible subgraph, namely the graph itself, so its expansion reduces to a naive Taylor series,*

$$\begin{aligned} F_{B,10}(D,x) &= -\Gamma(1-D/2) \\ &= \frac{1}{\varepsilon} + 1 + \left(1 + \frac{\zeta_2}{2}\right)\varepsilon + \left(1 + \frac{\zeta_2}{2} - \frac{\zeta_3}{3}\right)\varepsilon^2 + \mathcal{O}(\varepsilon^3) \,, \end{aligned} \tag{3.147}$$

$$\begin{aligned} F_{B,11}(D,x) &= F_{B,20}(D,x) + \frac{4-D}{D} x F_{B,30}(D,x) + \frac{4}{D} x F_{B,40}(D,x) + \mathcal{O}(x^2) \\ &= \frac{1}{\varepsilon} + \frac{\zeta_2}{2}\varepsilon - \frac{\zeta_3}{3}\varepsilon^2 + \mathcal{O}(\varepsilon^3) + \left(\frac{1}{6} + \frac{\zeta_2}{12}\varepsilon^2 + \mathcal{O}(\varepsilon^3)\right)x + \mathcal{O}(x^2) \,. \end{aligned} \tag{3.148}$$

3.3.6 Iterated Integrals

The solutions to the factorised differential equation are obtained by straightforward order-by-order integration in ε, and admit a natural expression in terms of Chen iterated integrals [103]. The rotated connection matrix decomposes as

$$B(\boldsymbol{x}) = \sum_{j=1}^{S_{\text{ext}}} \sum_{i \in \mathbb{N}} M_i \, \omega_{i,j}(\boldsymbol{x}) \, \mathrm{d}x_j \,, \tag{3.149}$$

where the sum involves only finitely many constant complex-valued matrices M_i and the functions $\omega_{i,j}$ are called *integral kernels*. In the univariate case the second index is dropped, and each kernel defines a differential one-form

$$\hat{\omega}_i = \omega_i(x) \, \mathrm{d}x \,, \tag{3.150}$$

on the space of kinematic invariants. For one-forms $\hat{\omega}_1, \ldots, \hat{\omega}_n$ and a curve γ from $\boldsymbol{x}_0$ to $\boldsymbol{x}$, the *Chen iterated integral* of length n reads

$$\mathrm{F}_{i_1,\ldots,i_n}[\gamma] = \int_{0 \le t_1 \le \cdots \le t_n \le 1} (\gamma^* \hat{\omega}_{i_1})(t_1) \cdots (\gamma^* \hat{\omega}_{i_n})(t_n) \,, \tag{3.151}$$

with the empty integral normalised by convention to $\mathrm{F}_\emptyset = 1$. Over $\mathbb{C}$, iterated integrals built from linearly independent one-forms are themselves linearly independent, yet their products need not be.

Iterated integrals possess a rich algebraic structure; in particular, they form a Hopf algebra [194,195], although this is not relevant for our present purposes. Therefore, we restrict attention to the properties that will be used in the subsequent computation. The product of two iterated integrals of lengths m and n satisfies the *shuffle relation*,

$$\mathrm{F}_{i_1,\ldots,i_m}[\gamma] \cdot \mathrm{F}_{j_1,\ldots,j_n}[\gamma] = \sum_{\sigma \, \in \, \mathrm{Sh}(m,n)} \mathrm{F}_{\sigma(i_1,\ldots,i_m,j_1,\ldots,j_n)}[\gamma] \,, \tag{3.152}$$

where $\mathrm{Sh}(m,n)$ denotes the set of permutations of $m+n$ elements preserving the relative order within each subsequence. Two further identities complete the algebraic structure. Under path reversal,

$$\mathrm{F}_{i_1,\ldots,i_n}[\gamma^{-1}] = (-1)^n \, \mathrm{F}_{i_n,\ldots,i_1}[\gamma] \,, \tag{3.153}$$

where γ^{-1} denotes the path traversed in the opposite direction. For path composition, where $\gamma_1 \cdot \gamma_2$ denotes the concatenation of two paths sharing an endpoint, the iterated integrals satisfy

$$\mathrm{F}_{i_1,\ldots,i_n}[\gamma_1 \cdot \gamma_2] = \sum_{k=0}^{n} \mathrm{F}_{i_1,\ldots,i_k}[\gamma_1] \, \mathrm{F}_{i_{k+1},\ldots,i_n}[\gamma_2] \,. \tag{3.154}$$

In the present work, integration is always performed along a straight line. The path dependence therefore reduces to dependence on the endpoints alone, and the path argument is suppressed in favour of the shorthand

$$\mathrm{F}_{i_1,\ldots,i_n}(\boldsymbol{x}) \equiv \mathrm{F}_{i_1,\ldots,i_n}[\gamma] \,. \tag{3.155}$$

Logarithmic one-forms, $\omega_i = \mathrm{d}\log\alpha_i$, give rise to the important special class of iterated integrals, namely *multiple polylogarithms*. Each rational function α_i is called a *letter*, and the finite collection of all letters the *alphabet*. In the univariate case the path may be chosen along the real axis, reducing the iterated integration to a one-dimensional nested integral. Letting $\alpha_i = t - a_i$, the resulting functions take the *Goncharov* form [196],

$$\mathrm{G}_{a_1,\ldots,a_n}(x) = \int_0^x \frac{\mathrm{d}t}{t-a_1}\,\mathrm{G}_{a_2,\ldots,a_n}(t)\,, \quad \exists\, i \le n \in \mathbb{N}: \quad a_i \neq 0\,, \tag{3.156}$$

$$\mathrm{G}_{a_1,\ldots,a_n}(x) = \frac{[\log(x)]^n}{n!}\,, \qquad \forall\, i \le n \in \mathbb{N}: \quad a_i = 0\,, \tag{3.157}$$

$$\mathrm{G}(x) = 1\,. \tag{3.158}$$

To obtain Eq. (3.157) from Eq. (3.156), we apply the tangential base point regularisation of [197]. The lower bound of the integral can be regularised by introducing a finite cut-off, which is expected to cancel in final expressions.

Of particular importance are the *harmonic polylogarithms* [198], obtained by restricting the alphabet to zero and the square roots of unity,

$$\mathrm{H}_{a_1,\ldots,a_n}(x) = \left[(-1)^{\sum_{i=1+}^{n}\delta_{1,a_i}}\right]\mathrm{G}_{a_1,\ldots,a_n}(x)\,, \qquad a_i \in \{-1,0,1\}\,, \tag{3.159}$$

and arising naturally in single-scale calculations. When the integral kernels involve algebraic functions of the kinematic invariants, two situations arise. If a rationalising change of variables exists [199, 200] that renders all kernels rational, the iterated integrals again reduce to multiple polylogarithms.

When no rationalisation exists, the iterated integrals define a broader class of special functions that do not reduce to multiple polylogarithms. Within this larger class, questions of linear independence in the functional sense remain an active area of research. Regardless of whether such relations are fully understood, numerical evaluation of iterated integrals proceeds by series expansion and term-by-term integration, though a finite radius of convergence may necessitate analytic continuation [201,202].

Example 14: *Returning to Ex. 12, the ε-factorised connection matrix, Eq.* (3.144), *decomposes into integral kernels as*

$$B(x) = \left\{\begin{bmatrix} 0 & 0 \\ -2 & 0 \end{bmatrix}\omega_1(x) + \begin{bmatrix} 0 & 0 \\ 0 & -1 \end{bmatrix}\omega_2(x)\right\}, \tag{3.160}$$

where the integral kernels read, together with their expansions around zero,

$$\begin{aligned}\omega_1(x) &= \frac{1}{x-4} \\ &= -\frac{1}{4} - \frac{x}{16} - \frac{x^2}{64} - \frac{x^3}{256} - \frac{x^4}{1024} + \mathcal{O}\big(x^5\big)\,,\end{aligned} \tag{3.161}$$

$$\begin{aligned}\omega_2(x) &= \frac{1}{\sqrt{x(4-x)}} \\ &= \frac{1}{\sqrt{x}}\left[\frac{1}{2x} + \frac{1}{16} + \frac{3x}{256} + \frac{5x^2}{2048} + \frac{35x^3}{65536} + \frac{63x^4}{524288} + \mathcal{O}\big(x^5\big)\right].\end{aligned} \tag{3.162}$$

Formally integrating the differential equation, rotating the boundary values to the ε-factorised basis, and matching with the integration constants yields, after some algebra,

$$F_{B,10}(D,x) = \frac{1}{\varepsilon} + 1 + \left(1 + \frac{\zeta_2}{2}\right)\varepsilon + \left(1 + \frac{\zeta_2}{2} - \frac{\zeta_3}{3}\right)\varepsilon^2 + \mathcal{O}\big(\varepsilon^3\big)\,, \tag{3.163}$$

$$\begin{aligned} F_{B,11}(D,x) = \frac{1}{\varepsilon} &+ \frac{1}{x}\Big(2x - r\mathrm{F}_2\Big) + \frac{\varepsilon}{2x}\Big(8x - 4r\mathrm{F}_2 + 2r\mathrm{F}_{2,1} + x\zeta_2\Big) \\ &+ \frac{\varepsilon^2}{6x}\Big(48x - 24r\mathrm{F}_4 + 12r\mathrm{F}_{2,1} - 6r\mathrm{F}_{2,1,1} + 6x\zeta_2 \\ &\qquad - 3r\mathrm{F}_2\zeta_2 - 2x\zeta_3\Big)\,. \end{aligned} \tag{3.164}$$

In Ex 14 we implicitly introduced the normalisation of the integrals used throughout this work,

$$C_{L,D} = \exp\left(-\gamma_{\mathrm{E}}\,\varepsilon\,L\right)\,, \tag{3.165}$$

where γ_{E} denotes the Euler–Mascheroni constant,

$$\gamma_{\mathrm{E}} = \lim_{n\to\infty}\left(\sum_{k=1}^{n}\frac{1}{k} - \ln n\right) = 0.57721566490153286061\ldots\,. \tag{3.166}$$

With this convention, our results, Eqs. (3.163) and (3.164), are expressed in terms of the classical polylogarithms and the associated zeta values,

$$\mathrm{Li}_n(x) = \sum_{k=1}^{\infty}\frac{x^k}{k^n}\,, \tag{3.167}$$

$$\zeta_n = \mathrm{Li}_n(1) \qquad \text{for } n > 1\,. \tag{3.168}$$

(This page is intentionally left blank.)

"She generally gave herself very good advice, (though she very seldom followed it)."

— *Alice's Adventures in Wonderland*, Lewis Carroll

Chapter 4

Heavy Quark Production

4.1 Harmonic Projection

4.1.1 Harmonic Tensor

The harmonic tensors introduced here underlie the method of harmonic projection (see Subsec 4.1.2), by which the moments of the coefficient functions are extracted. Constructed from a reference vector q and the metric tensor g, harmonic tensors of rank N are defined as symmetric, traceless tensors, normalised such that

$$H_N{}^{\mu_1\ldots\mu_i\ldots\mu_j\ldots\mu_N} = H_N{}^{\mu_1\ldots\mu_j\ldots\mu_i\ldots\mu_N}\,, \tag{4.1}$$

$$g_{\mu_i\mu_j} H_N{}^{\mu_1\ldots\mu_i\ldots\mu_j\ldots\mu_N} = 0\,, \tag{4.2}$$

$$q_{\mu_i} H_N{}^{\mu_1\ldots\mu_i\ldots\mu_n} = q^2 H_{N-1}{}^{\mu_1\ldots\hat{\mu}_i\ldots\mu_N}\,. \tag{4.3}$$

Here, the circumflex denotes an omitted index. With this normalisation, transversality is automatically ensured whenever the reference vector is light-like. For an already-transverse tensor, Fourier transformation reduces this condition to a harmonic differential equation.

Symmetric, traceless tensors arise throughout physics, from multipole expansions in electrodynamics to gravitational-wave analysis [203, 204]. The normalisation adopted here, however, departs from the standard convention and its rationale becomes apparent from the explicit construction of a general harmonic tensor [37],

$$H_N{}^{\mu_1\ldots\mu_N} = \sum_{K=0}^{\lfloor\frac{N}{2}\rfloor} (q^2)^K h_{2K}^N \sum_{\sigma} g^{\sigma(\mu_1)\sigma(\mu_2)} \ldots g^{\sigma(\mu_{2K-1})\sigma(\mu_{2K})} q^{\sigma(\mu_{2K+1})} \ldots q^{\sigma(\mu_N)}\,, \tag{4.4}$$

where the sum runs over all permutations σ of the indices, modulo those equivalent either by the intrinsic symmetry of the metric tensor or by the commutativity of product. The coefficients are given by

$$h_{2K}^N = (-1)^K 2^N \frac{\Gamma(D-2)\,\Gamma(D/2-1+N-K)}{\Gamma(D-2+N)\,\Gamma(D/2-1)}\,. \tag{4.5}$$

Absorbing all combinatorial factors into the coefficients ensures that the sum runs only over permutations distinct under these equivalences. The form of the coefficients itself accounts for the redundancies arising from the intrinsic symmetries of the metric tensor and from products of the reference vector.

To make the definition of harmonic tensors, Eq. (4.4), more concrete, we consider the explicit case of the rank-three harmonic tensor

$$H_3{}^{\mu_1\mu_2\mu_3} = h_0^3 q^{\mu_1} q^{\mu_2} q^{\mu_3} + h_2^3 q^2 \left(g^{\mu_1\mu_2} q^{\mu_3} + g^{\mu_3\mu_1} q^{\mu_2} + g^{\mu_2\mu_3} q^{\mu_1}\right) , \tag{4.6}$$

with the coefficients

$$h_0^3 = \frac{D+2}{D-1} , \tag{4.7}$$

$$h_2^3 = \frac{1}{1-D} . \tag{4.8}$$

Symmetry is by construction manifest. Tracelessness may be verified by contracting any two indices, for instance μ_1 and μ_2, and exploiting the symmetry of the tensor, yielding

$$g_{\mu_1\mu_2} H_3{}^{\mu_1\mu_2\mu_3} = q^2 q^{\mu_3} \left(h_0^3 + (D+2) h_2^3\right) = 0 . \tag{4.9}$$

This computation shows that the tracelessness, Eq. (4.2), is closely tied to a recursive relation between the coefficients h_{2K}^N for adjacent values of K. Along the same lines, the normalisation condition may be verified directly by contracting the harmonic tensor with the reference momentum, which gives

$$\begin{aligned} q_{\mu_1} H_3{}^{\mu_1\mu_2\mu_3} &= q^2 \left((h_0^3 + 2h_2^3) q^{\mu_2} q^{\mu_3} + h_2^3 q^2 g^{\mu_2\mu_3}\right) \\ &= q^2 \left(h_0^2 q^{\mu_2} q^{\mu_3} + h_2^2 q^2 g^{\mu_2\mu_3}\right) \\ &= q^2 H_2{}^{\mu_2\mu_3} , \end{aligned} \tag{4.10}$$

with the coefficients

$$h_0^2 = \frac{D}{D-1} , \tag{4.11}$$

$$h_2^2 = \frac{1}{1-D} . \tag{4.12}$$

Hence, the normalisation is likewise linked to the recursive nature of the coefficients h_{2K}^N, now across adjacent values of N at fixed K.

Turning now to the general case of a harmonic tensor of rank N, the construction, Eq. (4.4) can be shown to satisfy both the tracelessness and normalisation conditions for all N. The normalisation condition, Eq. (4.3), may, to this end, be equivalently written as

$$q_{\mu_1} ... q_{\mu_N} H_N{}^{\mu_1 ... \mu_N} = (q^2)^N . \tag{4.13}$$

In this form the normalisation relates all coefficients h_{2K}^N at fixed N, whilst also suggesting an even more practical condition,

$$\sum_{K=0}^{\lceil \frac{N}{2} \rceil} h_{2K}^N F_{2K}^N = 1 . \tag{4.14}$$

Here, F_{2K}^N is a coefficient accounting for the combinatorics of generating equivalent tensor structures upon contraction with N reference vectors. Each q may be paired with any of the N indices, then with any of the remaining $(N-1)$ indices, and so on, the process being repeated for all K metric tensors. To avoid over-counting, we must account for the intrinsic symmetry of each metric tensor as well as permutations amongst them, which yields

$$\begin{aligned} F_{2K}^{N} &= \frac{1}{2^K \Gamma(1+K)} \prod_{M=0}^{K-1} (N-2M)(N-2M-1) \\ &= \frac{\Gamma(2K-N)}{2^K \Gamma(-N)\,\Gamma(1+K)}\,. \end{aligned} \tag{4.15}$$

The sum representation of the normalisation, Eq. (4.14), is now combined with the combinatorial factors, Eq. (4.15). Applying Euler's reflection formula and using that $2K$ is a positive even integer, the condition can be rewritten as

$$\begin{aligned} \sum_{K=0}^{\lceil \frac{N}{2} \rceil} h_{2K}^{N} F_{2K}^{N} &= \frac{2^N \Gamma(D-2)}{\Gamma(D-2+N)} \sum_{K=0}^{\lceil \frac{N}{2} \rceil} \frac{(-1)^K}{4^K} \frac{\Gamma(2K-N)\,\Gamma(D/2-1+N-K)}{\Gamma(1+K)\,\Gamma(-N)\,\Gamma(D/2-1)} \\ &= \frac{2^N}{(D-2)_N} \sum_{K=0}^{\lceil \frac{N}{2} \rceil} \frac{(-1)^K}{4^K} \frac{\Gamma(2K-N)\,(D/2-1)_{N-K}}{\Gamma(1+K)\,\Gamma(-N)} \\ &= \frac{2^N \Gamma(N+1)}{(D-2)_N} \sum_{K=0}^{\lceil \frac{N}{2} \rceil} \frac{(-1)^K}{4^K} \frac{(D/2-1)_{N-K}}{\Gamma(1+K)\,\Gamma(N-2K+1)} \\ &= \frac{2^N \Gamma(N+1)}{(D-2)_N} \frac{(D-2)_N}{2^N \Gamma(N+1)} \\ &= 1\,, \end{aligned} \tag{4.16}$$

where $(x)_N$ denotes a Pochhammer symbol. As a consequence, the normalisation condition is satisfied by every harmonic tensor constructed.

Vanishing of the trace, Eq. (4.2), requires the sum of the coefficients associated with each independent tensor structure to vanish identically. Four distinct types of contraction may arise when taking a trace, of which only one contributes with a factor of $h_{2(K-1)}^{N}$, whilst the remaining three contribute with a factor of h_{2K}^{N}. Including the appropriate combinatorial weight in each case, we obtain

$$\underbrace{h_{2(K-1)}^{N}}_{g_{\mu\nu} q^\mu q^\nu} + \underbrace{D h_{2K}^{N}}_{g_{\mu\nu} g^{\mu\nu}} + \underbrace{(2K-2) h_{2K}^{N}}_{g_{\mu\nu} g^{\alpha\nu} g^{\beta\nu}} + \underbrace{(2N-4K) h_{2K}^{N}}_{g_{\mu\nu} g^{\mu\alpha} q^\nu} = 0\,. \tag{4.17}$$

Applying the recursion step by step, from the maximal value of K down to $K = 0$, makes all traces vanish. The harmonic tensors defined in Eq. (4.4) therefore exist for all N and are symmetric, traceless, and correctly normalised.

4.1.2 Projection Operators

To efficiently compute fixed-order moments of coefficient functions, an operator is introduced that projects reciprocal powers of x_{B} in the partonic invariants, as suggested by Eq. (2.104). The harmonic projection operator,

$$\mathcal{P}_M(\cdot) = \frac{H_M{}^{\mu_1 \ldots \mu_M}}{M!} \frac{\partial^M}{\partial p^{\mu_1} \ldots \partial p^{\mu_M}} \left(\cdot \right) \bigg|_{p=0}\,, \tag{4.18}$$

yields a non-zero result only when applied to a product of exactly M vectors p. This becomes clear when considering the case $M \neq N$ and evaluating the action of $\mathcal{P}_M$ explicitly. The indices can then be relabelled, using the symmetry of the product and the defining properties of harmonic tensors, to give

$$\mathcal{P}_M(p^{\lambda_1}\dots p^{\lambda_N}) = \begin{cases} \frac{N!}{M!} {H_M}^{\mu_1\dots\mu_M} \delta^{\lambda_1}{}_{\mu_1}\dots\delta^{\lambda_M}{}_{\mu_M} \partial^{\lambda_{M+1}}\dots\partial^{\lambda_N}\Big|_{p=0} & \text{if } N < M\,, \\ \frac{N!}{M!} {H_M}^{\mu_1\dots\mu_M} \delta^{\lambda_1}{}_{\mu_1}\dots\delta^{\lambda_M}{}_{\mu_M} p^{\lambda_{M+1}}\dots p^{\lambda_N}\Big|_{p=0} & \text{if } N > M\,. \end{cases} \tag{4.19}$$

Trivially, the first term vanishes, as the number of derivatives exceeds the number of available factors, meaning that at least one derivative necessarily acts on a constant and returns zero. For the second case, the projection also vanishes, since at least one factor of p survives in the expression and is subsequently nullified. The projection is therefore non-zero only when $M = N$, in which case

$$\mathcal{P}_N(p^{\lambda_1}\dots p^{\lambda_N}) = {H_N}^{\lambda_1\dots\lambda_N}\,, \tag{4.20}$$

so that the result itself is a harmonic tensor.

In practice, the harmonic projection is applied here to the forward scattering amplitude, and projecting the partonic invariants yields

$$\begin{aligned} \mathcal{P}_M(T_i(p,q)) &= \mathcal{P}_M\left(\sum_{N\in\mathbb{N}}\sum_{k\in\mathbb{S}^*}\left(\frac{1}{2x_{\mathrm{B}}}\right)^N A^N_{k,\mathrm{p}}(p) C^N_{i,k}(q)\right) \\ &= \mathcal{P}_M\left(\sum_{N\in\mathbb{N}}\sum_{k\in\mathbb{S}^*}\frac{q^{\lambda_1}\dots q^{\lambda_N}}{(-q^2)^N} p_{\lambda_1}\dots p_{\lambda_N} A^N_{k,\mathrm{p}}(p) C^N_{i,k}(q)\right) \\ &= \sum_{N\in\mathbb{N}}\sum_{k\in\mathbb{S}^*}\frac{q^{\lambda_1}\dots q^{\lambda_N}}{(-q^2)^N} C^N_{i,k}(q)\mathcal{P}_M\left(p_{\lambda_1}\dots p_{\lambda_N} A^N_{k,\mathrm{p}}(p)\right)\Big|_{p=0} \\ &= \sum_{N\in\mathbb{N}}\sum_{k\in\mathbb{S}^*} C^N_{i,k}(q)\frac{{H_q}^{\mu_1\dots\mu_M}}{M!}\frac{q^{\lambda_1}\dots q^{\lambda_N}}{(-q^2)^N} \\ &\quad\times \frac{\partial^M\left(p_{\lambda_1}\dots p_{\lambda_N} A^N_{k,\mathrm{p}}(p)\right)}{\partial p^{\mu_1}\dots\partial p^{\mu_M}}\Bigg|_{p=0} \\ &= \sum_{N\in\mathbb{N}}\sum_{k\in\mathbb{S}^*} C^N_{i,k}(q)\frac{{H_q}^{\mu_1\dots\mu_M}}{M!}\frac{q^{\lambda_1}\dots q^{\lambda_N}}{(-q^2)^N}\sum_{K=0}^{N}\binom{M-K}{K} \\ &\quad\times \frac{\partial^K\left(p_{\lambda_1}\dots p_{\lambda_N}\right)}{\partial p^{\mu_1}\dots\partial p^{\mu_K}}\frac{\partial^{M-K}\left(A^N_{k,\mathrm{p}}(p)\right)}{\partial p^{\mu_{K+1}}\dots\partial p^{\mu_M}}\Bigg|_{p=0} \qquad i\in\{\,L,2,3,S\,\}\,. \end{aligned} \tag{4.21}$$

Without further simplification, the harmonic projection would be of limited practical utility, since it acts not only on the products of momenta but also on the operator matrix elements. Derivatives acting on the operator matrix elements, however, do not contribute.

To see this, note that both harmonic tensors and derivatives are totally symmetric in all their indices, which greatly simplifies the combinatorics of taking derivatives, allowing the indices to be placed in canonical order. Applying the chain rule to differentiate the operator matrix elements, and observing that they depend only on p^2 since they are scalars, gives

$$\begin{aligned}\frac{\partial^{M-K}\left(A^N_{k,\mathrm{p}}(p)\right)}{\partial p^{\mu_{K+1}}\dots\partial p^{\mu_M}} = &\sum_{L=\lceil\frac{M-K}{2}\rceil}^{M-K} 2^{2L-(M-K)}\frac{(M-K)!}{L!}\binom{L}{M-K-L} \\ &\times\frac{\partial^L\left(A^N_{k,\mathrm{p}}(p)\right)}{\partial(p^2)^L}\, g_{\mu_1\mu_2}\dots g_{\mu_{2L-1}\mu_{2L}}p_{\mu_{2L+1}}\dots p_{\mu_M}\,.\end{aligned} \tag{4.22}$$

For $M-K\neq 0$ this expression does not contribute, because terms containing metric tensors are annihilated by the tracelessness of the harmonic tensors, whilst those containing p vanish once the partonic momentum is nullified. The inner sum may therefore be dropped,

$$\begin{aligned}\mathcal{P}_M(T_i(p,q)) &= \sum_{N\in\mathbb{N}}\sum_{k\in\mathbb{S}^*} A^N_{k,\mathrm{p}}(p)C^N_{i,k}(q) \\ &\quad\times\frac{H_q{}^{\mu_1\dots\mu_M}}{M!}\frac{q^{\lambda_1}\dots q^{\lambda_N}}{(-q^2)^N}\frac{\partial^M\left(p_{\lambda_1}\dots p_{\lambda_N}\right)}{\partial p^{\mu_1}\dots\partial p^{\mu_M}}\bigg|_{p=0} \\ &= \sum_{k\in\mathbb{S}^*} A^N_{k,\mathrm{p}}(p)C^N_{i,k}(q) \\ &\quad\times\frac{H_q{}^{\mu_1\dots\mu_M}q^{\lambda_1}\dots q^{\lambda_M}}{(-q^2)^M}g_{\lambda_1\mu_1}\dots g_{\lambda_N\mu_N}\bigg|_{p=0} \\ &= \sum_{k\in\mathbb{S}^*} A^N_{k,\mathrm{p}}(p)C^N_{i,k}(q)\frac{H_{q,\lambda_1\dots\lambda_M}q^{\lambda_1}\dots q^{\lambda_M}}{(-q^2)^M}\bigg|_{p=0} \\ &= (-1)^M\sum_{k\in\mathbb{S}^*} A^N_{k,\mathrm{p}}(p)C^N_{i,k}(q)\bigg|_{p=0} \\ &\equiv T^N_i(q)\quad i\in\{\,L,2,3,S\,\}\,.\end{aligned} \tag{4.23}$$

The harmonic projection must also be applied directly to the forward scattering amplitude, where it acts at the level of the integrand. Nullifying the hadronic momentum at the level of the integral would lead to infrared singularities that dimensional regularisation does not regulate, whereas at the integrand level such singularities are properly handled.

In this context, the harmonic projection acts on scalar products involving the hadronic momentum, in particular those arising from the numerator structure of the Feynman rules. Further scalar products may appear from the denominators, which can be expanded in powers of p, for instance

$$\frac{1}{(p+q)^2-m^2} = \frac{1}{q^2-m^2}\sum_{n=0}^{\infty}\left(-\frac{2(p\cdot q)}{q^2-m^2}\right)^n\,. \tag{4.24}$$

In this setting, the harmonic projection is conceptually straightforward, amounting simply to differentiating the integrands and contracting with harmonic tensors.

This expansion, however, introduces the first computational bottleneck of the method when higher moments are pursued. As a concrete example, consider a Feynman graph with E edges and L loops representing a typical forward scattering process with external bosonic momentum q, hadronic momentum p, and loop momenta k_ℓ. Each edge carries a momentum

$$\begin{aligned} p_i &= \sum_{\ell=1}^{L} \omega_{i\ell}^k k_\ell + \omega_i^q q + \omega_i^p p \\ &= q_i + \omega_i^p p \,, \qquad\qquad i = 1, \ldots, E \,, \end{aligned} \tag{4.25}$$

where the coefficients $\omega_{i\ell}^k$, ω_i^q, and ω_i^p are assumed to take values in the incidence set $\mathscr{X}$ (see also Subsec. 3.1.1). In the final line, the momenta are decomposed according to their dependence on p, and we define P to be the set of edge labels corresponding to momenta that depend on the partonic momentum.

All edge momenta q_i are assumed distinct for simplicity, though this need not hold in general for forward kinematics. The assumption serves only to facilitate the counting. Omitting constant prefactors and numerators to ease the combinatorics, a typical contribution to the amplitude takes the form,

$$\begin{aligned} I &= \prod_{i=1}^{E} \frac{1}{(p_i^2)^{\nu_i}} \\ &= \prod_{i \notin \mathcal{P}} \frac{1}{(q_i^2)^{\nu_i}} \prod_{i \in \mathcal{P}} \frac{1}{((q_i + \omega_i^p p)^2)^{\nu_i}} \\ &= \prod_{i=1}^{E} \frac{1}{(q_i^2)^{\nu_i}} \prod_{i \in \mathcal{P}} \left[\sum_{n=0}^{\infty} \left(-\omega_i^p \frac{2(p \cdot q_i)}{q_i^2} \right)^n \right] , \end{aligned} \tag{4.26}$$

where the propagators have been expanded in the limit $p \to 0$. The expansion is naturally truncated at order N by the action of the projection operator $\mathcal{P}_N$, such that

$$\mathcal{P}_N(I) = \prod_{i=1}^{E} \frac{1}{(q_i^2)^{\nu_i}} \mathcal{P}_N \left(\prod_{\sum n_i = N} \beta_{n_i} (p \cdot q_i)^{n_i} \right) . \tag{4.27}$$

Here the coefficients β_k absorb all combinatorial prefactors arising from the products and from the entries of the incidence matrix, as these factors are irrelevant for the counting problem. Applying the stars-and-bars theorem [205] then yields the number of terms arising before the derivatives are taken,

$$\binom{|\mathcal{P}| + N - 1}{N - 1} .$$

Once the derivatives have been taken, structurally similar expressions emerge, albeit with increased complexity. The source of this complication is that the quantity $|\mathcal{P}|$ must be replaced by the number of non-trivial scalar products appearing in each term. There are

$$2^{|\mathcal{P}|} - 1 = \sum_{m=1}^{|\mathcal{P}|} \binom{|\mathcal{P}|}{m} \tag{4.28}$$

different ways to set some, but not all, of the indices to zero. Substituting this into the counting formula, Eq. (4.27), gives

$$\begin{aligned}\#\text{terms}(\mathcal{P}_N(I)) &= \binom{|\mathcal{P}|+N-1}{N-1}\sum_{k=1}^{|\mathcal{P}|}\binom{|\mathcal{P}|}{k}\binom{k+N-1}{N-1} \\ &\sim \frac{N^{2|\mathcal{P}|}}{|\mathcal{P}|!^2} + \mathcal{O}(N^{2|\mathcal{P}|-1})\,.\end{aligned} \tag{4.29}$$

The counting makes clear that higher-order moments become increasingly demanding to compute as more edges carry the hadronic momentum. Growing $|\mathcal{P}|$ leads to less favourable scaling in the large-N limit, and to mitigate this effect the size of $\mathcal{P}$ is minimised separately for each graph.

4.2 Computational Setup

4.2.1 Conventions

The conventions adopted in this subsection address four points, namely the choice of gauge and polarisation sum, the decomposition of the current into vector and axial-vector components, the form of the projectors used to extract the partonic invariants, and the routing of momenta through each graph.

Turning first to the gauge choice, the Mellin moments of the forward scattering amplitude are obtained by summing over all gluon polarisations and light-quark spins, and averaging over all colours. For the polarisation sum, a physical gauge could in principle be employed,

$$\sum_{s\in\mathcal{S}_\mathrm{g}} \varepsilon_{s,\mu}(p){\varepsilon^*}_{s,\nu}(p) = -g_{\mu\nu} + \frac{p_\mu q_\nu + p_\nu q_\mu}{p\cdot q} - \frac{q^2}{(p\cdot q)^2}p_\nu p_\mu\,, \tag{4.30}$$

where $\mathcal{S}_g$ denotes the set of gluon polarisations and $\varepsilon_{s,\nu}$ the polarisation tensor of a gluon with respect to the partonic momentum p. This sum is well-defined, since q and p are not collinear. A physical gauge of this kind, however, introduces explicit factors of p into the polarisation sum. Because the harmonic projection is a derivative operator, every such factor produces a sizeable proliferation of terms. Instead, the polarisation sum adopted here reads

$$\sum_{s\in\mathcal{S}_\mathrm{g}} \varepsilon_{s,\mu}(p){\varepsilon^*}_{s,\nu}(p) = -g_{\mu\nu}\,. \tag{4.31}$$

This simplification comes at a price, namely the inclusion of ghosts as external partonic states, which compensate for the unphysical degrees of freedom. Internal gluons are treated in a general covariant gauge for the low moments and in Feynman gauge (see App. D) otherwise. Gauge invariance ensures that the parameter α cancels in the final result, providing a valuable consistency check.

With the gauge now fixed, we turn to the structure of the currents, which are decomposed into vector and axial-vector components, and with them the partonic invariants. The resulting partonic invariants fall into four categories,

$$T_{\mathrm{b}_1\mathrm{b}_2,i,\mathrm{q}} = T_i^{\mathrm{qb}_1\mathrm{qb}_2}\,, \qquad \mathrm{b}_1,\mathrm{b}_2\in\{\,\mathrm{v},\mathrm{a}\,\}\,,\quad i\in\{\,L,2,3\,\}\,, \tag{4.32}$$

$$T_{\mathrm{b}_1\mathrm{b}_2,i,\mathrm{g}} = T_i^{\mathrm{gb}_1\mathrm{gb}_2} + 2T_i^{\mathrm{cb}_1\mathrm{cb}_2}\,, \qquad \mathrm{b}_1,\mathrm{b}_2 \in \{\,\mathrm{v},\mathrm{a}\,\}\,, \quad i \in \{\,L,2,3\,\}\,. \tag{4.33}$$

Beyond the vector-current contributions, partonic invariants associated with scalar currents are decomposed as

$$T_{S,\mathrm{q}} = T_S^{\mathrm{qsqs}}\,, \tag{4.34}$$
$$T_{S,\mathrm{g}} = T_S^{\mathrm{gsqs}} + 2T_S^{\mathrm{cscs}}\,. \tag{4.35}$$

The superscripts label the external particle content contributing to the forward scattering amplitude, where c stands for external ghosts. A factor of two in the ghost contributions accounts for the sum over both ghosts and anti-ghosts in the initial state. Physical combinations of vector and axial-vector currents are then reconstructed by summing the corresponding results and inserting the appropriate flavour factors.

Having decomposed the invariants, we turn to the projection onto the partonic invariants. The projectors defined in Eqs. (2.54) to (2.56) have two shortcomings for efficient computation. First, they are redundant because the longitudinal part is effectively evaluated twice. Second, they depend on the dimensional regulator ε, which needlessly complicates the intermediate steps. Both issues are addressed by decomposing the projectors into simpler ones as

$$\mathcal{P}_{\mathrm{S},L}{}^{\mu\nu} = -\frac{1}{q^2}\mathcal{R}_2{}^{\mu\nu}\,, \tag{4.36}$$
$$\mathcal{P}_{\mathrm{S},2}{}^{\mu\nu} = -\frac{1}{q^2}\frac{3-2\varepsilon}{2-2\varepsilon}\mathcal{R}_2{}^{\mu\nu} - \frac{1}{2-2\varepsilon}\mathcal{R}_0{}^{\mu\nu}\,, \tag{4.37}$$
$$\mathcal{P}_{\mathrm{A},3}{}^{\mu\nu} = \frac{i}{(1-2\varepsilon)(2-2\varepsilon)}\mathcal{R}_1{}^{\mu\nu}\,, \tag{4.38}$$

where the new projectors are given by

$$\mathcal{R}_0{}^{\mu\nu} = g^{\mu\nu}\,, \tag{4.39}$$
$$\mathcal{R}_1{}^{\mu\nu} = 2x_{\mathrm{B}}\varepsilon_{\mu\nu\alpha\beta}p^\alpha q^\beta\,, \tag{4.40}$$
$$\mathcal{R}_2{}^{\mu\nu} = 4x_{\mathrm{B}}^2 p^\mu p^\nu\,. \tag{4.41}$$

Each of these projectors carries a definite power of x_{B}, so the forward amplitude can be expanded directly to a fixed power of the partonic momentum, without separating terms order by order in p. This decoupling of the Mellin moments enables a more modular and efficient implementation.

It remains to fix the routing of momenta through each graph. After harmonic projection, the forward amplitude is reduced to a two-point graph by stripping away the particle types, contracting all bridges, and contracting all edges with equivalent edge momenta until no two edge momenta coincide. This reduction is in general not unique.

Each internal edge then carries an edge momentum q_i inherited from the two-point function,

$$q_i \equiv \omega_{i0}q + \sum_{j=1}^{L}\omega_{i,j}k_j, \quad \omega_{i,j} \in \{\,-1,0,1\,\}\,, \tag{4.42}$$

and the original edge momenta differ from these by the partonic momentum alone,

$$p_i = q_i + \omega_i^p p\,, \quad \omega_i^p \in \mathscr{X}\,. \tag{4.43}$$

Only the momentum routing of p, encoded in the coefficients ω_i^p, then remains to be specified. Among all possible routings, the most natural one assigns the partonic momentum along a shortest path between the two external vertices to which the partons attach. This path is located by means of a breadth-first search algorithm. The number of p-dependent propagators is thereby minimised, and with it the term proliferation generated by the harmonic projection.

4.2.2 Amplitude Generation

Feynman graphs are generated and reduced to independent contributions following strategies similar to those employed for the massless case. All graphs contributing to the processes

$$\begin{aligned} \mathrm{p}+\mathrm{b}_1 &\longrightarrow \mathrm{p}+\mathrm{b}_2, \qquad && \mathrm{p}\in\{\,\mathrm{q},\mathrm{g},\mathrm{c}\,\}\,, \quad \mathrm{b}_1,\mathrm{b}_2\in\{\,\mathrm{v},\mathrm{a}\,\}\,, && (4.44)\\ \mathrm{p}+\mathrm{s} &\longrightarrow \mathrm{p}+\mathrm{s}, && \mathrm{p}\in\{\,\mathrm{q},\mathrm{g},\mathrm{c}\,\}\,, && (4.45) \end{aligned}$$

are produced with the built-in graph generator of FORM [139, 206] and processed by the routine `convdia.frm`[1], which assigns to each graph a topology together with edge momenta p_i of Eq. (4.43). Tadpoles are discarded, as they vanish in QCD by colour conservation, whilst snails are retained, since a heavy-quark insertion on a gluon line yields a non-vanishing contribution in dimensional regularisation.

Typically, these graphs contain many redundancies, making it more efficient to work with equivalence classes rather than individual graphs, where two graphs are treated as equivalent whenever their contributions to the moments agree up to an overall sign. Redundancies are removed in several stages, exploiting the pattern-matching capabilities of FORM.

The first stage discards graphs that do not contribute to the amplitude, beginning with those of vanishing colour factor. To expose the colour content, the four-gluon vertices are decomposed so that the colour structure is separated from the remainder of the numerator,

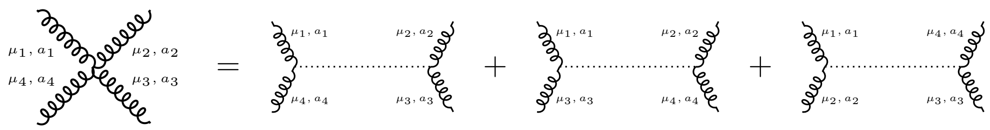

, (4.46)

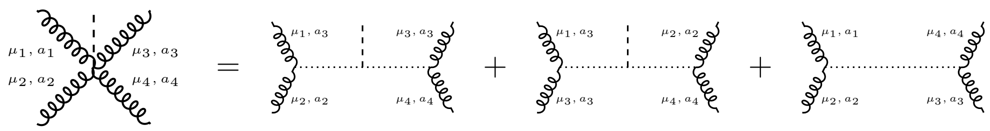

. (4.47)

For ease of implementation, only trivalent vertices are retained. The three-gluon-scalar vertex is therefore decomposed as well, even though this step is not strictly required for the colour factorisation,

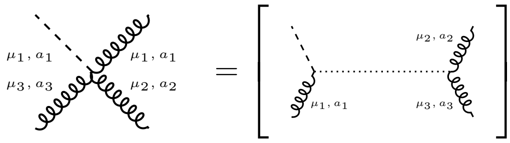

. (4.48)

[1]The code is not publicly available but may be provided upon reasonable request.

The left-hand side is symmetric under permutations of the three gluons, so the original vertex may be replaced by any representative of the resulting equivalence class. Such replacements can yield topologically distinct graphs, and any analysis of graph symmetries must therefore consider the full equivalence class. Once every vertex of valency greater than three has been reduced to a trivalent one, the colour structure decouples from the Lorentz and Dirac structures. The Feynman rules are then applied, with the colour and flavour traces evaluated separately [207].

A further source of redundancy arises from scaleless subgraphs, which emerge once the harmonic projection operator has been applied and the partonic momentum has been nullified. Their detection proceeds in three steps. Each edge is first classified as either massless or massive, with particle types discarded so that only the mass assignments and momentum flow are retained, yielding a scalar skeleton graph. The partonic momenta are then nullified and the partonic edges amputated. Finally, edges joined through bivalent vertices are identified, as illustrated by the sequence:

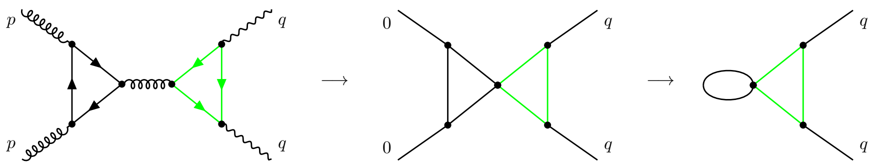

(4.49)

The reduced graph is then searched for articulation points, namely vertices whose removal disconnects the graph. Any disjoint component obtained by removing such a vertex that is free of both massive edges and the boson momentum q corresponds to a scaleless subgraph and therefore vanishes.

A final source of equivalences is charge conjugation, under which pairs of graphs either coincide and combine or cancel against one another. To see why, consider a closed quark loop carrying n external gluons, together with the graph obtained by reversing the direction of the loop. The absolute values of the corresponding colour traces read

$$\left|\operatorname{tr}\left(T^{a_1}T^{a_2}\dots T^{a_n}\right)\right| = \left|\operatorname{tr}\left((T^{a_1})^T(T^{a_2})^T\dots(T^{a_n})^T\right)\right|. \tag{4.50}$$

Equality holds only when the representation is real, symmetric or antisymmetric. For generic representations and arbitrary n, the relation therefore fails. It does hold, however, for exactly one or two generators, owing respectively to the invariance of the trace under transposition and to its cyclicity.

4.2.3 Graph Symmetries

Beyond its role in identifying trivial contributions, charge conjugation may also relate graphs to one another through symmetries that exceed graph automorphisms. Such relations require only that the orientation of individual lines be reversed, with the appropriate signs accounted for. This symmetry is referred to simply as *conjugation.*

Two further symmetry operations of a similar kind come into play, namely the *shuffle* and *swap* symmetries. Both, like conjugation, may be understood as relocating a subgraph without altering the overall amplitude.

The shuffle symmetry concerns bivalent subgraphs, that is, self-energy insertions along a given edge, which may be permuted amongst themselves. This is immediate in scalar theories. In other theories, the only possible obstruction stems from the numerator structures of the propagators. On ghost edges, where the propagators carry no non-trivial numerators, self-energy insertions may therefore be reordered freely. For quark edges, the numerators of the self-energy insertions are instead constrained by Lorentz symmetry to take the form

$$\not{\Sigma}_i = \Sigma_{i,p}\not{p} + \Sigma_{i,m} m\,, \tag{4.51}$$

with scalar functions $\Sigma_{i,p}$ and $\Sigma_{i,m}$. The same decomposition applies to tree-level quark propagators. For a product of quark numerators, we obtain

$$\begin{aligned}\not{\Sigma}_1\not{\Sigma}_2 &= \Sigma_{1,p}\Sigma_{2,p}\not{p}^2 + \Sigma_{1,m}\Sigma_{2,m}m^2 \\ &\quad + \Sigma_{1,m}\Sigma_{2,p}m\not{p} + \Sigma_{1,p}\Sigma_{2,m}\not{p}m = \not{\Sigma}_2\not{\Sigma}_1\,,\end{aligned} \tag{4.52}$$

which follows from the fact that m and $\not{p}$ commute with one another, and trivially with themselves. In direct analogy, the numerators of self-energy insertions on gluon edges take the form

$$\Pi_{i,\mu\nu} = \Pi_{i,p}p_\mu p_\nu + \Pi_{i,g}g_{\mu\nu}\,, \tag{4.53}$$

with the scalar functions $\Pi_{i,p}$ and $\Pi_{i,g}$. Hence, we find for a product of gluon numerators

$$\begin{aligned}\Pi_{1,\mu\rho}\Pi_{2,}{}^{\rho}{}_{\nu} &= \Pi_{1,g}\Pi_{2,g}g_{\mu\nu} + \big(\Pi_{1,p}\Pi_{2,g} + \Pi_{1,g}\Pi_{2,p} \\ &\quad + p^2\Pi_{1,p}\Pi_{2,p}\big)p_\mu p_\nu = \Pi_{2,\mu\rho}\Pi_{1,}{}^{\rho}{}_{\nu}\,,\end{aligned} \tag{4.54}$$

where the intermediate expression is manifestly symmetric. Self-energy insertions on gluon and quark edges therefore commute. The same argument extends to any number of numerators, including those arising from tree-level propagators.

Permutations of self-energy insertions on gluon, ghost, and quark edges along a given edge are accordingly equivalent, a fact depicted graphically as

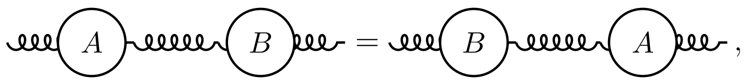
(4.55)

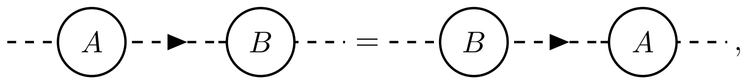
(4.56)

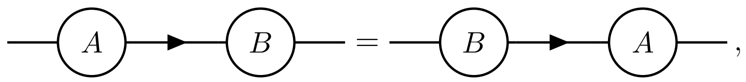
(4.57)

where these identities clearly fail to correspond to graph automorphisms once the edges are oriented. The same is true whenever an edge carries more than two self-energy insertions.

Forward-scattering kinematics give rise to the swap symmetry. It permits the exchange of self-energy insertions between two gluon or ghost edges connected by a line on which an external momentum both enters and leaves the graph. The external particles may be either scalars or gluons.

For ghost lines the symmetry is immediate, since the self-energy insertions reduce to scalar integrals and therefore commute. The gluon case is more involved, owing to the presence of numerators. In this case the shuffle symmetry allows the tree-level propagators to be shifted away from the two gluon-scalar vertices, leaving only the numerators of the adjacent self-energy insertions. Products of the form below are then encountered,

$$\begin{aligned}&\Pi_{1,}{}^{\mu}{}_{\lambda_1}(k)\,V_{\mathrm{g}^2}{}^{\lambda_1\lambda_2}(k,-k-p)\,\Pi_{2,\lambda_2\lambda_3}(k+p)\,V_{\mathrm{g}^2}{}^{\lambda_3\lambda_4}(-k,k+p)\,\Pi_{3,\lambda_4}{}^{\nu}(k) \\ &\quad = \Pi_{1,k}(k)\,\Pi_{2,k}(k+p)\,\Pi_{3,k}(k)\,X^{\mu\nu}(k,p)\,,\end{aligned} \tag{4.58}$$

$$\begin{aligned}&\Pi_{3,}{}^{\mu}{}_{\lambda_1}(k)\, V_{\mathrm{g}^2}{}^{\lambda_1\lambda_2}(k,-k-p)\, \Pi_{2,\lambda_2\lambda_3}(k+p)\, V_{\mathrm{g}^2}{}^{\lambda_3\lambda_4}(-k,k+p)\, \Pi_{1,\lambda_4}{}^{\nu}(k)\\ &\quad= \Pi_{1,k}(k)\, \Pi_{2,k}(k+p)\, \Pi_{3,k}(k)\, X^{\mu\nu}(k,p)\,,\end{aligned} \tag{4.59}$$

$$\begin{aligned}&\Pi_{1,}{}^{\mu}{}_{\lambda_1}(k)\, \Pi_{3,}{}^{\lambda_1}{}_{\lambda_2}(k)\, V_{\mathrm{g}^2}{}^{\lambda_2\lambda_3}(k,-k-p)\, \Pi_{2,\lambda_3\lambda_4}(k+p)\, V_{\mathrm{g}^2}{}^{\lambda_4\nu}(-k,k+p)\\ &\quad= \Pi_{1,k}(k)\, \Pi_{2,k}(k+p)\, \Pi_{3,k}(k)\, X^{\mu\nu}(k,p)\,,\end{aligned} \tag{4.60}$$

$$\begin{aligned}&\Pi_{1,}{}^{\mu}{}_{\lambda_1}(k)\, V_{\mathrm{g}^2}{}^{\lambda_1\lambda_2}(k,-k-p)\, \Pi_{2,\lambda_2\lambda_3}(k+p)\, V_{\mathrm{g}^2}{}^{\lambda_3\lambda_4}(-k,k+p)\, \Pi_{3,\lambda_4}{}^{\nu}(k)\\ &\quad= \Pi_{1,k}(k)\, \Pi_{2,k}(k+p)\, \Pi_{3,k}(k)\, X^{\mu\nu}(k,p)\,,\end{aligned} \tag{4.61}$$

with the shared tensor,

$$\begin{aligned}X^{\mu\nu}(k,p) \equiv{}& g^{\mu\nu}\big(k^2+(k\cdot p)\big)^2 + p^\mu p^\nu k^2 - k^\mu k^\nu\big(k^2+2(k\cdot p)\big) - \big(p^\mu k^\nu\\ &+ k^\mu p^\nu\big)(k\cdot p)\,.\end{aligned} \tag{4.62}$$

All equalities are obtained by direct computation, although the last two are special instances of the shuffle symmetry. Graphically, the swap symmetry translates into

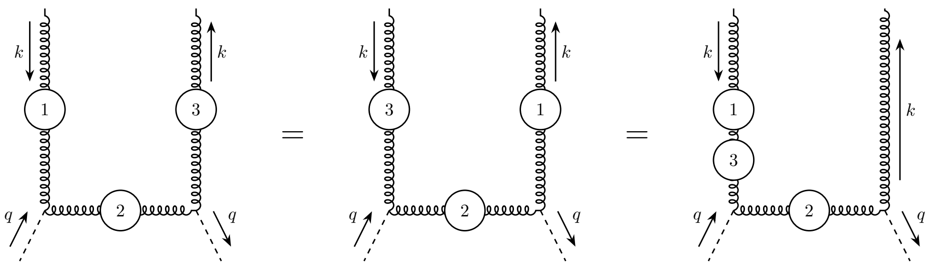

, (4.63)

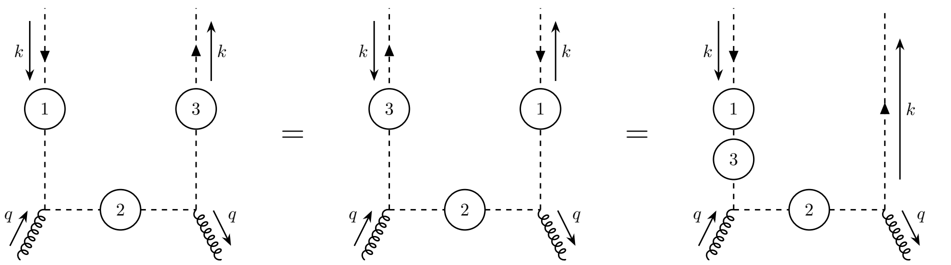

. (4.64)

No analogous identities exist for the three-gluon and gluon-quark vertices, owing to the non-commutativity of quark propagators and to tensor structures in the numerators that are neither manifestly symmetric nor antisymmetric. A notable consequence is that self-energies on a ghost line may be interchanged without reversing the direction of the line.

4.2.4 Amplitude Symmetries

Finally, graphs that differ only by the crossing of external particles are related. Unlike the symmetries discussed previously, those identified in this subsection act on Mellin moments of the amplitudes rather than on the amplitudes themselves.

At the level of the forward scattering amplitude, crossing corresponds to a parity transformation of the external momenta, accompanied where appropriate by an exchange of indices between identical external particles. To derive the corresponding symmetry relations, consider a graph Γ with L loops and only scalar external legs. Its amplitude $\mathcal{M}_\Gamma$ is built from the integrand $\mathcal{I}_\Gamma$. The N-th Mellin moment then follows through the harmonic projection operator,

$$\begin{aligned}\mathcal{P}_N(\mathcal{M}_\Gamma(p,q)) &\equiv \int \mathrm{d}^D k_1 \ldots \int \mathrm{d}^D k_L \, \mathcal{P}_N(\mathcal{I}_\Gamma(p,q)) \\ &= \int \mathrm{d}^D k_1 \ldots \int \mathrm{d}^D k_L \sum_{M=0}^{\infty} \mathcal{P}_N\left(p_{\mu_1} \ldots p_{\mu_M} \mathcal{J}^{\mu_1 \ldots \mu_M}(q)\right) \\ &= \int \mathrm{d}^D k_1 \ldots \int \mathrm{d}^D k_L \, \mathcal{P}_N\left(p_{\mu_1} \ldots p_{\mu_N} {\mathcal{J}_\Gamma}^{\mu_1 \ldots \mu_M}(q)\right) .\end{aligned} \tag{4.65}$$

By Lorentz invariance, the tensor $\mathcal{J}_\Gamma$ depends only on q and the metric tensor g. Since only the symmetric part survives contraction with a totally symmetric tensor, it may be taken to be totally symmetric without loss of generality.

Because each metric tensor contributes an even number of indices, and each power of the boson momentum contributes exactly one, the parity of the total index count must match that of the power of q. The remaining scalar coefficients are accordingly functions of q^2 alone, with the result

$$\begin{aligned}\int \mathrm{d}^D k_1 \ldots \int \mathrm{d}^D k_L \, {\mathcal{J}_\Gamma}^{\mu_1 \ldots \mu_M}(q) = \sum_{k=0}^{\lfloor \frac{M}{2} \rfloor} \hat{\mathcal{M}}^M_{\Gamma,2k}(q^2) \sum_\sigma g^{\sigma(\mu_1)\sigma(\mu_2)} \\ \times \ldots g^{\sigma(\mu_{2k-1})\sigma(\mu_{2k})} q^{\sigma(\mu_{2k+1})} \ldots q^{\sigma(\mu_M)} ,\end{aligned} \tag{4.66}$$

where the sum runs again over all independent permutations σ of the indices (see Subsec. 4.1.1). The N-th Mellin moment of the amplitude, Eq. (4.65), takes the form

$$\begin{aligned}\mathcal{P}_N(\mathcal{M}_\Gamma(p,q)) = \mathcal{P}_N\Bigg(p_{\mu_1} \ldots p_{\mu_N} \sum_{k=0}^{\lfloor \frac{M}{2} \rfloor} \hat{\mathcal{M}}^M_{\Gamma,2k}(q^2) \\ \times \sum_\sigma g^{\sigma(\mu_1)\sigma(\mu_2)} \ldots g^{\sigma(\mu_{2k-1})\sigma(\mu_{2k})} q^{\sigma(\mu_{2k+1})} \ldots q^{\sigma(\mu_M)} \Bigg) .\end{aligned} \tag{4.67}$$

Hence, the Mellin moment is an odd function of either external momentum when N is odd, and an even function when N is even.

Extending this symmetry to individual graphs requires recalling that the argument above applies only to scalar external edges. Attention now turns to the case where the edges carrying momentum p correspond to partons. For gluons, swapping one external leg for another is always permitted, since gluons are their own antiparticles. The polarisation sum is manifestly symmetric in the gluon indices, so the swap must be performed simultaneously on the momenta and their associated indices. For quarks and ghosts the situation differs, as reversing a quark line is not in general admissible, with analogous restrictions applying to ghost lines. The parity transformation is therefore permitted only for gluon legs, yielding the graphical identities

$\mathcal{P}_N\Big($ 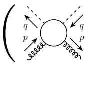 $\Big) = (-1)^N \mathcal{P}_N\Big($ 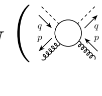 $\Big) = (-1)^N \mathcal{P}_N\Big($ 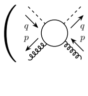 $\Big) = \mathcal{P}_N\Big($ 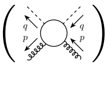 $\Big)$. (4.68)

If the external boson is a vector or an axial-vector rather than a scalar, it is contracted with a symmetric or antisymmetric tensor in the projection onto the partonic invariants. Depending on the projector, the simultaneous exchange of the bosonic momenta and their indices may therefore introduce an additional sign,

$\mathcal{P}_N$ (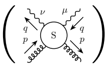) $= (-1)^N \mathcal{P}_N$ (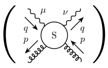) $= (-1)^N \quad \mathcal{P}_N$ (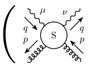) $= \quad \mathcal{P}_N$ (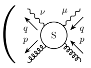) , (4.69)

$\mathcal{P}_N$ (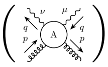) $= (-1)^N \mathcal{P}_N$ (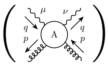) $= (-1)^{N+1} \mathcal{P}_N$ (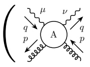) $= -\mathcal{P}_N$ (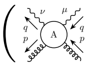) . (4.70)

Taken together, the conjugation, shuffle, swap, and crossing symmetries partition the graphs into equivalence classes. Non-trivial graphs contributing to the calculation are matched against these equivalence classes, with exchanges of external particles permitted and any resulting signs tracked explicitly.

The amplitudes are subsequently collected, up to overall numerical coefficients, into *super-amplitudes*, namely sums of all amplitudes that belong to the same integral family and share identical colour and flavour factors.

4.3 Integral Families

4.3.1 Momentum Routing

In practice, integral families are rarely complete, and the basis must be supplemented by adjoining auxiliary propagators. This choice is not unique, and different completions can yield inequivalent integral families of varying complexity. A common heuristic is to add the simplest propagators that generate the required scalar products, such as

$$\begin{aligned} k_i \cdot k_j \;&\leftrightarrow\; (k_i \pm k_j)^2 \,, \\ k_i \cdot p_j \;&\leftrightarrow\; (k_i \pm p_j)^2 \,. \end{aligned} \tag{4.71}$$

The rationale is that IBP identities act as derivative operators, and propagators involving fewer internal momenta produce fewer terms upon differentiation. This criterion is, however, insufficient on its own. A more complicated choice of auxiliary propagators may, after a suitable momentum shift, yield a simpler family overall, and it is not a priori clear whether the auxiliary propagators should be massless or massive. A more systematic approach is therefore required.

In what follows, we restrict attention to massless two-point functions from one to five loops, where the only external momentum is q, and construct *simple* integral families for these integrals. This restriction is practical, because two-point functions are precisely the objects required for the computation of Mellin moments in subsequent sections. The same strategies apply to problems with more external momenta, though the combinatorics become considerably more involved.

By a simple integral family we mean a family that maximises the number of graphs that can be mapped into it whilst minimising the number of internal momenta appearing in the propagators. The first criterion takes priority over the second. To make this concrete, we rank the propagators schematically in order of increasing complexity,

$$k_{i_1}^2, \quad (k_{i_1}+q)^2, \quad (k_{i_1}+k_{i_2})^2, \quad (k_{i_1}+k_{i_2}+q)^2, \quad (k_{i_1}+k_{i_2}+k_{i_3})^2, \quad \ldots\,, \tag{4.72}$$

and maximise, starting from the simplest type, the number of propagators of each kind in turn.

Not all graphs appearing in physical amplitudes need be considered. Every graph with a vertex of valence greater than three can be obtained from a trivalent one by contracting internal edges. It therefore suffices to work with trivalent graphs alone. At the level of integrals, contracted edges correspond to propagators raised to the zeroth power.

Trivalent graphs can be simplified further by contracting edges. Graphs that are not two-edge-connected contain *bridges*, edges carrying no internal momentum. Such bridges are purely multiplicative prefactors to the integral and may therefore be contracted without loss of information. Similar simplifications apply to graphs containing *self-energy insertions*, namely two-point subgraphs of lower loop order. By momentum conservation, both external edges of such a subgraph carry the same momentum, so one may be contracted whilst the other is assigned a suitable exponent to account for the subgraph.

A two-edge-connected trivalent graph without self-energy insertions will be referred to as an *independent graph*, and only such graphs are considered subsequently. Such a graph $G_{L,i}$ at L loops has

$$V(L) = 2L\,, \tag{4.73}$$
$$E(L) = 3L - 1\,, \tag{4.74}$$

vertices and edges respectively, consistent with the Euler characteristic for a single connected component.

Each edge is assigned an edge momentum $q_{i,j}$, with an implicit choice of orientation, subject to momentum conservation at every vertex. The set of propagators associated with the graph is

$$P_{L,i} = \bigcup_{j=1}^{E} \{\, q_{i,j}^2 \,\}\ . \tag{4.75}$$

In general, this set does not span the full space of scalar products, and completing the basis requires a suitable choice of auxiliary propagators (see Subsec. 3.1.1). The number of distinct momenta that can be formed from L internal momenta and only one external momentum grows rapidly with the loop order, following the sequence `A029858` [208],

$$N(L) = 3, 12, 39, 120, 363, 1092, 3279, 9840, \dots \tag{4.76}$$

Completing a family requires selecting $A(L)$ auxiliary propagators from amongst these, after excluding the $E(L)$ edges already present as propagators, giving

$$\hat{N}(L) = \binom{N(L) - E(L)}{A(L) - E(L)} \tag{4.77}$$

possible completions. Evaluating Eq. (4.77) for the first few loop orders reveals combinatorial growth,

$$\hat{N}(L) \approx 1, 1, 10, 10^5, 10^{12}, 10^{23}, 10^{40}, 10^{64}, \dots \tag{4.78}$$

Consequently, an exhaustive search for ideal auxiliary scalar products is feasible up to three loops, difficult at four, and entirely out of reach at five. Some more efficient strategy is required.

However, most of the available momenta are irrelevant, since they do not appear in the propagators of any of the independent graphs. The search may therefore be restricted to a smaller set of *candidate momenta*, large enough to contain all useful auxiliary propagators yet small enough to render the combinatorics tractable. To construct this set, we associate with each independent graph a collection of *reduced graphs*, obtained by contracting internal edges whilst preserving the Euler characteristic. Self-loops are never contracted, and the process terminates once a graph with L self-loops is reached. The propagators of any reduced graph form a subset of those of the original,

$$R_{L,i,k} \subseteq P_{L,i}\,, \tag{4.79}$$

with equality when no edges have been contracted. Using the parametric representation of the graph polynomials, isomorphisms between the reduced graphs can be identified (see Subsec. 3.1.4). At each loop order, there exists a reduced graph R_L that is isomorphic to a subgraph of every independent graph,

$$\exists\, R_{L,i,k} \subseteq P_{L,i}: \quad R_{L,i,k} \cong R_L\,. \tag{4.80}$$

Such a graph exists because every graph can be reduced to one containing only self-loops. The propagators of each independent graph admit the decomposition,

$$P_{L,i} = R_L \sqcup C_{L,i}\,, \tag{4.81}$$

where the sets $C_{L,i}$ contain the candidate momenta, that is, those propagators not already present in the reduced graph. Taking the union over all independent graphs yields the full set of candidate momenta,

$$C_L = \bigsqcup_{i=1}^{N_L} C_{L,i}\,, \tag{4.82}$$

which is typically much smaller than the set of all available momenta, reducing the combinatorial problem to a more tractable size.

Simple families are sought under the working assumption that a single family suffices to accommodate all independent graphs. Should such a family be found, the assumption is validated; otherwise, we attempt to cover all graphs with two families, establishing two as the minimum. Since every independent graph must be contained in the family, the construction may be seeded with any one of them, $R_{L,j}$. A natural choice is the reduced graph obtained from the ladder graph, which exists at each loop order and whose propagators take the form

$$\bigsqcup_{i=1}^{L} \left\{\, k_i^2, (k_i+q)^2 \,\right\} \sqcup \bigsqcup_{i=1}^{L-1} \left\{\, (k_i - k_{i+1})^2 \,\right\}\,, \tag{4.83}$$

as these involve the fewest internal momenta per propagator. The candidate families are constructed by augmenting this reduced graph with all subsets of candidate momenta of the appropriate size,

$$\mathcal{C}_L = \left\{\, C \subset C_L \,:\, |C| = S(L) - E(L) \,\right\}\,, \tag{4.84}$$

which yields the set of candidate integral families,

$$\mathcal{F}_L = \bigcup_{X \in \mathcal{C}_L} \left\{\, R_{L,j} \cup X \,\right\} / \sim\,, \tag{4.85}$$

where families equivalent under momentum shifts are identified. Each candidate family is tested against the full set of independent graphs, again using the parametric representation, to determine which graphs it accommodates.

At one and two loops, the number of scalar products coincides with the number of edges, and only a single independent graph exists at each loop order. The family is therefore uniquely determined, and such a family is called a *momentum routing*,

$$\mathcal{R}_1 = \{\, k_1, k_1 + q \,\} \;, \tag{4.86}$$
$$\mathcal{R}_2 = \{\, k_1, k_1 + q, k_2, k_2 + q, k_1 - k_2 \,\} \;. \tag{4.87}$$

The first non-trivial case occurs at three loops. Three independent graphs appear, giving rise to the sets of momenta

$$P_{3,1} = \{\, k_1, k_1 + q, k_2, k_2 + q, k_3, k_3 + q, k_1 - k_2, k_3 - k_2 \,\} \;, \tag{4.88}$$
$$P_{3,2} = \{\, k_1, k_1 + q, k_2 + q, k_3, k_3 + q, k_1 - k_2, k_3 - k_2, k_1 - k_2 + k_3 \,\} \;, \tag{4.89}$$
$$P_{3,3} = \{\, k_1, k_1 + q, k_2, k_2 + q, k_3, k_1 - k_2, k_3 - k_2, k_1 - k_2 + k_3 \,\} \;. \tag{4.90}$$

Contracting a single edge in each independent graph yields a collection of reduced graphs with the following sets of momenta,

$$R_{3,1,3} = \{\, k_1,\ k_1 + q,\ k_2,\ k_3,\ k_3 + q,\ k_1 - k_2,\ k_2 - k_3 \,\} \;, \tag{4.91}$$
$$R_{3,2,1} = \{\, k_1,\ k_1 + q,\ k_2 + q,\ k_3,\ k_3 + q,\ k_1 - k_2,\ k_2 - k_3 \,\} \;, \tag{4.92}$$
$$R_{3,3,3} = \{\, k_1,\ k_1 + q,\ k_2,\ k_2 + q,\ k_3,\ k_2 - k_3,\ k_1 - k_2 + k_3 \,\} \;. \tag{4.93}$$

The reduced graphs, Eqs. (4.91), (4.92) and (4.93), turn out to be isomorphic, with the latter two mapped to the first by the respective momentum shifts,

$$k_1 \to -q - k_1, \qquad k_2 \to -k_2 - q, \qquad k_3 \to -k_3 - q, \tag{4.94}$$
$$k_1 \to k_3, \qquad k_2 \to k_1, \qquad k_3 \to -k_2 + k_1. \tag{4.95}$$

Under these shifts, Eqs. (4.94) and (4.95), the full set of propagators of the respective independent graphs, Eqs. (4.89) and (4.90), becomes

$$P_{3,1} \cong \{\, k_1, k_1 + q, k_2, k_3, k_3 + q, k_1 - k_2, k_3 - k_2, k_2 + q \,\} \;, \tag{4.96}$$
$$P_{3,2} \cong \{\, k_1, k_1 + q, k_2, k_3, k_3 + q, k_1 - k_2, k_3 - k_2, k_1 - k_2 + k_3 + q \,\} \;, \tag{4.97}$$
$$P_{3,3} \cong \{\, k_1, k_1 + q, k_2, k_3, k_3 + q, k_1 - k_2, k_3 - k_2, k_1 - k_3 \,\} \;. \tag{4.98}$$

After these shifts, the first seven momenta across all three independent graphs coincide, showing that they share a common reduced graph. The ladder graph, Eq. (4.96), contributes no candidate momenta, whilst the remaining two each contribute one,

$$C_3 = \{\, k_1 - k_2 + k_3 + q,\ k_1 - k_3 \,\} \;. \tag{4.99}$$

Augmenting the reduced graph, Eq. (4.91), with each candidate momentum in turn yields two candidate families,

$$F_{3,1} = \{\, k_1, k_1 + q, k_2, k_3, k_3 + q, k_1 - k_2, k_3 - k_2, k_2 + q \,\} \;, \tag{4.100}$$
$$F_{3,2} = \{\, k_1, k_1 + q, k_2, k_3, k_3 + q, k_1 - k_2, k_3 - k_2, k_1 - k_2 + k_3 + q \,\} \;. \tag{4.101}$$

Testing these against all independent graphs, Eqs. (4.96) to (4.98), shows that the second family accommodates all three. Applying the momentum shift

$$k_1 \to -q - k_1, \quad k_2 \to -k_2 - q, \quad k_3 \to -k_3 - q\,, \tag{4.102}$$

already encountered in the reduction of the three-loop graphs, Eq. (4.94), brings the family into a form that manifestly contains the ladder graph. The single auxiliary propagator involves three internal momenta, reflecting the presence of non-planar graphs amongst the independent topologies. As a result, the minimal family reads

$$\mathcal{R}_3 = \{\, k_1, k_1+q, k_2, k_2+q, k_3, k_3+q, k_1-k_2, k_3-k_2, k_1-k_2+k_3 \,\}\,. \tag{4.103}$$

A new feature emerges at four loops, namely *chiral graphs*, defined as graphs related by the parity transformation of the external momentum. Fifteen independent graphs appear at this loop order, of which four pairs are related by parity and may be treated as equivalent. A further complication is that edge contractions can produce graphs that are not one-vertex-connected, for which the correspondence between graph automorphisms and integrand symmetries breaks down. Both issues are handled by the parametric representation without difficulty. Following the same procedure as at three loops, a single family is found to suffice for all independent graphs,

$$\begin{aligned}\mathcal{R}_4 = \big\{&k_1, k_1+q, k_2, k_2+q, k_3, k_3+q, k_4, k_4+q, k_1-k_2, k_2-k_3, k_3-k_4,\\ &k_1-k_3+k_4, k_1-k_2+k_4, k_1+k_4+q\big\}\,.\end{aligned} \tag{4.104}$$

At five loops the situation changes, and a single family no longer suffices. Of the one hundred independent graphs appearing at this order, sixty-four are inequivalent under parity. An exhaustive search shows that no single family accommodates more than sixty-two of them, so at least two families are required,

$$\begin{aligned}\mathcal{R}_{5,1} = \big\{&k_1, k_1+q, k_2, k_2+q, k_3, k_3+q, k_4, k_4+q, k_5, k_5+q, k_1-k_2,\\ &k_2-k_3, k_3-k_4, k_4-k_5, k_2-k_4, k_2-k_4+k_5, k_1-k_2+k_3+q,\\ &k_1+k_3-k_4+q, k_3-k_4+k_5+q, k_1+k_3-k_4+k_5+q\big\}\,,\end{aligned} \tag{4.105}$$

$$\begin{aligned}\mathcal{R}_{5,2} = \big\{&k_1, k_2, k_1+k_2, k_3, k_2-k_4, k_4, k_3+k_4, k_1+k_3+k_4, -k_2+k_3+k_4,\\ &k_2-k_5, k_1+k_4-k_5, k_5, k_3+k_5, k_4-k_5, k_1+k_4-q, k_1+k_2-q,\\ &k_3+k_4-q, k_1+k_3+k_4-q, k_5-q, k_3+k_5-q\big\}\,.\end{aligned} \tag{4.106}$$

The reduction from one hundred graphs to only two families is nonetheless a substantial simplification[2].

Four- and five-loop results demonstrate that the vast majority of choices of auxiliary propagators (see Fig. 4.1) yield little or no simplification. This observation carries considerable practical significance, as IBP reduction at higher loop orders can demand months or even years of computation, whereas identifying optimal integral families beforehand requires far less effort and dramatically reduces the overall cost. At four loops, the search procedure described here completes almost instantaneously on an ordinary laptop, whilst at five loops it requires approximately one week on a cluster of roughly one hundred cores. Since the analysis need only be performed once and requires minimal memory, the investment in optimisation is well worthwhile.

[2]To the best of the author's knowledge, this minimality result has not previously appeared in the literature.

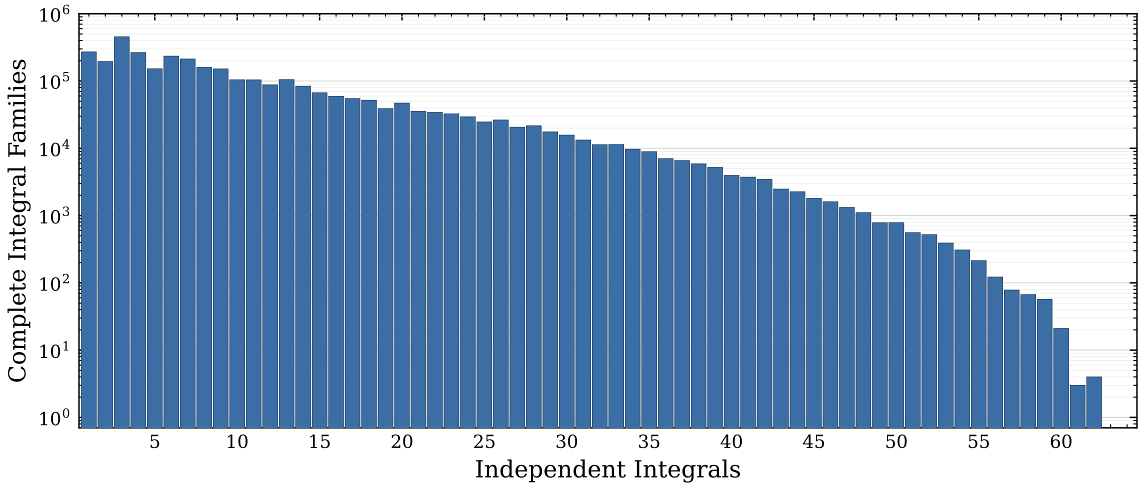

Figure 4.1: The bins show the number of complete families containing a fixed number of independent graphs.

Several extensions of these strategies are worth noting. Allowing contractions of multiple edges would yield reduced graphs specific to subsets of topologies, enabling candidate propagators to be ranked by their frequency of appearance. At higher loop orders or with additional external momenta, a greedy algorithm becomes practical, in which auxiliary propagators are added one at a time, each step selecting the momentum that covers the largest number of remaining independent graphs.

These results also have implications for vacuum integrals. Any two-point graph may be converted into a vacuum integral by treating the external momentum as an internal momentum, which at the level of the graph amounts to identifying the two external vertices. Conversely, a vacuum integral may be opened into a two-point graph by cutting any internal edge and routing the external momentum through it. The described method is also known as *glueing* and *cutting* [94, 209, 210]. Integral families constructed for two-point functions therefore automatically provide families for the corresponding vacuum integrals. Up to five loops a single family suffices for all of them, whilst at six loops two are required. For instance, through three loops we find the momentum routings for vacuum graphs,

$$\mathcal{R}_1^{\mathrm{V}} = \{\, k_1 \,\} \,, \tag{4.107}$$
$$\mathcal{R}_2^{\mathrm{V}} = \{\, k_1, k_2 - k_1, k_2 \,\} \,, \tag{4.108}$$
$$\mathcal{R}_3^{\mathrm{V}} = \{\, k_1, k_2 - k_1, k_2, k_3 - k_1, k_3 - k_2, k_3 \,\} \,. \tag{4.109}$$

An alternative route to two-point families, which we mention without pursuing in detail, is suggested by this correspondence. Rather than working with two-point graphs directly, we may first determine the minimal set of families covering all vacuum topologies and then promote one of the internal momenta to the external momentum q. Since vacuum graphs have fewer edges and vertices than the corresponding two-point graphs, the combinatorial search is simpler. The choice of which internal momentum to promote is not unique, however, and testing all possibilities reintroduces a combinatorial overhead.

4.3.2 Mass Assignments

Momentum routings are advantageous in that they already minimise the number of families required for the treatment of massless amplitudes. They also render cancellations manifest at the integrand level, since the master integrals within a single family are linearly independent, whereas this need not hold across distinct families. The routings alone would therefore suffice to define all integral families if all internal lines were massless. Since internal lines may, however, carry masses, the routings must be dressed accordingly.

To this end, recall that edges may be classified as either massive or massless, each edge i carrying a mass m_i equal to zero or to the heavy-quark mass m. The set of all graphs with L loops contributing to the forward scattering amplitude is denoted $\mathcal{G}_L$, and the edges of a graph $\Gamma \in \mathcal{G}_L$ are contained in the set $\mathcal{E}_\Gamma$. With each graph we associate the set of momentum-mass pairs encoding its denominator structure,

$$\mathcal{F}_\Gamma \equiv \bigcup_{i \in \mathcal{E}_\Gamma} \{ \, (p_i|_{p=0}, m_i) \, \} \setminus \sim \; . \tag{4.110}$$

Equivalent momenta, namely those differing by an overall sign, are identified here, as they always appear squared in the propagators. An auxiliary set is further defined as

$$\mathcal{R}(\mathcal{F}_\Gamma) \equiv \bigcup_{(p,m) \in \mathcal{F}_\Gamma} \{p\} \, . \tag{4.111}$$

All denominator structures are grouped into equivalence classes by identifying all sets of momenta related by momentum shift transformations. Such transformations are conveniently encoded in a linear operator T satisfying

$$T(\mathcal{F}_\Gamma) = \bigcup_{i \in \mathcal{E}_\Gamma} \{ \, (T(p_i)|_{p=0}, m_i) \, \} \setminus \sim \, , \tag{4.112}$$

$$T(l_i) = \omega_{i,0} q + \sum_{j=1}^{L} \omega_{i,j} k_j \, , \quad \omega_{i,j} \in \{ \, -1, 0, 1 \, \} \; . \tag{4.113}$$

All momentum-shift transformations are collected in the set $\mathcal{T}$. Among these, only those preserving the set size and remaining within the same momentum routing are admissible. The admissible transformations form the subset

$$\mathcal{T}_A = \big\{ T \in \mathcal{T} \mid (\mathcal{R}(T\mathcal{F}_\Gamma) \backslash R_L = \emptyset) \wedge (|T\mathcal{F}_\Gamma| = |\mathcal{F}_\Gamma|) \big\} \, . \tag{4.114}$$

Size constraints arise because certain shifts cause two or more edge momenta to coincide, rendering the corresponding Jacobian matrix non-invertible and the shift itself invalid. An equivalence class of denominator structures may be defined as

$$\big[\mathcal{F}_\Gamma\big] = \bigcup_{T \in \mathcal{T}_A} \big\{ T\mathcal{F}_\Gamma \big\} \, . \tag{4.115}$$

These equivalence classes are free of duplicate entries, being unions of sets by construction. Remaining redundancies arise only from classes whose members are contained within those of larger cardinality. This translates into the requirement that the power set P of each equivalence class must not be a subset of that of any class of larger cardinality. Independent equivalence classes are then defined as

$$\mathcal{C}_L = \bigcup_{\substack{\Gamma\in\mathcal{G}_L, \\ P([\mathcal{F}_\Gamma])\not\subset P([\mathcal{F}_{\Gamma'}])\ \forall\Gamma'\in\mathcal{G}_L:|[\mathcal{F}_{\Gamma'}]|>|[\mathcal{F}_\Gamma]|}} \left\{[\mathcal{F}_\Gamma]\right\}. \tag{4.116}$$

To determine the minimal set of families, a given momentum routing is dressed with masses, yielding a basis such as

$$\mathcal{B}_{L,b} = \{(q_1, b_1), \ldots, (q_n, b_n)\}, \quad b = \sum_{i=1}^{n} 2^{i-1}\frac{b_{n-i+1}}{m_i}. \tag{4.117}$$

Constructing the sets for all possible mass assignments of the momentum routings is equivalent to taking the union over all such sets for every binary representation of b with n digits. The full set of integral families is therefore obtained by the union

$$\mathcal{B}_L = \bigcup_{b=0}^{2^n-1} \left\{\mathcal{B}_{L,b}\right\}. \tag{4.118}$$

For notational convenience, two auxiliary functions are introduced. The first is a bijective index function g mapping each independent equivalence class to an index in the set $\mathcal{I} \subset \mathbb{N}$ with $|\mathcal{I}| = |\mathcal{C}_\Gamma|$, where the values may be chosen arbitrarily,

$$g_L : \mathcal{C}_L \to \mathcal{I}, \quad g_L(C) = i, \quad C \in \mathcal{C}_L, i \in \mathcal{I}. \tag{4.119}$$

Since the map is applied to equivalence classes, it induces a canonical map assigning to each member of a class the index of the class itself,

$$\tilde{g}_L : C \in \mathcal{C}_L \to \mathcal{I}, \quad \tilde{g}_L(c) = g_L(C), \quad c \in C. \tag{4.120}$$

This follows because the equivalence classes are by construction disjoint, and hence their members are independent. The index function is then used to define an indicator function,

$$f_L : \mathcal{C}_L \times \mathcal{B} \to P_{\leq 1}(\mathcal{I}), \quad f_L(c, b) = \begin{cases} \{\tilde{g}_L(c)\}, & c \setminus b = \emptyset, \\ \emptyset, & c \setminus b \neq \emptyset, \end{cases} \quad c \in \mathcal{C}_L, b \in \mathcal{B}, \tag{4.121}$$

where $P_{\leq 1}$ denotes the power set restricted to the empty set and sets of cardinality one. This indicator function then assigns to each basis family the independent classes it contains,

$$\mathcal{S}_{L,b} = \bigcup_{C\in\mathcal{C}} \left(\bigcup_{c\in C} f_L(c, \mathcal{B}_{L,b})\right). \tag{4.122}$$

With this family of sets, the construction of a minimal set of integral families reduces to a standard set-covering problem, with the family $\mathcal{S}_L$ and the universe $\mathcal{U}_L$ given by

$$\mathcal{S}_L = \bigcup_{b=0}^{2^n-1} \left\{\mathcal{S}_{L,b}\right\}, \tag{4.123}$$

$$\mathcal{U}_L = \bigcup_{b=0}^{2^n-1} \mathcal{S}_{L,b} \,. \tag{4.124}$$

The set-covering problem may be further optimised by restricting the candidates to inequivalent integral families.

Up to three loops, the problem remains sufficiently small for non-greedy implementations of the set-covering algorithm to be applied. This is feasible because the covering sets are sparse, with most entries empty. The integral families obtained in this way constitute a minimal set. Solving the set-covering problem yields the integral families for the neutral current,

$$\mathcal{B}_1^{\mathrm{NC}} = \left\{\mathcal{B}_{1,0}, \mathcal{B}_{1,3}\right\}, \tag{4.125}$$

$$\mathcal{B}_2^{\mathrm{NC}} = \left\{\mathcal{B}_{2,0}, \mathcal{B}_{2,7}, \mathcal{B}_{2,30}\right\}, \tag{4.126}$$

$$\mathcal{B}_3^{\mathrm{NC}} = \left\{\mathcal{B}_{3,0}, \mathcal{B}_{3,27}, \mathcal{B}_{3,103}, \mathcal{B}_{3,414}, \mathcal{B}_{3,482}, \mathcal{B}_{3,505}\right\}, \tag{4.127}$$

and those exclusive to the charged current,

$$\mathcal{B}_1^{\mathrm{CC}} = \left\{\mathcal{B}_{1,2}\right\}, \tag{4.128}$$

$$\mathcal{B}_2^{\mathrm{CC}} = \left\{\mathcal{B}_{2,10}, \mathcal{B}_{2,13}\right\}, \tag{4.129}$$

$$\mathcal{B}_3^{\mathrm{CC}} = \left\{\mathcal{B}_{3,168}, \mathcal{B}_{3,179}, \mathcal{B}_{3,207}, \mathcal{B}_{3,310}, \mathcal{B}_{3,330}, \mathcal{B}_{3,337}\right\}. \tag{4.130}$$

Assigning integral families to the graphs of the forward scattering amplitude is the final step. Since the assignment was performed at the level of equivalence classes, the momenta in the amplitude must be shifted accordingly to bring each graph into the form of its assigned family. Determining these shifts is a matter of bookkeeping and poses no conceptual difficulty.

Two natural generalisations of the algorithm present themselves. First, it extends to theories involving n distinct masses by replacing the binary encoding of the mass assignments with a base-n representation, leaving the remainder of the procedure unchanged. Second, it applies to problems requiring several momentum routings, in which case the equivalence classes must be broadened to allow shifted incomplete families to be embedded in any of the available routings rather than in a single one. With these modifications, the procedure is otherwise unaltered. For a detailed discussion of the NLO results, see Ref. [211].

4.4 Differential Equations

4.4.1 Selection of Master Integrals

The computation of the master integrals proceeds in several steps. Once the full amplitude has been generated and the integral families have been assigned, all of the integrals that appear are read out, with the trivial ones discarded immediately and equivalent ones identified (see Sec. 3.1.4). The remaining integrals are reduced with `Kira` [177–179] and `FireFly` [212, 213], and the master integrals are chosen so as to build a dot basis. A single constraint is placed on the basis, namely that the denominators of the reduced integrals are sufficiently simple, with no mixing of the dimension and the kinematic scales.

For the reduction, we exploit the scaling relation for Feynman integrals, Eq. (3.128), and set $m^2 = 1$, which fixes the mass scale and leaves a single kinematic variable

$$x = \frac{q^2}{m^2} \,. \tag{4.131}$$

Reducing the full amplitude requires more integral families than the computation of the master integrals alone, because master integrals that are linearly independent within a given family need not stay independent across different integral families. A dot basis makes symmetries of the master integrals manifest, and equivalent sectors can in particular be assigned the same master integrals across families. The resulting set is linearly independent, but non-linear relations may potentially exist amongst its elements. By the factorisation criterion (see Subsec. 3.1.2), about a third of the master integrals are found to factorise.

An exhaustive list of all master integrals required is given for the neutral current (see Tab. A.1) and for the charged current (see Tab. A.2), where we also record their factorisation and the sector symmetries, with a single representative master integral listed in each case. In total we find three, ten and seventy-one master integrals for the neutral current and two, eight and fifty-seven for the charged current, at one, two and three loops respectively. Of these, three, four and forty-five are independent for the neutral current and two, five and forty-seven for the charged current, in the sense that they do not factorise. In contrast to the reduction, the calculation of the master integrals themselves requires only two, three and five integral families for the neutral current and one, one and three for the charged current.

4.4.2 Classification of Master Integrals

All massive master integrals are computed by the method of differential equations, which yields a series expansion in the dimensional regulator. Each integral is then characterised in two respects, namely the depth to which this expansion is required and the class of functions in which it can be expressed, the latter being either polylogarithmic or elliptic.

The depths are not immediately apparent, since IBP reduction introduces spurious poles. Each master integral is therefore assigned a depth by taking the fully reduced Mellin moments, inserting the formal expansions of the master integrals, and collecting the highest order that contributes to the finite part through three loops, including contributions from renormalisation.

Since x is the only kinematic variable, all differential equations are univariate (see Sec. 3.3.3). Each master integral, and hence its family, is broadly labelled either as an elliptic candidate or as strictly polylogarithmic, a distinction that remains somewhat loose and is justified later. Two heuristics guide this labelling. One rests on the fact that an elliptic curve requires at least three singular points, flagging as elliptic candidates all families whose sectors contain a homogeneous system with three such points (see Fig. 4.2). Another checks whether a family contains a known elliptic subgraph, namely one of the fully massive two- or three-loop banana graphs.

Elliptic integrals further separate into two classes, those carrying an elliptic homogeneous sector, termed homogeneously elliptic, and those coupling to such a block only through the inhomogeneity, termed inhomogeneously elliptic. For the neutral and charged currents, three and twelve homogeneously elliptic integrals arise respectively,

$$\mathcal{E}^{\mathrm{NC}} = \left\{ I^{\mathrm{NC}}_{3,10},\, I^{\mathrm{NC}}_{3,11},\, I^{\mathrm{NC}}_{3,12} \right\} , \tag{4.132}$$

$$\mathcal{E}^{\mathrm{CC}} = \left\{ I^{\mathrm{CC}}_{2,3},\, I^{\mathrm{CC}}_{2,4},\, I^{\mathrm{CC}}_{3,05},\, I^{\mathrm{CC}}_{3,06},\, I^{\mathrm{CC}}_{3,10},\, I^{\mathrm{CC}}_{3,11},\, I^{\mathrm{CC}}_{3,12},\, I^{\mathrm{CC}}_{3,17},\, I^{\mathrm{CC}}_{3,18},\, I^{\mathrm{CC}}_{3,22},\, I^{\mathrm{CC}}_{3,23},\, I^{\mathrm{CC}}_{3,24} \right\} . \tag{4.133}$$

A further eleven and twenty-seven inhomogeneous elliptic integrals are present for the neutral and charged currents respectively, and are not listed explicitly.

In the neutral current case, the one- and two-loop families are purely polylogarithmic, and only at three loops do three of the six families become elliptic. The charged current turns elliptic sooner. Beyond the polylogarithmic one-loop family, two loops bring one elliptic and one polylogarithmic family, and at three loops five of the six families are elliptic.

All one- and two-loop integrals are determined by the three-loop ones, because factorisation allows each to be obtained from a three-loop integral up to signs fixed by inexpensive numerical evaluations. It therefore suffices to focus the discussion on the three-loop case, even though every integral may be computed from its respective differential equation.

Polylogarithmic and elliptic differential equations are solved separately for computational reasons, as the former can be solved almost fully automatically whilst the latter require case-by-case analysis. Within each current, an elliptic system is constructed by augmenting the elliptic master integrals with polylogarithmic ones until the system closes. For the neutral current three systems arise, whilst the charged current yields a single one into which all polylogarithmic integrals are absorbed.

4.5 Integration of the Master Integrals

4.5.1 Polylogarithmic Integrals

Purely polylogarithmic differential equations are essentially trivial, as the corresponding system can be brought into ε-factorised form using the Mathematica package `Canonica` [214]. Because the package supports only rational transformations, any algebraic factors appearing in the transformation, namely square roots, must first be anticipated and rationalised. Care is needed, however, as the change of variables used to achieve this must respect the underlying kinematics.

In terms of the original variable x, the singular points of the polylogarithmic differential equations are

$$x_*^{\mathrm{phys}} \in \{ -4,\ 0,\ 1,\ 4 \} , \tag{4.134}$$

where the singularity at infinity is set aside. Constructing a transformation to ε-factorised form requires the introduction of the square roots

$$\left\{ \sqrt{x(x-4)},\ \sqrt{x(x+4)} \right\} . \tag{4.135}$$

For $m^2 > 0$ and spacelike $q^2 < 0$, the variable x lies in the interval $(-\infty, 0)$, on which the square roots are partially rationalised by the parametrisation

$$x(y) = -\frac{(1-y)^2}{y} , \tag{4.136}$$

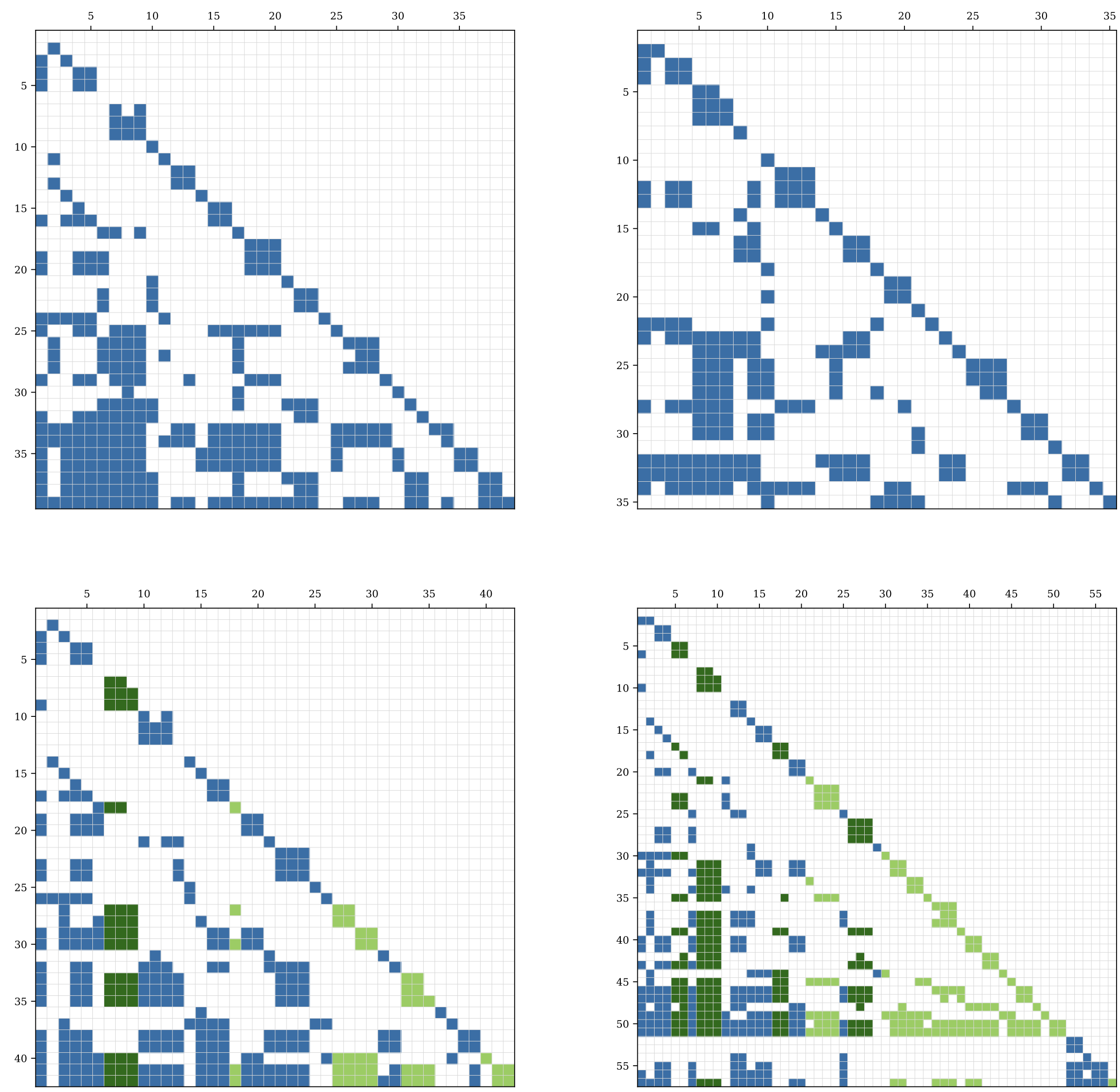

Figure 4.2: Differential equations for the master integrals. The top row shows the polylogarithmic systems, the bottom row the elliptic ones, with the neutral current on the left and the charged current on the right. Homogeneous elliptic sectors are shown in dark green, inhomogeneous ones in light green.

inverted by

$$y(x) = 1 - \frac{x}{2} - \frac{1}{2}\sqrt{x(x-4)}\,. \tag{4.137}$$

The endpoints $x \to -\infty$ and $x \to 0^-$ map to $y \to 0^+$ and $y \to 1^-$ respectively, so that $y \in (0,1)$. Beyond the singular points of the original differential equation, the reparametrisation introduces further ones. Images of the initial four singular points, Eq. (4.134),

$$y_*^{\text{phys}} \in \left\{ -1,\ 1,\ 3-2\sqrt{2},\ \frac{1}{2}(1-i\sqrt{3}) \right\}, \tag{4.138}$$

are accompanied by three spurious ones,

$$y_*^{\text{spur}} \in \left\{ 0,\ 3+2\sqrt{2},\ \frac{1}{2}(1+i\sqrt{3}) \right\}, \tag{4.139}$$

which are artefacts of the rationalisation procedure and must cancel in any physical result. Under the substitution, the square roots, Eq. (4.135), transform as

$$\sqrt{x(x-4)} \longmapsto -\frac{(y-1)(y+1)}{y}\,, \tag{4.140}$$

$$\sqrt{x(x+4)} \longmapsto -\frac{(y-1)}{y}\sqrt{1-6y+y^2}\,, \tag{4.141}$$

where the sign reflects the branch convention implied by $x \in (-\infty, 0)$. Only the first root is rationalised by this parametrisation. Simultaneous rationalisation of the second root is accomplished through a further change of variables, found with the Mathematica package `RationalizeRoots` [199],

$$y(z) = \frac{2(z-3)}{z^2-1}\,, \tag{4.142}$$

inverted by

$$z(y) = \frac{1-\sqrt{1-6y+y^2}}{y}\,. \tag{4.143}$$

Under this change of variables, z is no longer real but traces a curve in the complex plane with endpoints $z(0) = 3$ and $z(1) = 1 - 2i$. Working along a complex curve causes no difficulty, as the differential equations remain rational, and hence single-valued, in z. Eleven singular points appear, four of them physical,

$$z_*^{\mathrm{phys}} \in \Big\{ -1+2\sqrt{2},\ 1-2i,\ 3+2\sqrt{2},\ \frac{1}{2}\big[1+\sqrt{5}-i(\sqrt{15}-\sqrt{3})\big] \Big\}\,, \tag{4.144}$$

the remaining seven being spurious,

$$\begin{aligned} z_*^{\mathrm{spur}} \in \Big\{ & -1-2\sqrt{2},\ 3-2\sqrt{2},\ 1+2i,\ \frac{1}{2}\big[1+\sqrt{5}+i(\sqrt{15}-\sqrt{3})\big], \\ & \frac{1}{2}\big[1-\sqrt{5}+i(\sqrt{15}+\sqrt{3})\big],\ \frac{1}{2}\big[1-\sqrt{5}-i(\sqrt{15}+\sqrt{3})\big],\ 3 \Big\}\,. \end{aligned} \tag{4.145}$$

The second square root is now rationalised,

$$\sqrt{1-6y+y^2} \longmapsto \frac{z^2-6z+1}{(z-1)(z+1)}\,, \tag{4.146}$$

and the first remains so by virtue of the transformation being itself rational. Both square roots are thereby rationalised, and every polylogarithmic differential equation can be brought into ε-factorised form without complication.

4.5.2 Neutral Current Elliptic Integrals

This section presents the calculation of the elliptic integrals encountered in the neutral current. Discussion focuses on the homogeneous block of the fully massive three-loop banana graph which, whilst more involved than the two-loop banana of the charged current, is the more illustrative case. Remaining elliptic integrals follow by direct analogy and are not discussed separately.

Similar calculations have appeared in the literature [215], and all results obtained here agree with them up to some typographical errors in those works, whilst the QCD exclusive integrals are structurally compatible with existing results. The three-loop banana integrals have been studied extensively in the literature [216–219]. However, complete derivations are still included here, as most references omit intermediate steps. To obtain ε-factorisation, we employ the method of splitting the Wronskian in a semi-simple and unipotent part, see Refs. [220, 221] for details.

Three master integrals contribute to the homogeneous part of the three-loop banana graph,

$$I_{\mathrm{B}}^{\mathrm{NC}} = \left(I_{3,10}^{\mathrm{NC}}, I_{3,11}^{\mathrm{NC}}, I_{3,12}^{\mathrm{NC}}\right), \tag{4.147}$$

and satisfy a first-order differential system inherited from the full elliptic system,

$$A_{\mathrm{B}}^{\mathrm{NC}} = A_{\mathrm{B}}^{\mathrm{NC},(0)} + \varepsilon A_{\mathrm{B}}^{\mathrm{NC},(1)} \tag{4.148}$$

with the connection matrices

$$A_{\mathrm{B}}^{\mathrm{NC},(0)} = \begin{pmatrix} -\frac{1}{x} & -\frac{4}{x} & 0 \\ \frac{1}{4x} & \frac{4-x}{4x} & -\frac{1}{2} \\ -\frac{x^2-28x+120}{8(16-x)(4-x)x} & \frac{x^3-40x^2+392x-800}{8(16-x)(4-x)x} & \frac{x^3-36x^2+264x-256}{4(16-x)(4-x)x} \end{pmatrix}, \tag{4.149}$$

$$A_{\mathrm{B}}^{\mathrm{NC},(1)} = \begin{pmatrix} -\frac{3}{x} & 0 & 0 \\ \frac{7}{4x} & \frac{16-x}{4x} & 0 \\ -\frac{x^2-29x+127}{(16-x)(4-x)x} & \frac{x^3-52x^2+644x-1616}{4(16-x)(4-x)x} & \frac{x^3-48x^2+384x-256}{4(16-x)(4-x)x} \end{pmatrix}. \tag{4.150}$$

A first step towards an ε-factorised basis is to pass to a derivative basis, in which the connection takes the form

$$I_{\mathrm{B,d}}^{\mathrm{NC}} \equiv \left(I_{\mathrm{B},1}^{\mathrm{NC}}, \frac{\mathrm{d}}{\mathrm{d}x} I_{\mathrm{B},1}^{\mathrm{NC}}, \frac{\mathrm{d}^2}{\mathrm{d}x^2} I_{\mathrm{B},1}^{\mathrm{NC}}\right). \tag{4.151}$$

Repeated use of the homogeneous differential equation allows all derivatives to be expressed in terms of the connection matrix and its derivatives. This relates the original master integrals to those of the derivative basis,

$$I_{\mathrm{B,d}}^{\mathrm{NC}} = T_{\mathrm{B,d}}^{\mathrm{NC}} I_{\mathrm{B}}^{\mathrm{NC}}, \tag{4.152}$$

with the rotation matrix

$$T_{\mathrm{B,d}}^{\mathrm{NC}} = \begin{pmatrix} 1 & 0 & 0 \\ -\frac{3\varepsilon+1}{x} & -\frac{4}{x} & 0 \\ -\frac{(\varepsilon-1)(3\varepsilon+1)}{x^2} & \frac{x\varepsilon+x-4\varepsilon+4}{x^2} & \frac{2}{x} \end{pmatrix}. \tag{4.153}$$

Restricting henceforth to the maximal cut [222, 223], defined by letting $\varepsilon \to 0$, the transformed connection matrix reads

$$A_{\mathrm{B,d}}^{\mathrm{NC}} = \begin{pmatrix} 0 & 1 & 0 \\ 0 & 0 & 1 \\ \frac{1}{(16-x)x^2} & -\frac{7x^2-68x+64}{(16-x)(4-x)x^2} & -\frac{6\left(x^2-15x+32\right)}{(16-x)(4-x)x} \end{pmatrix}. \tag{4.154}$$

The last row in Eq. (4.154) defines a Picard–Fuchs operator of degree three [222]. Being irreducible and admitting no factorisation, this third-order operator possesses three linearly independent solutions. Geometrically, the underlying equation describes a K3 surface [224, 225], equivalently a Calabi–Yau two-fold, though the precise geometry plays no role in what follows. An alternative derivation of the geometry can be obtained from the Baikov representation [226–228] evaluated on the maximal cut [222, 223]. The three solutions, namely the periods ϖ_i^{NC}, form the solution space and satisfy

$$L_3^{\mathrm{NC}}\varpi_i^{\mathrm{NC}} = 0\,, \qquad i \in \{0, 1, 2\}\,, \tag{4.155}$$

with the Picard–Fuchs operator

$$L_3^{\mathrm{NC}} = \frac{\mathrm{d}^3}{\mathrm{d}x^3} + \frac{7x^2 - 68x + 64}{(16-x)(4-x)x^2}\frac{\mathrm{d}^2}{\mathrm{d}x^2} + \frac{1}{(16-x)x^2}\frac{\mathrm{d}}{\mathrm{d}x} - \frac{1}{(16-x)x^2}\,. \tag{4.156}$$

Although direct integration of Eq. (4.155) is possible in closed form, the exact solutions are Heun functions [229], which are poorly suited to practical calculations. The Frobenius method instead produces an iterative solution expanded around a chosen singular point, and is therefore the approach adopted here. Since the case of interest is deep-inelastic scattering, the expansion[3] is taken around zero, specifically in the limit $x \to 0^-$,

$$\varpi_0^{\mathrm{NC}} = 1 + \frac{x}{16} + \frac{7x^2}{1024} + \frac{x^3}{1024} + \frac{679x^4}{4194304} + \mathcal{O}\big(x^5\big)\,, \tag{4.157}$$

$$\varpi_1^{\mathrm{NC}} = \varpi_0^{\mathrm{NC}}\log x + \frac{3x}{32} + \frac{57x^2}{4096} + \frac{73x^3}{32768} + \frac{13081x^4}{33554432} + \mathcal{O}\big(x^5\big)\,, \tag{4.158}$$

$$\varpi_2^{\mathrm{NC}} = \frac{\varpi_0^{\mathrm{NC}}\log^2 x}{2} - \varpi_0^{\mathrm{NC}}\log x + \frac{9x^2}{2048} + \frac{135x^3}{131072} + \frac{7089x^4}{33554432} + \mathcal{O}\big(x^5\big)\,. \tag{4.159}$$

Among these, the first solution is the *holomorphic* one, whose expansion is used later to fix the boundary conditions.

Notably, this Picard–Fuchs operator is the symmetric square of a second-order operator [230, 231]. To see this, consider generic second- and third-order Picard–Fuchs operators

$$L_2^{\mathrm{NC}} = \frac{\mathrm{d}^2}{\mathrm{d}x^2} + c_{2,1}\frac{\mathrm{d}}{\mathrm{d}x} + c_{2,0}\,, \tag{4.160}$$

$$L_3^{\mathrm{NC}} = \frac{\mathrm{d}^3}{\mathrm{d}x^3} + c_{3,2}\frac{\mathrm{d}^2}{\mathrm{d}x^2} + c_{3,1}\frac{\mathrm{d}}{\mathrm{d}x} + c_{3,0}\,, \tag{4.161}$$

related through the symmetric square property [232],

$$L_2^{\mathrm{NC}}\pi^{\mathrm{NC}} = 0 \quad \text{and} \quad \varpi^{\mathrm{NC}} = (\pi^{\mathrm{NC}})^2 \quad \Longrightarrow \quad L_3^{\mathrm{NC}}\varpi^{\mathrm{NC}} = 0\,. \tag{4.162}$$

This property fixes the coefficients $c_{3,i}$ uniquely in terms of the $c_{2,i}$. Repeated differentiation of ϖ^{NC} yields

$$\varpi^{\mathrm{NC}} = \big(\pi^{\mathrm{NC}}\big)^2\,, \tag{4.163}$$

$$\dot{\varpi}^{\mathrm{NC}} = 2\dot{\pi}^{\mathrm{NC}}\pi^{\mathrm{NC}}\,, \tag{4.164}$$

$$\ddot{\varpi}^{\mathrm{NC}} = 2\big(\dot{\pi}^{\mathrm{NC}}\big)^2 - 2c_{2,1}\dot{\pi}^{\mathrm{NC}}\pi^{\mathrm{NC}} - 2c_{2,0}\big(\pi^{\mathrm{NC}}\big)^2\,, \tag{4.165}$$

$$\begin{aligned}\dddot{\varpi}^{\mathrm{NC}} &= -6c_{2,1}\big(\dot{\pi}^{\mathrm{NC}}\big)^2 + \big(2c_{2,1}^2 - 2\dot{c}_{2,1} - 8c_{2,0}\big)\dot{\pi}^{\mathrm{NC}}\pi^{\mathrm{NC}} \\ &\quad + \big(2c_{2,0}c_{2,1} - 2\dot{c}_{2,0}\big)\big(\pi^{\mathrm{NC}}\big)^2\,,\end{aligned} \tag{4.166}$$

[3]Digital results are provided; see App. E for details.

where the second-order operator, Eq. (4.160), has been used repeatedly to eliminate second derivatives.

Substituting Eqs. (4.163)–(4.165) into Eq. (4.166) eliminates π^{NC} and $\dot{\pi}^{\mathrm{NC}}$ in favour of ϖ^{NC} and its derivatives, yielding a third-order ordinary differential equation. Subtracting the general third-order operator of Eq. (4.161) then provides a system of equations on the coefficients, whose solution characterises precisely when a third-order operator is a symmetric square,

$$0 = c_{3,0} - 4c_{2,0}c_{2,1} - 2\dot{c}_{2,0}\,, \tag{4.167}$$
$$0 = c_{3,1} - 2c_{2,1}^2 - \dot{c}_{2,1} - 4c_{2,0}\,, \tag{4.168}$$
$$0 = c_{3,2} - 3c_{2,1}\,. \tag{4.169}$$

Returning to the operator of the banana graph in Eq. (4.156), solving the second and third equation, Eqs. (4.168) and Eq. (4.169), for $c_{2,1}$ and $c_{2,0}$ gives, respectively,

$$c_{2,0} = \frac{x-8}{4(16-x)(4-x)x}\,, \tag{4.170}$$
$$c_{2,1} = \frac{2(x^2-15x+32)}{(16-x)(4-x)x}\,. \tag{4.171}$$

These solutions satisfy the first equation, Eq. (4.167), as well, confirming that the operator is indeed a symmetric square.

As a second-order linear operator, L_2^{NC} admits two independent solutions π_1^{NC} and π_2^{NC}, and any linear combination thereof is again a solution. Linearity of L_3^{NC} together with the symmetric-square condition of Eq. (4.162) implies that

$$0 = L_3^{\mathrm{NC}}\big((\pi_1^{\mathrm{NC}} + \pi_2^{\mathrm{NC}})^2\big) = L_3^{\mathrm{NC}}\big(\pi_1^{\mathrm{NC}}\pi_2^{\mathrm{NC}}\big)\,. \tag{4.172}$$

The three pairwise products of π_1^{NC} and π_2^{NC} therefore furnish a basis of solutions, which we take to be

$$\varpi_0^{\mathrm{NC}} = (\pi_1^{\mathrm{NC}})^2\,, \tag{4.173}$$
$$\varpi_1^{\mathrm{NC}} = \pi_1^{\mathrm{NC}}\pi_2^{\mathrm{NC}}\,, \tag{4.174}$$
$$\varpi_2^{\mathrm{NC}} = \frac{1}{2}(\pi_2^{\mathrm{NC}})^2\,. \tag{4.175}$$

Conventions for the normalisation are chosen to match the existing literature. Expanding these periods in a series around zero to fourth order[4], we find

$$\pi_0^{\mathrm{NC}} = 1 + \frac{x}{32} + \frac{3x^2}{1024} + \frac{13x^3}{32768} + \frac{539x^4}{8388608} + \mathcal{O}\big(x^5\big)\,, \tag{4.176}$$
$$\pi_1^{\mathrm{NC}} = \pi_0^{\mathrm{NC}}\log(x) + \frac{3x}{32} + \frac{45x^2}{4096} + \frac{211x^3}{131072} + \frac{9065x^4}{33554432} + \mathcal{O}\big(x^5\big)\,. \tag{4.177}$$

Taking the appropriate products in Eqs. (4.173)–(4.175) reproduces the expansions given in Eqs. (4.157)–(4.159).

A crucial ingredient in obtaining the ε-factorised form is the Picard–Fuchs operator, which enters through a splitting of the Wronskian matrix into its unipotent

[4]Deeper expansions are provided as ancillary files; see App. E for details.

and semi-simple parts. This approach extends the familiar method of normalising integrals by their leading singularities beyond the polylogarithmic case. Explicitly, the Wronskian matrices read

$$W^{\mathrm{NC}}_{\mathrm{B},2} = \begin{pmatrix} \pi^{\mathrm{NC}}_0 & \pi^{\mathrm{NC}}_1 \\ \dot{\pi}^{\mathrm{NC}}_0 & \dot{\pi}^{\mathrm{NC}}_1 \end{pmatrix} \tag{4.178}$$

and

$$W^{\mathrm{NC}}_{\mathrm{B},3} = \begin{pmatrix} \varpi^{\mathrm{NC}}_0 & \varpi^{\mathrm{NC}}_1 & \varpi^{\mathrm{NC}}_2 \\ \dot{\varpi}^{\mathrm{NC}}_0 & \dot{\varpi}^{\mathrm{NC}}_1 & \dot{\varpi}^{\mathrm{NC}}_2 \\ \ddot{\varpi}^{\mathrm{NC}}_0 & \ddot{\varpi}^{\mathrm{NC}}_1 & \ddot{\varpi}^{\mathrm{NC}}_2 \end{pmatrix}, \tag{4.179}$$

where each entry of the latter may be expressed in terms of π^{NC}_1 and π^{NC}_2 via the symmetric-square property. The determinant of Eq. (4.178) takes the form

$$\det\left(W^{\mathrm{NC}}_{\mathrm{B},2}\right) = \pi^{\mathrm{NC}}_0 \dot{\pi}^{\mathrm{NC}}_1 - \pi^{\mathrm{NC}}_1 \dot{\pi}^{\mathrm{NC}}_0 \,. \tag{4.180}$$

Imposing the second-order Picard–Fuchs equation, Eq. (4.160), this determinant is seen to satisfy

$$\frac{\mathrm{d}}{\mathrm{d}x} \log\left(\det\big(W^{\mathrm{NC}}_{\mathrm{B},2}\big)\right) = \frac{\pi^{\mathrm{NC}}_1 \ddot{\pi}^{\mathrm{NC}}_0 - \pi^{\mathrm{NC}}_0 \ddot{\pi}^{\mathrm{NC}}_1}{\pi^{\mathrm{NC}}_1 \dot{\pi}^{\mathrm{NC}}_0 - \pi^{\mathrm{NC}}_0 \dot{\pi}^{\mathrm{NC}}_1} = -\frac{2(x^2 - 15x + 32)}{(16-x)(4-x)x} \,. \tag{4.181}$$

The differential equation, Eq. (4.181), may be integrated to give

$$R^{\mathrm{NC}} \equiv \det\big(W^{\mathrm{NC}}_{\mathrm{B},2}\big) = \frac{8}{\sqrt{(16-x)(4-x)x}} \,, \tag{4.182}$$

where the integration constant has been fixed for later convenience. Together with the Picard–Fuchs equation, Eq. (4.160), this relation permits all derivatives of π^{NC}_1 in the Wronskian matrix of Eq. (4.179) to be eliminated.

To decompose the matrix into its semi-simple and unipotent parts, we make the ansatz

$$W^{\mathrm{NC}}_{\mathrm{B},3} = W^{\mathrm{NC}}_{\mathrm{B},3,\mathrm{s}} W^{\mathrm{NC}}_{\mathrm{B},3,\mathrm{u}} \implies W^{\mathrm{NC}}_{\mathrm{B},3,\mathrm{s}} = W^{\mathrm{NC}}_{\mathrm{B},3} \big(W^{\mathrm{NC}}_{\mathrm{B},3,\mathrm{u}}\big)^{-1} \,, \tag{4.183}$$

where the semi-simple part is taken to be lower triangular and the unipotent part upper triangular,

$$W^{\mathrm{NC}}_{\mathrm{B},3,\mathrm{u}} = \begin{pmatrix} 1 & a^{\mathrm{NC}}_{1,2} & a^{\mathrm{NC}}_{1,3} \\ 0 & 1 & a^{\mathrm{NC}}_{2,3} \\ 0 & 0 & 1 \end{pmatrix} . \tag{4.184}$$

Imposing this triangular structure yields three equations that may be solved for the unknown coefficients,

$$a^{\mathrm{NC}}_{1,2} = \frac{\pi_1}{\pi_0} \,, \tag{4.185}$$

$$a_{1,3}^{\mathrm{NC}} = \frac{1}{2}\frac{\pi_1^2}{\pi_0^2}\,, \tag{4.186}$$

$$a_{2,3}^{\mathrm{NC}} = \frac{\pi_1}{\pi_0}\,. \tag{4.187}$$

The unipotent part of the Wronskian matrix is intimately related to its monodromy matrix. To see this, we may consider the transformation $x \to xe^{2i\pi\tau}$ with $\tau \in (0,1)$ acting on the Wronskian matrix. Under this transformation, the holomorphic parts, namely those free of logarithms, remain invariant, so

$$\varpi_0^{\mathrm{NC}} \to \varpi_0^{\mathrm{NC}}\,, \tag{4.188}$$

$$\varpi_1^{\mathrm{NC}} \to \varpi_1^{\mathrm{NC}} + (2\pi i)\tau\varpi_0^{\mathrm{NC}}\quad , \tag{4.189}$$

$$\varpi_2^{\mathrm{NC}} \to \varpi_2^{\mathrm{NC}} + (2\pi i)\tau\varpi_1^{\mathrm{NC}} + \frac{(2\pi i)^2}{2}\tau^2\varpi_0^{\mathrm{NC}} \tag{4.190}$$

with τ the ratio of periods,

$$\tau = \frac{1}{2\pi i}\frac{\varpi_1^{\mathrm{NC}}}{\varpi_0^{\mathrm{NC}}}\,, \tag{4.191}$$

the resulting matrix reads, noting that the period vector is here taken as a row vector,

$$W_{\mathrm{B,3,m}}^{\mathrm{NC}} = \varpi_0^{\mathrm{NC}}\begin{pmatrix} 1 & \frac{\varpi_1^{\mathrm{NC}}}{\varpi_0^{\mathrm{NC}}} & \frac{1}{2}\frac{(\varpi_1^{\mathrm{NC}})^2}{(\varpi_0^{\mathrm{NC}})^2} \\ 0 & 1 & \frac{\varpi_1^{\mathrm{NC}}}{\varpi_0^{\mathrm{NC}}} \\ 0 & 0 & 1 \end{pmatrix} = \varpi_0^{\mathrm{NC}}\begin{pmatrix} 1 & \frac{\pi_1^{\mathrm{NC}}}{\pi_0^{\mathrm{NC}}} & \frac{1}{2}\frac{(\pi_1^{\mathrm{NC}})^2}{(\pi_0^{\mathrm{NC}})^2} \\ 0 & 1 & \frac{\pi_1^{\mathrm{NC}}}{\pi_0^{\mathrm{NC}}} \\ 0 & 0 & 1 \end{pmatrix} \sim W_{\mathrm{B,3,u}}^{\mathrm{NC}}\,. \tag{4.192}$$

The semi-simple part can thus be constructed explicitly, with second derivatives eliminated via the Picard–Fuchs equation and first derivatives via the Wronskian determinant,

$$W_{\mathrm{B,3,s}}^{\mathrm{NC}} \equiv \begin{pmatrix} \varpi_0^{\mathrm{NC}} & 0 & 0 \\ \dot{\varpi}_0^{\mathrm{NC}} & R^{\mathrm{NC}} & 0 \\ \ddot{\varpi}_0^{\mathrm{NC}} & \dot{R}^{\mathrm{NC}} + R^{\mathrm{NC}}\dot{\varpi}_0^{\mathrm{NC}}\left(\varpi_0^{\mathrm{NC}}\right)^{-1} & \left(R^{\mathrm{NC}}\right)^2\left(\varpi_0^{\mathrm{NC}}\right)^{-1} \end{pmatrix}\,, \tag{4.193}$$

in exact agreement with the literature, up to typographical errors. With both Picard–Fuchs operators in hand, second derivatives can be eliminated from subsequent equations through the identity

$$\ddot{\varpi}_0^{\mathrm{NC}} = -\frac{x-8}{(16-x)(4-x)x}\varpi_0^{\mathrm{NC}} - \frac{2(x^2-15x+32)}{(16-x)(4-x)x}\dot{\varpi}_0^{\mathrm{NC}} + \frac{(\dot{\varpi}_0^{\mathrm{NC}})^2}{2\varpi_0^{\mathrm{NC}}}\,. \tag{4.194}$$

This identity is known as a Griffiths transversality relation [219], the analogue of the Legendre relation in the elliptic case. A final rescaling accounts for the fact that the periods carry different transcendental weights,

$$T_{\mathrm{B,e}}^{\mathrm{NC}} = \begin{pmatrix} \varepsilon^2 & 0 & 0 \\ 0 & \varepsilon & 0 \\ 0 & 0 & 1 \end{pmatrix}\,. \tag{4.195}$$

Chaining the rotations obtained so far yields a pre-factorised form which is not linear in ε and contains undesired derivatives of the periods. Both issues are removed

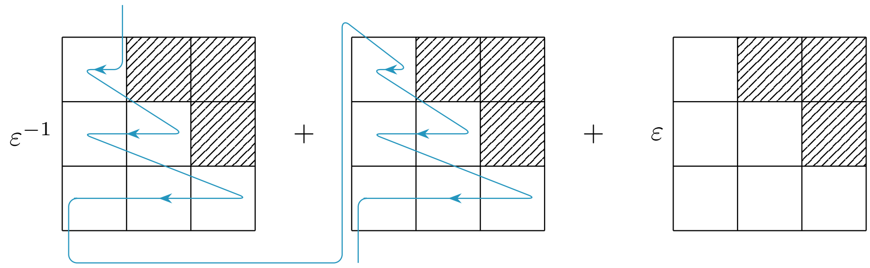

Figure 4.3: Schematic representation of the clean-up procedure for traversing the connection matrix order by order, entry by entry. Hatched entries vanish by virtue of the triangular structure of the differential equations.

by further rotation, the so-called *clean-up*. The intermediate matrix is rather involved, so its explicit form is omitted here, but it has the structural form

$$A_{\mathrm{B},3}^{\mathrm{NC}} = \varepsilon^{-1} A_{\mathrm{B},3}^{\mathrm{NC},(-1)} + A_{\mathrm{B},3}^{\mathrm{NC},(0)} + \varepsilon A_{\mathrm{B},3}^{\mathrm{NC},(1)} \,. \tag{4.196}$$

Bringing the system into ε-factorised form requires a sequence of rotations removing all contributions except those linear in ε. These are applied order by order in ε, starting from the most singular terms and working upwards (see Fig. 4.3). At each step, the offending entry in row i and column j of the connection matrix is identified and removed by a transformation of the form

$$\left(T_{mn}^{(k)}\right)_{ab} = \left(\varepsilon^{k}(\delta_{mn} + \delta_{im}\delta_{jn}(\ldots))\right)_{ab} \,, \tag{4.197}$$

where the ellipsis indicates an ansatz built from the periods, their derivatives and any algebraic or transcendental functions that must be introduced in the course of bringing the connection matrix into ε-factorised form.

In what follows, by a slight abuse of notation, the connection matrix is understood to incorporate all preceding rotations. At each step, we identify the offending entry (E), state the ansatz (A), and introduce when necessary new algebraic or transcendental functions (F) to obtain factorisation, with explicit entries and coefficients collected in App. B.1. Bringing the homogeneous block into ε-factorised form demands four such steps, which we now carry out in turn:

Step 1.

E: $$\left(A_{\mathrm{B}}^{\mathrm{NC},(-1)}\right)_{3,1} = a_{\mathrm{B},3,1,1}^{\mathrm{NC},(-1)}\left(\varpi_0^{\mathrm{NC}}\right)^2 + a_{\mathrm{B},3,1,2}^{\mathrm{NC},(-1)}\varpi_0^{\mathrm{NC}}\dot{\varpi}_0^{\mathrm{NC}} + a_{\mathrm{B},3,1,3}^{\mathrm{NC},(-1)}\left(\dot{\varpi}_0^{\mathrm{NC}}\right)^2 \tag{4.198}$$

A: $$\left(T_{\mathrm{B}}^{\mathrm{NC},(-1)}\right)_{3,1} = \varepsilon^{-1}\left(t_{\mathrm{B},3,1,1}^{\mathrm{NC},(-1)}\left(\varpi_0^{\mathrm{NC}}\right)^2 + t_{\mathrm{B},3,1,2}^{\mathrm{NC},(-1)}\varpi_0^{\mathrm{NC}}\dot{\varpi}_0^{\mathrm{NC}} - G_1^{\mathrm{NC}}\right) \tag{4.199}$$

F: $$\dot{G}_1^{\mathrm{NC}} = -\frac{(x-8)(x+8)^3\left(\varpi_0^{\mathrm{NC}}\right)^2}{32(16-x)^2(4-x)^2} \tag{4.200}$$

Step 2.

E: $$\left(A_{\mathrm{B}}^{\mathrm{NC},(0)}\right)_{2,1} = a_{\mathrm{B},2,1,1}^{\mathrm{NC},(0)}\varpi_0^{\mathrm{NC}} + a_{\mathrm{B},2,1,2}^{\mathrm{NC},(0)}\dot{\varpi}_0^{\mathrm{NC}} + a_{\mathrm{B},2,1,3}^{\mathrm{NC},(0)}\frac{G_1^{\mathrm{NC}}}{\varpi_0^{\mathrm{NC}}} \tag{4.201}$$

A: $$\left(T_{\mathrm{B}}^{\mathrm{NC},(0)}\right)_{2,1} = t_{\mathrm{B},2,1,1}^{\mathrm{NC},(0)}\varpi_0^{\mathrm{NC}} - G_2^{\mathrm{NC}} \tag{4.202}$$

F:
$$\dot{G}_2^{\mathrm{NC}} = \frac{8G_1^{\mathrm{NC}}}{x\sqrt{(16-x)(4-x)}\varpi_0^{\mathrm{NC}}} \tag{4.203}$$

Step 3.

E:
$$\left(A_{\mathrm{B}}^{\mathrm{NC},(0)}\right)_{3,2} = a_{\mathrm{B},3,2,1}^{\mathrm{NC},(0)}\varpi_0^{\mathrm{NC}} + a_{\mathrm{B},3,2,2}^{\mathrm{NC},(0)}\dot{\varpi}_0^{\mathrm{NC}} + a_{\mathrm{B},3,2,3}^{\mathrm{NC},(0)}\frac{G_1^{\mathrm{NC}}}{\varpi_0^{\mathrm{NC}}} \tag{4.204}$$

A:
$$\left(T_{\mathrm{B}}^{\mathrm{NC},(0)}\right)_{3,2} = t_{\mathrm{B},3,2,1}^{\mathrm{NC},(0)}\varpi_0^{\mathrm{NC}} + t_{\mathrm{B},3,2,2}^{\mathrm{NC},(0)}G_2^{\mathrm{NC}} \tag{4.205}$$

Step 4.

E:
$$\left(A_{\mathrm{B}}^{\mathrm{NC},(0)}\right)_{3,1} = a_{\mathrm{B},3,1,1}^{\mathrm{NC},(0)}\left(\varpi_0^{\mathrm{NC}}\right)^2 + a_{\mathrm{B},3,1,2}^{\mathrm{NC},(0)}\varpi_0^{\mathrm{NC}}\dot{\varpi}_0^{\mathrm{NC}} + a_{\mathrm{B},3,1,3}^{\mathrm{NC},(0)}G_1^{\mathrm{NC}} \tag{4.206}$$
$$+ a_{\mathrm{B},3,1,4}^{\mathrm{NC},(0)}\varpi_0^{\mathrm{NC}}G_2^{\mathrm{NC}} + a_{\mathrm{B},3,1,5}^{\mathrm{NC},(0)}\dot{\varpi}_0^{\mathrm{NC}}G_2^{\mathrm{NC}} + a_{\mathrm{B},3,1,6}^{\mathrm{NC},(0)}\frac{G_1^{\mathrm{NC}}G_2^{\mathrm{NC}}}{\varpi_0^{\mathrm{NC}}} \tag{4.207}$$

A:
$$\left(T_{\mathrm{B}}^{\mathrm{NC},(0)}\right)_{3,1} = t_{\mathrm{B},3,1,1}^{\mathrm{NC},(0)}\left(\varpi_0^{\mathrm{NC}}\right)^2 + t_{\mathrm{B},3,1,2}^{\mathrm{NC},(0)}\left(G_2^{\mathrm{NC}}\right)^2 + t_{\mathrm{B},3,1,2}^{\mathrm{NC},(0)}\varpi_0^{\mathrm{NC}}G_2^{\mathrm{NC}} \tag{4.208}$$

The steps above yield a rotation that brings the only homogeneous elliptic block of the neutral current into ε-factorised form. This comes at the cost of introducing two auxiliary functions, which are themselves integrals over the periods, in agreement with the literature.

Remaining inhomogeneous blocks are treated analogously and are not discussed further. Three heuristics facilitate the search for a rotation,

1. Master integrals are normalised by their leading singularities, a step which in practice is often sufficient to achieve factorisation on its own.

2. Integrals that factorise into two-point functions are treated in two dimensions, making use of dimensional shift matrices.

3. The basis is rotated via IBP relations to a mixed form, admitting both dots and scalar products in the numerators.

These steps are motivated by the observation that a judicious choice of master integrals can render the search for a transformation considerably more tractable, whilst a poor choice may make it extremely cumbersome or obstruct it entirely.

All integrals of the neutral current are brought into ε-factorised form[5]. The rotation for the QED-type master integrals coincides with the results in the literature [215], requiring only one further transcendental function beyond those introduced here, whilst the QCD-specific part is structurally similar.

Table 4.1: Complete set of master integrals contributing to the neutral-current contribution. Massive propagators are displayed in green.

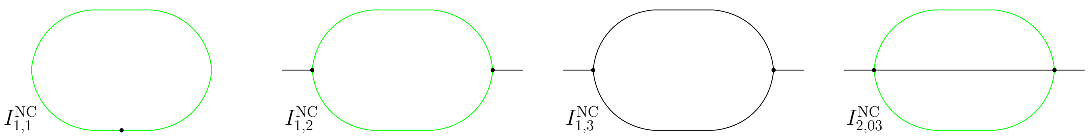

[5]All NC master integrals are provided as ancillary files; see App. E for details.

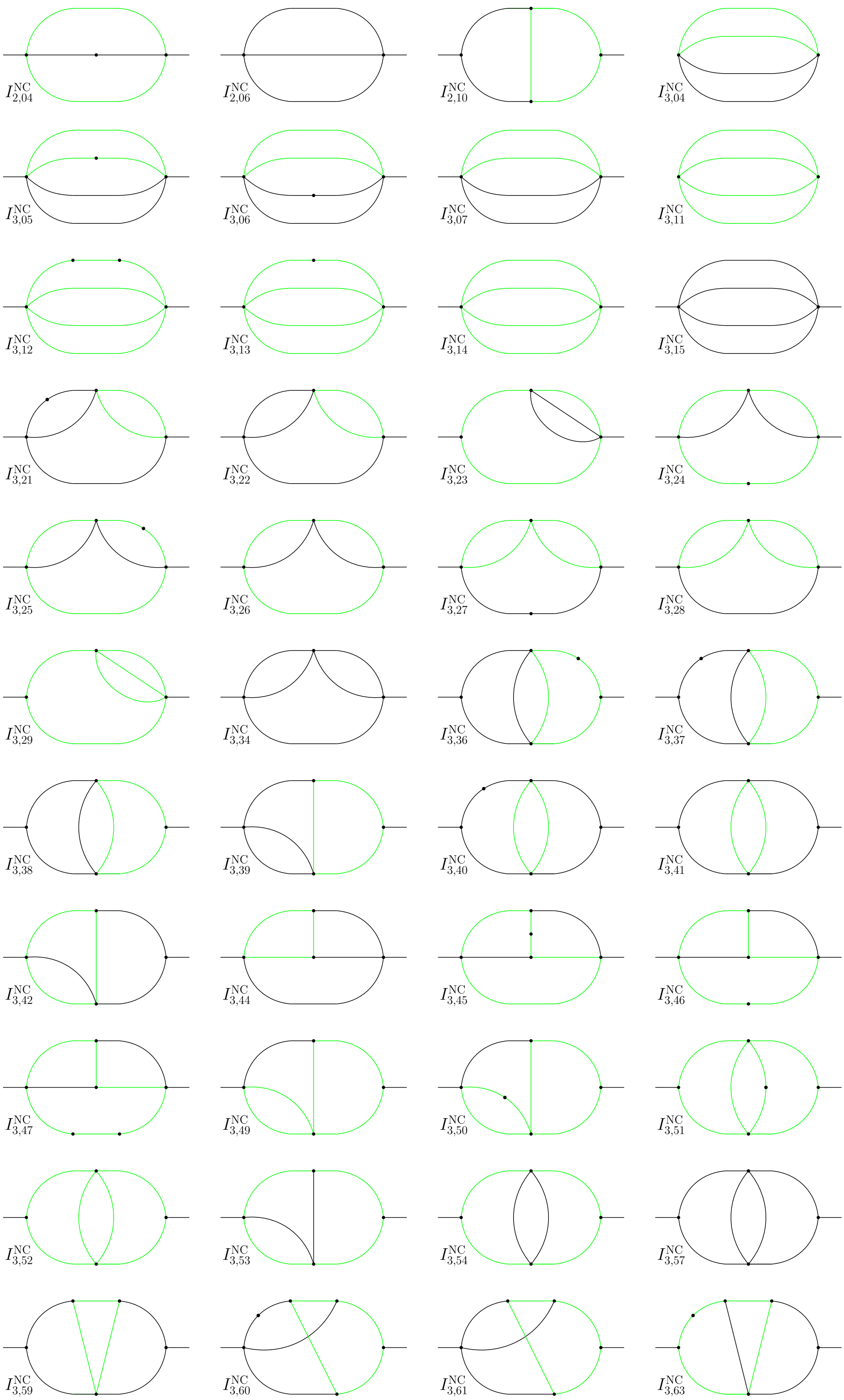

$I^{\mathrm{NC}}_{2,04}$
$I^{\mathrm{NC}}_{2,06}$
$I^{\mathrm{NC}}_{2,10}$
$I^{\mathrm{NC}}_{3,04}$
$I^{\mathrm{NC}}_{3,05}$
$I^{\mathrm{NC}}_{3,06}$
$I^{\mathrm{NC}}_{3,07}$
$I^{\mathrm{NC}}_{3,11}$
$I^{\mathrm{NC}}_{3,12}$
$I^{\mathrm{NC}}_{3,13}$
$I^{\mathrm{NC}}_{3,14}$
$I^{\mathrm{NC}}_{3,15}$
$I^{\mathrm{NC}}_{3,21}$
$I^{\mathrm{NC}}_{3,22}$
$I^{\mathrm{NC}}_{3,23}$
$I^{\mathrm{NC}}_{3,24}$
$I^{\mathrm{NC}}_{3,25}$
$I^{\mathrm{NC}}_{3,26}$
$I^{\mathrm{NC}}_{3,27}$
$I^{\mathrm{NC}}_{3,28}$
$I^{\mathrm{NC}}_{3,29}$
$I^{\mathrm{NC}}_{3,34}$
$I^{\mathrm{NC}}_{3,36}$
$I^{\mathrm{NC}}_{3,37}$
$I^{\mathrm{NC}}_{3,38}$
$I^{\mathrm{NC}}_{3,39}$
$I^{\mathrm{NC}}_{3,40}$
$I^{\mathrm{NC}}_{3,41}$
$I^{\mathrm{NC}}_{3,42}$
$I^{\mathrm{NC}}_{3,44}$
$I^{\mathrm{NC}}_{3,45}$
$I^{\mathrm{NC}}_{3,46}$
$I^{\mathrm{NC}}_{3,47}$
$I^{\mathrm{NC}}_{3,49}$
$I^{\mathrm{NC}}_{3,50}$
$I^{\mathrm{NC}}_{3,51}$
$I^{\mathrm{NC}}_{3,52}$
$I^{\mathrm{NC}}_{3,53}$
$I^{\mathrm{NC}}_{3,54}$
$I^{\mathrm{NC}}_{3,57}$
$I^{\mathrm{NC}}_{3,59}$
$I^{\mathrm{NC}}_{3,60}$
$I^{\mathrm{NC}}_{3,61}$
$I^{\mathrm{NC}}_{3,63}$

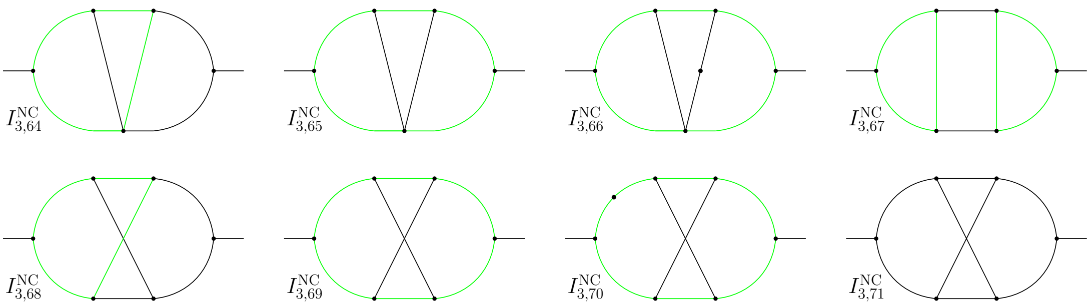

4.5.3 Charged Current Elliptic Integrals

Having discussed the three-loop banana in detail (see Subsec. 4.5.2), the two-loop banana encountered in the charged current is unsurprisingly conceptually much simpler, with its computation proceeding in close analogy with the previous case. Research on two-loop banana integrals is extensive; see, for example, Refs. [233–236]. As will become clear, the only genuinely novel elliptic homogeneous block appears at this order, where the two-loop banana sector is governed by two master integrals,

$$I_{\mathrm{B}}^{\mathrm{CC}} = \left(I_{2,3}^{\mathrm{CC}},\, I_{2,4}^{\mathrm{CC}}\right), \tag{4.209}$$

and a first-order differential system inherited from the full elliptic system,

$$A_{\mathrm{B}}^{\mathrm{CC}} = A_{\mathrm{B}}^{\mathrm{CC},(0)} + \varepsilon\, A_{\mathrm{B}}^{\mathrm{CC},(1)}, \tag{4.210}$$

with the matrices

$$A_{\mathrm{B}}^{\mathrm{CC},(0)} = \begin{pmatrix} -\frac{1}{x} & -\frac{3}{x} \\ -\frac{x-3}{(x-9)(x-1)x} & -\frac{x^2-9}{(x-9)(x-1)x} \end{pmatrix}, \tag{4.211}$$

$$A_{\mathrm{B}}^{\mathrm{CC},(1)} = \begin{pmatrix} -\frac{2}{x} & 0 \\ -\frac{5(x-3)}{(x-9)(x-1)x} & -\frac{x^2+10x-27}{(x-9)(x-1)x} \end{pmatrix}. \tag{4.212}$$

As for the neutral current, the first step towards an ε-factorised basis is to pass to a derivative basis,

$$I_{\mathrm{B,d}}^{\mathrm{CC}} \equiv \left(I_{\mathrm{B},1}^{\mathrm{CC}},\, \frac{\mathrm{d}}{\mathrm{d}x} I_{\mathrm{B},1}^{\mathrm{CC}}\right). \tag{4.213}$$

Repeated use of the homogeneous differential equation expresses all derivatives in terms of the connection matrix and its derivatives, relating the original master integrals to those of the derivative basis via

$$I_{\mathrm{B,d}}^{\mathrm{CC}} = T_{\mathrm{B,d}}^{\mathrm{CC}} I_{\mathrm{B}}^{\mathrm{CC}}, \tag{4.214}$$

with the rotation matrix

$$T_{\mathrm{B,d}}^{\mathrm{CC}} = \begin{pmatrix} 1 & 0 \\ -\frac{2\varepsilon+1}{x} & -\frac{3}{x} \end{pmatrix}. \tag{4.215}$$

Restricting henceforth to the maximal cut, defined by $\varepsilon \to 0$, the transformed connection matrix reads

$$A_{\mathrm{B,d}}^{\mathrm{CC}} = \begin{pmatrix} 0 & 1 \\ -\frac{x-3}{(x-9)(x-1)x} & -\frac{3x^2-20x+9}{(x-9)(x-1)x} \end{pmatrix}. \tag{4.216}$$

The last row of the rotated connection matrix, Eq. (4.216), defines an irreducible Picard–Fuchs operator of degree two, admitting no factorisation and possessing two linearly independent solutions, the periods π_i^{CC}, which are annihilated by the Picard–Fuchs operator

$$L_2^{\mathrm{CC}} = \frac{\mathrm{d}^2}{\mathrm{d}x^2} + \frac{(3x^2-20x+9)}{(x-9)(x-1)x}\frac{\mathrm{d}}{\mathrm{d}x} + \frac{(x-3)}{(x-9)(x-1)x}\,. \tag{4.217}$$

Exact solutions are expressed in terms of Heun functions and are therefore poorly suited to practical calculations. The solutions of the Picard–Fuchs operator L_2^{CC} are the periods of an elliptic curve [237]. As before, the Frobenius method instead yields an iterative solution expanded around a chosen singular point. This expansion is taken around zero, specifically in the limit $x \to 0^-$,

$$\pi_0^{\mathrm{CC}} = 1 + \frac{x}{3} + \frac{5x^2}{27} + \frac{31x^3}{243} + \frac{71x^4}{729} + \mathcal{O}\big(x^5\big)\,, \tag{4.218}$$

$$\pi_1^{\mathrm{CC}} = \pi_0^{\mathrm{CC}}\log(x) + \frac{4x}{9} + \frac{26x^2}{81} + \frac{526x^3}{2187} + \frac{1253x^4}{6561} + \mathcal{O}\big(x^5\big)\,. \tag{4.219}$$

Following the neutral current closely, the determinant of the degree-two Wronskian matrix is

$$\det\left(W_{\mathrm{B},2}^{\mathrm{CC}}\right) = \pi_0^{\mathrm{CC}}\dot{\pi}_1^{\mathrm{CC}} - \pi_1^{\mathrm{CC}}\dot{\pi}_0^{\mathrm{CC}}\,, \tag{4.220}$$

and is found to be

$$R^{\mathrm{CC}} \equiv \det\big(W_{\mathrm{B},2}^{\mathrm{CC}}\big) = \frac{1}{(9-x)(1-x)x}\,. \tag{4.221}$$

Once the unipotent part has been constructed, the semi-simple part follows explicitly, with the first derivatives of the periods eliminated via the Wronskian determinant,

$$W_{\mathrm{B,s}}^{\mathrm{CC}} = \begin{pmatrix} \pi_0^{\mathrm{CC}} & 0 \\ \dot{\pi}_0^{\mathrm{CC}} & R^{\mathrm{CC}}\pi_0^{\mathrm{CC}} \end{pmatrix}\,. \tag{4.222}$$

Finally, a rescaling is required to account for the differing transcendental weights of the periods,

$$W_{\mathrm{B,e}}^{\mathrm{CC}} = \begin{pmatrix} \varepsilon^2 & 0 \\ 0 & \varepsilon \end{pmatrix}\,. \tag{4.223}$$

Chaining these rotations yields again a pre-factorised form. The intermediate matrix is again omitted here, but it has the structure

$$A_{\mathrm{B}}^{\mathrm{CC}} = A_{\mathrm{B}}^{\mathrm{CC},(0)} + \varepsilon A_{\mathrm{B}}^{\mathrm{CC},(1)}\,, \tag{4.224}$$

which is simpler than that for the neutral current. In this case, the clean-up requires only one step:

Step 1.

$$\textbf{E:}\quad \big(A_{\mathrm{B}}^{\mathrm{CC},(0)}\big)_{2,1} = a_{\mathrm{B},2,1,1}^{\mathrm{CC},(0)}\big(\pi_0^{\mathrm{CC}}\big)^2 + a_{\mathrm{B},2,1,2}^{\mathrm{CC},(0)}\pi_0^{\mathrm{CC}}\dot{\pi}_0^{\mathrm{CC}} \tag{4.225}$$

$$\textbf{A:}\quad \big(T_{\mathrm{B}}^{\mathrm{CC},(0)}\big)_{2,1} = t_{\mathrm{B},2,1,1}^{\mathrm{CC},(0)}\big(\pi_0^{\mathrm{CC}}\big)^2 \tag{4.226}$$

After this step, the clean-up procedure is completed and the homogeneous block is in ε-factorised form. Unlike the neutral current, no additional functions need be introduced. The inhomogeneous blocks are treated following the same strategy as for the neutral current, the principal difference being that at three loops there are four elliptic blocks rather than one.

Although the strategy carries over, it is not clear whether the same periods appear across all homogeneous blocks with an elliptic system. Examining the gauge transformations of the Picard–Fuchs operators reveals that two sectors admit operators of degree two, which may therefore be brought into direct correspondence with the two-loop operator. For the remaining two sectors the operators are of degree three, and establishing such a correspondence requires factorisation. The four systems read

$$I_{\mathrm{E1}}^{\mathrm{CC}} = \left(I_{3,05}^{\mathrm{CC}},\, I_{3,06}^{\mathrm{CC}}\right) \tag{4.227}$$

$$I_{\mathrm{E2}}^{\mathrm{CC}} = \left(I_{3,10}^{\mathrm{CC}},\, I_{3,11}^{\mathrm{CC}},\, I_{3,12}^{\mathrm{CC}}\right), \tag{4.228}$$

$$I_{\mathrm{E3}}^{\mathrm{CC}} = \left(I_{3,17}^{\mathrm{CC}},\, I_{3,18}^{\mathrm{CC}}\right), \tag{4.229}$$

$$I_{\mathrm{E4}}^{\mathrm{CC}} = \left(I_{3,22}^{\mathrm{CC}},\, I_{3,23}^{\mathrm{CC}},\, I_{3,24}^{\mathrm{CC}}\right). \tag{4.230}$$

The first elliptic block, Eq. (4.227), is a one-loop vacuum integral multiplied by the two-loop banana. Being independent of q^2, and hence of x, the vacuum integral leaves the Picard–Fuchs operator unchanged from that of the two-loop banana,

$$L_{\mathrm{E1},2}^{\mathrm{CC}} = \frac{\mathrm{d}^2}{\mathrm{d}x^2} + \frac{(3x^2-20x+9)}{(x-9)(x-1)x}\frac{\mathrm{d}}{\mathrm{d}x} + \frac{(x-3)}{(x-9)(x-1)x}\,. \tag{4.231}$$

Arising from the product of a one-loop two-point integral and the two-loop banana, the third elliptic block, Eq. (4.229), has a Picard–Fuchs operator that does not reduce to the two-loop banana operator in any obvious way,

$$L_{\mathrm{E3},2}^{\mathrm{CC}} = \frac{\mathrm{d}^2}{\mathrm{d}x^2} - \frac{(-9+38x-5x^2)}{(x-9)(x-1)x}\frac{\mathrm{d}}{\mathrm{d}x} + \frac{2(6x-12x^2+2x^3)}{(x-9)(x-1)^2x^2}\,. \tag{4.232}$$

However, under the gauge transformation

$$\pi_i^{\mathrm{CC}} \to \frac{\pi_i^{\mathrm{CC}}}{1-x}\,, \tag{4.233}$$

the operator reduces to that of the two-loop banana. This gauge transformation corresponds to normalising the one-loop two-point integral by its maximal cut.

Contained within the second elliptic block, Eq. (4.228), is the three-loop banana with one massless and three massive lines, whose Picard–Fuchs operator is of degree three,

$$L_{\mathrm{E2},3}^{\mathrm{CC}} = \frac{\mathrm{d}^3}{\mathrm{d}x^3} - \frac{(-6x^2+40x-18)}{(x-9)(x-1)x}\frac{\mathrm{d}^2}{\mathrm{d}x^2} - \frac{(23x-7x^2)}{(x-9)(x-1)x^2}\frac{\mathrm{d}}{\mathrm{d}x} + \frac{1}{(x-9)(x-1)x}\,. \tag{4.234}$$

The operator $L_{\mathrm{E2},3}^{\mathrm{CC}}$ admits a factorisation $L_{\mathrm{E2},3}^{\mathrm{CC}} = L_{\mathrm{E2},1}^{\mathrm{CC}} L_{\mathrm{E2},2}^{\mathrm{CC}}$, where $L_{\mathrm{E2},2}^{\mathrm{CC}}$ is precisely the Picard–Fuchs operator of the two-loop banana, with the remaining operator of degree one

$$L_{\mathrm{E2},1}^{\mathrm{CC}} = \frac{\mathrm{d}}{\mathrm{d}x} - \frac{3x^2-20x+9}{(x-9)(x-1)x}\,. \tag{4.235}$$

Factorisation is verified using the `DEtools` package in MAPLE. A further Picard–Fuchs operator of degree three arises in the remaining elliptic sector, Eq. (4.230), from an integral that reduces to a two-loop banana only upon integrating out a one-loop two-point function,

$$
\begin{aligned}
L^{\mathrm{CC}}_{\mathrm{E}4,3} = {} & \frac{\mathrm{d}^3}{\mathrm{d}x^3} - \frac{(-8x^2+66x-18)}{(x-9)(x-1)x}\frac{\mathrm{d}^2}{\mathrm{d}x^2} - \frac{(-14x^4+236x^3-990x^2+576x)}{(x-9)^2(x-1)^2x^2}\frac{\mathrm{d}}{\mathrm{d}x} \\
& + \frac{2\,(2x^3-32x^2+78x)}{(x-9)^2(x-1)^2x^2}\,.
\end{aligned} \tag{4.236}
$$

Carrying out the factorisation yields $L^{\mathrm{CC}}_{\mathrm{E}4,3} = L^{\mathrm{CC}}_{\mathrm{E}4,2}L^{\mathrm{CC}}_{\mathrm{E}4,1}$, with the order of the factors reversed relative to the previous case. This reversal reflects the graph reducing to a two-loop banana only after integrating out the two-point function,

$$
L^{\mathrm{CC}}_{\mathrm{E}4,1} = \frac{\mathrm{d}}{\mathrm{d}x} - \frac{x-3}{(x+3)\,x}\,, \tag{4.237}
$$

$$
\begin{aligned}
L^{\mathrm{CC}}_{\mathrm{E}4,2} = {} & \frac{\mathrm{d}^2}{\mathrm{d}x^2} - \frac{-81+15x+37x^2-3x^3}{(x-9)(x-1)x(x+3)}\frac{\mathrm{d}}{\mathrm{d}x} \\
& + \frac{243+243x-468x^2+260x^3-23x^4+x^5}{(x-9)^2(x-1)^2x^2(x+3)}\,.
\end{aligned} \tag{4.238}
$$

To relate $L^{\mathrm{CC}}_{\mathrm{E}4,2}$ to the Picard–Fuchs operator of the two-loop banana, a gauge transformation is applied by inserting $\mathrm{id} = UU^{-1}$ between the two factors. The matrix

$$
U = \frac{(x-9)(x-1)}{x(x+3)}\,, \tag{4.239}
$$

maps $L^{\mathrm{CC}}_{\mathrm{E}4,2}$ to the two-loop banana operator, with the remainder absorbed into $L^{\mathrm{CC}}_{\mathrm{E}4,1}$.

Once all factorisations of the Picard–Fuchs operators are established, the solutions of the two-loop banana are seen to satisfy the elliptic systems appearing at three loops as well. The remaining steps proceed in direct analogy with the neutral current. All integrals of the charged current are brought into ε-factorised form[6]. For the QED-type master integrals, the differential equations and rotation matrices agree with the literature [238] up to constant rotations, whilst those for the QCD-specific master integrals are again structurally similar.

Table 4.2: Complete set of master integrals contributing to the charged-current contribution. Massive propagators are displayed in green.

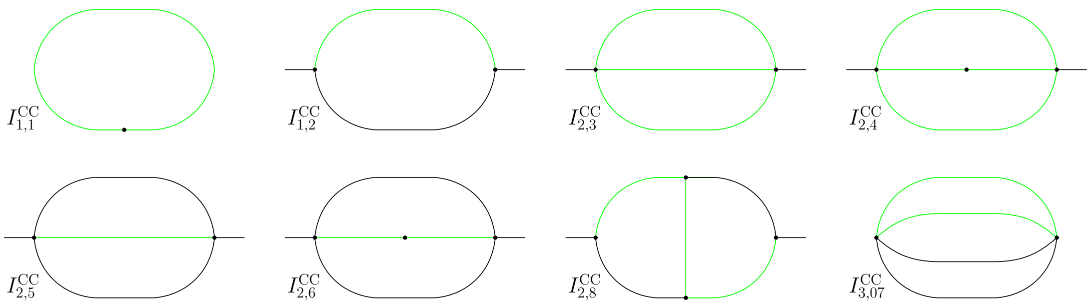

[6]All CC master integrals are provided as ancillary files; see App. E for details.

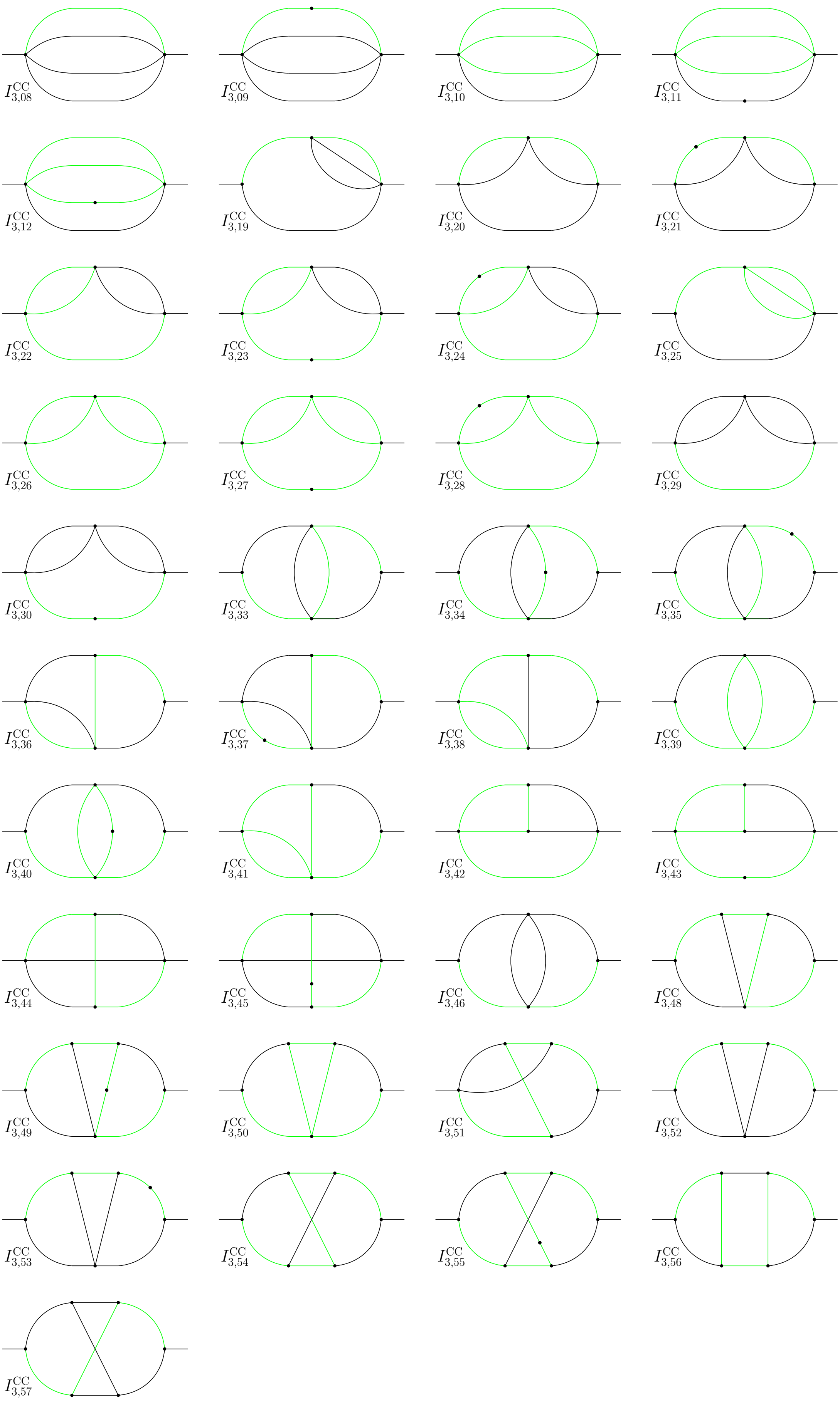
$I^{\rm CC}_{3,08}$
$I^{\rm CC}_{3,09}$
$I^{\rm CC}_{3,10}$
$I^{\rm CC}_{3,11}$
$I^{\rm CC}_{3,12}$
$I^{\rm CC}_{3,19}$
$I^{\rm CC}_{3,20}$
$I^{\rm CC}_{3,21}$
$I^{\rm CC}_{3,22}$
$I^{\rm CC}_{3,23}$
$I^{\rm CC}_{3,24}$
$I^{\rm CC}_{3,25}$
$I^{\rm CC}_{3,26}$
$I^{\rm CC}_{3,27}$
$I^{\rm CC}_{3,28}$
$I^{\rm CC}_{3,29}$
$I^{\rm CC}_{3,30}$
$I^{\rm CC}_{3,33}$
$I^{\rm CC}_{3,34}$
$I^{\rm CC}_{3,35}$
$I^{\rm CC}_{3,36}$
$I^{\rm CC}_{3,37}$
$I^{\rm CC}_{3,38}$
$I^{\rm CC}_{3,39}$
$I^{\rm CC}_{3,40}$
$I^{\rm CC}_{3,41}$
$I^{\rm CC}_{3,42}$
$I^{\rm CC}_{3,43}$
$I^{\rm CC}_{3,44}$
$I^{\rm CC}_{3,45}$
$I^{\rm CC}_{3,46}$
$I^{\rm CC}_{3,48}$
$I^{\rm CC}_{3,49}$
$I^{\rm CC}_{3,50}$
$I^{\rm CC}_{3,51}$
$I^{\rm CC}_{3,52}$
$I^{\rm CC}_{3,53}$
$I^{\rm CC}_{3,54}$
$I^{\rm CC}_{3,55}$
$I^{\rm CC}_{3,56}$
$I^{\rm CC}_{3,57}$

4.5.4 Boundary Values

The boundary values for all differential equations are obtained from the asymptotic limit $x \to 0$, evaluated by the method of expansion by subgraphs (see Subsec. 3.3.5), implemented in the FORM code `expdia.frm`[7].

Under this expansion, each integral decomposes into a sum of products of massive vacuum graphs and massless two-point functions. Applying the method first requires translating each master integral into a graph, which the use of a dot basis makes possible and which, in part, motivates that choice. Each graph is then mapped onto the previously derived momentum routings and assigned an integral family. For the two-point functions, the massless families defined earlier suffice, whereas the massive vacuum integrals call for the additional families

$$\hat{\mathcal{B}}_1 = \left\{\hat{\mathcal{B}}_{1,1}\right\}, \tag{4.240}$$

$$\hat{\mathcal{B}}_2 = \left\{\hat{\mathcal{B}}_{2,1}, \hat{\mathcal{B}}_{2,3}, \hat{\mathcal{B}}_{2,7}\right\}, \tag{4.241}$$

$$\hat{\mathcal{B}}_3 = \left\{\hat{\mathcal{B}}_{3,01}, \hat{\mathcal{B}}_{3,03}, \hat{\mathcal{B}}_{3,07}, \hat{\mathcal{B}}_{3,11}, \hat{\mathcal{B}}_{3,13}, \hat{\mathcal{B}}_{3,15}, \hat{\mathcal{B}}_{3,29}, \hat{\mathcal{B}}_{3,31}\right\}, \tag{4.242}$$

which are derived from the momentum routings for the vacuum integrals, Eqs. (4.107) to (4.109), and dressed with masses in the binary notation introduced earlier. From here the workflow mirrors that of the amplitude itself, the integrals being reduced with `Kira` to a small set of master integrals (see Tab. A.3), the only new step being the tensor reduction of the non-trivial numerators with `Opiter` [239].

The massless two-point functions arising in these expansions are themselves master integrals, encountered earlier in the calculation, and, being single-scale, may equally be regarded as pure boundary integrals. They are evaluated with the MAPLE package `HyperInt` [240,241] or equivalently its FORM implementation `HyperForm` [242], which proceeds via the parametric representation and exploits the linear reducibility of the integrals to yield an iterative integration in terms of multiple polylogarithms.

By contrast, the massive vacuum integrals are not all known analytically at three loops, although high-precision numerical values are available [243]. These were computed using dimensional recurrence relations [244, 245] and subsequently identified via the integer-relation algorithm `PSLQ` [246], allowing their reconstruction in terms of harmonic polylogarithms evaluated at the sixth root of unity [247].

Following the reference, the integrals are parametrised by a set of constants from which all pure zeta values have been factored out, retaining only those constants not expressible through zeta values alone. The rationale for this choice is twofold. First, zeta values appear in every vacuum integral and frequently cancel against one another, so separating them avoids carrying redundant contributions through the calculation. Second, the remaining transcendental constants form an independent basis and yield more compact expressions for the master integrals. The parametrisation adopted here departs from the reference in one further respect: one of the master integrals is related by IBP to its counterpart there, whilst the remaining integrals coincide. Explicitly, the integral $I_{3,10}$ is replaced by a top-sector integral with a massless and five massive lines, namely

$$I'_{3,10} = \frac{(D-2)^2}{6(D-4)(D-3)}\hat{I}_{3,01} - \frac{2(D-2)}{3(D-4)}\hat{I}_{3,06} + \frac{3D-8}{12(D-4)}\hat{I}_{3,07} + \frac{2(D-3)}{3(D-4)}\hat{I}_{3,10}\,. \tag{4.243}$$

[7]The code is not publicly available but may be provided upon reasonable request.

Fixing the boundary values to the needed expansion depth (see Subsec. 4.4.2) requires twenty-four constants, which may not be linearly independent[8]. Their values are obtained by matching the analytic parametrisation of each vacuum integral to its high-precision numerical value from the reference.

Finally, in the asymptotic limit each master integral takes the form of a log-Puiseux expansion in x combined with a Laurent series in ε,

$$I = \sum_k \varepsilon^k \sum_{m,n} c^{(k)}_{m/2,n} x^{m/2} [\log x]^n. \tag{4.244}$$

However, in the ε-factorised basis the constant terms do not derive entirely from those of the original basis. Since the transformation relating the two bases may contain inverse powers of the scale, higher orders of the original expansion feed into the constant part. The remaining orders in x and its logarithms may then be used as consistency checks.

A full set of boundary conditions[9] has been cross-checked numerically against the asymptotic expansions obtained through the Mathematica package `Fiesta` [248], agreeing within the numerical uncertainty.

Table 4.3: Complete set of master integrals contributing to the boundary integrals. Massive propagators are displayed in green.

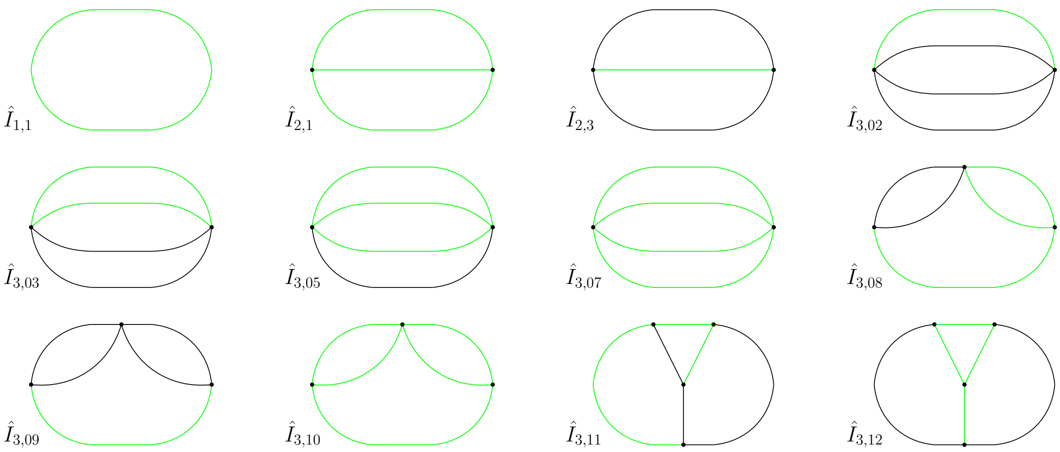

4.5.5 Solutions

Now that all differential equations have been transformed into ε-factorised form, they can be integrated formally, with the solutions expressed in terms of iterated integrals. Fixing the boundary conditions, however, requires expanding the iterated integrals in the limit $x \to 0$. The following therefore discusses the expansions of the integral kernels and special functions in turn.

For the neutral current, ε-factorisation requires the introduction of three transcendental functions, whereas none are needed for the charged current. Their expansions

[8] Checking linear independence is more parctical at the level of the renormalised amplitude, where additional transcendental constants may appear, while others can cancel completely

[9] A complete set of boundary values is not provided, since they can be derived from the full master integrals for both NC and CC by means of a series expansion.

around zero read

$$G_1^{\mathrm{NC}}(x) = \frac{1}{32}\int_0^x \mathrm{d}t\, \frac{(t-8)(8+t)^3[\varpi_0^{\mathrm{NC}}(t)]^2}{(t-16)^2(t-4)^2} \\ = \frac{x}{32} + \frac{x^2}{64} + \frac{93x^3}{16384} + \frac{1841x^4}{1048576} + \frac{33637x^5}{67108864} + \mathcal{O}\big(x^6\big)\,, \tag{4.245}$$

$$G_2^{\mathrm{NC}}(x) = 8\int_0^x \mathrm{d}t\, \frac{G_1^{\mathrm{NC}}(t)}{t r_2^{\mathrm{NC}}(t)\varpi_0^{\mathrm{NC}}(t)} \\ = \frac{x}{32} + \frac{19x^2}{2048} + \frac{167x^3}{65536} + \frac{5539x^4}{8388608} + \frac{44561x^5}{268435456} + \mathcal{O}\big(x^6\big)\,, \tag{4.246}$$

$$G_3^{\mathrm{NC}}(x) = \int_0^x \mathrm{d}t\, \frac{(2+t) r_1^{\mathrm{NC}}(t)\varpi_0^{\mathrm{NC}}(t)}{t(t-4)^2} \\ = \frac{1}{\sqrt{x}}\left[\frac{x}{2} + \frac{5x^2}{32} + \frac{75x^3}{2048} + \frac{139x^4}{16384} + \mathcal{O}\big(x^5\big)\right]\,, \tag{4.247}$$

where G_1^{NC} and G_2^{NC} are holomorphic near zero, whilst G_3^{NC} is not. The ε-factorised differential equation itself holds on the punctured complex plane, since its derivation relies only on algebraic properties of the periods, but never on their explicit form; by contrast, the series expansions above are valid only in some neighbourhood of zero, with radii of convergence that may vary between the functions.

Across all differential equations, the transformations require the introduction of three square roots for the neutral current,

$$r_1^{\mathrm{NC}}(x) = \sqrt{x(4-x)}\,, \tag{4.248}$$

$$r_2^{\mathrm{NC}}(x) = \sqrt{(16-x)(4-x)}\,, \tag{4.249}$$

$$r_3^{\mathrm{NC}}(x) = \sqrt{x(4+x)}\,, \tag{4.250}$$

and two for the charged current,

$$r_1^{\mathrm{CC}}(x) = \sqrt{(3+x)(1-x)}\,, \tag{4.251}$$

$$r_2^{\mathrm{CC}}(x) = \sqrt{(9-x)(1-x)}\,. \tag{4.252}$$

Here, the threshold square roots r_1^{NC}, r_2^{NC}, r_1^{CC}, and r_2^{CC} correspond to two-, four-, one-, and three-heavy-quark production respectively, whilst r_3^{NC} is spurious and corresponds to no physical threshold.

The integral kernels appearing in the neutral current are collected here, together with their series expansions around zero to fifth order, from which their analytic properties can be read off. With the exception of the QCD-exclusive kernels $\omega_{25}^{\mathrm{NC}}$ and $\omega_{26}^{\mathrm{NC}}$, which are not covered by the existing literature [215], all kernels are in agreement with QED-like results. Explicitly, the kernels read

$$\omega_1^{\mathrm{NC}}(x) = \frac{1}{x} \tag{4.253}$$

$$\omega_2^{\mathrm{NC}}(x) = \frac{1}{x-1} \\ = -1 - x - x^2 - x^3 - x^4 + \mathcal{O}\big(x^5\big)\,, \tag{4.254}$$

$$\omega_3^{\mathrm{NC}}(x) = \frac{1}{x-4} \\ = -\frac{1}{4} - \frac{x}{16} - \frac{x^2}{64} - \frac{x^3}{256} - \frac{x^4}{1024} + \mathcal{O}\big(x^5\big)\,, \tag{4.255}$$

$$\begin{aligned}\omega_4^{\rm NC}(x) &= \frac{1}{r_1^{\rm NC}} \\ &= \frac{1}{\sqrt{x}}\left[\frac{1}{2} + \frac{x}{16} + \frac{3x^2}{256} + \frac{5x^3}{2048} + \frac{35x^4}{65536} + \mathcal{O}\big(x^5\big)\right],\end{aligned} \tag{4.256}$$

$$\begin{aligned}\omega_5^{\rm NC}(x) &= \frac{1}{x-16} \\ &= -\frac{1}{16} - \frac{x}{256} - \frac{x^2}{4096} - \frac{x^3}{65536} - \frac{x^4}{1048576} + \mathcal{O}\big(x^5\big),\end{aligned} \tag{4.257}$$

$$\begin{aligned}\omega_6^{\rm NC}(x) &= \frac{1}{x r_2^{\rm NC}\varpi_0^{\rm NC}} \\ &= \frac{1}{8x} + \frac{3}{256} + \frac{33x}{16384} + \frac{213x^2}{524288} + \frac{5889x^3}{67108864} + \frac{42159x^4}{2147483648} + \mathcal{O}\big(x^5\big),\end{aligned} \tag{4.258}$$

$$\begin{aligned}\omega_7^{\rm NC}(x) &= \frac{G_2^{\rm NC}}{x r_2^{\rm NC}\varpi_0^{\rm NC}} \\ &= \frac{1}{256} + \frac{25x}{16384} + \frac{257x^2}{524288} + \frac{9649x^3}{67108864} + \frac{86183x^4}{2147483648} + \mathcal{O}\big(x^5\big),\end{aligned} \tag{4.259}$$

$$\begin{aligned}\omega_8^{\rm NC}(x) &= \frac{[G_2^{\rm NC}]^2}{x r_2^{\rm NC}\varpi_0^{\rm NC}} \\ &= \frac{x}{8192} + \frac{11x^2}{131072} + \frac{1323x^3}{33554432} + \frac{4163x^4}{268435456} + \mathcal{O}\big(x^5\big),\end{aligned} \tag{4.260}$$

$$\begin{aligned}\omega_9^{\rm NC}(x) &= \frac{[G_2^{\rm NC}]^3}{x r_2^{\rm NC}\varpi_0^{\rm NC}} \\ &= \frac{x^2}{262144} + \frac{63x^3}{16777216} + \frac{2493x^4}{1073741824} + \mathcal{O}\big(x^5\big),\end{aligned} \tag{4.261}$$

$$\begin{aligned}\omega_{10}^{\rm NC}(x) &= \frac{G_3^{\rm NC}}{x r_2^{\rm NC}\varpi_0^{\rm NC}} \\ &= \frac{1}{\sqrt{x}}\left[\frac{1}{16} + \frac{13x}{512} + \frac{243x^2}{32768} + \frac{2105x^3}{1048576} + \mathcal{O}\big(x^5\big)\right],\end{aligned} \tag{4.262}$$

$$\begin{aligned}\omega_{11}^{\rm NC}(x) &= \frac{G_2^{\rm NC}G_3^{\rm NC}}{x r_2^{\rm NC}\varpi_0^{\rm NC}} \\ &= \frac{1}{\sqrt{x}}\left[\frac{x}{512} + \frac{45x^2}{32768} + \frac{657x^3}{1048576} + \mathcal{O}\big(x^5\big)\right],\end{aligned} \tag{4.263}$$

$$\begin{aligned}\omega_{12}^{\rm NC}(x) &= \frac{G_3^{\rm NC}}{r_1^{\rm NC}} \\ &= \frac{1}{4} + \frac{7x}{64} + \frac{139x^2}{4096} + \frac{157x^3}{16384} + \frac{43567x^4}{16777216} + \mathcal{O}\big(x^5\big),\end{aligned} \tag{4.264}$$

$$\begin{aligned}\omega_{13}^{\rm NC}(x) &= \frac{G_3^{\rm NC}}{x} \\ &= \frac{1}{\sqrt{x}}\left[\frac{1}{2} + \frac{5x}{32} + \frac{75x^2}{2048} + \frac{139x^3}{16384} + \frac{16591x^4}{8388608} + \mathcal{O}\big(x^5\big)\right],\end{aligned} \tag{4.265}$$

$$\begin{aligned}\omega_{14}^{\mathrm{NC}}(x) &= \frac{G_3^{\mathrm{NC}}}{x-4} \\ &= \frac{1}{\sqrt{x}}\left[-\frac{x}{8}-\frac{9x^2}{128}-\frac{219x^3}{8192}-\frac{577x^4}{65536}+\mathcal{O}\big(x^5\big)\right],\end{aligned} \tag{4.266}$$

$$\begin{aligned}\omega_{15}^{\mathrm{NC}}(x) &= \frac{G_3^{\mathrm{NC}}}{x-16} \\ &= \frac{1}{\sqrt{x}}\left[-\frac{x}{32}-\frac{3x^2}{256}-\frac{99x^3}{32768}-\frac{377x^4}{524288}+\mathcal{O}\big(x^5\big)\right],\end{aligned} \tag{4.267}$$

$$\begin{aligned}\omega_{16}^{\mathrm{NC}}(x) &= \varpi_0^{\mathrm{NC}} \\ &= 1+\frac{x}{16}+\frac{7x^2}{1024}+\frac{x^3}{1024}+\frac{679x^4}{4194304}+\mathcal{O}\big(x^5\big),\end{aligned} \tag{4.268}$$

$$\begin{aligned}\omega_{17}^{\mathrm{NC}}(x) &= \frac{\varpi_0^{\mathrm{NC}}}{x} \\ &= \frac{1}{x}+\frac{1}{16}+\frac{7x}{1024}+\frac{x^2}{1024}+\frac{679x^3}{4194304}+\frac{1969x^4}{67108864}+\mathcal{O}\big(x^5\big),\end{aligned} \tag{4.269}$$

$$\begin{aligned}\omega_{18}^{\mathrm{NC}}(x) &= \frac{\varpi_0^{\mathrm{NC}}}{x-4} \\ &= -\frac{1}{4}-\frac{5x}{64}-\frac{87x^2}{4096}-\frac{91x^3}{16384}-\frac{23975x^4}{16777216}+\mathcal{O}\big(x^5\big),\end{aligned} \tag{4.270}$$

$$\begin{aligned}\omega_{19}^{\mathrm{NC}}(x) &= \frac{r_1^{\mathrm{NC}}\varpi_0^{\mathrm{NC}}}{x} \\ &= \frac{1}{\sqrt{x}}\left[2-\frac{x}{8}-\frac{9x^2}{512}-\frac{11x^3}{4096}-\frac{953x^4}{2097152}+\mathcal{O}\big(x^5\big)\right],\end{aligned} \tag{4.271}$$

$$\begin{aligned}\omega_{20}^{\mathrm{NC}}(x) &= \frac{r_1^{\mathrm{NC}}\varpi_0^{\mathrm{NC}}}{x-4} \\ &= \frac{1}{\sqrt{x}}\left[-\frac{x}{2}-\frac{3x^2}{32}-\frac{39x^3}{2048}-\frac{67x^4}{16384}+\mathcal{O}\big(x^5\big)\right],\end{aligned} \tag{4.272}$$

$$\begin{aligned}\omega_{21}^{\mathrm{NC}}(x) &= \frac{r_1^{\mathrm{NC}}\varpi_0^{\mathrm{NC}}}{(x-4)^2} \\ &= \frac{1}{\sqrt{x}}\left[\frac{x}{8}+\frac{7x^2}{128}+\frac{151x^3}{8192}+\frac{369x^4}{65536}+\mathcal{O}\big(x^5\big)\right],\end{aligned} \tag{4.273}$$

$$\begin{aligned}\omega_{22}^{\mathrm{NC}}(x) &= \frac{(x+8)^2(x^2-8x+64)r_2^{\mathrm{NC}}\varpi_0^{\mathrm{NC}}}{(x-16)^2(x-4)^2x} \\ &= \frac{8}{x}+\frac{21}{4}+\frac{537x}{256}+\frac{5835x^2}{8192}+\frac{232869x^3}{1048576}+\frac{2195805x^4}{33554432}+\mathcal{O}\big(x^5\big),\end{aligned} \tag{4.274}$$

$$\begin{aligned}\omega_{23}^{\mathrm{NC}}(x) &= \frac{(x+8)^2(x^2-8x+64)r_2^{\mathrm{NC}}G_2^{\mathrm{NC}}\varpi_0^{\mathrm{NC}}}{(x-16)^2(x-4)^2x} \\ &= \frac{1}{4}+\frac{61x}{256}+\frac{1103x^2}{8192}+\frac{63313x^3}{1048576}+\frac{794837x^4}{33554432}+\mathcal{O}\big(x^5\big),\end{aligned} \tag{4.275}$$

$$\begin{aligned}\omega_{24}^{\mathrm{NC}}(x) &= \frac{(x+8)^3(x-8)[\varpi_0^{\mathrm{NC}}]^2}{(x-16)^2(x-4)^2} \\ &= -1-x-\frac{279x^2}{512}-\frac{1841x^3}{8192}-\frac{168185x^4}{2097152}+\mathcal{O}\big(x^5\big),\end{aligned} \tag{4.276}$$

$$
\begin{aligned}
\omega_{25}^{\mathrm{NC}}(x) &= \frac{1}{r_3^{\mathrm{NC}}} \\
&= \frac{1}{\sqrt{x}}\left[\frac{1}{2} - \frac{x}{16} + \frac{3x^2}{256} - \frac{5x^3}{2048} + \frac{35x^4}{65536} + \mathcal{O}\big(x^5\big)\right],
\end{aligned}
\tag{4.277}
$$

$$
\begin{aligned}
\omega_{26}^{\mathrm{NC}}(x) &= \frac{1}{x+4} \\
&= \frac{1}{4} - \frac{x}{16} + \frac{x^2}{64} - \frac{x^3}{256} + \frac{x^4}{1024} + \mathcal{O}\big(x^5\big)\,.
\end{aligned}
\tag{4.278}
$$

The kernels ω_i^{NC} admit a natural partition according to the analytic structure of their primitives,

$$\mathcal{H}^{\mathrm{NC}} = \big\{\,\omega_i^{\mathrm{NC}}\;\big|\; i \in \{\,2,3,5,7,8,9,12,16,18,23,24,26\,\}\,\big\}\,, \tag{4.279}$$

$$\mathcal{L}^{\mathrm{NC}} = \big\{\,\omega_i^{\mathrm{NC}}\;\big|\; i \in \{\,1,6,17,22\,\}\,\big\}\,, \tag{4.280}$$

$$\mathcal{A}^{\mathrm{NC}} = \big\{\,\omega_i^{\mathrm{NC}}\;\big|\; i \in \{\,4,10,11,13,14,15,19,20,21,25\,\}\,\big\}\,, \tag{4.281}$$

where the set $\mathcal{H}^{\mathrm{NC}}$ collects kernels whose primitives are holomorphic, $\mathcal{L}^{\mathrm{NC}}$ those that are logarithmic, and $\mathcal{A}^{\mathrm{NC}}$ those with algebraic, square-root, branch points.

The iterated integrals over these kernels are real for all $x \in (-\infty, 0)$, but not manifestly so, which is an obstacle for numerical evaluation. This is remedied by the change of variables

$$\hat{x}(x) = -x\,, \tag{4.282}$$

with $\hat{x} \in (0,\infty)$ and the Jacobian contributing an overall sign to each transformed kernel. All holomorphic kernels in $\mathcal{H}^{\mathrm{NC}}$ transform by direct substitution,

$$\hat{\omega}_k^{\mathrm{NC}}(\hat{x}) \equiv -\omega_k^{\mathrm{NC}}(-x)\,, \qquad k \in \mathcal{H}^{\mathrm{NC}}\,. \tag{4.283}$$

For the kernels with algebraic branch-points, the branch of the square root is chosen so that the transformed kernels remain real,

$$
\begin{aligned}
r_1^{\mathrm{NC}}(-x) &= -i\sqrt{\hat{x}(4+\hat{x})} \\
&\equiv -i\,\hat{r}_1^{\mathrm{NC}}(\hat{x})\,,
\end{aligned}
\tag{4.284}
$$

$$
\begin{aligned}
r_2^{\mathrm{NC}}(-x) &= \sqrt{(16+\hat{x})(4+\hat{x})} \\
&\equiv \hat{r}_2^{\mathrm{NC}}(\hat{x})\,,
\end{aligned}
\tag{4.285}
$$

$$
\begin{aligned}
r_3^{\mathrm{NC}}(-x) &= -i\sqrt{\hat{x}(4-\hat{x})} \\
&\equiv -i\hat{r}_3^{\mathrm{NC}}(\hat{x})\,,
\end{aligned}
\tag{4.286}
$$

where $\hat{r}_1^{\mathrm{NC}}$ and $\hat{r}_2^{\mathrm{NC}}$ are real for all $\hat{x} \in (0,\infty)$, and $\hat{r}_3^{\mathrm{NC}}$ for all $\hat{x} \in (0,4)$. Since $\hat{r}_3^{\mathrm{NC}}$ enters the master integrals only at even powers, its branch ambiguity drops out.

The algebraic kernels split into two cases according to whether their denominators contain r_1^{NC} or r_3^{NC}, or feature these square roots in the numerator implicitly through G_3^{NC}. This implies the transformations

$$\hat{\omega}_k^{\mathrm{NC}}(\hat{x}) \equiv +i\,\omega_k^{\mathrm{NC}}(-x)\,, \qquad k \in \mathcal{A}^{\mathrm{NC}} \setminus \{4,25\}\,, \tag{4.287}$$

$$\hat{\omega}_k^{\mathrm{NC}}(\hat{x}) \equiv -i\,\omega_k^{\mathrm{NC}}(-x) \qquad k \in \{4,25\}\,. \tag{4.288}$$

Kernels with logarithmic branch points transform by direct substitution

$$\hat{\omega}_k^{\mathrm{NC}}(\hat{x}) \equiv -\omega_k^{\mathrm{NC}}(-x)\,, \qquad k \in \mathcal{L}^{\mathrm{NC}}\,. \tag{4.289}$$

Iterated integrals over these kernels require more care. For the general weight-n case with $a_k = 1$ for all k, we find

$$\begin{aligned} \mathrm{F}^{\mathrm{NC}}_{a_1,\ldots,a_n}(x) &= \frac{1}{n!}\big[\log(x)\big]^n \\ &= \frac{1}{n!}\big[\log(\hat{x}) + i\pi\big]^n \\ &= \sum_{k=0}^{n} \frac{(i\pi)^{n-k}}{(n-k)!}\, \hat{\mathrm{F}}^{\mathrm{NC}}_{a_1,\ldots,a_k}(\hat{x})\,, \end{aligned} \tag{4.290}$$

which generalises straightforwardly to other logarithmic letters and to the presence of trailing kernels,

$$\mathrm{F}^{\mathrm{NC}}_{a_1,\ldots,a_n,a_{n+1},\ldots,a_m}(x) = \sum_{k=0}^{n} \frac{(i\pi)^{n-k}}{(n-k)!} \left(\prod_{l=0}^{k} \mathrm{Res}(\hat{\omega}_l^{\mathrm{NC}}, 0) \right) \hat{\mathrm{F}}^{\mathrm{NC}}_{a_1,\ldots,a_k,a_n,a_{n+1},\ldots,a_m}(\hat{x})\,. \tag{4.291}$$

Finally, the change of variables acts on the periods and their derivatives. Being holomorphic, these transform trivially,

$$\left.\frac{\mathrm{d}^n}{\mathrm{d}x^n} \varpi_0^{\mathrm{NC}}(x)\right|_{x=-\hat{x}} = (-1)^n \frac{\mathrm{d}^n}{\mathrm{d}\hat{x}^n} \varpi_0^{\mathrm{NC}}(\hat{x})\,. \tag{4.292}$$

The same is true for the transcendental functions needed to bring the differential equation into ε-factorised form. Their transformations are inherited from those of the square roots and periods,

$$G_1^{\mathrm{NC}}(-x) = \hat{G}_1^{\mathrm{NC}}(\hat{x})\,, \tag{4.293}$$
$$G_2^{\mathrm{NC}}(-x) = \hat{G}_2^{\mathrm{NC}}(\hat{x})\,, \tag{4.294}$$
$$G_3^{\mathrm{NC}}(-x) = -i\,\hat{G}_3^{\mathrm{NC}}(\hat{x})\,. \tag{4.295}$$

Much the same applies to the charged current integral kernels, which agree precisely with the corresponding QED kernels. Their expansions to fifth order read,

$$\begin{aligned} \omega_1^{\mathrm{CC}}(x) &= \frac{1}{x+3} \\ &= \frac{1}{3} - \frac{x}{9} + \frac{x^2}{27} - \frac{x^3}{81} + \frac{x^4}{243} + \mathcal{O}\big(x^5\big)\,, \end{aligned} \tag{4.296}$$

$$\begin{aligned} \omega_2^{\mathrm{CC}}(x) &= \frac{1}{x+1} \\ &= 1 - x + x^2 - x^3 + x^4 + \mathcal{O}\big(x^5\big)\,, \end{aligned} \tag{4.297}$$

$$\omega_3^{\mathrm{CC}}(x) = \frac{1}{x} \tag{4.298}$$

$$\begin{aligned} \omega_4^{\mathrm{CC}}(x) &= \frac{1}{x-1} \\ &= -1 - x - x^2 - x^3 - x^4 + \mathcal{O}\big(x^5\big)\,, \end{aligned} \tag{4.299}$$

$$\begin{aligned}\omega_5^{\mathrm{CC}}(x) &= \frac{1}{x-2} \\ &= -\frac{1}{2} - \frac{x}{4} - \frac{x^2}{8} - \frac{x^3}{16} - \frac{x^4}{32} + \mathcal{O}\big(x^5\big)\,,\end{aligned} \tag{4.300}$$

$$\begin{aligned}\omega_6^{\mathrm{CC}}(x) &= \frac{1}{x-9} \\ &= -\frac{1}{9} - \frac{x}{81} - \frac{x^2}{729} - \frac{x^3}{6561} - \frac{x^4}{59049} + \mathcal{O}\big(x^5\big)\,,\end{aligned} \tag{4.301}$$

$$\begin{aligned}\omega_7^{\mathrm{CC}}(x) &= \frac{1}{r_1^{\mathrm{CC}}} \\ &= \frac{1}{\sqrt{3}}\left[1 + \frac{x}{3} + \frac{x^2}{3} + \frac{7x^3}{27} + \frac{19x^4}{81} + \mathcal{O}\big(x^5\big)\right],\end{aligned} \tag{4.302}$$

$$\begin{aligned}\omega_8^{\mathrm{CC}}(x) &= \frac{1}{r_2^{\mathrm{CC}}} \\ &= \frac{1}{3} + \frac{5x}{27} + \frac{11x^2}{81} + \frac{245x^3}{2187} + \frac{1921x^4}{19683} + \mathcal{O}\big(x^5\big)\,,\end{aligned} \tag{4.303}$$

$$\begin{aligned}\omega_9^{\mathrm{CC}}(x) &= \frac{1}{x r_2^{\mathrm{CC}}} \\ &= \frac{1}{3x} + \frac{5}{27} + \frac{11x}{81} + \frac{245x^2}{2187} + \frac{1921x^3}{19683} + \frac{575x^4}{6561} + \mathcal{O}\big(x^5\big)\,,\end{aligned} \tag{4.304}$$

$$\begin{aligned}\omega_{10}^{\mathrm{CC}}(x) &= \frac{1}{(x-9)(x-1)x[\pi_0^{\mathrm{CC}}]^2} \\ &= \frac{1}{9x} + \frac{4}{81} + \frac{28x}{729} + \frac{220x^2}{6561} + \frac{1804x^3}{59049} + \frac{15124x^4}{531441} + \mathcal{O}\big(x^5\big)\,,\end{aligned} \tag{4.305}$$

$$\begin{aligned}\omega_{11}^{\mathrm{CC}}(x) &= \pi_0^{\mathrm{CC}} \\ &= 1 + \frac{x}{3} + \frac{5x^2}{27} + \frac{31x^3}{243} + \frac{71x^4}{729} + \mathcal{O}\big(x^5\big)\,,\end{aligned} \tag{4.306}$$

$$\begin{aligned}\omega_{12}^{\mathrm{CC}}(x) &= \frac{\pi_0^{\mathrm{CC}}}{x-1} \\ &= -1 - \frac{4x}{3} - \frac{41x^2}{27} - \frac{400x^3}{243} - \frac{1271x^4}{729} + \mathcal{O}\big(x^5\big)\,,\end{aligned} \tag{4.307}$$

$$\begin{aligned}\omega_{13}^{\mathrm{CC}}(x) &= \frac{(x-3)\pi_0^{\mathrm{CC}}}{r_2^{\mathrm{CC}}} \\ &= -1 - \frac{5x}{9} - \frac{13x^2}{27} - \frac{323x^3}{729} - \frac{2719x^4}{6561} + \mathcal{O}\big(x^5\big)\,,\end{aligned} \tag{4.308}$$

$$\begin{aligned}\omega_{14}^{\mathrm{CC}}(x) &= \frac{(x+3)^4[\pi_0^{\mathrm{CC}}]^2}{(x-9)(x-1)x} \\ &= \frac{9}{x} + 28 + \frac{436x}{9} + \frac{5284x^2}{81} + \frac{57124x^3}{729} + \frac{583948x^4}{6561} + \mathcal{O}\big(x^5\big)\,,\end{aligned} \tag{4.309}$$

$$\begin{aligned}\omega_{15}^{\mathrm{CC}}(x) &= \frac{(x+3)(x-1)[\pi_0^{\mathrm{CC}}]^2}{(x-9)x} \\ &= \frac{1}{3x} + \frac{1}{27} - \frac{23x}{243} - \frac{143x^2}{2187} - \frac{791x^3}{19683} - \frac{4679x^4}{177147} + \mathcal{O}\big(x^5\big)\,,\end{aligned} \tag{4.310}$$

$$\begin{aligned}\omega_{16}^{\mathrm{CC}}(x) &= \frac{[\pi_0^{\mathrm{CC}}]^2}{(x-9)(x-1)} \\ &= \frac{1}{9} + \frac{16x}{81} + \frac{190x^2}{729} + \frac{2032x^3}{6561} + \frac{20671x^4}{59049} + \mathcal{O}\big(x^5\big)\,.\end{aligned} \tag{4.311}$$

For the charged current, all integral kernels agree with those found in the existing literature [238] and are consistent with QED-like results.

In direct analogy to the neutral current, the integral kernels ω_i^{CC} admit partitions according to the analytic structure of their primitives,

$$\mathcal{H}^{\mathrm{CC}} = \left\{ \omega_i^{\mathrm{CC}} \;\middle|\; i \in \{1,2,4,5,6,7,8,11,12,16\} \right\}\,, \tag{4.312}$$

$$\mathcal{L}^{\mathrm{CC}} = \left\{ \omega_i^{\mathrm{CC}} \;\middle|\; i \in \{3,9,10,14,15\} \right\}\,, \tag{4.313}$$

$$\mathcal{A}^{\mathrm{CC}} = \emptyset\,. \tag{4.314}$$

The holomorphic kernels in $\mathcal{H}^{\mathrm{CC}}$ transform once more by direct substitution,

$$\hat{\omega}_k^{\mathrm{CC}}(\hat{x}) \equiv -\omega_k^{\mathrm{CC}}(-x)\,, \qquad k \in \mathcal{H}^{\mathrm{CC}}\,. \tag{4.315}$$

For the kernels with algebraic branch-points, the branch of the square root is chosen so that the transformed kernels remain real,

$$\begin{aligned} r_1^{\mathrm{CC}}(-x) &= \sqrt{(3-\hat{x})(1+\hat{x})} \\ &\equiv \hat{r}_1^{\mathrm{CC}}(\hat{x})\,, \end{aligned} \tag{4.316}$$

$$\begin{aligned} r_2^{\mathrm{CC}}(-x) &= -i\sqrt{(9+\hat{x})(1+\hat{x})} \\ &\equiv -i\hat{r}_3^{\mathrm{CC}}(\hat{x})\,. \end{aligned} \tag{4.317}$$

where $\hat{r}_1^{\mathrm{CC}}$ is real only for $\hat{x} \in (0,3)$, and $\hat{r}_2^{\mathrm{CC}}$ for all $\hat{x} \in (0,\infty)$. In contrast to the neutral current, no algebraic kernels arise here. The logarithmic kernels transform as

$$\hat{\omega}_k^{\mathrm{CC}}(\hat{x}) \equiv -\omega_k^{\mathrm{CC}}(-x)\,, \qquad k \in \mathcal{L}^{\mathrm{CC}}\,. \tag{4.318}$$

with the iterated integrals transforming as

$$\mathrm{F}^{\mathrm{CC}}_{a_1,\ldots,a_n,a_{n+1},\ldots,a_m}(x) = \sum_{k=0}^{n} \frac{(i\pi)^{n-k}}{(n-k)!} \left(\prod_{l=0}^{k} \mathrm{Res}(\hat{\omega}_l^{\mathrm{CC}},0) \right) \hat{\mathrm{F}}^{\mathrm{CC}}_{a_1,\ldots,a_k,a_n,a_{n+1},\ldots,a_m}(\hat{x})\,. \tag{4.319}$$

Finally, being holomorphic functions, the period of the charged current, ϖ_0^{CC}, also transforms trivially,

$$\frac{\mathrm{d}^n}{\mathrm{d}x^n}\varpi_0^{\mathrm{CC}}(x) = (-1)^n \frac{\mathrm{d}^n}{\mathrm{d}\hat{x}^n}\varpi_0^{\mathrm{CC}}(\hat{x})\,. \tag{4.320}$$

All master integrals were verified numerically with the Mathematica package `AMFlow` [249] to twenty digits at $\hat{x} = 1/2$, both before and after the change of variables. This point was chosen because the singularity structure restricts the series to a disc of radius one around the origin. Such a check does not validate the integrals themselves, but it does confirm that the change of variables is implemented consistently.

(This page is intentionally left blank.)

"Wake up, Alice dear!' said her sister; 'Why, what a long sleep you've had!' 'Oh, I've had such a curious dream!' said Alice, and she told her sister, as well as she could remember them, all these strange Adventures of hers that you have just been reading about; and when she had finished, her sister kissed her, and said, 'It was a curious dream, dear, certainly: but now run in to your tea; it's getting late."

— *Alice's Adventures in Wonderland*, Lewis Carroll

Chapter 5

Results

5.1 Neutral Current at NLO

5.1.1 Vector-Vector

The complete NLO results for the Mellin moments of the transverse and longitudinal heavy-quark coefficient functions, retaining their full mass dependence, are rather lengthy, and in our computation they have been evaluated up to $N = 22$. As highlighted in the previous chapters, the setup also allows for the calculation of the Mellin moments of the massless coefficient functions, which we include here for completeness. These massless contributions were first obtained in Refs. [31, 38], with which our results agree.

For illustration, we display explicitly only the lowest non-vanishing Mellin moment, namely $N = 2$. All results are written in the auxiliary variable υ defined in Eq. (1.29), since this change of variables casts them in terms of harmonic polylogarithms. The iterated integrals can be transformed directly, at the price of a rather subtle treatment of boundary terms. Integrating the differential equation in the new variable instead avoids that subtlety, and is the route adopted here.

Several conventions keep the expressions compact. Throughout, H denotes the harmonic polylogarithms defined in Eq. (3.159) evaluated at υ, whose argument we suppress, whilst ζ_n stands for the Riemann zeta values. After partial fraction decomposition, all denominators are abbreviated as

$$\mathrm{d}_a = \frac{1}{a+\upsilon}, \qquad a \in \{\, -1, 0, 1 \,\} \,, \tag{5.1}$$

and coincide with the kernels of the harmonic polylogarithms. For the scale choice, we adopt $\mu^2 = -q^2$ as the common value of the renormalisation and factorisation scales. Under this choice the Mellin moments take the form given in Eqs. (5.2)–(5.19).

$$c^{2,(0,0)}_{2,\mathrm{g,vv}} = 0 \tag{5.2}$$

$$\begin{aligned} c^{2,(1,0)}_{2,\mathrm{g,vv}} = {} & -T_F \langle \mathrm{l}_{\{\,\mathrm{v,v}\,\}} \rangle^{\mathrm{g}} n_\mathrm{l} + T_F \langle \mathrm{h}_{\{\,\mathrm{v,v}\,\}} \rangle^{\mathrm{g}} n_\mathrm{h} \Big[-1 + 6\mathrm{d}_1 - 6\mathrm{d}_1^2 \\ & + \mathrm{H}_0 \Big(\frac{4}{3} - \frac{1}{2}\mathrm{d}_{-1} - \frac{37}{6}\mathrm{d}_1 + 9\mathrm{d}_1^2 - 6\mathrm{d}_1^3 \Big) \Big] \end{aligned} \tag{5.3}$$

$$c^{2,(2,0)}_{2,\mathrm{g,vv}} = C_A T_F \langle \mathrm{l}_{\{\,\mathrm{v,v}\,\}} \rangle^{\mathrm{g}} n_\mathrm{l} \Big(\frac{115}{162} - 4\zeta_3 \Big) + C_F T_F \langle \mathrm{l}_{\{\,\mathrm{v,v}\,\}} \rangle^{\mathrm{g}} n_\mathrm{l} \Big(-\frac{4799}{405} + \frac{32}{5}\zeta_3 \Big)$$

$$+ C_F T_F \langle \mathrm{h}_{\{\mathrm{v},\mathrm{v}\}} \rangle^{\mathrm{g}} n_{\mathrm{h}} \Big[\frac{371}{45} - \frac{29}{6}\upsilon - \frac{62}{45}\upsilon^2 - \frac{29}{6}\mathrm{d}_0 - \frac{62}{45}\mathrm{d}_0^2 + \frac{284}{15}\mathrm{d}_1 - \frac{284}{15}\mathrm{d}_1^2$$

$$+ \mathrm{H}_0 \Big(\frac{604}{45} - \frac{19}{5}\upsilon - \frac{62}{45}\upsilon^2 - \frac{98}{45}\mathrm{d}_{-1} + \frac{19}{5}\mathrm{d}_0 + \frac{62}{45}\mathrm{d}_0^2 - \frac{3778}{45}\mathrm{d}_1 - \frac{1648}{15}\mathrm{d}_1^3 \Big)$$

$$+ \mathrm{H}_{-1,0} \Big(- \frac{144}{5} + \frac{76}{45}\upsilon + \frac{176}{15}\upsilon^2 + \frac{124}{45}\upsilon^3 - \frac{64}{15}\mathrm{d}_{-1} - \frac{76}{45}\mathrm{d}_0 - \frac{176}{15}\mathrm{d}_0^2 - \frac{124}{45}\mathrm{d}_0^3$$

$$+ \frac{160}{3}\mathrm{d}_1 \Big)$$

$$+ \mathrm{H}_{0,0} \Big(\frac{1784}{45} - \frac{38}{15}\upsilon - \frac{88}{5}\upsilon^2 - \frac{62}{15}\upsilon^3 + \frac{434}{45}\mathrm{d}_{-1} + \frac{58}{9}\mathrm{d}_{-1}^2 + \frac{98}{9}\mathrm{d}_1 - \frac{10474}{45}\mathrm{d}_1^2$$

$$+ \frac{5456}{15}\mathrm{d}_1^3 - \frac{2728}{15}\mathrm{d}_1^4 \Big)$$

$$+ \mathrm{H}_{1,0} \Big(\frac{72}{5} - \frac{38}{45}\upsilon - \frac{88}{15}\upsilon^2 - \frac{62}{45}\upsilon^3 + \frac{32}{15}\mathrm{d}_{-1} + \frac{38}{45}\mathrm{d}_0 + \frac{88}{15}\mathrm{d}_0^2 + \frac{62}{45}\mathrm{d}_0^3 - \frac{80}{3}\mathrm{d}_1 \Big)$$

$$+ \mathrm{H}_{-1,0,0} \Big(- \frac{128}{15} - \frac{64}{15}\mathrm{d}_{-1} - \frac{64}{15}\mathrm{d}_{-1}^2 \Big)$$

$$+ \mathrm{H}_{0,-1,0} \Big(\frac{128}{15} + \frac{64}{15}\mathrm{d}_{-1} + \frac{64}{15}\mathrm{d}_{-1}^2 \Big)$$

$$+ \mathrm{H}_{0,1,0} \Big(- \frac{64}{15} - \frac{32}{15}\mathrm{d}_{-1} - \frac{32}{15}\mathrm{d}_{-1}^2 \Big)$$

$$+ \mathrm{H}_{1,0,0} \Big(\frac{64}{15} + \frac{32}{15}\mathrm{d}_{-1} + \frac{32}{15}\mathrm{d}_{-1}^2 \Big)$$

$$+ \zeta_3 \Big(\frac{32}{5} + \frac{16}{5}\mathrm{d}_{-1} + \frac{16}{5}\mathrm{d}_{-1}^2 \Big) \Big]$$

$$+ C_A T_F \langle \mathrm{h}_{\{\mathrm{v},\mathrm{v}\}} \rangle^{\mathrm{g}} n_{\mathrm{h}} \Big[\frac{547}{90} - \frac{353}{90}\upsilon - \frac{58}{45}\upsilon^2 - \frac{353}{90}\mathrm{d}_0 - \frac{58}{45}\mathrm{d}_0^2 - \frac{121}{15}\mathrm{d}_1 + \frac{121}{15}\mathrm{d}_1^2$$

$$+ \mathrm{H}_0 \Big(\frac{2626}{135} - \frac{133}{45}\upsilon - \frac{58}{45}\upsilon^2 + \frac{481}{180}\mathrm{d}_{-1} + \frac{133}{45}\mathrm{d}_0 + \frac{58}{45}\mathrm{d}_0^2 - \frac{37619}{540}\mathrm{d}_1 + \frac{783}{10}\mathrm{d}_1^2$$

$$- \frac{563}{15}\mathrm{d}_1^3 \Big)$$

$$+ \mathrm{H}_1 \Big(\frac{22}{3} - 44\mathrm{d}_1 + 44\mathrm{d}_1^2 \Big)$$

$$+ \mathrm{H}_{-1,0} \Big(\frac{248}{45} - \frac{236}{45}\upsilon + \frac{88}{9}\upsilon^2 + \frac{116}{45}\upsilon^3 + \frac{142}{15}\mathrm{d}_{-1} + \frac{236}{45}\mathrm{d}_0 - \frac{88}{9}\mathrm{d}_0^2 - \frac{116}{45}\mathrm{d}_0^3$$

$$+ \frac{238}{9}\mathrm{d}_1 - 84\mathrm{d}_1^2 + 56\mathrm{d}_1^3 \Big)$$

$$+ \mathrm{H}_{0,0} \Big(- \frac{344}{15} + \frac{118}{15}\upsilon - \frac{44}{3}\upsilon^2 - \frac{58}{15}\upsilon^3 - \frac{449}{90}\mathrm{d}_{-1} - \frac{14}{9}\mathrm{d}_{-1}^2 + \frac{1553}{90}\mathrm{d}_1 + \frac{389}{15}\mathrm{d}_1^2$$

$$- \frac{198}{5}\mathrm{d}_1^3 + \frac{104}{5}\mathrm{d}_1^4 \Big)$$

$$+ \mathrm{H}_{0,1} \Big(- \frac{88}{9} + \frac{11}{3}\mathrm{d}_{-1} + \frac{407}{9}\mathrm{d}_1 - 66\mathrm{d}_1^2 + 44\mathrm{d}_1^3 \Big)$$

$$+ \mathrm{H}_{1,0} \Big(- \frac{188}{15} + \frac{118}{45}\upsilon - \frac{44}{9}\upsilon^2 - \frac{58}{45}\upsilon^3 - \frac{16}{15}\mathrm{d}_{-1} - \frac{118}{45}\mathrm{d}_0 + \frac{44}{9}\mathrm{d}_0^2 + \frac{58}{45}\mathrm{d}_0^3$$

$$+ 32\mathrm{d}_1 - 24\mathrm{d}_1^2 + 16\mathrm{d}_1^3 \Big)$$

$$
\begin{aligned}
&+ \mathrm{H}_{-1,0,0}\Big(\frac{16}{3} + \frac{32}{15}\mathrm{d}_{-1} + \frac{32}{15}\mathrm{d}_{-1}^2\Big) \\
&+ \mathrm{H}_{0,-1,0}\Big(-\frac{16}{3} - \frac{32}{15}\mathrm{d}_{-1} - \frac{32}{15}\mathrm{d}_{-1}^2\Big) \\
&+ \mathrm{H}_{0,1,0}\Big(\frac{8}{3} + \frac{16}{15}\mathrm{d}_{-1} + \frac{16}{15}\mathrm{d}_{-1}^2\Big) \\
&+ \mathrm{H}_{1,0,0}\Big(-\frac{8}{3} - \frac{16}{15}\mathrm{d}_{-1} - \frac{16}{15}\mathrm{d}_{-1}^2\Big) \\
&+ \zeta_3\Big(-4 - \frac{8}{5}\mathrm{d}_{-1} - \frac{8}{5}\mathrm{d}_{-1}^2\Big)\Big]
\end{aligned} \tag{5.4}
$$

$$
c_{L,\mathrm{g,vv}}^{2,(0,0)} = 0 \tag{5.5}
$$

$$
\begin{aligned}
c_{L,\mathrm{g,vv}}^{2,(1,0)} = &\frac{4}{3}T_F\langle \mathrm{l}_{\{\mathrm{v,v}\}}\rangle^{\mathrm{g}} n_\mathrm{l} T_F\langle \mathrm{h}_{\{\mathrm{v,v}\}}\rangle^{\mathrm{g}} n_\mathrm{h}\Big[\frac{4}{3} + \frac{20}{3}\mathrm{d}_1 - \frac{44}{3}\mathrm{d}_1^2 + 16\mathrm{d}_1^3 - 8\mathrm{d}_1^4 \\
&+ \mathrm{H}_0\Big(-\frac{5}{2}\mathrm{d}_{-1} - \frac{11}{2}\mathrm{d}_1 + 13\mathrm{d}_1^2 - 22\mathrm{d}_1^3 + 20\mathrm{d}_1^4 - 8\mathrm{d}_1^5\Big)\Big]
\end{aligned} \tag{5.6}
$$

$$
\begin{aligned}
c_{L,\mathrm{g,vv}}^{2,(2,0)} = &\frac{346}{27}C_A T_F\langle \mathrm{l}_{\{\mathrm{v,v}\}}\rangle^{\mathrm{g}} n_\mathrm{l} + C_F T_F\langle \mathrm{l}_{\{\mathrm{v,v}\}}\rangle^{\mathrm{g}} n_\mathrm{l}\Big[-\frac{232}{135} - \frac{32}{5}\zeta_3\Big] \\
&+ C_A T_F\langle \mathrm{h}_{\{\mathrm{v,v}\}}\rangle^{\mathrm{g}} n_\mathrm{h}\Big[\frac{12412}{135} - \frac{229}{5}\upsilon + \frac{116}{15}\upsilon^2 - \frac{229}{5}\mathrm{d}_0 + \frac{116}{15}\mathrm{d}_0^2 - \frac{8506}{135}\mathrm{d}_1 \\
&+ \frac{10726}{135}\mathrm{d}_1^2 - \frac{296}{9}\mathrm{d}_1^3 + \frac{148}{9}\mathrm{d}_1^4 \\
&+ \mathrm{H}_0\Big(\frac{1516}{15} - \frac{258}{5}\upsilon + \frac{116}{15}\upsilon^2 - \frac{1027}{60}\mathrm{d}_{-1} + \frac{258}{5}\mathrm{d}_0 - \frac{116}{15}\mathrm{d}_0^2 - \frac{47927}{180}\mathrm{d}_1 \\
&+ \frac{12473}{90}\mathrm{d}_1^2 - \frac{12151}{45}\mathrm{d}_1^3 + \frac{2354}{9}\mathrm{d}_1^4 - \frac{836}{9}\mathrm{d}_1^5\Big) \\
&+ \mathrm{H}_1\Big(-\frac{88}{9} - \frac{440}{9}\mathrm{d}_1 + \frac{968}{9}\mathrm{d}_1^2 - \frac{352}{3}\mathrm{d}_1^3 + \frac{176}{3}\mathrm{d}_1^4\Big) \\
&+ \mathrm{H}_{-1,0}\Big(\frac{1664}{15} - \frac{1448}{15}\upsilon + 80\upsilon^2 - \frac{232}{15}\upsilon^3 + \frac{358}{15}\mathrm{d}_{-1} + \frac{1448}{15}\mathrm{d}_0 - 80\mathrm{d}_0^2 + \frac{232}{15}\mathrm{d}_0^3 \\
&- 154\mathrm{d}_1 - \frac{572}{3}\mathrm{d}_1^2 + \frac{968}{3}\mathrm{d}_1^3 - \frac{880}{3}\mathrm{d}_1^4 + \frac{352}{3}\mathrm{d}_1^5\Big) \\
&+ \mathrm{H}_{0,0}\Big(-\frac{832}{5} + \frac{724}{5}\upsilon - 120\upsilon^2 + \frac{116}{5}\upsilon^3 + \frac{163}{30}\mathrm{d}_{-1} + 5\mathrm{d}_{-1}^2 + \frac{4349}{30}\mathrm{d}_1 + \frac{1186}{15}\mathrm{d}_1^2 \\
&- \frac{2066}{15}\mathrm{d}_1^3 + \frac{2128}{15}\mathrm{d}_1^4 - \frac{232}{3}\mathrm{d}_1^5 + 16\mathrm{d}_1^6\Big) \\
&+ \mathrm{H}_{0,1}\Big(\frac{55}{3}\mathrm{d}_{-1} + \frac{121}{3}\mathrm{d}_1 - \frac{286}{3}\mathrm{d}_1^2 + \frac{484}{3}\mathrm{d}_1^3 - \frac{440}{3}\mathrm{d}_1^4 + \frac{176}{3}\mathrm{d}_1^5\Big) \\
&+ \mathrm{H}_{1,0}\Big(-\frac{832}{15} + \frac{724}{15}\upsilon - 40\upsilon^2 + \frac{116}{15}\upsilon^3 + \frac{32}{5}\mathrm{d}_{-1} - \frac{724}{15}\mathrm{d}_0 + 40\mathrm{d}_0^2 - \frac{116}{15}\mathrm{d}_0^3 \\
&+ \frac{352}{3}\mathrm{d}_1\Big) \\
&+ \mathrm{H}_{-1,0,0}\Big(-\frac{64}{5}\mathrm{d}_{-1} - \frac{64}{5}\mathrm{d}_{-1}^2\Big) \\
&+ \mathrm{H}_{0,-1,0}\Big(\frac{64}{5}\mathrm{d}_{-1} + \frac{64}{5}\mathrm{d}_{-1}^2\Big)
\end{aligned}
$$

$$
\begin{aligned}
&+ \mathrm{H}_{0,1,0}\Big(-\frac{32}{5}\mathrm{d}_{-1} - \frac{32}{5}\mathrm{d}_{-1}^2\Big)\\
&+ \mathrm{H}_{1,0,0}\Big(\frac{32}{5}\mathrm{d}_{-1} + \frac{32}{5}\mathrm{d}_{-1}^2\Big)\\
&+ \zeta_3\Big(\frac{48}{5}\mathrm{d}_{-1} + \frac{48}{5}\mathrm{d}_{-1}^2\Big)\Big]\\
+ C_F T_F \langle \mathrm{h}_{\{\mathrm{v,v}\}}\rangle^{\mathrm{g}} n_{\mathrm{h}} &\Big[\frac{1238}{15} - \frac{161}{3}\upsilon + \frac{124}{15}\upsilon^2 - \frac{161}{3}\mathrm{d}_0 + \frac{124}{15}\mathrm{d}_0^2 + \frac{376}{15}\mathrm{d}_1 - \frac{232}{5}\mathrm{d}_1^2\\
&+ \frac{128}{3}\mathrm{d}_1^3 - \frac{64}{3}\mathrm{d}_1^4\\
&+ \mathrm{H}_0\Big(\frac{1852}{15} - \frac{898}{15}\upsilon + \frac{124}{15}\upsilon^2 + \frac{196}{15}\mathrm{d}_{-1} + \frac{898}{15}\mathrm{d}_0 - \frac{124}{15}\mathrm{d}_0^2 - \frac{1348}{5}\mathrm{d}_1 + \frac{2888}{15}\mathrm{d}_1^2\\
&- \frac{2064}{5}\mathrm{d}_1^3 + \frac{1280}{3}\mathrm{d}_1^4 - \frac{512}{3}\mathrm{d}_1^5\Big)\\
&+ \mathrm{H}_{-1,0}\Big(\frac{384}{5} - \frac{1432}{15}\upsilon + \frac{1424}{15}\upsilon^2 - \frac{248}{15}\upsilon^3 + \frac{128}{5}\mathrm{d}_{-1} + \frac{1432}{15}\mathrm{d}_0 - \frac{1424}{15}\mathrm{d}_0^2\\
&+ \frac{248}{15}\mathrm{d}_0^3 - \frac{448}{3}\mathrm{d}_1 + 64\mathrm{d}_1^2 - \frac{128}{3}\mathrm{d}_1^3\Big)\\
&+ \mathrm{H}_{0,0}\Big(-\frac{576}{5} + \frac{716}{5}\upsilon - \frac{712}{5}\upsilon^2 + \frac{124}{5}\upsilon^3 - \frac{868}{15}\mathrm{d}_{-1} - \frac{116}{3}\mathrm{d}_{-1}^2 + \frac{508}{3}\mathrm{d}_1\\
&- \frac{1684}{5}\mathrm{d}_1^2 + \frac{3968}{5}\mathrm{d}_1^3 - \frac{16912}{15}\mathrm{d}_1^4 + 896\mathrm{d}_1^5 - \frac{896}{3}\mathrm{d}_1^6\Big)\\
&+ \mathrm{H}_{1,0}\Big(-\frac{192}{5} + \frac{716}{15}\upsilon - \frac{712}{15}\upsilon^2 + \frac{124}{15}\upsilon^3 - \frac{64}{5}\mathrm{d}_{-1} - \frac{716}{15}\mathrm{d}_0 + \frac{712}{15}\mathrm{d}_0^2\\
&- \frac{124}{15}\mathrm{d}_0^3 + \frac{224}{3}\mathrm{d}_1 - 32\mathrm{d}_1^2 + \frac{64}{3}\mathrm{d}_1^3\Big)\\
&+ \mathrm{H}_{-1,0,0}\Big(\frac{128}{15} + \frac{128}{5}\mathrm{d}_{-1} + \frac{128}{5}\mathrm{d}_{-1}^2\Big)\\
&+ \mathrm{H}_{0,-1,0}\Big(-\frac{128}{15} - \frac{128}{5}\mathrm{d}_{-1} - \frac{128}{5}\mathrm{d}_{-1}^2\Big)\\
&+ \mathrm{H}_{0,1,0}\Big(\frac{64}{15} + \frac{64}{5}\mathrm{d}_{-1} + \frac{64}{5}\mathrm{d}_{-1}^2\Big)\\
&+ \mathrm{H}_{1,0,0}\Big(-\frac{64}{15} - \frac{64}{5}\mathrm{d}_{-1} - \frac{64}{5}\mathrm{d}_{-1}^2\Big)\\
&+ \zeta_3\Big(-\frac{32}{5} - \frac{96}{5}\mathrm{d}_{-1} - \frac{96}{5}\mathrm{d}_{-1}^2\Big)\Big]
\end{aligned} \tag{5.7}
$$

$$
c_{2,\mathrm{q,vv}}^{2,(0,0)} = \langle \bar{\mathrm{l}}_{\{\mathrm{v,v}\}}\rangle^{\mathrm{q}} \tag{5.8}
$$

$$
c_{2,\mathrm{q,vv}}^{2,(1,0)} = \frac{1}{3}C_F\langle \bar{\mathrm{l}}_{\{\mathrm{v,v}\}}\rangle^{\mathrm{q}} \tag{5.9}
$$

$$
\begin{aligned}
c_{2,\mathrm{q,vv}}^{2,(2,0)} = & -8C_F T_F\langle \bar{\mathrm{l}}_{\{\mathrm{v,v}\}}\rangle^{\mathrm{q}} n_{\mathrm{l}} - \frac{266}{81}C_F T_F\langle \mathrm{l}_{\{\mathrm{v,v}\}}\rangle^{\mathrm{q}} n_{\mathrm{l}} + C_A C_F\langle \bar{\mathrm{l}}_{\{\mathrm{v,v}\}}\rangle^{\mathrm{q}}\Big[\frac{3677}{135} - \frac{128}{5}\zeta_3\Big]\\
&+ C_F^2\langle \bar{\mathrm{l}}_{\{\mathrm{v,v}\}}\rangle^{\mathrm{q}}\Big[-\frac{4189}{810} + \frac{96}{5}\zeta_3\Big]\\
&+ C_F T_F\langle \bar{\mathrm{l}}_{\{\mathrm{v,v}\}}\rangle^{\mathrm{q}} n_{\mathrm{h}}\Big[-\frac{509317}{42525} - \frac{26}{2025}\upsilon - \frac{16}{14175}\upsilon^2 + \frac{6484}{2835}\mathrm{d}_{-1} + \frac{6484}{2835}\mathrm{d}_{-1}^2
\end{aligned}
$$

$$
\begin{aligned}
&\quad - \frac{26}{2025}\mathrm{d}_0 - \frac{16}{14175}\mathrm{d}_0^2 \\
&\quad + \mathrm{H}_0\Big(\frac{18992}{2835} - \frac{104}{135}\upsilon + \frac{58}{4725}\upsilon^2 + \frac{16}{14175}\upsilon^3 + \frac{1576}{135}\mathrm{d}_{-1} - \frac{596}{945}\mathrm{d}_{-1}^2 - \frac{1192}{2835}\mathrm{d}_{-1}^3\Big) \\
&\quad + \mathrm{H}_1\Big(\frac{4292}{2835} - \frac{104}{135}\upsilon + \frac{58}{4725}\upsilon^2 + \frac{16}{14175}\upsilon^3 - \frac{104}{135}\mathrm{d}_0 + \frac{58}{4725}\mathrm{d}_0^2 + \frac{16}{14175}\mathrm{d}_0^3\Big) \\
&\quad + \mathrm{H}_{0,0}\Big(- \frac{32}{9} - \frac{56}{15}\mathrm{d}_{-1}^2 - \frac{112}{15}\mathrm{d}_{-1}^3 - \frac{56}{15}\mathrm{d}_{-1}^4\Big)\Big] \\
&+ C_F T_F \langle \mathrm{h}_{\{\,\mathrm{v,v}\,\}}\rangle^{\mathrm{q}} n_{\mathrm{h}}\Big[- \frac{266}{45} - \frac{38}{45}\upsilon - \frac{56}{45}\upsilon^2 - \frac{38}{45}\mathrm{d}_0 - \frac{56}{45}\mathrm{d}_0^2 + \frac{176}{3}\mathrm{d}_1 - \frac{176}{3}\mathrm{d}_1^2 \\
&\quad + \mathrm{H}_0\Big(\frac{8}{135} + \frac{4}{45}\upsilon - \frac{56}{45}\upsilon^2 - \frac{82}{45}\mathrm{d}_{-1} - \frac{4}{45}\mathrm{d}_0 + \frac{56}{45}\mathrm{d}_0^2 + \frac{1538}{135}\mathrm{d}_1 - 24\mathrm{d}_1^2 + \frac{16}{3}\mathrm{d}_1^3\Big) \\
&\quad + \mathrm{H}_1\Big(- \frac{16}{3} + 32\mathrm{d}_1 - 32\mathrm{d}_1^2\Big) \\
&\quad + \mathrm{H}_{-1,0}\Big(\frac{128}{9} - \frac{16}{45}\upsilon + \frac{32}{9}\upsilon^2 + \frac{112}{45}\upsilon^3 - \frac{16}{3}\mathrm{d}_{-1} + \frac{16}{45}\mathrm{d}_0 - \frac{32}{9}\mathrm{d}_0^2 - \frac{112}{45}\mathrm{d}_0^3 \\
&\quad - \frac{592}{9}\mathrm{d}_1 + 96\mathrm{d}_1^2 - 64\mathrm{d}_1^3\Big) \\
&\quad + \mathrm{H}_{0,0}\Big(- \frac{32}{3} + \frac{8}{15}\upsilon - \frac{16}{3}\upsilon^2 - \frac{56}{15}\upsilon^3 + \frac{52}{45}\mathrm{d}_{-1} - \frac{8}{45}\mathrm{d}_{-1}^2 + \frac{2324}{45}\mathrm{d}_1 \\
&\quad - \frac{296}{5}\mathrm{d}_1^2 + 16\mathrm{d}_1^3\Big) \\
&\quad + \mathrm{H}_{0,1}\Big(\frac{64}{9} - \frac{8}{3}\mathrm{d}_{-1} - \frac{296}{9}\mathrm{d}_1 + 48\mathrm{d}_1^2 - 32\mathrm{d}_1^3\Big) \\
&\quad + \mathrm{H}_{1,0}\Big(\frac{8}{45}\upsilon - \frac{16}{9}\upsilon^2 - \frac{56}{45}\upsilon^3 - \frac{8}{45}\mathrm{d}_0 + \frac{16}{9}\mathrm{d}_0^2 + \frac{56}{45}\mathrm{d}_0^3\Big)\Big] \qquad (5.10)
\end{aligned}
$$

$$
c_{L,\mathrm{q,vv}}^{2,(0,0)} = 0 \qquad (5.11)
$$

$$
c_{L,\mathrm{q,vv}}^{2,(1,0)} = \frac{4}{3} C_F \langle \bar{\mathrm{l}}_{\{\,\mathrm{v,v}\,\}}\rangle^{\mathrm{q}} \qquad (5.12)
$$

$$
\begin{aligned}
c_{L,\mathrm{q,vv}}^{2,(2,0)} &= - \frac{184}{27} C_F T_F \langle \bar{\mathrm{l}}_{\{\,\mathrm{v,v}\,\}}\rangle^{\mathrm{q}} n_{\mathrm{l}} - \frac{160}{27} C_F T_F \langle \mathrm{l}_{\{\,\mathrm{v,v}\,\}}\rangle^{\mathrm{q}} n_{\mathrm{l}} + C_F^2 \langle \bar{\mathrm{l}}_{\{\,\mathrm{v,v}\,\}}\rangle^{\mathrm{q}}\Big[- \frac{1906}{135} + \frac{64}{5}\zeta_3\Big] \\
&+ C_A C_F \langle \bar{\mathrm{l}}_{\{\,\mathrm{v,v}\,\}}\rangle^{\mathrm{q}}\Big[\frac{2878}{135} - \frac{32}{5}\zeta_3\Big] \\
&+ C_F T_F \langle \bar{\mathrm{l}}_{\{\,\mathrm{v,v}\,\}}\rangle^{\mathrm{q}} n_{\mathrm{h}}\Big[- \frac{95416}{14175} - \frac{176}{4725}\upsilon + \frac{32}{4725}\upsilon^2 - \frac{10208}{135}\mathrm{d}_{-1} - \frac{10208}{135}\mathrm{d}_{-1}^2 \\
&\quad - \frac{176}{4725}\mathrm{d}_0 + \frac{32}{4725}\mathrm{d}_0^2 \\
&\quad + \mathrm{H}_0\Big(\frac{1808}{945} - \frac{32}{315}\upsilon + \frac{64}{1575}\upsilon^2 - \frac{32}{4725}\upsilon^3 + \frac{10048}{315}\mathrm{d}_{-1} + \frac{3808}{45}\mathrm{d}_{-1}^2 + \frac{7616}{135}\mathrm{d}_{-1}^3\Big) \\
&\quad + \mathrm{H}_1\Big(\frac{128}{945} - \frac{32}{315}\upsilon + \frac{64}{1575}\upsilon^2 - \frac{32}{4725}\upsilon^3 - \frac{32}{315}\mathrm{d}_0 + \frac{64}{1575}\mathrm{d}_0^2 - \frac{32}{4725}\mathrm{d}_0^3\Big) \\
&\quad + \mathrm{H}_{0,0}\Big(\frac{192}{5}\mathrm{d}_{-1}^2 + \frac{384}{5}\mathrm{d}_{-1}^3 + \frac{192}{5}\mathrm{d}_{-1}^4\Big)\Big] \\
&+ C_F T_F \langle \mathrm{h}_{\{\,\mathrm{v,v}\,\}}\rangle^{\mathrm{q}} n_{\mathrm{h}}\Big[\frac{8168}{135} - \frac{188}{5}\upsilon + \frac{112}{15}\upsilon^2 - \frac{188}{5}\mathrm{d}_0 + \frac{112}{15}\mathrm{d}_0^2 + \frac{1088}{27}\mathrm{d}_1
\end{aligned}
$$

$$
\begin{aligned}
& - \frac{2864}{27}\mathrm{d}_1^2 + \frac{1184}{9}\mathrm{d}_1^3 - \frac{592}{9}\mathrm{d}_1^4 \\
& + \mathrm{H}_0\Big(\frac{496}{5} - \frac{216}{5}\upsilon + \frac{112}{15}\upsilon^2 + \frac{33}{5}\mathrm{d}_{-1} + \frac{216}{5}\mathrm{d}_0 - \frac{112}{15}\mathrm{d}_0^2 - \frac{7201}{45}\mathrm{d}_1 - \frac{626}{9}\mathrm{d}_1^2 \\
& + \frac{860}{9}\mathrm{d}_1^3 - \frac{632}{9}\mathrm{d}_1^4 + \frac{176}{9}\mathrm{d}_1^5\Big) \\
& + \mathrm{H}_1\Big(\frac{64}{9} + \frac{320}{9}\mathrm{d}_1 - \frac{704}{9}\mathrm{d}_1^2 + \frac{256}{3}\mathrm{d}_1^3 - \frac{128}{3}\mathrm{d}_1^4\Big) \\
& + \mathrm{H}_{-1,0}\Big(\frac{256}{3} - \frac{416}{5}\upsilon + 64\upsilon^2 - \frac{224}{15}\upsilon^3 - \frac{80}{3}\mathrm{d}_{-1} + \frac{416}{5}\mathrm{d}_0 - 64\mathrm{d}_0^2 + \frac{224}{15}\mathrm{d}_0^3 \\
& - \frac{688}{3}\mathrm{d}_1 + \frac{416}{3}\mathrm{d}_1^2 - \frac{704}{3}\mathrm{d}_1^3 + \frac{640}{3}\mathrm{d}_1^4 - \frac{256}{3}\mathrm{d}_1^5\Big) \\
& + \mathrm{H}_{0,0}\Big(- 128 + \frac{624}{5}\upsilon - 96\upsilon^2 + \frac{112}{5}\upsilon^3 + \frac{116}{15}\mathrm{d}_{-1} + \frac{16}{15}\mathrm{d}_{-1}^2 + \frac{2812}{15}\mathrm{d}_1 - \frac{1832}{15}\mathrm{d}_1^2 \\
& + 144\mathrm{d}_1^3 - 96\mathrm{d}_1^4 + \frac{64}{3}\mathrm{d}_1^5\Big) \\
& + \mathrm{H}_{0,1}\Big(- (\frac{40}{3}\mathrm{d}_{-1}) - \frac{88}{3}\mathrm{d}_1 + \frac{208}{3}\mathrm{d}_1^2 - \frac{352}{3}\mathrm{d}_1^3 + \frac{320}{3}\mathrm{d}_1^4 - \frac{128}{3}\mathrm{d}_1^5\Big) \\
& + \mathrm{H}_{1,0}\Big(- \frac{128}{3} + \frac{208}{5}\upsilon - 32\upsilon^2 + \frac{112}{15}\upsilon^3 - \frac{208}{5}\mathrm{d}_0 + 32\mathrm{d}_0^2 - \frac{112}{15}\mathrm{d}_0^3 \\
& + \frac{256}{3}\mathrm{d}_1\Big)\Big]
\end{aligned} \tag{5.13}
$$

$$c_{2,a}^{2,(0,0)} = \langle \bar{\mathrm{l}}_{\{\,\mathrm{v},\mathrm{v}\,\}}\rangle^{\mathrm{q}} \tag{5.14}$$

$$c_{2,a}^{2,(1,0)} = \frac{1}{3}C_F\langle \bar{\mathrm{l}}_{\{\,\mathrm{v},\mathrm{v}\,\}}\rangle^{\mathrm{q}} \tag{5.15}$$

$$
\begin{aligned}
c_{2,a}^{2,(2,0)} = & -8C_F T_F\langle \bar{\mathrm{l}}_{\{\,\mathrm{v},\mathrm{v}\,\}}\rangle^{a} n_{\mathrm{l}} + C_A C_F\langle \bar{\mathrm{l}}_{\{\,\mathrm{v},\mathrm{v}\,\}}\rangle^{a}\Big(\frac{3677}{135} - \frac{128}{5}\zeta_3\Big) + C_F^2\langle \bar{\mathrm{l}}_{\{\,\mathrm{v},\mathrm{v}\,\}}\rangle^{\mathrm{q}}\Big[- \frac{4189}{810} \\
& + \frac{96}{5}\zeta_3\Big] \\
& + C_F T_F\langle \bar{\mathrm{l}}_{\{\,\mathrm{v},\mathrm{v}\,\}}\rangle^{a} n_{\mathrm{h}}\Big[- \frac{509317}{42525} - \frac{26}{2025}\upsilon - \frac{16}{14175}\upsilon^2 + \frac{6484}{2835}\mathrm{d}_{-1} + \frac{6484}{2835}\mathrm{d}_{-1}^2 \\
& - \frac{26}{2025}\mathrm{d}_0 - \frac{16}{14175}\mathrm{d}_0^2 \\
& + \mathrm{H}_0\Big(\frac{18992}{2835} - \frac{104}{135}\upsilon + \frac{58}{4725}\upsilon^2 + \frac{16}{14175}\upsilon^3 + \frac{1576}{135}\mathrm{d}_{-1} - \frac{596}{945}\mathrm{d}_{-1}^2 - \frac{1192}{2835}\mathrm{d}_{-1}^3\Big) \\
& + \mathrm{H}_1\Big(\frac{4292}{2835} - \frac{104}{135}\upsilon + \frac{58}{4725}\upsilon^2 + \frac{16}{14175}\upsilon^3 - \frac{104}{135}\mathrm{d}_0 + \frac{58}{4725}\mathrm{d}_0^2 + \frac{16}{14175}\mathrm{d}_0^3\Big) \\
& + \mathrm{H}_{0,0}\Big(- \frac{32}{9} - \frac{56}{15}\mathrm{d}_{-1}^2 - \frac{112}{15}\mathrm{d}_{-1}^3 - \frac{56}{15}\mathrm{d}_{-1}^4\Big)\Big]
\end{aligned} \tag{5.16}
$$

$$c_{L,a,\mathrm{vv}}^{2,(0,0)} = 0 \tag{5.17}$$

$$c_{L,a,\mathrm{vv}}^{2,(1,0)} = \frac{4}{3}C_F\langle \bar{\mathrm{l}}_{\{\,\mathrm{v},\mathrm{v}\,\}}\rangle^{a} \tag{5.18}$$

$$
\begin{aligned}
c_{L,a,\mathrm{vv}}^{2,(2,0)} = &-\frac{184}{27} C_F T_F \langle \bar{\mathrm{l}}_{\{\mathrm{v,v}\}}\rangle^a n_\mathrm{l} + C_F^2 \langle \bar{\mathrm{l}}_{\{\mathrm{v,v}\}}\rangle^a \Big[-\frac{1906}{135} + \frac{64}{5}\zeta_3 \Big] + C_A C_F \langle \bar{\mathrm{l}}_{\{\mathrm{v,v}\}}\rangle^\mathrm{q} \Big[\frac{2878}{135} \\
&\quad - \frac{32}{5}\zeta_3 \Big] \\
&+ C_F T_F \langle \bar{\mathrm{l}}_{\{\mathrm{v,v}\}}\rangle^a n_\mathrm{h} \Big[-\frac{95416}{14175} - \frac{176}{4725}\upsilon + \frac{32}{4725}\upsilon^2 - \frac{10208}{135}\mathrm{d}_{-1} - \frac{10208}{135}\mathrm{d}_{-1}^2 \\
&\quad - \frac{176}{4725}\mathrm{d}_0 + \frac{32}{4725}\mathrm{d}_0^2 \\
&\quad + \mathrm{H}_0 \Big(\frac{1808}{945} - \frac{32}{315}\upsilon + \frac{64}{1575}\upsilon^2 - \frac{32}{4725}\upsilon^3 + \frac{10048}{315}\mathrm{d}_{-1} + \frac{3808}{45}\mathrm{d}_{-1}^2 + \frac{7616}{135}\mathrm{d}_{-1}^3 \Big) \\
&\quad + \mathrm{H}_1 \Big(\frac{128}{945} - \frac{32}{315}\upsilon + \frac{64}{1575}\upsilon^2 - \frac{32}{4725}\upsilon^3 - \frac{32}{315}\mathrm{d}_0 + \frac{64}{1575}\mathrm{d}_0^2 - \frac{32}{4725}\mathrm{d}_0^3 \Big) \\
&\quad + \mathrm{H}_{0,0} \Big(\frac{192}{5}\mathrm{d}_{-1}^2 + \frac{384}{5}\mathrm{d}_{-1}^3 + \frac{192}{5}\mathrm{d}_{-1}^4 \Big) \Big]
\end{aligned}
\tag{5.19}
$$

5.1.2 Numerical Comparison

A non-trivial consistency check compares our results (denoted KMS in the following) with the semi-analytical results of Ref. [76] (RSvN) and Ref. [77] (LeProHQ). Both references parametrise the heavy-quark coefficient functions in terms of $\hat{z}$ and x_B. Since these parametrisations live in $\hat{z}$-space, any comparison with the present results first requires a numerical integration to recover a Mellin moment. That integration reaches around six significant figures here. Any residual deviation amongst the three sets may therefore be ascribed to the accuracy of the parametrisations rather than to the integration itself.

The numerical data are collected in Tab. 5.1. At LO the results agree exactly, whilst at NLO they display very good overall consistency with the semi-analytical parametrisations. In the gluon channel, where no independent analytic comparison is available, the agreement reaches the permille level, matching the accuracy quoted for those parametrisations.

Quark non-singlet contributions require additional care. Through the optical theorem, the forward amplitude includes vertex corrections with heavy quarks in the loops. These are encoded in the two-loop heavy-quark virtual contribution to the light-quark form factor $F_\mathrm{h}^{(2)}$, given in Eq. (5.20) and discussed for example in Refs. [78, 250]. Because it is proportional to $\delta(1-\hat{z})$, this contribution is constant in Mellin N-space. Such corrections are absent from the RSvN calculation, which retains only open heavy-quark lines in the final state, as appropriate for the charm- and bottom-quark structure functions. A meaningful comparison of the non-singlet coefficient-function moments with the RSvN results therefore requires this form factor to be subtracted twice. At NLO, the quantity compared with RSvN is

$$
c_{2,a,\mathrm{vv}}^{N,(2,0)}\Big|_{\mathrm{RSvN}} = c_{2,a,\mathrm{vv}}^{N,(2,0)}\Big|_{\mathrm{KMS}} - 2\,F_\mathrm{h}^{(2)}\,, \qquad \mu = Q\,.
\tag{5.20}
$$

Further subtractions are not necessary, since our calculation uses $a_{s,\mathrm{ren}}$ with n_l active flavours, where the heavy quark is decoupled, matching the renormalisation scheme of RSvN. For comparison, Ref. [78] employs $a_{s,\mathrm{ren}}$ with $n_\mathrm{l}+n_\mathrm{h}$ active flavours, so that the heavy quark is treated as active. In that scheme, additional contributions from heavy-quark self-energy insertions on external gluon lines must be subtracted, whereas the decoupled-flavour definition adopted here leaves them absent at NLO. The explicit form factor, taken from Ref. [78], is given in the notation of Subsec.1.3 as follows

$$F_{\mathrm{h}}^{(2)}(\xi) = 2C_F T_F n_{\mathrm{h}} \Bigg\{ \frac{3355}{81} - \frac{952}{9}\xi + \left(32\xi^2 - \frac{16}{3}\right)\zeta_3 - \left(\frac{440}{9}\xi - \frac{530}{27}\right)\ln(\xi) \\ + \beta\left(\frac{184}{9}\xi - \frac{76}{9}\right)\left(\mathrm{Li}_2\left(\frac{\beta+1}{\beta-1}\right) - \mathrm{Li}_2\left(\frac{\beta-1}{\beta+1}\right)\right) \\ + \left(\frac{8}{3} - 16\xi^2\right)\left(\mathrm{Li}_3\left(\frac{\beta-1}{\beta+1}\right) + \mathrm{Li}_3\left(\frac{\beta+1}{\beta-1}\right)\right)\Bigg\}. \tag{5.21}$$

For the non-singlet coefficient-function moments at NLO, KMS reproduces LeProHQ exactly, since these functions are implemented in analytical form. At the same order, the singlet moments from KMS and RSvN agree across both the gluon and quark channels. A comparison with LeProHQ, by contrast, exposes deviations of up to twenty percent for larger N in the quark channel.

Table 5.1: Comparison of the numerical values of the moments of the coefficient functions at LO and NLO for $m = 2\sqrt{2}\,\mathrm{GeV}$ and $Q = 7\,\mathrm{GeV}$, corresponding to $\xi = 8/49$, with the scale choice $\mu = Q$.

N	KMS	RSvN	LeProHQ	KMS/RSvN	KMS/LeProHQ
			$c_{L,\mathrm{g}}^{N,(1,0)}$		
2	$8.867283709e-02$	$8.8673e-02$	$8.8673e-02$	1.0000	1.0000
4	$1.103046457e-02$	$1.1030e-02$	$1.1030e-02$	1.0000	1.0000
6	$1.917444241e-03$	$1.9174e-03$	$1.9174e-03$	1.0000	1.0000
8	$3.966816131e-04$	$3.9668e-04$	$3.9668e-04$	1.0000	1.0000
10	$9.137167103e-05$	$9.1372e-05$	$9.1372e-05$	1.0000	1.0000
12	$2.264262570e-05$	$2.2643e-05$	$2.2643e-05$	1.0000	1.0000
14	$5.916619363e-06$	$5.9166e-06$	$5.9166e-06$	1.0000	1.0000
16	$1.609557695e-06$	$1.6096e-06$	$1.6096e-06$	1.0000	1.0000
18	$4.519332213e-07$	$4.5193e-07$	$4.5193e-07$	1.0000	1.0000
20	$1.301724905e-07$	$1.3017e-07$	$1.3017e-07$	1.0000	1.0000
22	$3.829032869e-08$	$3.8290e-08$	$3.8290e-08$	1.0000	1.0000
			$c_{2,\mathrm{g}}^{N,(1,0)}$		
2	$5.028907767e-01$	$5.0289e-01$	$5.0289e-01$	1.0000	1.0000
4	$6.175564320e-02$	$6.1756e-02$	$6.1756e-02$	1.0000	1.0000
6	$1.183561754e-02$	$1.1836e-02$	$1.1836e-02$	1.0000	1.0000
8	$2.731109006e-03$	$2.7311e-03$	$2.7311e-03$	1.0000	1.0000
10	$6.987846232e-04$	$6.9878e-04$	$6.9878e-04$	1.0000	1.0000
12	$1.909719930e-04$	$1.9097e-04$	$1.9097e-04$	1.0000	1.0000
14	$5.463077020e-05$	$5.4631e-05$	$5.4631e-05$	1.0000	1.0000
16	$1.616052219e-05$	$1.6161e-05$	$1.6161e-05$	1.0000	1.0000
18	$4.904449068e-06$	$4.9044e-06$	$4.9045e-06$	1.0000	1.0000
20	$1.518757609e-06$	$1.5188e-06$	$1.5188e-06$	1.0000	1.0000
22	$4.780440303e-07$	$4.7804e-07$	$4.7805e-07$	1.0000	1.0000
			$c_{L,\mathrm{g}}^{N,(2,0)}$		

Continued on next page

N	KMS	RSvN	LeProHQ	KMS/RSvN	KMS/LeProHQ
2	3.378659570e + 00	3.4037e + 00	3.3799e + 00	0.9926	0.9996
4	7.289865120e − 01	7.3158e − 01	7.2948e − 01	0.9965	0.9993
6	1.676777828e − 01	1.6809e − 01	1.6786e − 01	0.9976	0.9989
8	4.148549496e − 02	4.1576e − 02	4.1548e − 02	0.9978	0.9985
10	1.087276123e − 02	1.0897e − 02	1.0895e − 02	0.9977	0.9980
12	2.977571974e − 03	2.9849e − 03	2.9852e − 03	0.9975	0.9974
14	8.436717814e − 04	8.4599e − 04	8.4636e − 04	0.9973	0.9968
16	2.455922015e − 04	2.4633e − 04	2.4652e − 04	0.9970	0.9962
18	7.307379587e − 05	7.3315e − 05	7.3396e − 05	0.9967	0.9956
20	2.213903270e − 05	2.2218e − 05	2.2260e − 05	0.9965	0.9946
22	6.809936693e − 06	6.8358e − 06	6.8402e − 06	0.9962	0.9956
		$c_{2,\mathrm{g}}^{N,(2,0)}$			
2	1.606527957e + 01	1.6121e + 01	1.6047e + 01	0.9966	1.0011
4	3.680483878e + 00	3.6872e + 00	3.6743e + 00	0.9982	1.0017
6	9.457069517e − 01	9.4677e − 01	9.4356e − 01	0.9989	1.0023
8	2.623839998e − 01	2.6259e − 01	2.6164e − 01	0.9992	1.0029
10	7.663126763e − 02	7.6681e − 02	7.6370e − 02	0.9993	1.0034
12	2.319720217e − 02	2.3211e − 02	2.3106e − 02	0.9994	1.0039
14	7.208613114e − 03	7.2126e − 03	7.1769e − 03	0.9994	1.0044
16	2.285220881e − 03	2.2865e − 03	2.2742e − 03	0.9995	1.0049
18	7.358664768e − 04	7.3627e − 04	7.3200e − 04	0.9995	1.0053
20	2.399582635e − 04	2.4009e − 04	2.3860e − 04	0.9995	1.0057
22	7.906076590e − 05	7.9104e − 05	7.8587e − 05	0.9994	1.0060
		$c_{L,\mathrm{q}}^{N,(2,0)}$			
2	−2.663968441e − 01	−2.6599e − 01	−2.6379e − 01	1.0015	1.0099
4	−2.291865727e − 02	−2.2898e − 02	−2.2309e − 02	1.0009	1.0273
6	−3.037959700e − 03	−3.0392e − 03	−2.8930e − 03	0.9996	1.0501
8	−5.184054510e − 04	−5.1947e − 04	−4.8333e − 04	0.9980	1.0726
10	−1.027971471e − 04	−1.0318e − 04	−9.4155e − 05	0.9963	1.0918
12	−2.252325062e − 05	−2.2641e − 05	−2.0354e − 05	0.9948	1.1066
14	−5.299818794e − 06	−5.3350e − 06	−4.7487e − 06	0.9934	1.1161
16	−1.315786777e − 06	−1.3262e − 06	−1.1719e − 06	0.9921	1.1228
18	−3.406331187e − 07	−3.4374e − 07	−3.0241e − 07	0.9910	1.1264
20	−9.119679388e − 08	−9.2130e − 08	−8.1052e − 08	0.9899	1.1252
22	−2.509868611e − 08	−2.5381e − 08	−2.2298e − 08	0.9889	1.1256
		$c_{2,\mathrm{q}}^{N,(2,0)}$			
2	−1.819031902e + 00	−1.8187e + 00	−1.7819e + 00	1.0002	1.0208
4	−1.440499763e − 01	−1.4401e − 01	−1.3525e − 01	1.0002	1.0651
6	−2.040592390e − 02	−2.0418e − 02	−1.8276e − 02	0.9994	1.1166
8	−3.811432361e − 03	−3.8175e − 03	−3.2852e − 03	0.9984	1.1602
10	−8.290910647e − 04	−8.3117e − 04	−6.9627e − 04	0.9975	1.1908
12	−1.985751721e − 04	−1.9923e − 04	−1.6434e − 04	0.9967	1.2083
14	−5.082020292e − 05	−5.1024e − 05	−4.1804e − 05	0.9960	1.2157
16	−1.365120445e − 05	−1.3714e − 05	−1.1227e − 05	0.9954	1.2159
18	−3.804753682e − 06	−3.8243e − 06	−3.1416e − 06	0.9949	1.2111
20	−1.091674299e − 06	−1.0978e − 06	−9.0873e − 07	0.9944	1.2013
22	−3.206582357e − 07	−3.2258e − 07	−2.6837e − 07	0.9940	1.1948
		$c_{L,a}^{N,(2,0)}$			
2	1.269706065e − 01	1.2691e − 01	1.2697e − 01	1.0004	1.0000

Continued on next page

N	KMS	RSvN	LeProHQ	KMS/RSvN	KMS/LeProHQ
4	$7.773989042e-03$	$7.7697e-03$	$7.7740e-03$	1.0006	1.0000
6	$8.451385732e-04$	$8.4611e-04$	$8.4514e-04$	0.9989	1.0000
8	$1.218724089e-04$	$1.2232e-04$	$1.2187e-04$	0.9964	1.0000
10	$2.086984108e-05$	$2.1002e-05$	$2.0870e-05$	0.9937	1.0000
12	$4.015640039e-06$	$4.0518e-06$	$4.0156e-06$	0.9911	1.0000
14	$8.409051715e-07$	$8.5059e-07$	$8.4091e-07$	0.9886	1.0000
16	$1.878096423e-07$	$1.9041e-07$	$1.8781e-07$	0.9863	1.0000
18	$4.413049803e-08$	$4.4839e-08$	$4.4130e-08$	0.9842	1.0000
20	$1.080458841e-08$	$1.1000e-08$	$1.0805e-08$	0.9823	1.0000
22	$2.736748775e-09$	$2.7912e-09$	$2.7367e-09$	0.9805	1.0000
			$c_{2,a}^{N,(2,0)}$		
2	$3.828697684e-01$	$3.8268e-01$	$3.8287e-01$	1.0005	1.0000
4	$1.899084702e-02$	$1.8981e-02$	$1.8991e-02$	1.0005	1.0000
6	$1.953555304e-03$	$1.9556e-03$	$1.9536e-03$	0.9989	1.0000
8	$2.757969313e-04$	$2.7672e-04$	$2.7580e-04$	0.9967	1.0000
10	$4.678690020e-05$	$4.7059e-05$	$4.6787e-05$	0.9942	1.0000
12	$8.963806878e-06$	$9.0378e-06$	$8.9638e-06$	0.9918	1.0000
14	$1.873670645e-06$	$1.8935e-06$	$1.8737e-06$	0.9895	1.0000
16	$4.182500377e-07$	$4.2360e-07$	$4.1825e-07$	0.9874	1.0000
18	$9.829615433e-08$	$9.9755e-08$	$9.8296e-08$	0.9854	1.0000
20	$2.408000184e-08$	$2.4483e-08$	$2.4080e-08$	0.9835	1.0000
22	$6.104188218e-09$	$6.2172e-09$	$6.1042e-09$	0.9818	1.0000

5.1.3 Asymptotic Limit

As a further consistency check on the Mellin moments, we extend the comparison to the region $\upsilon \to 0$, that is the limit of asymptotically small masses. This limit is of particular interest because exact results are not available for all heavy-quark coefficient functions at NLO, so the asymptotic expansion provides the only independent benchmark against which our Mellin moments can be validated.

Here the Mellin moments $C_{2,i}^{N}$ are found to agree with the literature, which Ref. [43] expresses in terms of harmonic sums [251, 252]. Our calculation recovers the correct factorisation into heavy-quark operator matrix elements and massless coefficient functions, confirming the consistency of the results with the expected structure of the expansion. These asymptotic expressions are obtained using the MATHEMATICA packages `HPL` [253] and `HypExp` [254], collected in Eqs. (5.22)–(5.33), further yield the higher-order corrections, previously unavailable, in a straightforward manner:

$$c_{2,\mathrm{g,vv}}^{2,(0,0)} = 0 \tag{5.22}$$

$$\begin{aligned} c_{2,\mathrm{g,vv}}^{2,(1,0)} &= -T_F \langle \mathrm{l}_{\{\mathrm{v,v}\}} \rangle^{\mathrm{g}} n_\mathrm{l} + T_F \langle \mathrm{h}_{\{\mathrm{v,v}\}} \rangle^{\mathrm{g}} n_\mathrm{h} \Bigg[-12\upsilon^2 - \frac{44}{3}\upsilon^2 \log(\upsilon) + 6\upsilon \\ &\quad + \frac{20}{3}\upsilon \log(\upsilon) - \frac{4}{3}\log(\upsilon) - 1 + \mathcal{O}\big(\upsilon^3\big) \Bigg] \end{aligned} \tag{5.23}$$

$$\begin{aligned} c_{2,\mathrm{g,vv}}^{2,(2,0)} &= C_A T_F \langle \mathrm{l}_{\{\mathrm{v,v}\}} \rangle^{\mathrm{g}} n_\mathrm{l} \left[\frac{115}{162} - 4\zeta_3 \right] + C_F T_F \langle \mathrm{l}_{\{\mathrm{v,v}\}} \rangle^{\mathrm{g}} n_\mathrm{l} \left[-\frac{4799}{405} + \frac{32}{5}\zeta_3 \right] \\ &\quad + C_F T_F \langle \mathrm{h}_{\{\mathrm{v,v}\}} \rangle^{\mathrm{g}} n_\mathrm{h} \Bigg[-\frac{7364}{45}\upsilon^2 \log^2(\upsilon) - \frac{196786}{675}\upsilon^2 \log(\upsilon) + \frac{131}{3}\upsilon \log^2(\upsilon) \end{aligned}$$

$$- \frac{16}{9}\log^2(\upsilon) + \frac{1901}{18}\upsilon\log(\upsilon) - \frac{160}{27}\log(\upsilon) + \upsilon^2\left(\frac{32}{5}\zeta_3 - \frac{147959}{20250}\right)$$
$$+ \upsilon\left(\frac{16}{5}\zeta_3 - \frac{14407}{1080}\right) + \frac{32}{5}\zeta_3 + \frac{1961}{405} + \mathcal{O}(\upsilon^3)\Bigg]$$
$$+ C_A T_F \langle \mathrm{h}_{\{\mathrm{v,v}\}}\rangle^{\mathrm{g}} n_{\mathrm{h}}\Bigg[\frac{1084}{45}\upsilon^2\log^2(\upsilon) - \frac{79799}{675}\upsilon^2\log(\upsilon) - \frac{95}{9}\upsilon\log^2(\upsilon)$$
$$+ \frac{22}{9}\log^2(\upsilon) + \frac{925}{54}\upsilon\log(\upsilon) - \frac{70}{27}\log(\upsilon) + \upsilon^2\left(-\frac{16}{5}\zeta_3 - \frac{321337}{40500}\right)$$
$$+ \upsilon\left(\frac{27113}{3240} - \frac{8}{5}\zeta_3\right) - 4\zeta_3 - \frac{11}{162} + \mathcal{O}(\upsilon^3)\Bigg], \tag{5.24}$$

$$c_{L,\mathrm{g,vv}}^{2,(0,0)} = 0 \tag{5.25}$$

$$c_{L,\mathrm{g,vv}}^{2,(1,0)} = \frac{4}{3}T_F\langle \mathrm{l}_{\{\mathrm{v,v}\}}\rangle^{\mathrm{g}} n_{\mathrm{l}} + T_F\langle \mathrm{h}_{\{\mathrm{v,v}\}}\rangle^{\mathrm{g}} n_{\mathrm{h}}\Bigg[-\frac{64\upsilon^2}{3} - 16\upsilon^2\log(\upsilon) + \frac{20}{3}\upsilon + 8\upsilon\log(\upsilon)$$
$$+ \frac{4}{3} + \mathcal{O}(\upsilon^3)\Bigg] \tag{5.26}$$

$$c_{L,\mathrm{g,vv}}^{2,(2,0)} = \frac{346}{27}C_A T_F\langle \mathrm{l}_{\{\mathrm{v,v}\}}\rangle^{\mathrm{g}} n_{\mathrm{l}} + C_F T_F\langle \mathrm{l}_{\{\mathrm{v,v}\}}\rangle^{\mathrm{g}} n_{\mathrm{l}}\left[-\frac{232}{135} - \frac{32}{5}\zeta_3\right]$$
$$+ C_F T_F\langle \mathrm{h}_{\{\mathrm{v,v}\}}\rangle^{\mathrm{g}} n_{\mathrm{h}}\Bigg[-\frac{2852}{15}\upsilon^2\log^2(\upsilon) - \frac{81278}{225}\upsilon^2\log(\upsilon) + \frac{110}{3}\upsilon\log^2(\upsilon)$$
$$+ \frac{505}{9}\upsilon\log(\upsilon) - \frac{16\log(\upsilon)}{9} + \upsilon^2\left(-\frac{192}{5}\zeta_3 - \frac{587707}{6750}\right) + \upsilon\left(\frac{35221}{540}\right.$$
$$\left. - \frac{96}{5}\zeta_3\right) - \frac{32}{5}\zeta_3 - \frac{232}{135} + \mathcal{O}(\upsilon^3)\Bigg]$$
$$+ C_A T_F\langle \mathrm{h}_{\{\mathrm{v,v}\}}\rangle^{\mathrm{g}} n_{\mathrm{h}}\Bigg[\frac{84}{5}\upsilon^2\log^2(\upsilon) - \frac{9134}{75}\upsilon^2\log(\upsilon) - \frac{26}{3}\upsilon\log^2(\upsilon)$$
$$+ \frac{323}{9}\upsilon\log(\upsilon) + \upsilon^2\left(\frac{96}{5}\zeta_3 + \frac{38087}{6750}\right) + \upsilon\left(\frac{48}{5}\zeta_3 - \frac{11353}{540}\right)$$
$$+ \frac{346}{27} + \mathcal{O}(\upsilon^3)\Bigg], \tag{5.27}$$

$$c_{2,\mathrm{q,vv}}^{2,(0,0)} = \langle \bar{\mathrm{l}}_{\{\mathrm{v,v}\}}\rangle^{\mathrm{q}} \tag{5.28}$$

$$c_{2,\mathrm{q,vv}}^{2,(1,0)} = \frac{1}{3}C_F\langle \bar{\mathrm{l}}_{\{\mathrm{v,v}\}}\rangle^{\mathrm{q}} \tag{5.29}$$

$$c_{2,\mathrm{q,vv}}^{2,(2,0)} = -8C_F T_F\langle \bar{\mathrm{l}}_{\{\mathrm{v,v}\}}\rangle^{\mathrm{q}} n_{\mathrm{l}} - \frac{266}{81}C_F T_F\langle \mathrm{l}_{\{\mathrm{v,v}\}}\rangle^{\mathrm{q}} n_{\mathrm{l}} + C_A C_F\langle \bar{\mathrm{l}}_{\{\mathrm{v,v}\}}\rangle^{\mathrm{q}}\left[\frac{3677}{135} - \frac{128}{5}\zeta_3\right]$$
$$+ C_F^2\langle \bar{\mathrm{l}}_{\{\mathrm{v,v}\}}\rangle^{\mathrm{q}}\left[-\frac{4189}{810} + \frac{96}{5}\zeta_3\right]$$
$$+ C_F T_F\langle \bar{\mathrm{l}}_{\{\mathrm{v,v}\}}\rangle^{\mathrm{q}} n_{\mathrm{h}}\Bigg[\frac{9689}{2250}\upsilon^2 - \frac{28}{15}\upsilon^2\log^2(\upsilon) - \frac{2482}{225}\upsilon^2\log(\upsilon) + \frac{92}{27}\upsilon$$

$$
\begin{aligned}
&- \frac{16}{9}\log^2(\upsilon) - \frac{112}{9}\upsilon\log(\upsilon) - \frac{140}{27}\log(\upsilon) - \frac{344}{27} + \mathcal{O}\big(\upsilon^3\big)\Big] \\
&+ C_F T_F \langle \mathrm{h}_{\{\mathrm{v},\mathrm{v}\}}\rangle^{\mathrm{q}} n_{\mathrm{h}} \Big[- \frac{1318871}{10125}\upsilon^2 - \frac{832}{45}\upsilon^2\log^2(\upsilon) + \frac{34532}{675}\upsilon^2\log(\upsilon) \\
&+ \frac{9671}{162}\upsilon + \frac{80}{9}\upsilon\log^2(\upsilon) - \frac{16}{9}\log^2(\upsilon) + \frac{226}{27}\upsilon\log(\upsilon) - \frac{80}{27} \\
&- \frac{590}{81}\log(\upsilon) + \mathcal{O}\big(\upsilon^3\big)\Big] ,
\end{aligned} \tag{5.30}
$$

$$
c_{L,\mathrm{q},\mathrm{vv}}^{2,(0,0)} = 0 \tag{5.31}
$$

$$
c_{L,\mathrm{q},\mathrm{vv}}^{2,(1,0)} = \frac{4}{3} C_F \langle \bar{\mathrm{l}}_{\{\mathrm{v},\mathrm{v}\}}\rangle^{\mathrm{q}} \tag{5.32}
$$

$$
\begin{aligned}
c_{L,\mathrm{q},\mathrm{vv}}^{2,(2,0)} = &-\frac{184}{27} C_F T_F \langle \bar{\mathrm{l}}_{\{\mathrm{v},\mathrm{v}\}}\rangle^{\mathrm{q}} n_{\mathrm{l}} - \frac{160}{27} C_F T_F \langle \mathrm{l}_{\{\mathrm{v},\mathrm{v}\}}\rangle^{\mathrm{q}} n_{\mathrm{l}} + C_F^2 \langle \bar{\mathrm{l}}_{\{\mathrm{v},\mathrm{v}\}}\rangle^{\mathrm{q}} \Big[- \frac{1906}{135} + \frac{64}{5}\zeta_3 \Big] \\
&+ C_A C_F \langle \bar{\mathrm{l}}_{\{\mathrm{v},\mathrm{v}\}}\rangle^{\mathrm{q}} \Big[\frac{2878}{135} - \frac{32}{5}\zeta_3 \Big] \\
&+ C_F T_F \langle \bar{\mathrm{l}}_{\{\mathrm{v},\mathrm{v}\}}\rangle^{\mathrm{q}} n_{\mathrm{h}} \Big[- \frac{170192}{1125}\upsilon^2 + \frac{96}{5}\upsilon^2\log^2(\upsilon) - \frac{2912}{25}\upsilon^2\log(\upsilon) - \frac{680}{9}\upsilon \\
&- 32\upsilon\log(\upsilon) - \frac{16}{9}\log(\upsilon) - \frac{184}{27} + \mathcal{O}\big(\upsilon^3\big)\Big] \\
&+ C_F T_F \langle \mathrm{h}_{\{\mathrm{v},\mathrm{v}\}}\rangle^{\mathrm{q}} n_{\mathrm{h}} \Big[- \frac{773258}{3375}\upsilon^2 - \frac{416}{15}\upsilon^2\log^2(\upsilon) + \frac{6536}{225}\upsilon^2\log(\upsilon) \\
&+ \frac{2393}{27}\upsilon + \frac{32}{3}\upsilon\log^2(\upsilon) + \frac{220}{9}\upsilon\log(\upsilon) - \frac{160}{27} + \mathcal{O}\big(\upsilon^3\big)\Big] .
\end{aligned} \tag{5.33}
$$

Ultimately, we highlight that the limit $\upsilon \to 0$ agrees with the limit $\xi \to 0$ only at leading power. Beyond this order, corrections are need,

$$
\upsilon = \xi - 2\xi^2 + 5\xi^3 + \mathcal{O}\big(\xi^4\big) , \tag{5.34}
$$

$$
\log \upsilon = \log(\xi) - 2\xi + 3\xi^2 + \frac{22\xi^3}{3} + \mathcal{O}\big(\xi^4\big) . \tag{5.35}
$$

5.1.4 Axial-Axial

For products of two axial-vector currents, we computed only the first non-vanishing Mellin moment, namely $N = 2$. Higher Mellin moments follow in direct analogy, since all master integrals and IBP tables can be recycled. Unlike the VV case, the extraction of the finite coefficient function is no longer straightforward whilst the numbers of light and heavy quarks, n_{l} and n_{h}, are kept general. To simplify the notation, we write Eq. (2.105) as

$$
T_{i,\mathrm{p}}^{N,\mathrm{ren}}(p,q) = (-1)^N \sum_{j,k\in\mathbb{S}} C_{i,j}^N(q) Z_{jk} A_{k,\mathrm{p}}^{N,\mathrm{ren}}(p)\Big|_{p=0} + \sum_{m=1}^{\infty}\sum_{n=1}^{m} \frac{a_{s,\mathrm{ren}}^m}{\varepsilon^n} c_{i,\mathrm{p}}^{N,(m,n)} , \tag{5.36}
$$

which introduces new constants that vanish once the coefficient functions are successfully renormalised and mass factorisation holds.

Gluon-initiated processes renormalise as they should, whereas the quark-initiated ones leave behind divergent contributions,

$$c_{2,\mathrm{q}}^{2,(2,-1)} = 24 C_F T_F \langle \bar{\mathrm{l}}_{\{\mathrm{a}\}} \mathrm{l}_{\{\mathrm{a}\}} \rangle^{\mathrm{q}} n_{\mathrm{l}} + 24 C_F T_F \langle \bar{\mathrm{l}}_{\{\mathrm{a}\}} \mathrm{h}_{\{\mathrm{a}\}} \rangle^{\mathrm{q}} n_{\mathrm{h}} \,. \tag{5.37}$$

This phenomenon admits two interpretations. On the one hand, no physical requirements on the neutral current have been imposed so far. The Mellin moments are renormalisable when, for example, the theory contains even numbers of both heavy and light quarks, with equal numbers of up-type and down-type quarks in each case. In such cases the traces over the charge matrices vanish. Within the full electroweak theory they also vanish, because the charge traces are independent of the mass and become trivial once the quark masses are non-degenerate. On the other hand, the products of two axial-vector and of two vector currents acquire anomalous dimensions that agree only at LO and may differ at higher orders in perturbation theory [255]. Renormalisation is therefore expected to fail if the anomalous dimensions of the product of two vector currents are used.

What should be noted, however, is that even with the correct anomalous dimensions the result would remain non-renormalisable, since the anomalous dimensions depend only on the number of light flavours. The heavy-quark contributions would then survive, which suggests that the results are meaningful *only* when a physical theory is considered.

The Mellin moments of the AA and VV contributions to the coefficient functions are in general not identical. As a non-trivial consistency check, they should nevertheless coincide in the massless limit, where chiral symmetry is restored, provided the currents have identical coupling constants and anomalous contributions are discarded.

Discrepancies arise in the massless limit solely from anomalous contributions, which are unique to the product of two axial-vector currents. These originate from fermion-triangle subgraphs containing merely one γ_5. In the VV case, such contributions vanish by Furry's theorem. Explicitly, for the differences between Eqs. (5.2)–(5.13) and (C.1)–(C.12), we find

$$c_{2,\mathrm{g,aa}}^{2,(0,0)} - c_{2,\mathrm{g,vv}}^{2,(0,0)} = 0 \,, \tag{5.38}$$

$$c_{2,\mathrm{g,aa}}^{2,(1,0)} - c_{2,\mathrm{g,vv}}^{2,(1,0)} = T_F n_{\mathrm{h}} \upsilon \left[8 + \frac{16}{3} \log(\upsilon) \right] + \mathcal{O}\big(\upsilon^2\big) \,, \tag{5.39}$$

$$\begin{aligned} c_{2,\mathrm{g,aa}}^{2,(2,0)} - c_{2,\mathrm{g,vv}}^{2,(2,0)} = {} & C_A T_F n_{\mathrm{h}} \upsilon \left[\frac{56}{9} \log^2(\upsilon) + \frac{688}{27} \log(\upsilon) + \frac{16}{5}\zeta_3 - \frac{2392}{405} \right] \\ & + C_F T_F n_{\mathrm{h}} \upsilon \left[-32 \log^2(\upsilon) - \frac{392}{9} \log(\upsilon) - \frac{288}{5}\zeta_3 + \frac{12352}{135} \right] \\ & + 10 T_F^2 \langle \mathrm{h}_{\{\mathrm{a}\}} \mathrm{h}_{\{\mathrm{a}\}} \rangle^{\mathrm{g}} n_{\mathrm{h}}^2 \\ & + T_F^2 \langle \mathrm{h}_{\{\mathrm{a}\}} \mathrm{h}_{\{\mathrm{a}\}} \rangle^{\mathrm{g}} n_{\mathrm{h}}^2 \Big[40 \upsilon \log(\upsilon) + 10 \Big] \\ & + T_F^2 \langle \mathrm{l}_{\{\mathrm{a}\}} \mathrm{h}_{\{\mathrm{a}\}} \rangle^{\mathrm{g}} n_{\mathrm{h}} n_{\mathrm{l}} \Big[40 \upsilon \log(\upsilon) + 20 \Big] + \mathcal{O}\big(\upsilon^2\big) \,, \end{aligned} \tag{5.40}$$

$$c_{L,\mathrm{g,aa}}^{2,(0,0)} - c_{L,\mathrm{g,vv}}^{2,(0,0)} = 0 \,, \tag{5.41}$$

$$c_{L,\mathrm{g,aa}}^{2,(1,0)} - c_{L,\mathrm{g,vv}}^{2,(1,0)} = 0\,, \tag{5.42}$$

$$\begin{aligned}
c_{L,\mathrm{g,aa}}^{2,(2,0)} - c_{L,\mathrm{g,vv}}^{2,(2,0)} = {} & C_F T_F n_\mathrm{h} v\left[-\frac{176}{9}\log(v) - \frac{1232}{135} - \frac{192}{5}\zeta_3\right] \\
& + C_A T_F n_\mathrm{h} v\left[\frac{1048}{45} - \frac{96}{5}\zeta_3\right] \\
& + 4T_F^2 \langle \mathrm{l}_{\{\mathrm{a}\}} \mathrm{l}_{\{\mathrm{a}\}} \rangle^\mathrm{g} n_\mathrm{l}^2 \\
& + T_F^2 \langle \mathrm{h}_{\{\mathrm{a}\}} \mathrm{h}_{\{\mathrm{a}\}} \rangle^\mathrm{g} n_\mathrm{h}^2 \Big[16 v\log(v) + 4\Big] \\
& + T_F^2 \langle \mathrm{l}_{\{\mathrm{a}\}} \mathrm{h}_{\{\mathrm{a}\}} \rangle^\mathrm{g} n_\mathrm{h} n_\mathrm{l} \Big[16 v\log(v) + 8\Big] + \mathcal{O}\big(v^2\big)\,,
\end{aligned} \tag{5.43}$$

$$c_{2,\mathrm{q,aa}}^{2,(0,0)} - c_{2,\mathrm{q,vv}}^{2,(0,0)} = 0\,, \tag{5.44}$$

$$c_{2,\mathrm{q,aa}}^{2,(1,0)} - c_{2,\mathrm{q,vv}}^{2,(1,0)} = 0\,, \tag{5.45}$$

$$\begin{aligned}
c_{2,\mathrm{q,aa}}^{2,(2,0)} - c_{2,\mathrm{q,vv}}^{2,(2,0)} = {} & C_F T_F n_\mathrm{h} v\left[\frac{7544}{81} + \frac{64}{9}\log^2(v) + \frac{992}{27}\log(v)\right] \\
& + C_F T_F \langle \bar{\mathrm{l}}_{\{\mathrm{a}\}} \mathrm{h}_{\{\mathrm{a}\}} \rangle^\mathrm{q} n_\mathrm{h} \Bigg[v\left(\frac{1004}{15} - 32\log(v) + \frac{496}{5}\zeta_3\right) \\
& \quad - \frac{32}{5}\zeta_3 - \frac{658}{15}\Bigg] \\
& + C_F T_F \langle \bar{\mathrm{l}}_{\{\mathrm{a}\}} \mathrm{l}_{\{\mathrm{a}\}} \rangle^\mathrm{q} n_\mathrm{l} \left[-\frac{32}{5}\zeta_3 - \frac{658}{15}\right] + \mathcal{O}\big(v^2\big)\,,
\end{aligned} \tag{5.46}$$

$$c_{L,\mathrm{q,aa}}^{2,(0,0)} - c_{L,\mathrm{q,vv}}^{2,(0,0)} = 0\,, \tag{5.47}$$

$$c_{L,\mathrm{q,aa}}^{2,(1,0)} - c_{L,\mathrm{q,vv}}^{2,(1,0)} = 0\,, \tag{5.48}$$

$$\begin{aligned}
c_{L,\mathrm{q,aa}}^{2,(2,0)} - c_{L,\mathrm{q,vv}}^{2,(2,0)} = {} & C_F T_F n_\mathrm{h} v\left[\frac{16}{9}\right] \\
& + C_F T_F \langle \bar{\mathrm{l}}_{\{\mathrm{a}\}} \mathrm{h}_{\{\mathrm{a}\}} \rangle^\mathrm{q} n_\mathrm{h} \Bigg[v\left(\frac{312}{5} - \frac{96}{5}\zeta_3\right) \\
& \quad - \frac{128}{5}\zeta_3 + \frac{368}{15}\Bigg] \\
& + C_F T_F \langle \bar{\mathrm{l}}_{\{\mathrm{a}\}} \mathrm{l}_{\{\mathrm{a}\}} \rangle^\mathrm{q} n_\mathrm{l} \left[-\frac{128}{5}\zeta_3 + \frac{368}{15}\right] + \mathcal{O}\big(v^2\big)\,.
\end{aligned} \tag{5.49}$$

5.1.5 Axial-Vector

For the parity-violating coefficient function the gluon-channel contributions vanish identically. In the quark channel, by contrast, a non-vanishing result appears already at the first Mellin moment, namely $N = 1$, since only the odd moments contribute here, unlike the AA and VV cases where only the even Mellin moments do. Explicitly, the residual divergence of the quark channel reads

$$c_{3,\mathrm{q}}^{1,(2,-1)} = -6C_F T_F \langle \bar{\mathrm{l}}_{\{\mathrm{v}\}} \mathrm{l}_{\{\mathrm{a}\}} \rangle^{\mathrm{q}} n_{\mathrm{l}} - 6C_F T_F \langle \bar{\mathrm{l}}_{\{\mathrm{v}\}} \mathrm{h}_{\{\mathrm{a}\}} \rangle^{\mathrm{q}} n_{\mathrm{h}} \,. \tag{5.50}$$

Following the discussion of the axial–axial anomaly in Eq. (5.37), the same reasoning applies here. Restricting the light- and heavy-quark numbers to a physically sensible flavour content, as discussed in Subsec. 5.1.4, removes the anomalous remainder. The Mellin moment of the parity-violating coefficient function are given in Eqs. (C.13)–(C.15).

5.2 Scalar Current at NLO

The computation of the scalar current serves as a consistency check on the setup, with the first non-vanishing Mellin moments, at $N = 2$, given in Eqs. (C.16)–(C.21). Gauge invariance provides a first non-trivial test here, since, unlike the vector-current case, only the sum of the ghost and gluon contributions is gauge invariant. Renormalisation offers a further and more informative check, as a second operator, the Yukawa coupling, must be introduced to renormalise the coefficient functions and account for the Weyl anomaly. Along the way the calculation yields every anomalous dimension needed for the finite Mellin moments, and is in that sense self-contained. Were the Yukawa coupling omitted, the coefficient function would not be renormalisable and the divergent part

$$c_{S,\mathrm{g}}^{1,(2,-1)} = C_F T_F n_h \mathrm{H}_0 \Big[-48\mathrm{d}_{-1}^3 - 24\mathrm{d}_{-1}^2 + 12\mathrm{d}_{-1} - 12\mathrm{d}_1 \Big] \tag{5.51}$$

would remain. Its cancellation is non-trivial and therefore constitutes a strong check on the setup.

Scalar currents typically require more master integrals than the neutral current, since scalars couple directly to gluons and thereby generate additional non-Abelian vertices, admitting graphs with mass configurations absent from the neutral current case. These extra configurations have been computed as well and, being mass-preserving, included among the master integrals of the neutral current.

5.3 Neutral Current at NNLO

At NNLO, only the explicit expressions involving the cubic Casimir operator are given, since the full moments are quite lengthy. Two reasons motivate the choice of this specific term. First, the cubic Casimir colour factor makes its first appearance at NNLO, and the moment already captures almost the entire analytic structure of the result, with most of the integral kernels present. Second, it showcases a flavour factor that at two loops was exclusive to the product of two axial-vector currents, yet now arises for vector currents as well.

Presentation is once again restricted to the first non-vanishing Mellin moment, namely $N = 2$, and specifically to the $c_{2,\mathrm{g,vv}}^{2,(3,0)}$, although the other coefficient functions have, of course, been computed as well. Unlike at NLO, the restriction here is not a matter of convenience. Only this moment could be obtained, since computing higher moments at this order becomes exceedingly expensive and demands further optimisation and computing resources.

Notably, the full Mellin moment comprises merely 142 iterated integrals, with not all kernels contributing, whereas the master integrals contain 2216 in total. Such a disparity is a recurring feature. Most intermediate results in amplitude computations amount to unphysical content, an effect far more pronounced in the presence of masses than in the massless case.

Before the result is presented, a few structural remarks are in order. Confirmed here is the observation that no kernels with a squared period survive at the amplitude level [215], whether directly or implicitly through the transcendental functions, even though such kernels do appear in the master integrals and in the rotations to the canonical basis. Interestingly, under the transformation

$$\varpi_0^{\mathrm{NC}} = \epsilon\varpi_0^{\mathrm{NC}}\Big|_{\epsilon=1}\,, \tag{5.52}$$

the Mellin moment turns out to be an affine function of the parameter ϵ. Only the zeroth and first powers therefore occur. Likewise, square roots enter solely at even powers, either directly or indirectly through the integral kernels. Physics must not depend on the branch choice, so such behaviour is only to be expected. Along similar lines, the observation regarding the periods may indicate that a comparable mechanism is at work.

The structure of the result warrants further investigation in future work, in particular in relation to approaches such as the Landau bootstrap [256]. In this context, it would be ideal to find criteria that exclude certain integral kernels, thereby enabling a more constrained ansatz.

$$
\begin{aligned}
c_{2,\mathrm{g,vv}}^{2,(3,0)} = \frac{d^{abc}d_{abc}T_F^3}{N_A}\langle \mathrm{h}_{\{\mathrm{v}\}}\mathrm{h}_{\{\mathrm{v}\}}\rangle^{\mathrm{g}} n_{\mathrm{h}}^2 \Bigg[& \frac{10}{9} + \frac{143}{270}\hat{x} - \frac{32}{45}\hat{\omega}_1 - \frac{32}{45}\hat{\omega}_4 \\
& + \mathrm{C}_{3,11,1}\left(-\frac{27}{20} - \frac{409}{960}\hat{x} - \frac{153}{1280}\hat{x}^2 + \frac{16}{5}\hat{\omega}_1 \right) \\
& + \hat{\mathrm{F}}_1\left(\frac{508}{15} - \frac{8}{15}\hat{x} + \frac{11}{270}\hat{x}^2 \right) \\
& + \mathrm{C}_{3,11,1}\hat{\mathrm{F}}_{12}\left(-\frac{11}{20} - \frac{4}{5}\hat{\omega}_1 \right) \\
& + \mathrm{C}_{3,11,1}\hat{\mathrm{F}}_{16}\left(\frac{11}{80} + \frac{1}{5}\hat{\omega}_1 \right) \\
& + \mathrm{C}_{3,11,1}\hat{\mathrm{F}}_{18}\left(-\frac{33}{20} - \frac{12}{5}\hat{\omega}_1 \right) \\
& + \hat{\mathrm{F}}_{4,4}\left(-\frac{4711}{45} - \frac{19}{30}\hat{x} - 260\hat{\omega}_1 + \frac{896}{15}\hat{\omega}_1^2 + \frac{512}{5}\hat{\omega}_1^3 - \frac{736}{15}\hat{\omega}_4 \right) \\
& + \mathrm{C}_{3,11,1}\hat{\mathrm{F}}_{4,4}\left(-\frac{1}{3} + \frac{4}{5}\hat{\omega}_1 - \frac{32}{15}\hat{\omega}_1^2 \right) \\
& + \mathrm{C}_{3,11,1}\hat{\mathrm{F}}_{12,1}\left(-\frac{3}{10} - \frac{2}{15}\hat{\omega}_1 \right) \\
& + \mathrm{C}_{3,11,1}\hat{\mathrm{F}}_{13,4}\left(-\frac{1}{3} + \frac{4}{5}\hat{\omega}_1 - \frac{32}{15}\hat{\omega}_1^2 \right) \\
& + \mathrm{C}_{3,11,1}\hat{\mathrm{F}}_{14,4}\left(\frac{1}{3} - \frac{4}{5}\hat{\omega}_1 + \frac{32}{15}\hat{\omega}_1^2 \right)
\end{aligned}
$$

$$
\begin{aligned}
&+ \mathrm{C}_{3,11,1}\hat{\mathrm{F}}_{16,1}\bigg(\frac{3}{40} + \frac{1}{30}\hat{\omega}_1\bigg)\\
&+ \mathrm{C}_{3,11,1}\hat{\mathrm{F}}_{18,1}\bigg(- \frac{9}{10} - \frac{2}{5}\hat{\omega}_1\bigg)\\
&+ \mathrm{C}_{3,11,1}\hat{\mathrm{F}}_{19,4}\bigg(\frac{1}{6} - \frac{2}{5}\hat{\omega}_1 + \frac{16}{15}\hat{\omega}_1^2\bigg)\\
&+ \mathrm{C}_{3,11,1}\hat{\mathrm{F}}_{20,4}\bigg(- \frac{5}{24} + \frac{1}{2}\hat{\omega}_1 - \frac{4}{3}\hat{\omega}_1^2\bigg)\\
&+ \mathrm{C}_{3,11,1}\hat{\mathrm{F}}_{21,4}\bigg(1 - \frac{12}{5}\hat{\omega}_1 + \frac{32}{5}\hat{\omega}_1^2\bigg)\\
&+ \hat{\mathrm{F}}_{1,4,4}\bigg(\frac{476}{45} + \frac{248}{15}\hat{\omega}_1 - \frac{616}{15}\hat{\omega}_4\bigg)\\
&+ \hat{\mathrm{F}}_{4,1,4}\bigg(\frac{476}{45} + \frac{248}{15}\hat{\omega}_1 - \frac{616}{15}\hat{\omega}_4\bigg)\\
&+ \hat{\mathrm{F}}_{4,4,1}\bigg(\frac{946}{45} - \frac{107}{30}\hat{x} - \frac{29}{24}\hat{x}^2 + \frac{2992}{15}\hat{\omega}_1 - \frac{616}{15}\hat{\omega}_4\bigg)\\
&+ \hat{\mathrm{F}}_{4,4,3}\bigg(- \frac{106}{5} - \frac{61}{30}\hat{x} - \frac{191}{120}\hat{x}^2 - \frac{536}{5}\hat{\omega}_1\bigg)\\
&+ \hat{\mathrm{F}}_{4,4,4,4}\bigg(- \frac{88}{5} - \frac{128}{5}\hat{\omega}_1\bigg)\\
&+ \hat{\mathrm{F}}_{16,6,6,12}\bigg(- \frac{352}{5} - \frac{512}{5}\hat{\omega}_1\bigg)\\
&+ \hat{\mathrm{F}}_{16,6,6,16}\bigg(\frac{88}{5} + \frac{128}{5}\hat{\omega}_1\bigg)\\
&+ \hat{\mathrm{F}}_{16,6,6,18}\bigg(- \frac{1056}{5} - \frac{1536}{5}\hat{\omega}_1\bigg)\\
&+ \hat{\mathrm{F}}_{16,6,10,4}\bigg(- \frac{352}{5} - \frac{512}{5}\hat{\omega}_1\bigg)\\
&+ \hat{\mathrm{F}}_{1,4,4,4,4}\bigg(\frac{112}{5} - \frac{64}{5}\hat{\omega}_1 + \frac{256}{5}\hat{\omega}_1^2\bigg)\\
&+ \hat{\mathrm{F}}_{4,1,4,4,4}\bigg(\frac{112}{5} - \frac{64}{5}\hat{\omega}_1 + \frac{256}{5}\hat{\omega}_1^2\bigg)\\
&+ \hat{\mathrm{F}}_{4,4,1,4,4}\bigg(- 16 + \frac{192}{5}\hat{\omega}_1 - \frac{512}{5}\hat{\omega}_1^2\bigg)\\
&+ \hat{\mathrm{F}}_{4,4,3,4,4}\bigg(- \frac{64}{3} + \frac{256}{5}\hat{\omega}_1 - \frac{2048}{15}\hat{\omega}_1^2\bigg)\\
&+ \hat{\mathrm{F}}_{4,4,4,1,4}\bigg(- \frac{352}{15} - \frac{128}{5}\hat{\omega}_1 + \frac{512}{15}\hat{\omega}_1^2\bigg)\\
&+ \hat{\mathrm{F}}_{4,4,4,3,4}\bigg(\frac{32}{3} - \frac{128}{5}\hat{\omega}_1 + \frac{1024}{15}\hat{\omega}_1^2\bigg)\\
&+ \hat{\mathrm{F}}_{4,4,4,4,1}\bigg(- \frac{48}{5} - \frac{64}{15}\hat{\omega}_1\bigg)\\
&+ \hat{\mathrm{F}}_{16,6,6,12,1}\bigg(- \frac{192}{5} - \frac{256}{15}\hat{\omega}_1\bigg)\\
&+ \hat{\mathrm{F}}_{16,6,6,13,4}\bigg(- \frac{128}{3} + \frac{512}{5}\hat{\omega}_1 - \frac{4096}{15}\hat{\omega}_1^2\bigg)
\end{aligned}
$$

$$
\begin{aligned}
&+ \hat{\mathrm{F}}_{16,6,6,14,4}\bigg(\frac{128}{3} - \frac{512}{5}\hat{\omega}_1 + \frac{4096}{15}\hat{\omega}_1^2\bigg)\\
&+ \hat{\mathrm{F}}_{16,6,6,16,1}\bigg(\frac{48}{5} + \frac{64}{15}\hat{\omega}_1\bigg)\\
&+ \hat{\mathrm{F}}_{16,6,6,18,1}\bigg(-\frac{576}{5} - \frac{256}{5}\hat{\omega}_1\bigg)\\
&+ \hat{\mathrm{F}}_{16,6,6,19,4}\bigg(\frac{64}{3} - \frac{256}{5}\hat{\omega}_1 + \frac{2048}{15}\hat{\omega}_1^2\bigg)\\
&+ \hat{\mathrm{F}}_{16,6,6,20,4}\bigg(-\frac{80}{3} + 64\hat{\omega}_1 - \frac{512}{3}\hat{\omega}_1^2\bigg)\\
&+ \hat{\mathrm{F}}_{16,6,6,21,4}\bigg(128 - \frac{1536}{5}\hat{\omega}_1 + \frac{4096}{5}\hat{\omega}_1^2\bigg)\\
&+ \hat{\mathrm{F}}_{16,6,10,1,4}\bigg(\frac{128}{3} - \frac{512}{5}\hat{\omega}_1 + \frac{4096}{15}\hat{\omega}_1^2\bigg)\\
&+ \hat{\mathrm{F}}_{16,6,10,3,4}\bigg(-\frac{128}{3} + \frac{512}{5}\hat{\omega}_1 - \frac{4096}{15}\hat{\omega}_1^2\bigg)\\
&+ \hat{\mathrm{F}}_{16,6,10,4,1}\bigg(-\frac{192}{5} - \frac{256}{15}\hat{\omega}_1\bigg)\\
&+ \hat{r}_1\hat{\mathrm{F}}_{4}\bigg(-\frac{1117}{270} - \frac{829}{270}\hat{x} + \frac{6854}{45}\hat{\omega}_1 - \frac{32}{3}\hat{\omega}_1^2 - \frac{128}{5}\hat{\omega}_1^3 - \frac{116}{45}\hat{\omega}_4\bigg)\\
&+ \hat{r}_1\mathrm{C}_{3,11,1}\hat{\mathrm{F}}_{4}\bigg(-\frac{37}{60}\hat{\omega}_1 - \frac{28}{15}\hat{\omega}_1^2 + \frac{23}{60}\hat{\omega}_4\bigg)\\
&+ \hat{r}_1\mathrm{C}_{3,11,1}\hat{\mathrm{F}}_{13}\bigg(-\frac{37}{60}\hat{\omega}_1 - \frac{28}{15}\hat{\omega}_1^2 + \frac{23}{60}\hat{\omega}_4\bigg)\\
&+ \hat{r}_1\mathrm{C}_{3,11,1}\hat{\mathrm{F}}_{14}\bigg(\frac{37}{60}\hat{\omega}_1 + \frac{28}{15}\hat{\omega}_1^2 - \frac{23}{60}\hat{\omega}_4\bigg)\\
&+ \hat{r}_1\mathrm{C}_{3,11,1}\hat{\mathrm{F}}_{19}\bigg(\frac{37}{120}\hat{\omega}_1 + \frac{14}{15}\hat{\omega}_1^2 - \frac{23}{120}\hat{\omega}_4\bigg)\\
&+ \hat{r}_1\mathrm{C}_{3,11,1}\hat{\mathrm{F}}_{20}\bigg(-\frac{37}{96}\hat{\omega}_1 - \frac{7}{6}\hat{\omega}_1^2 + \frac{23}{96}\hat{\omega}_4\bigg)\\
&+ \hat{r}_1\mathrm{C}_{3,11,1}\hat{\mathrm{F}}_{21}\bigg(\frac{37}{20}\hat{\omega}_1 + \frac{28}{5}\hat{\omega}_1^2 - \frac{23}{20}\hat{\omega}_4\bigg)\\
&+ \hat{r}_1\hat{\mathrm{F}}_{1,4}\bigg(\frac{2}{45} - \frac{404}{15}\hat{\omega}_1 + \frac{452}{45}\hat{\omega}_4\bigg)\\
&+ \hat{r}_1\hat{\mathrm{F}}_{4,1}\bigg(\frac{2}{45} - \frac{404}{15}\hat{\omega}_1 + \frac{452}{45}\hat{\omega}_4\bigg)\\
&+ \hat{r}_1\hat{\mathrm{F}}_{4,4,4}\bigg(-\frac{14}{5}\hat{x} + \frac{1372}{45}\hat{\omega}_1 + \frac{2824}{45}\hat{\omega}_1^2 - \frac{128}{5}\hat{\omega}_1^3 - \frac{256}{5}\hat{\omega}_1^4 + \frac{64}{15}\hat{\omega}_4\\
&\quad - 8\hat{\omega}_4^2\bigg)\\
&+ \hat{r}_1\hat{\mathrm{F}}_{16,6,10}\bigg(-\frac{76}{15} - \frac{38}{5}\hat{x} - \frac{1904}{9}\hat{\omega}_1 - \frac{30784}{45}\hat{\omega}_1^2 - \frac{1024}{5}\hat{\omega}_1^3 - \frac{2048}{5}\hat{\omega}_1^4\\
&\quad - \frac{352}{15}\hat{\omega}_4 + 32\hat{\omega}_4^2\bigg)\\
&+ \hat{r}_1\hat{\mathrm{F}}_{1,4,4,4}\bigg(4\hat{\omega}_1 + \frac{144}{5}\hat{\omega}_1^2 - \frac{124}{5}\hat{\omega}_4\bigg)
\end{aligned}
$$

$$
\begin{aligned}
&+ \hat{r}_1 \hat{\mathrm{F}}_{4,1,4,4}\bigg(4\hat{\omega}_1 + \frac{144}{5}\hat{\omega}_1^2 - \frac{124}{5}\hat{\omega}_4\bigg) \\
&+ \hat{r}_1 \hat{\mathrm{F}}_{4,4,1,4}\bigg(- \frac{148}{5}\hat{\omega}_1 - \frac{448}{5}\hat{\omega}_1^2 + \frac{92}{5}\hat{\omega}_4\bigg) \\
&+ \hat{r}_1 \hat{\mathrm{F}}_{4,4,3,4}\bigg(- \frac{592}{15}\hat{\omega}_1 - \frac{1792}{15}\hat{\omega}_1^2 + \frac{368}{15}\hat{\omega}_4\bigg) \\
&+ \hat{r}_1 \hat{\mathrm{F}}_{4,4,4,1}\bigg(\frac{472}{15}\hat{\omega}_1 + \frac{928}{15}\hat{\omega}_1^2 + \frac{376}{15}\hat{\omega}_4\bigg) \\
&+ \hat{r}_1 \hat{\mathrm{F}}_{4,4,4,3}\bigg(\frac{296}{15}\hat{\omega}_1 + \frac{896}{15}\hat{\omega}_1^2 - \frac{184}{15}\hat{\omega}_4\bigg) \\
&+ \hat{r}_1 \hat{\mathrm{F}}_{16,6,6,13}\bigg(- \frac{1184}{15}\hat{\omega}_1 - \frac{3584}{15}\hat{\omega}_1^2 + \frac{736}{15}\hat{\omega}_4\bigg) \\
&+ \hat{r}_1 \hat{\mathrm{F}}_{16,6,6,14}\bigg(\frac{1184}{15}\hat{\omega}_1 + \frac{3584}{15}\hat{\omega}_1^2 - \frac{736}{15}\hat{\omega}_4\bigg) \\
&+ \hat{r}_1 \hat{\mathrm{F}}_{16,6,6,19}\bigg(\frac{592}{15}\hat{\omega}_1 + \frac{1792}{15}\hat{\omega}_1^2 - \frac{368}{15}\hat{\omega}_4\bigg) \\
&+ \hat{r}_1 \hat{\mathrm{F}}_{16,6,6,20}\bigg(- \frac{148}{3}\hat{\omega}_1 - \frac{448}{3}\hat{\omega}_1^2 + \frac{92}{3}\hat{\omega}_4\bigg) \\
&+ \hat{r}_1 \hat{\mathrm{F}}_{16,6,6,21}\bigg(\frac{1184}{5}\hat{\omega}_1 + \frac{3584}{5}\hat{\omega}_1^2 - \frac{736}{5}\hat{\omega}_4\bigg) \\
&+ \hat{r}_1 \hat{\mathrm{F}}_{16,6,10,1}\bigg(\frac{1184}{15}\hat{\omega}_1 + \frac{3584}{15}\hat{\omega}_1^2 - \frac{736}{15}\hat{\omega}_4\bigg) \\
&+ \hat{r}_1 \hat{\mathrm{F}}_{16,6,10,3}\bigg(- \frac{1184}{15}\hat{\omega}_1 - \frac{3584}{15}\hat{\omega}_1^2 + \frac{736}{15}\hat{\omega}_4\bigg) \\
&+ \hat{r}_1 \hat{G}_3 \mathrm{C}_{3,11,1}\bigg(- \frac{19}{480} - \frac{19}{320}\hat{x} - \frac{119}{72}\hat{\omega}_1 - \frac{481}{90}\hat{\omega}_1^2 - \frac{8}{5}\hat{\omega}_1^3 - \frac{16}{5}\hat{\omega}_1^4 - \frac{11}{60}\hat{\omega}_4 \\
&\qquad + \frac{1}{4}\hat{\omega}_4^2\bigg) \\
&+ \hat{r}_1 \hat{G}_3 \hat{\mathrm{F}}_{16,6,6}\bigg(- \frac{76}{15} - \frac{38}{5}\hat{x} - \frac{1904}{9}\hat{\omega}_1 - \frac{30784}{45}\hat{\omega}_1^2 - \frac{1024}{5}\hat{\omega}_1^3 - \frac{2048}{5}\hat{\omega}_1^4 \\
&\qquad - \frac{352}{15}\hat{\omega}_4 + 32\hat{\omega}_4^2\bigg) \\
&+ \hat{r}_2 \hat{\mathrm{F}}_{16,6}\bigg(\frac{34}{45} - \frac{28}{9}\hat{x} + \frac{1424}{45}\hat{\omega}_1 + \frac{8}{3}\hat{\omega}_1^2 + \frac{64}{5}\hat{\omega}_1^3 - \frac{224}{45}\hat{\omega}_4 - \frac{968}{45}\hat{\omega}_4^2 \\
&\qquad - \frac{32}{15}\hat{\omega}_4^3\bigg) \\
&+ \hat{\varpi}_0^{-1} \hat{\mathrm{F}}_{16}\bigg(\frac{62}{15} + \frac{28}{9}\hat{x} - \frac{1724}{15}\hat{\omega}_1 + \frac{112}{9}\hat{\omega}_1^2 + \frac{128}{5}\hat{\omega}_1^3 + \frac{124}{45}\hat{\omega}_4 \\
&\qquad + \frac{16}{15}\hat{\omega}_4^2\bigg) \\
&+ \hat{r}_2 \hat{\varpi}_0^{-1} \dot{\hat{\varpi}}_0 \hat{\mathrm{F}}_{16,6}\bigg(- \frac{5048}{45} + \frac{62}{15}\hat{x} + \frac{28}{9}\hat{x}^2 + \frac{112}{9}\hat{\omega}_1 + \frac{128}{5}\hat{\omega}_1^2 - \frac{448}{45}\hat{\omega}_4 \\
&\qquad - \frac{64}{15}\hat{\omega}_4^2\bigg) \\
&+ \hat{\varpi}_0^{-1} \dot{\hat{\varpi}}_0^2 \mathrm{C}_{3,11,1}\bigg(\frac{221}{45} - \frac{497}{18}\hat{x} - \frac{1853}{240}\hat{x}^2 + \frac{53}{80}\hat{x}^3 + \frac{1493}{5760}\hat{x}^4 + \frac{7}{576}\hat{x}^5 + \frac{32}{5}\hat{\omega}_1
\end{aligned}
$$

$$
\begin{aligned}
&+\frac{4}{5}\hat{\omega}_4\Big) \\
&+\hat{\varpi}_0^{-1}\dot{\hat{\varpi}}_0^2\hat{\mathrm{F}}_{16,6,6}\Big(\frac{28288}{45}-\frac{31808}{9}\hat{x}-\frac{14824}{15}\hat{x}^2+\frac{424}{5}\hat{x}^3+\frac{1493}{45}\hat{x}^4+\frac{14}{9}\hat{x}^5 \\
&\quad+\frac{4096}{5}\hat{\omega}_1+\frac{512}{5}\hat{\omega}_4\Big) \\
&+\dot{\hat{\varpi}}_0\mathrm{C}_{3,11,1}\Big(\frac{515}{36}+\frac{1639}{360}\hat{x}-\frac{59}{48}\hat{x}^2-\frac{461}{960}\hat{x}^3-\frac{7}{288}\hat{x}^4+\frac{10}{3}\hat{\omega}_1+\frac{32}{5}\hat{\omega}_1^2 \\
&\quad+\frac{119}{15}\hat{\omega}_4+\frac{4}{5}\hat{\omega}_4^2\Big) \\
&+\dot{\hat{\varpi}}_0\hat{\mathrm{F}}_{16,6,6}\Big(\frac{16480}{9}+\frac{26224}{45}\hat{x}-\frac{472}{3}\hat{x}^2-\frac{922}{15}\hat{x}^3-\frac{28}{9}\hat{x}^4+\frac{1280}{3}\hat{\omega}_1 \\
&\quad+\frac{4096}{5}\hat{\omega}_1^2+\frac{15232}{15}\hat{\omega}_4+\frac{512}{5}\hat{\omega}_4^2\Big) \\
&+\hat{\varpi}_0\mathrm{C}_{3,11,1}\Big(\frac{29}{16}+\frac{119}{288}\hat{x}+\frac{323}{1152}\hat{x}^2+\frac{7}{576}\hat{x}^3+\frac{163}{90}\hat{\omega}_1+\frac{4}{5}\hat{\omega}_1^2+\frac{16}{5}\hat{\omega}_1^3 \\
&\quad-\frac{41}{18}\hat{\omega}_4+\frac{46}{15}\hat{\omega}_4^2\Big) \\
&+\hat{\varpi}_0\hat{\mathrm{F}}_{16,6,6}\Big(232+\frac{476}{9}\hat{x}+\frac{323}{9}\hat{x}^2+\frac{14}{9}\hat{x}^3+\frac{10432}{45}\hat{\omega}_1+\frac{512}{5}\hat{\omega}_1^2 \\
&\quad+\frac{2048}{5}\hat{\omega}_1^3-\frac{2624}{9}\hat{\omega}_4+\frac{5888}{15}\hat{\omega}_4^2\Big)\Big]+\cdots
\end{aligned}
\tag{5.53}
$$

5.4 Conclusion

Heavy-quark production in deep-inelastic scattering has been investigated here for neutral, charged and scalar currents. For the neutral current, the first eleven even Mellin moments of the VV contribution were obtained at NLO [211]. It was found that AA and VV contributions agree only at LO as a consequence of the chiral anomaly. However, agreement is restored in the limit of vanishing masses where chiral symmetry is recovered.

At NNLO, the first even Mellin moment was determined, where the earliest elliptic structures in the neutral current case emerge through the K3 cohomology underlying the Picard–Fuchs operator of the three-loop banana integral [217–219]. The charged current case was treated in direct analogy, although elliptic structures already appear at two loops via the two-loop banana subtopology [234, 236, 237]. A scalar current was also computed, serving as a consistency check of the setup, both through gauge invariance and through the renormalisation of the additional Yukawa operator.

Many of the master integrals obtained along the way suffice for a range of further structure functions, remaining unaffected by changes of the projectors. Beyond deep-inelastic scattering, these same integrals serve the study of QCD self-energies in the presence of heavy quarks [133].

Computation of higher moments at NNLO is a natural first extension, both for the VV contribution and for the AV and AA contributions, the latter pair still undetermined. Such contributions gain phenomenological weight in light of the Electron–Ion Collider [26, 27], where Z-boson exchange and parity-violating observables become accessible and where the projected experimental precision on heavy-flavour observables demands theory beyond NLO. On the charged current side, the same holds for the neutrino programmes at the intensity frontier, most notably the SHiP facility at the CERN SPS [257], whose neutrino-interaction data will probe charm production in charged current scattering at momentum transfers where the full mass dependence of the coefficient functions is indispensable. Conceptually the calculation should be straightforward, since no new master integrals arise and the IBP tables already assembled cover most, if not all, of the integrals encountered. This same reasoning carries over to polarised scattering, where no structural difference appears at the amplitude level and only the projectors require adjustment. Polarised coefficient functions may at first appear as low-hanging fruit, yet in the presence of masses the additional γ_5 insertions bring the full subtleties of dimensional regularisation and of the axial anomaly [258, 259], rendering them both more demanding and physically more intriguing than a first glance suggests.

The Mellin moments may be used to improve the approximate parametrisations of the coefficient functions at NNLO [87,260], in the same spirit in which fixed moments have long sharpened massless analyses, although an analytic reconstruction may be out of the question, given the complexity of the moments.

Pushing to higher moments is obstructed chiefly by the IBP reduction itself. Already at the fourth moment the Laporta algorithm becomes unfeasible, owing to the proliferation of dotted propagators alongside the many scalar products appearing in the numerators. Memory on the order of terabytes is demanded by the reductions at this stage. Progress will most plausibly come from improved reduction strategies, for instance a fully symbolic reduction within FORM [139], by analogy with the FORCER framework [171], which trades the memory bottleneck for a more manageable demand on disk space.

Even the moments already obtained retain significant value for this purpose, although two caveats should be noted. The present results are fully inclusive. In particular, for neutral current final states, configurations containing two and four heavy quarks cannot be separated. Similarly, for charged currents, contributions with one and three heavy quarks are not distinguished.

Furthermore, the Mellin moments computed in this work are valid for all strictly positive $\hat{x}$, although the evaluation of the iterated integrals may not be straightforward. This reflects the singularity structure of the amplitude. While no singularities are present in the deep-inelastic scattering regime, singularities do occur in the physical region and constrain the radius of convergence of series expansions of the iterated integrals and the associated periods. As a result, several expansions are required to cover the full kinematic range. One caveat is that, at each stage, it must be verified that expansions respect the Picard–Fuchs equations used to derive the ε-factorised form of the master integrals [220, 230]. Otherwise the construction would become inconsistent.

Extension to four loops is a further natural step (see Fig. 5.1), where the same formalism applies, in particular because a single momentum routing suffices to cover all independent graphs. Four loops nonetheless remain out of reach for the moment, as the IBP reductions become a severe bottleneck. No new elliptic curves are expected for the neutral current, since all elliptic contributions should descend from the two- and three-loop banana subtopologies. More interesting is the charged current, where the four-loop banana subtopology appears for the first time and brings with it Calabi–Yau threefolds [218, 219, 224]. Unlike the K3 surfaces of three loops, these threefolds are genuinely new objects, since their Picard–Fuchs operators are no longer symmetric squares of second-order operators, so a richer class of special functions must be anticipated.

Scattering of heavy quarks with two distinct masses offers a further, phenomenologically motivated direction, relevant wherever the charm and bottom scales act together, as studied at asymptotic virtualities in Ref. [64, 65, 67, 68, 261]. Here the set-covering construction extends to that case almost verbatim, the only change being a move from a binary to a ternary basis.

As a closing and more mathematical remark, this work ranks amongst the first applications of the method of differential equations [97, 99, 100, 189] involving elliptic integrals at NNLO to a physical observable in deep-inelastic scattering, confirming in a genuine QCD setting many structural observations previously made only for QED propagator-type integrals [215, 238].

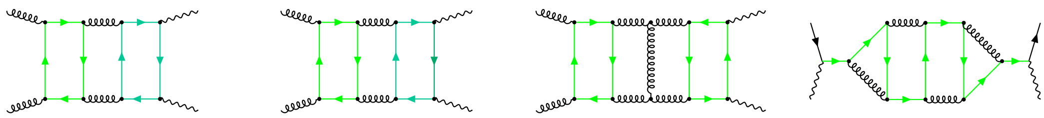

Figure 5.1: The graphs on the left show contributions to the forward scattering amplitude involving two and three distinct heavy quarks in the neutral current, where the quark masses are indicated by different shades of green. The two graphs on the right show the extension to four loops: in the neutral current case, only four heavy-quark cuts are present, whereas in the charged current case five heavy-quark cuts appear, opening the door to new geometries.

(This page is intentionally left blank.)

Adapted from J. Tenniel, "Shower of Playing Cards," in Lewis Carroll, Alice's Adventures in Wonderland (1865).

Appendix A

Integrals

A.1 Neutral Current

Table A.1: Master integrals contributing to the moments of the neutral current through three loops, ordered by their e-values. For each master integral, its factorisation, its sector symmetries and a single representative are provided.

Int.	Family	Weights	Sector Symmetries	Factors
$I^{\rm NC}_{1,1}$	$B^{\rm NC}_{1,3}$	$(1,0)$	$(B^{\rm NC}_{1,3})$	–
$I^{\rm NC}_{1,2}$	$B^{\rm NC}_{1,3}$	$(1,1)$	$(B^{\rm NC}_{1,3})$	–
$I^{\rm NC}_{1,3}$	$B^{\rm NC}_{1,0}$	$(1,1)$	$(B^{\rm NC}_{1,0})$	–
$I^{\rm NC}_{2,01}$	$B^{\rm NC}_{2,30}$	$(1,0,1,0,0)$	$(B^{\rm NC}_{2,07},\, B^{\rm NC}_{2,30})$	$(I^{\rm NC}_{1,1})^2$
$I^{\rm NC}_{2,02}$	$B^{\rm NC}_{2,30}$	$(1,1,1,0,0)$	$(B^{\rm NC}_{2,07},\, B^{\rm NC}_{2,30})$	$I^{\rm NC}_{1,1}\ I^{\rm NC}_{1,2}$
$I^{\rm NC}_{2,03}$	$B^{\rm NC}_{2,30}$	$(0,1,1,0,1)$	$(B^{\rm NC}_{2,07},\, B^{\rm NC}_{2,30})$	–
$I^{\rm NC}_{2,04}$	$B^{\rm NC}_{2,30}$	$(0,1,1,0,2)$	$(B^{\rm NC}_{2,07},\, B^{\rm NC}_{2,30})$	–
$I^{\rm NC}_{2,05}$	$B^{\rm NC}_{2,07}$	$(1,1,0,0,1)$	$(B^{\rm NC}_{2,07})$	$I^{\rm NC}_{1,1}\ I^{\rm NC}_{1,3}$
$I^{\rm NC}_{2,06}$	$B^{\rm NC}_{2,00}$	$(0,1,1,0,1)$	$(B^{\rm NC}_{2,00})$	–
$I^{\rm NC}_{2,07}$	$B^{\rm NC}_{2,30}$	$(1,1,1,1,0)$	$(B^{\rm NC}_{2,30})$	$(I^{\rm NC}_{1,2})^2$
$I^{\rm NC}_{2,08}$	$B^{\rm NC}_{2,07}$	$(1,1,1,1,0)$	$(B^{\rm NC}_{2,07})$	$I^{\rm NC}_{1,2}\ I^{\rm NC}_{1,3}$
$I^{\rm NC}_{2,09}$	$B^{\rm NC}_{2,00}$	$(1,1,1,1,0)$	$(B^{\rm NC}_{2,00})$	$(I^{\rm NC}_{1,3})^2$
$I^{\rm NC}_{2,10}$	$B^{\rm NC}_{2,07}$	$(1,1,1,1,1)$	$(B^{\rm NC}_{2,07})$	–
$I^{\rm NC}_{3,01}$	$B^{\rm NC}_{3,027}$	$(0,0,0,0,1,0,0,1,1)$	$(B^{\rm NC}_{3,027},\, B^{\rm NC}_{3,103},\, B^{\rm NC}_{3,414},\, B^{\rm NC}_{3,482},\, B^{\rm NC}_{3,505})$	$(I^{\rm NC}_{1,1})^3$
$I^{\rm NC}_{3,02}$	$B^{\rm NC}_{3,027}$	$(0,1,1,0,1,0,1,0,0)$	$(B^{\rm NC}_{3,027},\, B^{\rm NC}_{3,482})$	$I^{\rm NC}_{1,1}\ I^{\rm NC}_{2,6}$
$I^{\rm NC}_{3,03}$	$B^{\rm NC}_{3,027}$	$(1,1,0,0,1,0,0,1,0)$	$(B^{\rm NC}_{3,027},\, B^{\rm NC}_{3,103},\, B^{\rm NC}_{3,414},\, B^{\rm NC}_{3,482})$	$(I^{\rm NC}_{1,1})^2\ I^{\rm NC}_{1,3}$
$I^{\rm NC}_{3,04}$	$B^{\rm NC}_{3,027}$	$(1,0,0,0,1,0,1,1,0)$	$(B^{\rm NC}_{3,027},\, B^{\rm NC}_{3,103},\, B^{\rm NC}_{3,414},\, B^{\rm NC}_{3,482},\, B^{\rm NC}_{3,505})$	–
$I^{\rm NC}_{3,05}$	$B^{\rm NC}_{3,027}$	$(0,1,0,0,2,0,1,1,0)$	$(B^{\rm NC}_{3,027},\, B^{\rm NC}_{3,103},\, B^{\rm NC}_{3,414},\, B^{\rm NC}_{3,482},\, B^{\rm NC}_{3,505})$	–
$I^{\rm NC}_{3,06}$	$B^{\rm NC}_{3,027}$	$(0,2,0,0,1,0,1,1,0)$	$(B^{\rm NC}_{3,027},\, B^{\rm NC}_{3,103},\, B^{\rm NC}_{3,414},\, B^{\rm NC}_{3,482},\, B^{\rm NC}_{3,505})$	–
$I^{\rm NC}_{3,07}$	$B^{\rm NC}_{3,027}$	$(0,1,0,0,1,0,1,1,0)$	$(B^{\rm NC}_{3,027},\, B^{\rm NC}_{3,103},\, B^{\rm NC}_{3,414},\, B^{\rm NC}_{3,482},\, B^{\rm NC}_{3,505})$	–
$I^{\rm NC}_{3,08}$	$B^{\rm NC}_{3,027}$	$(0,2,0,0,1,0,0,1,1)$	$(B^{\rm NC}_{3,027},\, B^{\rm NC}_{3,103},\, B^{\rm NC}_{3,414},\, B^{\rm NC}_{3,482},\, B^{\rm NC}_{3,505})$	$I^{\rm NC}_{1,1}\ I^{\rm NC}_{2,4}$
$I^{\rm NC}_{3,09}$	$B^{\rm NC}_{3,027}$	$(0,1,0,0,1,0,0,1,1)$	$(B^{\rm NC}_{3,027},\, B^{\rm NC}_{3,103},\, B^{\rm NC}_{3,414},\, B^{\rm NC}_{3,482},\, B^{\rm NC}_{3,505})$	$I^{\rm NC}_{1,1}\ I^{\rm NC}_{2,3}$
$I^{\rm NC}_{3,10}$	$B^{\rm NC}_{3,027}$	$(0,0,0,0,1,1,0,1,1)$	$(B^{\rm NC}_{3,027},\, B^{\rm NC}_{3,103},\, B^{\rm NC}_{3,414},\, B^{\rm NC}_{3,482},\, B^{\rm NC}_{3,505})$	$(I^{\rm NC}_{1,1})^2\ I^{\rm NC}_{1,2}$
$I^{\rm NC}_{3,11}$	$B^{\rm NC}_{3,414}$	$(1,0,0,0,1,0,1,1,0)$	$(B^{\rm NC}_{3,103},\, B^{\rm NC}_{3,414},\, B^{\rm NC}_{3,505})$	–
$I^{\rm NC}_{3,12}$	$B^{\rm NC}_{3,414}$	$(0,1,0,0,1,0,1,3,0)$	$(B^{\rm NC}_{3,103},\, B^{\rm NC}_{3,414},\, B^{\rm NC}_{3,505})$	–
$I^{\rm NC}_{3,13}$	$B^{\rm NC}_{3,414}$	$(0,1,0,0,1,0,1,2,0)$	$(B^{\rm NC}_{3,103},\, B^{\rm NC}_{3,414},\, B^{\rm NC}_{3,505})$	–
$I^{\rm NC}_{3,14}$	$B^{\rm NC}_{3,414}$	$(0,1,0,0,1,0,1,1,0)$	$(B^{\rm NC}_{3,103},\, B^{\rm NC}_{3,414},\, B^{\rm NC}_{3,505})$	–
$I^{\rm NC}_{3,15}$	$B^{\rm NC}_{3,000}$	$(0,1,0,0,1,0,1,1,0)$	$(B^{\rm NC}_{3,000})$	–
$I^{\rm NC}_{3,16}$	$B^{\rm NC}_{3,027}$	$(1,1,1,1,1,0,0,0,0)$	$(B^{\rm NC}_{3,027},\, B^{\rm NC}_{3,103})$	$I^{\rm NC}_{1,1}\ (I^{\rm NC}_{1,3})^2$
$I^{\rm NC}_{3,17}$	$B^{\rm NC}_{3,027}$	$(0,1,1,0,1,1,1,0,0)$	$(B^{\rm NC}_{3,027},\, B^{\rm NC}_{3,482})$	$I^{\rm NC}_{1,2}\ I^{\rm NC}_{2,6}$

Continued on next page

Int.	Family	Weights	Sector Symmetries	Factors
$I^{\mathrm{NC}}_{3,18}$	$B^{\mathrm{NC}}_{3,027}$	$(1,1,0,1,1,0,0,1,0)$	$(B^{\mathrm{NC}}_{3,027},\, B^{\mathrm{NC}}_{3,103},\, B^{\mathrm{NC}}_{3,482})$	$I^{\mathrm{NC}}_{1,3}\ I^{\mathrm{NC}}_{2,3}$
$I^{\mathrm{NC}}_{3,19}$	$B^{\mathrm{NC}}_{3,027}$	$(1,1,0,1,2,0,0,1,0)$	$(B^{\mathrm{NC}}_{3,027},\, B^{\mathrm{NC}}_{3,103},\, B^{\mathrm{NC}}_{3,482})$	IBP
$I^{\mathrm{NC}}_{3,20}$	$B^{\mathrm{NC}}_{3,027}$	$(1,1,0,0,1,1,0,1,0)$	$(B^{\mathrm{NC}}_{3,027},\, B^{\mathrm{NC}}_{3,414},\, B^{\mathrm{NC}}_{3,482})$	$I^{\mathrm{NC}}_{1,1}\ I^{\mathrm{NC}}_{1,2}\ I^{\mathrm{NC}}_{1,3}$
$I^{\mathrm{NC}}_{3,21}$	$B^{\mathrm{NC}}_{3,027}$	$(2,0,0,1,1,0,1,1,0)$	$(B^{\mathrm{NC}}_{3,027},\, B^{\mathrm{NC}}_{3,482})$	–
$I^{\mathrm{NC}}_{3,22}$	$B^{\mathrm{NC}}_{3,027}$	$(1,0,0,1,1,0,1,1,0)$	$(B^{\mathrm{NC}}_{3,027},\, B^{\mathrm{NC}}_{3,482})$	–
$I^{\mathrm{NC}}_{3,23}$	$B^{\mathrm{NC}}_{3,027}$	$(1,0,0,0,1,1,1,1,0)$	$(B^{\mathrm{NC}}_{3,027},\, B^{\mathrm{NC}}_{3,103},\, B^{\mathrm{NC}}_{3,414},\, B^{\mathrm{NC}}_{3,482},\, B^{\mathrm{NC}}_{3,505})$	–
$I^{\mathrm{NC}}_{3,24}$	$B^{\mathrm{NC}}_{3,027}$	$(0,1,0,1,1,0,0,2,1)$	$(B^{\mathrm{NC}}_{3,027},\, B^{\mathrm{NC}}_{3,103},\, B^{\mathrm{NC}}_{3,414},\, B^{\mathrm{NC}}_{3,482},\, B^{\mathrm{NC}}_{3,505})$	–
$I^{\mathrm{NC}}_{3,25}$	$B^{\mathrm{NC}}_{3,027}$	$(0,1,0,1,2,0,0,1,1)$	$(B^{\mathrm{NC}}_{3,027},\, B^{\mathrm{NC}}_{3,103},\, B^{\mathrm{NC}}_{3,414},\, B^{\mathrm{NC}}_{3,482},\, B^{\mathrm{NC}}_{3,505})$	–
$I^{\mathrm{NC}}_{3,26}$	$B^{\mathrm{NC}}_{3,027}$	$(0,1,0,1,1,0,0,1,1)$	$(B^{\mathrm{NC}}_{3,027},\, B^{\mathrm{NC}}_{3,103},\, B^{\mathrm{NC}}_{3,414},\, B^{\mathrm{NC}}_{3,482},\, B^{\mathrm{NC}}_{3,505})$	–
$I^{\mathrm{NC}}_{3,27}$	$B^{\mathrm{NC}}_{3,414}$	$(1,0,0,2,1,0,1,1,0)$	$(B^{\mathrm{NC}}_{3,103},\, B^{\mathrm{NC}}_{3,414},\, B^{\mathrm{NC}}_{3,505})$	–
$I^{\mathrm{NC}}_{3,28}$	$B^{\mathrm{NC}}_{3,414}$	$(1,0,0,1,1,0,1,1,0)$	$(B^{\mathrm{NC}}_{3,103},\, B^{\mathrm{NC}}_{3,414},\, B^{\mathrm{NC}}_{3,505})$	–
$I^{\mathrm{NC}}_{3,29}$	$B^{\mathrm{NC}}_{3,414}$	$(1,1,0,0,1,0,1,1,0)$	$(B^{\mathrm{NC}}_{3,103},\, B^{\mathrm{NC}}_{3,414},\, B^{\mathrm{NC}}_{3,505})$	–
$I^{\mathrm{NC}}_{3,30}$	$B^{\mathrm{NC}}_{3,482}$	$(1,1,1,1,0,0,0,1,0)$	$(B^{\mathrm{NC}}_{3,414},\, B^{\mathrm{NC}}_{3,482},\, B^{\mathrm{NC}}_{3,505})$	$I^{\mathrm{NC}}_{1,1}\ (I^{\mathrm{NC}}_{1,2})^2$
$I^{\mathrm{NC}}_{3,31}$	$B^{\mathrm{NC}}_{3,482}$	$(1,1,0,2,1,0,0,1,0)$	$(B^{\mathrm{NC}}_{3,414},\, B^{\mathrm{NC}}_{3,482},\, B^{\mathrm{NC}}_{3,505})$	IBP
$I^{\mathrm{NC}}_{3,32}$	$B^{\mathrm{NC}}_{3,482}$	$(1,1,0,1,1,0,0,1,0)$	$(B^{\mathrm{NC}}_{3,414},\, B^{\mathrm{NC}}_{3,482},\, B^{\mathrm{NC}}_{3,505})$	$I^{\mathrm{NC}}_{1,2}\ I^{\mathrm{NC}}_{2,3}$
$I^{\mathrm{NC}}_{3,33}$	$B^{\mathrm{NC}}_{3,000}$	$(0,1,1,0,1,1,1,0,0)$	$(B^{\mathrm{NC}}_{3,000})$	$I^{\mathrm{NC}}_{1,3}\ I^{\mathrm{NC}}_{2,6}$
$I^{\mathrm{NC}}_{3,34}$	$B^{\mathrm{NC}}_{3,000}$	$(1,0,0,1,1,0,1,1,0)$	$(B^{\mathrm{NC}}_{3,000})$	–
$I^{\mathrm{NC}}_{3,35}$	$B^{\mathrm{NC}}_{3,027}$	$(1,1,1,1,1,1,0,0,0)$	$(B^{\mathrm{NC}}_{3,027})$	$I^{\mathrm{NC}}_{1,2}\ (I^{\mathrm{NC}}_{1,3})^2$
$I^{\mathrm{NC}}_{3,36}$	$B^{\mathrm{NC}}_{3,027}$	$(1,1,0,0,2,1,1,1,0)$	$(B^{\mathrm{NC}}_{3,027},\, B^{\mathrm{NC}}_{3,482})$	–
$I^{\mathrm{NC}}_{3,37}$	$B^{\mathrm{NC}}_{3,027}$	$(2,1,0,0,1,1,1,1,0)$	$(B^{\mathrm{NC}}_{3,027},\, B^{\mathrm{NC}}_{3,482})$	–
$I^{\mathrm{NC}}_{3,38}$	$B^{\mathrm{NC}}_{3,027}$	$(1,1,0,0,1,1,1,1,0)$	$(B^{\mathrm{NC}}_{3,027},\, B^{\mathrm{NC}}_{3,482})$	–
$I^{\mathrm{NC}}_{3,39}$	$B^{\mathrm{NC}}_{3,027}$	$(0,1,1,0,1,1,1,1,0)$	$(B^{\mathrm{NC}}_{3,027},\, B^{\mathrm{NC}}_{3,482})$	–
$I^{\mathrm{NC}}_{3,40}$	$B^{\mathrm{NC}}_{3,027}$	$(2,1,1,1,1,0,0,0,1)$	$(B^{\mathrm{NC}}_{3,027})$	–
$I^{\mathrm{NC}}_{3,41}$	$B^{\mathrm{NC}}_{3,027}$	$(1,1,1,1,1,0,0,0,1)$	$(B^{\mathrm{NC}}_{3,027})$	–
$I^{\mathrm{NC}}_{3,42}$	$B^{\mathrm{NC}}_{3,027}$	$(1,1,0,1,1,0,0,1,1)$	$(B^{\mathrm{NC}}_{3,027},\, B^{\mathrm{NC}}_{3,482})$	–
$I^{\mathrm{NC}}_{3,43}$	$B^{\mathrm{NC}}_{3,027}$	$(0,0,1,1,1,1,0,1,1)$	$(B^{\mathrm{NC}}_{3,027},\, B^{\mathrm{NC}}_{3,414},\, B^{\mathrm{NC}}_{3,482})$	$I^{\mathrm{NC}}_{1,1}\ I^{\mathrm{NC}}_{2,10}$
$I^{\mathrm{NC}}_{3,44}$	$B^{\mathrm{NC}}_{3,027}$	$(0,1,1,0,1,0,1,1,1)$	$(B^{\mathrm{NC}}_{3,027},\, B^{\mathrm{NC}}_{3,482})$	–
$I^{\mathrm{NC}}_{3,45}$	$B^{\mathrm{NC}}_{3,414}$	$(0,1,1,0,2,0,1,1,1)$	$(B^{\mathrm{NC}}_{3,103},\, B^{\mathrm{NC}}_{3,414},\, B^{\mathrm{NC}}_{3,505})$	–
$I^{\mathrm{NC}}_{3,46}$	$B^{\mathrm{NC}}_{3,414}$	$(0,2,1,0,1,0,1,1,1)$	$(B^{\mathrm{NC}}_{3,103},\, B^{\mathrm{NC}}_{3,414},\, B^{\mathrm{NC}}_{3,505})$	–
$I^{\mathrm{NC}}_{3,47}$	$B^{\mathrm{NC}}_{3,414}$	$(0,3,1,0,1,0,1,1,1)$	$(B^{\mathrm{NC}}_{3,103},\, B^{\mathrm{NC}}_{3,414},\, B^{\mathrm{NC}}_{3,505})$	–
$I^{\mathrm{NC}}_{3,48}$	$B^{\mathrm{NC}}_{3,414}$	$(1,1,1,1,1,1,0,0,0)$	$(B^{\mathrm{NC}}_{3,414})$	$(I^{\mathrm{NC}}_{1,2})^2\ I^{\mathrm{NC}}_{1,3}$
$I^{\mathrm{NC}}_{3,49}$	$B^{\mathrm{NC}}_{3,414}$	$(1,1,0,1,1,0,1,1,0)$	$(B^{\mathrm{NC}}_{3,414},\, B^{\mathrm{NC}}_{3,505})$	–
$I^{\mathrm{NC}}_{3,50}$	$B^{\mathrm{NC}}_{3,414}$	$(1,1,0,1,2,0,1,1,0)$	$(B^{\mathrm{NC}}_{3,414},\, B^{\mathrm{NC}}_{3,505})$	–
$I^{\mathrm{NC}}_{3,51}$	$B^{\mathrm{NC}}_{3,414}$	$(1,1,0,0,1,1,2,1,0)$	$(B^{\mathrm{NC}}_{3,414},\, B^{\mathrm{NC}}_{3,505})$	–
$I^{\mathrm{NC}}_{3,52}$	$B^{\mathrm{NC}}_{3,414}$	$(1,1,0,0,1,1,1,1,0)$	$(B^{\mathrm{NC}}_{3,414},\, B^{\mathrm{NC}}_{3,505})$	–
$I^{\mathrm{NC}}_{3,53}$	$B^{\mathrm{NC}}_{3,482}$	$(1,1,0,1,1,0,1,1,0)$	$(B^{\mathrm{NC}}_{3,482},\, B^{\mathrm{NC}}_{3,505})$	–
$I^{\mathrm{NC}}_{3,54}$	$B^{\mathrm{NC}}_{3,482}$	$(1,1,1,1,1,0,0,0,1)$	$(B^{\mathrm{NC}}_{3,482},\, B^{\mathrm{NC}}_{3,505})$	–
$I^{\mathrm{NC}}_{3,55}$	$B^{\mathrm{NC}}_{3,505}$	$(1,1,1,1,1,1,0,0,0)$	$(B^{\mathrm{NC}}_{3,505})$	$(I^{\mathrm{NC}}_{1,2})^3$
$I^{\mathrm{NC}}_{3,56}$	$B^{\mathrm{NC}}_{3,000}$	$(1,1,1,1,1,1,0,0,0)$	$(B^{\mathrm{NC}}_{3,000})$	$(I^{\mathrm{NC}}_{1,3})^3$
$I^{\mathrm{NC}}_{3,57}$	$B^{\mathrm{NC}}_{3,000}$	$(1,1,0,0,1,1,1,1,0)$	$(B^{\mathrm{NC}}_{3,000})$	–
$I^{\mathrm{NC}}_{3,58}$	$B^{\mathrm{NC}}_{3,027}$	$(1,1,1,1,1,1,0,1,0)$	$(B^{\mathrm{NC}}_{3,027})$	$I^{\mathrm{NC}}_{1,3}\ I^{\mathrm{NC}}_{2,10}$
$I^{\mathrm{NC}}_{3,59}$	$B^{\mathrm{NC}}_{3,027}$	$(1,1,1,1,1,0,0,1,1)$	$(B^{\mathrm{NC}}_{3,027})$	–
$I^{\mathrm{NC}}_{3,60}$	$B^{\mathrm{NC}}_{3,027}$	$(2,0,0,1,1,1,1,1,1)$	$(B^{\mathrm{NC}}_{3,027},\, B^{\mathrm{NC}}_{3,482})$	–
$I^{\mathrm{NC}}_{3,61}$	$B^{\mathrm{NC}}_{3,027}$	$(1,0,0,1,1,1,1,1,1)$	$(B^{\mathrm{NC}}_{3,027},\, B^{\mathrm{NC}}_{3,482})$	–
$I^{\mathrm{NC}}_{3,62}$	$B^{\mathrm{NC}}_{3,414}$	$(1,1,1,1,1,1,1,0,0)$	$(B^{\mathrm{NC}}_{3,414})$	$I^{\mathrm{NC}}_{1,2}\ I^{\mathrm{NC}}_{2,10}$
$I^{\mathrm{NC}}_{3,63}$	$B^{\mathrm{NC}}_{3,482}$	$(1,2,1,0,1,1,1,1,0)$	$(B^{\mathrm{NC}}_{3,482})$	–
$I^{\mathrm{NC}}_{3,64}$	$B^{\mathrm{NC}}_{3,482}$	$(1,1,1,0,1,1,1,1,0)$	$(B^{\mathrm{NC}}_{3,482})$	–
$I^{\mathrm{NC}}_{3,65}$	$B^{\mathrm{NC}}_{3,482}$	$(1,1,1,1,1,0,0,1,1)$	$(B^{\mathrm{NC}}_{3,482},\, B^{\mathrm{NC}}_{3,505})$	–
$I^{\mathrm{NC}}_{3,66}$	$B^{\mathrm{NC}}_{3,482}$	$(1,1,1,1,2,0,0,1,1)$	$(B^{\mathrm{NC}}_{3,482},\, B^{\mathrm{NC}}_{3,505})$	–
$I^{\mathrm{NC}}_{3,67}$	$B^{\mathrm{NC}}_{3,414}$	$(1,1,1,1,1,1,1,1,0)$	$(B^{\mathrm{NC}}_{3,414})$	–
$I^{\mathrm{NC}}_{3,68}$	$B^{\mathrm{NC}}_{3,482}$	$(1,1,0,1,1,1,1,1,1)$	$(B^{\mathrm{NC}}_{3,482})$	–
$I^{\mathrm{NC}}_{3,69}$	$B^{\mathrm{NC}}_{3,505}$	$(1,1,0,1,1,1,1,1,1)$	$(B^{\mathrm{NC}}_{3,505})$	–
$I^{\mathrm{NC}}_{3,70}$	$B^{\mathrm{NC}}_{3,505}$	$(2,1,0,1,1,1,1,1,1)$	$(B^{\mathrm{NC}}_{3,505})$	–
$I^{\mathrm{NC}}_{3,71}$	$B^{\mathrm{NC}}_{3,000}$	$(1,1,0,1,1,1,1,1,1)$	$(B^{\mathrm{NC}}_{3,000})$	–

A.2 Charged Current

Table A.2: Master integrals contributing to the moments of the charged current through three loops, ordered by their e-values. For each master integral, its factorisation, its sector symmetries and a single representative are provided.

Int.	Family	Weights	Sector Symmetries	Factors
$I^{\rm CC}_{1,1}$	$\mathcal{B}^{\rm CC}_{1,2}$	$(1,0)$	$(\mathcal{B}^{\rm CC}_{1,2})$	–
$I^{\rm CC}_{1,2}$	$\mathcal{B}^{\rm CC}_{1,2}$	$(1,1)$	$(\mathcal{B}^{\rm CC}_{1,2})$	–
$I^{\rm CC}_{2,1}$	$\mathcal{B}^{\rm CC}_{2,13}$	$(0,1,1,0,0)$	$(\mathcal{B}^{\rm CC}_{2,10},\mathcal{B}^{\rm CC}_{2,13})$	$(I^{\rm CC}_{1,1})^2$
$I^{\rm CC}_{2,2}$	$\mathcal{B}^{\rm CC}_{2,13}$	$(1,1,1,0,0)$	$(\mathcal{B}^{\rm CC}_{2,10},\mathcal{B}^{\rm CC}_{2,13})$	$I^{\rm CC}_{1,1}\ I^{\rm CC}_{1,2}$
$I^{\rm CC}_{2,3}$	$\mathcal{B}^{\rm CC}_{2,13}$	$(0,1,1,0,1)$	$(\mathcal{B}^{\rm CC}_{2,13})$	–
$I^{\rm CC}_{2,4}$	$\mathcal{B}^{\rm CC}_{2,13}$	$(0,2,1,0,1)$	$(\mathcal{B}^{\rm CC}_{2,13})$	–
$I^{\rm CC}_{2,5}$	$\mathcal{B}^{\rm CC}_{2,13}$	$(1,0,0,1,1)$	$(\mathcal{B}^{\rm CC}_{2,10},\mathcal{B}^{\rm CC}_{2,13})$	–
$I^{\rm CC}_{2,6}$	$\mathcal{B}^{\rm CC}_{2,13}$	$(1,0,0,1,2)$	$(\mathcal{B}^{\rm CC}_{2,10},\mathcal{B}^{\rm CC}_{2,13})$	–
$I^{\rm CC}_{2,7}$	$\mathcal{B}^{\rm CC}_{2,13}$	$(1,1,1,1,0)$	$(\mathcal{B}^{\rm CC}_{2,10},\mathcal{B}^{\rm CC}_{2,13})$	$(I^{\rm CC}_{1,2})^2$
$I^{\rm CC}_{2,8}$	$\mathcal{B}^{\rm CC}_{2,13}$	$(1,1,1,1,1)$	$(\mathcal{B}^{\rm CC}_{2,13})$	–
$I^{\rm CC}_{3,01}$	$\mathcal{B}^{\rm CC}_{3,179}$	$(0,1,0,1,1,0,0,0,0)$	$(\mathcal{B}^{\rm CC}_{3,168},\mathcal{B}^{\rm CC}_{3,179},\mathcal{B}^{\rm CC}_{3,207},\mathcal{B}^{\rm CC}_{3,310},\mathcal{B}^{\rm CC}_{3,330},\mathcal{B}^{\rm CC}_{3,337})$	$(I^{\rm CC}_{1,1})^3$
$I^{\rm CC}_{3,02}$	$\mathcal{B}^{\rm CC}_{3,179}$	$(1,1,0,1,1,0,0,0,0)$	$(\mathcal{B}^{\rm CC}_{3,168},\mathcal{B}^{\rm CC}_{3,179},\mathcal{B}^{\rm CC}_{3,207},\mathcal{B}^{\rm CC}_{3,310},\mathcal{B}^{\rm CC}_{3,330},\mathcal{B}^{\rm CC}_{3,337})$	$(I^{\rm CC}_{1,1})^2\ I^{\rm CC}_{1,2}$
$I^{\rm CC}_{3,03}$	$\mathcal{B}^{\rm CC}_{3,179}$	$(0,1,1,0,1,0,1,0,0)$	$(\mathcal{B}^{\rm CC}_{3,168},\mathcal{B}^{\rm CC}_{3,179},\mathcal{B}^{\rm CC}_{3,207},\mathcal{B}^{\rm CC}_{3,310},\mathcal{B}^{\rm CC}_{3,330},\mathcal{B}^{\rm CC}_{3,337})$	$(I^{\rm CC}_{1,1})\ I^{\rm CC}_{2,5}$
$I^{\rm CC}_{3,04}$	$\mathcal{B}^{\rm CC}_{3,179}$	$(0,2,1,0,1,0,1,0,0)$	$(\mathcal{B}^{\rm CC}_{3,168},\mathcal{B}^{\rm CC}_{3,179},\mathcal{B}^{\rm CC}_{3,207},\mathcal{B}^{\rm CC}_{3,310},\mathcal{B}^{\rm CC}_{3,330},\mathcal{B}^{\rm CC}_{3,337})$	$(I^{\rm CC}_{1,1})\ I^{\rm CC}_{2,6}$
$I^{\rm CC}_{3,05}$	$\mathcal{B}^{\rm CC}_{3,179}$	$(0,1,0,1,1,0,0,1,0)$	$(\mathcal{B}^{\rm CC}_{3,179},\mathcal{B}^{\rm CC}_{3,207},\mathcal{B}^{\rm CC}_{3,310},\mathcal{B}^{\rm CC}_{3,330})$	$(I^{\rm CC}_{1,1})\ I^{\rm CC}_{2,3}$
$I^{\rm CC}_{3,06}$	$\mathcal{B}^{\rm CC}_{3,179}$	$(0,1,0,2,1,0,0,1,0)$	$(\mathcal{B}^{\rm CC}_{3,179},\mathcal{B}^{\rm CC}_{3,207},\mathcal{B}^{\rm CC}_{3,310},\mathcal{B}^{\rm CC}_{3,330})$	$(I^{\rm CC}_{1,1})\ I^{\rm CC}_{2,4}$
$I^{\rm CC}_{3,07}$	$\mathcal{B}^{\rm CC}_{3,179}$	$(1,0,0,0,1,0,1,1,0)$	$(\mathcal{B}^{\rm CC}_{3,168},\mathcal{B}^{\rm CC}_{3,179},\mathcal{B}^{\rm CC}_{3,207},\mathcal{B}^{\rm CC}_{3,310},\mathcal{B}^{\rm CC}_{3,330},\mathcal{B}^{\rm CC}_{3,337})$	–
$I^{\rm CC}_{3,08}$	$\mathcal{B}^{\rm CC}_{3,179}$	$(1,0,0,0,0,1,1,1,0)$	$(\mathcal{B}^{\rm CC}_{3,168},\mathcal{B}^{\rm CC}_{3,179},\mathcal{B}^{\rm CC}_{3,207},\mathcal{B}^{\rm CC}_{3,310},\mathcal{B}^{\rm CC}_{3,330},\mathcal{B}^{\rm CC}_{3,337})$	–
$I^{\rm CC}_{3,09}$	$\mathcal{B}^{\rm CC}_{3,179}$	$(1,0,0,0,0,1,1,2,0)$	$(\mathcal{B}^{\rm CC}_{3,168},\mathcal{B}^{\rm CC}_{3,179},\mathcal{B}^{\rm CC}_{3,207},\mathcal{B}^{\rm CC}_{3,310},\mathcal{B}^{\rm CC}_{3,330},\mathcal{B}^{\rm CC}_{3,337})$	–
$I^{\rm CC}_{3,10}$	$\mathcal{B}^{\rm CC}_{3,179}$	$(0,1,0,0,1,0,1,1,0)$	$(\mathcal{B}^{\rm CC}_{3,179},\mathcal{B}^{\rm CC}_{3,207},\mathcal{B}^{\rm CC}_{3,310},\mathcal{B}^{\rm CC}_{3,330},\mathcal{B}^{\rm CC}_{3,337})$	–
$I^{\rm CC}_{3,11}$	$\mathcal{B}^{\rm CC}_{3,179}$	$(0,1,0,0,1,0,2,1,0)$	$(\mathcal{B}^{\rm CC}_{3,179},\mathcal{B}^{\rm CC}_{3,207},\mathcal{B}^{\rm CC}_{3,310},\mathcal{B}^{\rm CC}_{3,330},\mathcal{B}^{\rm CC}_{3,337})$	–
$I^{\rm CC}_{3,12}$	$\mathcal{B}^{\rm CC}_{3,179}$	$(0,2,0,0,1,0,1,1,0)$	$(\mathcal{B}^{\rm CC}_{3,179},\mathcal{B}^{\rm CC}_{3,207},\mathcal{B}^{\rm CC}_{3,310},\mathcal{B}^{\rm CC}_{3,330},\mathcal{B}^{\rm CC}_{3,337})$	–
$I^{\rm CC}_{3,13}$	$\mathcal{B}^{\rm CC}_{3,179}$	$(0,1,0,1,1,0,0,0,1)$	$(\mathcal{B}^{\rm CC}_{3,179},\mathcal{B}^{\rm CC}_{3,207},\mathcal{B}^{\rm CC}_{3,310},\mathcal{B}^{\rm CC}_{3,337})$	–
$I^{\rm CC}_{3,14}$	$\mathcal{B}^{\rm CC}_{3,179}$	$(1,1,1,1,1,0,0,0,0)$	$(\mathcal{B}^{\rm CC}_{3,168},\mathcal{B}^{\rm CC}_{3,179},\mathcal{B}^{\rm CC}_{3,207},\mathcal{B}^{\rm CC}_{3,310},\mathcal{B}^{\rm CC}_{3,330},\mathcal{B}^{\rm CC}_{3,337})$	$I^{\rm CC}_{1,1}\ (I^{\rm CC}_{1,2})^2$
$I^{\rm CC}_{3,15}$	$\mathcal{B}^{\rm CC}_{3,179}$	$(0,1,1,0,1,1,1,0,0)$	$(\mathcal{B}^{\rm CC}_{3,168},\mathcal{B}^{\rm CC}_{3,179},\mathcal{B}^{\rm CC}_{3,207},\mathcal{B}^{\rm CC}_{3,310},\mathcal{B}^{\rm CC}_{3,330},\mathcal{B}^{\rm CC}_{3,337})$	$(I^{\rm CC}_{1,2})\ I^{\rm CC}_{2,5}$
$I^{\rm CC}_{3,16}$	$\mathcal{B}^{\rm CC}_{3,179}$	$(0,2,1,0,1,1,1,0,0)$	$(\mathcal{B}^{\rm CC}_{3,168},\mathcal{B}^{\rm CC}_{3,179},\mathcal{B}^{\rm CC}_{3,207},\mathcal{B}^{\rm CC}_{3,310},\mathcal{B}^{\rm CC}_{3,330},\mathcal{B}^{\rm CC}_{3,337})$	$(I^{\rm CC}_{1,2})\ I^{\rm CC}_{2,6}$
$I^{\rm CC}_{3,17}$	$\mathcal{B}^{\rm CC}_{3,179}$	$(1,1,0,1,1,0,0,1,0)$	$(\mathcal{B}^{\rm CC}_{3,179},\mathcal{B}^{\rm CC}_{3,207},\mathcal{B}^{\rm CC}_{3,310},\mathcal{B}^{\rm CC}_{3,330})$	$(I^{\rm CC}_{1,2})\ I^{\rm CC}_{2,3}$
$I^{\rm CC}_{3,18}$	$\mathcal{B}^{\rm CC}_{3,179}$	$(1,1,0,2,1,0,0,1,0)$	$(\mathcal{B}^{\rm CC}_{3,179},\mathcal{B}^{\rm CC}_{3,207},\mathcal{B}^{\rm CC}_{3,310},\mathcal{B}^{\rm CC}_{3,330})$	$(I^{\rm CC}_{1,2})\ I^{\rm CC}_{2,4}$
$I^{\rm CC}_{3,19}$	$\mathcal{B}^{\rm CC}_{3,179}$	$(1,0,0,0,1,1,1,1,0)$	$(\mathcal{B}^{\rm CC}_{3,168},\mathcal{B}^{\rm CC}_{3,179},\mathcal{B}^{\rm CC}_{3,207},\mathcal{B}^{\rm CC}_{3,310},\mathcal{B}^{\rm CC}_{3,330},\mathcal{B}^{\rm CC}_{3,337})$	–
$I^{\rm CC}_{3,20}$	$\mathcal{B}^{\rm CC}_{3,179}$	$(0,1,1,0,0,1,1,1,0)$	$(\mathcal{B}^{\rm CC}_{3,168},\mathcal{B}^{\rm CC}_{3,179},\mathcal{B}^{\rm CC}_{3,207},\mathcal{B}^{\rm CC}_{3,310},\mathcal{B}^{\rm CC}_{3,330},\mathcal{B}^{\rm CC}_{3,337})$	–
$I^{\rm CC}_{3,21}$	$\mathcal{B}^{\rm CC}_{3,179}$	$(0,2,1,0,0,1,1,1,0)$	$(\mathcal{B}^{\rm CC}_{3,168},\mathcal{B}^{\rm CC}_{3,179},\mathcal{B}^{\rm CC}_{3,207},\mathcal{B}^{\rm CC}_{3,310},\mathcal{B}^{\rm CC}_{3,330},\mathcal{B}^{\rm CC}_{3,337})$	–
$I^{\rm CC}_{3,22}$	$\mathcal{B}^{\rm CC}_{3,179}$	$(1,0,0,1,1,0,1,1,0)$	$(\mathcal{B}^{\rm CC}_{3,179},\mathcal{B}^{\rm CC}_{3,207},\mathcal{B}^{\rm CC}_{3,310},\mathcal{B}^{\rm CC}_{3,330})$	–
$I^{\rm CC}_{3,23}$	$\mathcal{B}^{\rm CC}_{3,179}$	$(1,0,0,2,1,0,1,1,0)$	$(\mathcal{B}^{\rm CC}_{3,179},\mathcal{B}^{\rm CC}_{3,207},\mathcal{B}^{\rm CC}_{3,310},\mathcal{B}^{\rm CC}_{3,330})$	–
$I^{\rm CC}_{3,24}$	$\mathcal{B}^{\rm CC}_{3,179}$	$(1,0,0,1,2,0,1,1,0)$	$(\mathcal{B}^{\rm CC}_{3,179},\mathcal{B}^{\rm CC}_{3,207},\mathcal{B}^{\rm CC}_{3,310},\mathcal{B}^{\rm CC}_{3,330})$	–
$I^{\rm CC}_{3,25}$	$\mathcal{B}^{\rm CC}_{3,179}$	$(1,1,0,1,1,0,0,0,1)$	$(\mathcal{B}^{\rm CC}_{3,179},\mathcal{B}^{\rm CC}_{3,207},\mathcal{B}^{\rm CC}_{3,310},\mathcal{B}^{\rm CC}_{3,337})$	–
$I^{\rm CC}_{3,26}$	$\mathcal{B}^{\rm CC}_{3,179}$	$(0,1,0,1,1,0,0,1,1)$	$(\mathcal{B}^{\rm CC}_{3,179},\mathcal{B}^{\rm CC}_{3,207},\mathcal{B}^{\rm CC}_{3,310})$	–
$I^{\rm CC}_{3,27}$	$\mathcal{B}^{\rm CC}_{3,179}$	$(0,1,0,1,1,0,0,2,1)$	$(\mathcal{B}^{\rm CC}_{3,179},\mathcal{B}^{\rm CC}_{3,207},\mathcal{B}^{\rm CC}_{3,310})$	–
$I^{\rm CC}_{3,28}$	$\mathcal{B}^{\rm CC}_{3,179}$	$(0,2,0,1,1,0,0,1,1)$	$(\mathcal{B}^{\rm CC}_{3,179},\mathcal{B}^{\rm CC}_{3,207},\mathcal{B}^{\rm CC}_{3,310})$	–
$I^{\rm CC}_{3,29}$	$\mathcal{B}^{\rm CC}_{3,330}$	$(0,1,0,1,1,0,0,1,1)$	$(\mathcal{B}^{\rm CC}_{3,168},\mathcal{B}^{\rm CC}_{3,330},\mathcal{B}^{\rm CC}_{3,337})$	–
$I^{\rm CC}_{3,30}$	$\mathcal{B}^{\rm CC}_{3,330}$	$(0,1,0,1,1,0,0,2,1)$	$(\mathcal{B}^{\rm CC}_{3,168},\mathcal{B}^{\rm CC}_{3,330},\mathcal{B}^{\rm CC}_{3,337})$	–
$I^{\rm CC}_{3,31}$	$\mathcal{B}^{\rm CC}_{3,179}$	$(1,1,1,1,1,1,0,0,0)$	$(\mathcal{B}^{\rm CC}_{3,168},\mathcal{B}^{\rm CC}_{3,179},\mathcal{B}^{\rm CC}_{3,207},\mathcal{B}^{\rm CC}_{3,310},\mathcal{B}^{\rm CC}_{3,330},\mathcal{B}^{\rm CC}_{3,337})$	$(I^{\rm CC}_{1,2})^3$
$I^{\rm CC}_{3,32}$	$\mathcal{B}^{\rm CC}_{3,179}$	$(0,1,1,1,1,1,0,1,0)$	$(\mathcal{B}^{\rm CC}_{3,179},\mathcal{B}^{\rm CC}_{3,207},\mathcal{B}^{\rm CC}_{3,310},\mathcal{B}^{\rm CC}_{3,330})$	$I^{\rm CC}_{1,1}\ I^{\rm CC}_{2,8}$
$I^{\rm CC}_{3,33}$	$\mathcal{B}^{\rm CC}_{3,179}$	$(1,1,0,0,1,1,1,1,0)$	$(\mathcal{B}^{\rm CC}_{3,179},\mathcal{B}^{\rm CC}_{3,207},\mathcal{B}^{\rm CC}_{3,310},\mathcal{B}^{\rm CC}_{3,330})$	–
$I^{\rm CC}_{3,34}$	$\mathcal{B}^{\rm CC}_{3,179}$	$(1,1,0,0,1,1,1,2,0)$	$(\mathcal{B}^{\rm CC}_{3,179},\mathcal{B}^{\rm CC}_{3,207},\mathcal{B}^{\rm CC}_{3,310},\mathcal{B}^{\rm CC}_{3,330})$	–
$I^{\rm CC}_{3,35}$	$\mathcal{B}^{\rm CC}_{3,179}$	$(1,2,0,0,1,1,1,1,0)$	$(\mathcal{B}^{\rm CC}_{3,179},\mathcal{B}^{\rm CC}_{3,207},\mathcal{B}^{\rm CC}_{3,310},\mathcal{B}^{\rm CC}_{3,330})$	–

Continued on next page

Int.	Family	Weights	Sector Symmetries	Factors
$I^{\rm CC}_{3,36}$	$\mathcal{B}^{\rm CC}_{3,179}$	$(0,1,1,0,1,1,1,1,0)$	$(\mathcal{B}^{\rm CC}_{3,179}, \mathcal{B}^{\rm CC}_{3,207}, \mathcal{B}^{\rm CC}_{3,310}, \mathcal{B}^{\rm CC}_{3,330}, \mathcal{B}^{\rm CC}_{3,337})$	–
$I^{\rm CC}_{3,37}$	$\mathcal{B}^{\rm CC}_{3,179}$	$(0,2,1,0,1,1,1,1,0)$	$(\mathcal{B}^{\rm CC}_{3,179}, \mathcal{B}^{\rm CC}_{3,207}, \mathcal{B}^{\rm CC}_{3,310}, \mathcal{B}^{\rm CC}_{3,330}, \mathcal{B}^{\rm CC}_{3,337})$	–
$I^{\rm CC}_{3,38}$	$\mathcal{B}^{\rm CC}_{3,179}$	$(1,1,0,1,1,0,1,1,0)$	$(\mathcal{B}^{\rm CC}_{3,179}, \mathcal{B}^{\rm CC}_{3,207}, \mathcal{B}^{\rm CC}_{3,310}, \mathcal{B}^{\rm CC}_{3,330})$	–
$I^{\rm CC}_{3,39}$	$\mathcal{B}^{\rm CC}_{3,179}$	$(1,1,1,1,1,0,0,0,1)$	$(\mathcal{B}^{\rm CC}_{3,179}, \mathcal{B}^{\rm CC}_{3,207}, \mathcal{B}^{\rm CC}_{3,310}, \mathcal{B}^{\rm CC}_{3,337})$	–
$I^{\rm CC}_{3,40}$	$\mathcal{B}^{\rm CC}_{3,179}$	$(1,1,1,1,2,0,0,0,1)$	$(\mathcal{B}^{\rm CC}_{3,179}, \mathcal{B}^{\rm CC}_{3,207}, \mathcal{B}^{\rm CC}_{3,310}, \mathcal{B}^{\rm CC}_{3,337})$	–
$I^{\rm CC}_{3,41}$	$\mathcal{B}^{\rm CC}_{3,179}$	$(1,1,0,1,1,0,0,1,1)$	$(\mathcal{B}^{\rm CC}_{3,179}, \mathcal{B}^{\rm CC}_{3,207}, \mathcal{B}^{\rm CC}_{3,310})$	–
$I^{\rm CC}_{3,42}$	$\mathcal{B}^{\rm CC}_{3,179}$	$(0,1,1,0,1,0,1,1,1)$	$(\mathcal{B}^{\rm CC}_{3,179}, \mathcal{B}^{\rm CC}_{3,207}, \mathcal{B}^{\rm CC}_{3,310}, \mathcal{B}^{\rm CC}_{3,330})$	–
$I^{\rm CC}_{3,43}$	$\mathcal{B}^{\rm CC}_{3,179}$	$(0,2,1,0,1,0,1,1,1)$	$(\mathcal{B}^{\rm CC}_{3,179}, \mathcal{B}^{\rm CC}_{3,207}, \mathcal{B}^{\rm CC}_{3,310}, \mathcal{B}^{\rm CC}_{3,330})$	–
$I^{\rm CC}_{3,44}$	$\mathcal{B}^{\rm CC}_{3,179}$	$(1,0,0,1,0,1,1,1,1)$	$(\mathcal{B}^{\rm CC}_{3,179}, \mathcal{B}^{\rm CC}_{3,207}, \mathcal{B}^{\rm CC}_{3,310}, \mathcal{B}^{\rm CC}_{3,330}, \mathcal{B}^{\rm CC}_{3,337})$	–
$I^{\rm CC}_{3,45}$	$\mathcal{B}^{\rm CC}_{3,179}$	$(1,0,0,1,0,1,1,2,1)$	$(\mathcal{B}^{\rm CC}_{3,179}, \mathcal{B}^{\rm CC}_{3,207}, \mathcal{B}^{\rm CC}_{3,310}, \mathcal{B}^{\rm CC}_{3,330}, \mathcal{B}^{\rm CC}_{3,337})$	–
$I^{\rm CC}_{3,46}$	$\mathcal{B}^{\rm CC}_{3,330}$	$(1,1,1,1,1,0,0,0,1)$	$(\mathcal{B}^{\rm CC}_{3,168}, \mathcal{B}^{\rm CC}_{3,330}, \mathcal{B}^{\rm CC}_{3,337})$	–
$I^{\rm CC}_{3,47}$	$\mathcal{B}^{\rm CC}_{3,179}$	$(1,1,1,1,1,1,0,1,0)$	$(\mathcal{B}^{\rm CC}_{3,179}, \mathcal{B}^{\rm CC}_{3,207}, \mathcal{B}^{\rm CC}_{3,310}, \mathcal{B}^{\rm CC}_{3,330})$	$I^{\rm CC}_{1,2}\ I^{\rm CC}_{2,8}$
$I^{\rm CC}_{3,48}$	$\mathcal{B}^{\rm CC}_{3,179}$	$(1,1,0,1,1,1,1,1,0)$	$(\mathcal{B}^{\rm CC}_{3,179}, \mathcal{B}^{\rm CC}_{3,207}, \mathcal{B}^{\rm CC}_{3,310}, \mathcal{B}^{\rm CC}_{3,330})$	–
$I^{\rm CC}_{3,49}$	$\mathcal{B}^{\rm CC}_{3,179}$	$(1,1,0,1,1,1,1,2,0)$	$(\mathcal{B}^{\rm CC}_{3,179}, \mathcal{B}^{\rm CC}_{3,207}, \mathcal{B}^{\rm CC}_{3,310}, \mathcal{B}^{\rm CC}_{3,330})$	–
$I^{\rm CC}_{3,50}$	$\mathcal{B}^{\rm CC}_{3,179}$	$(1,1,1,1,1,0,0,1,1)$	$(\mathcal{B}^{\rm CC}_{3,179}, \mathcal{B}^{\rm CC}_{3,207}, \mathcal{B}^{\rm CC}_{3,310})$	–
$I^{\rm CC}_{3,51}$	$\mathcal{B}^{\rm CC}_{3,179}$	$(1,0,0,1,1,1,1,1,1)$	$(\mathcal{B}^{\rm CC}_{3,179}, \mathcal{B}^{\rm CC}_{3,207}, \mathcal{B}^{\rm CC}_{3,310}, \mathcal{B}^{\rm CC}_{3,330})$	–
$I^{\rm CC}_{3,52}$	$\mathcal{B}^{\rm CC}_{3,330}$	$(1,1,1,1,1,0,0,1,1)$	$(\mathcal{B}^{\rm CC}_{3,168}, \mathcal{B}^{\rm CC}_{3,330}, \mathcal{B}^{\rm CC}_{3,337})$	–
$I^{\rm CC}_{3,53}$	$\mathcal{B}^{\rm CC}_{3,330}$	$(1,1,2,1,1,0,0,1,1)$	$(\mathcal{B}^{\rm CC}_{3,168}, \mathcal{B}^{\rm CC}_{3,330}, \mathcal{B}^{\rm CC}_{3,337})$	–
$I^{\rm CC}_{3,54}$	$\mathcal{B}^{\rm CC}_{3,179}$	$(1,1,0,1,1,1,1,1,1)$	$(\mathcal{B}^{\rm CC}_{3,179})$	–
$I^{\rm CC}_{3,55}$	$\mathcal{B}^{\rm CC}_{3,179}$	$(1,1,0,1,1,1,1,2,1)$	$(\mathcal{B}^{\rm CC}_{3,179})$	–
$I^{\rm CC}_{3,56}$	$\mathcal{B}^{\rm CC}_{3,207}$	$(1,1,1,1,1,1,1,1,0)$	$(\mathcal{B}^{\rm CC}_{3,207}, \mathcal{B}^{\rm CC}_{3,310})$	–
$I^{\rm CC}_{3,57}$	$\mathcal{B}^{\rm CC}_{3,330}$	$(1,1,0,1,1,1,1,1,1)$	$(\mathcal{B}^{\rm CC}_{3,330})$	–

A.3 Boundary Values

Table A.3: Master integrals contributing to the boundary values through three loops, ordered by their e-values. For each master integral, its factorisation, its sector symmetries and a single representative are provided.

Int.	Family	Weights	Sector Symmetries	Factors
$\hat{I}_{1,1}$	$\hat{\mathcal{B}}_{1,1}$	(1)	$(\hat{\mathcal{B}}_{1,1})$	–
$\hat{I}_{2,1}$	$\hat{\mathcal{B}}_{2,1}$	$(1,1,1)$	$(\hat{\mathcal{B}}_{2,1})$	$(\hat{I}_{1,1})^2$
$\hat{I}_{2,2}$	$\hat{\mathcal{B}}_{2,3}$	$(0,1,1)$	$(\hat{\mathcal{B}}_{2,3},\hat{\mathcal{B}}_{2,7})$	–
$\hat{I}_{2,3}$	$\hat{\mathcal{B}}_{2,7}$	$(1,1,1)$	$(\hat{\mathcal{B}}_{2,7})$	–
$\hat{I}_{3,01}$	$\hat{\mathcal{B}}_{3,07}$	$(0,0,0,1,1,1)$	$(\hat{\mathcal{B}}_{3,13}, \hat{\mathcal{B}}_{3,15}, \hat{\mathcal{B}}_{3,29}, \hat{\mathcal{B}}_{3,31}, \hat{\mathcal{B}}_{3,07})$	$(\hat{I}_{1,1})^3$
$\hat{I}_{3,02}$	$\hat{\mathcal{B}}_{3,01}$	$(0,1,1,1,0,1)$	$(\hat{\mathcal{B}}_{3,03}, \hat{\mathcal{B}}_{3,13}, \hat{\mathcal{B}}_{3,01})$	–
$\hat{I}_{3,03}$	$\hat{\mathcal{B}}_{3,03}$	$(1,1,0,0,1,1)$	$(\hat{\mathcal{B}}_{3,07}, \hat{\mathcal{B}}_{3,11}, \hat{\mathcal{B}}_{3,12}, \hat{\mathcal{B}}_{3,13}, \hat{\mathcal{B}}_{3,15}, \hat{\mathcal{B}}_{3,29}, \hat{\mathcal{B}}_{3,03})$	–
$\hat{I}_{3,04}$	$\hat{\mathcal{B}}_{3,03}$	$(1,0,0,1,1,1)$	$(\hat{\mathcal{B}}_{3,11}, \hat{\mathcal{B}}_{3,12}, \hat{\mathcal{B}}_{3,13}, \hat{\mathcal{B}}_{3,15}, \hat{\mathcal{B}}_{3,03})$	$\hat{I}_{1,1}\hat{I}_{2,1}$
$\hat{I}_{3,05}$	$\hat{\mathcal{B}}_{3,13}$	$(0,1,1,1,0,1)$	$(\hat{\mathcal{B}}_{3,15}, \hat{\mathcal{B}}_{3,31}, \hat{\mathcal{B}}_{3,13})$	–
$\hat{I}_{3,06}$	$\hat{\mathcal{B}}_{3,15}$	$(0,0,1,1,1,1)$	$(\hat{\mathcal{B}}_{3,31}, \hat{\mathcal{B}}_{3,15})$	$\hat{I}_{1,1}\hat{I}_{2,3}$
$\hat{I}_{3,07}$	$\hat{\mathcal{B}}_{3,29}$	$(0,1,1,1,0,1)$	$(\hat{\mathcal{B}}_{3,31}, \hat{\mathcal{B}}_{3,29})$	–
$\hat{I}_{3,08}$	$\hat{\mathcal{B}}_{3,11}$	$(1,1,1,0,1,1)$	$(\hat{\mathcal{B}}_{3,15}, \hat{\mathcal{B}}_{3,11})$	–
$\hat{I}_{3,09}$	$\hat{\mathcal{B}}_{3,01}$	$(1,0,1,1,1,1)$	$(\hat{\mathcal{B}}_{3,01})$	–
$\hat{I}_{3,10}$	$\hat{\mathcal{B}}_{3,31}$	$(0,1,1,1,1,1)$	$(\hat{\mathcal{B}}_{3,31})$	–
$\hat{I}_{3,11}$	$\hat{\mathcal{B}}_{3,13}$	$(1,1,1,1,1,1)$	$(\hat{\mathcal{B}}_{3,13})$	–
$\hat{I}_{3,12}$	$\hat{\mathcal{B}}_{3,15}$	$(1,1,1,1,1,1)$	$(\hat{\mathcal{B}}_{3,15})$	–

Appendix B

Bananas

B.1 Three-Loop Banana

B.1.1 Ansatz Functions

$$a^{\mathrm{NC},(-1)}_{\mathrm{B},3,1,1} = \frac{5x^4 - 132x^3 + 912x^2 + 256x - 6144}{512(x-16)(x-4)} \tag{B.1}$$

$$a^{\mathrm{NC},(-1)}_{\mathrm{B},3,1,2} = \frac{x\left(2x^4 - 83x^3 + 1164x^2 - 5840x + 11264\right)}{128(x-16)(x-4)} \tag{B.2}$$

$$a^{\mathrm{NC},(-1)}_{\mathrm{B},3,1,3} = \frac{3}{512}x\left(x^3 - 44x^2 + 464x - 1024\right) \tag{B.3}$$

$$a^{\mathrm{NC},(0)}_{\mathrm{B},2,1,1} = \frac{x^3 - 30x^2 + 336x - 640}{8(x-16)(x-4)\sqrt{(x-16)(x-4)}} \tag{B.4}$$

$$a^{\mathrm{NC},(0)}_{\mathrm{B},2,1,2} = \frac{x^2 - 40x + 192}{8\sqrt{(x-16)(x-4)}} \tag{B.5}$$

$$a^{\mathrm{NC},(0)}_{\mathrm{B},2,1,3} = -\frac{8}{x\sqrt{(x-16)(x-4)}} \tag{B.6}$$

$$a^{\mathrm{NC},(0)}_{\mathrm{B},3,2,1} = \frac{x^4 - 45x^3 + 696x^2 - 3952x + 8448}{16(x-16)(x-4)\sqrt{(x-16)(x-4)}} \tag{B.7}$$

$$a^{\mathrm{NC},(0)}_{\mathrm{B},3,2,2} = \frac{x^3 - 40x^2 + 304x - 256}{32\sqrt{(x-16)(x-4)}} \tag{B.8}$$

$$a^{\mathrm{NC},(0)}_{\mathrm{B},3,2,3} = \frac{8}{x\sqrt{(x-16)(x-4)}} \tag{B.9}$$

$$a^{\mathrm{NC},(0)}_{\mathrm{B},3,1,1} = \frac{3x^6 - 148x^5 + 2872x^4 - 29184x^3 + 143872x^2 - 360448x + 688128}{256(x-16)^2(x-4)^2} \tag{B.10}$$

$$a^{\mathrm{NC},(0)}_{\mathrm{B},3,1,2} = \frac{x^5 - 34x^4 + 512x^3 - 2688x^2 + 8192x + 8192}{128(x-16)(x-4)} \tag{B.11}$$

$$a^{\mathrm{NC},(0)}_{\mathrm{B},3,1,3} = -\frac{x^3 - 40x^2 + 304x - 256}{4(x-16)(x-4)x} \tag{B.12}$$

$$a^{\mathrm{NC},(0)}_{\mathrm{B},3,1,4} = -\frac{\sqrt{(x-16)(x-4)}\left(x^4 - 45x^3 + 696x^2 - 3952x + 8448\right)}{16(x-16)^2(x-4)^2} \tag{B.13}$$

$$a^{\mathrm{NC},(0)}_{\mathrm{B},3,1,5} = -\frac{\sqrt{(x-16)(x-4)}\,(x^3-40x^2+304x-256)}{32(x-16)(x-4)} \tag{B.14}$$

$$a^{\mathrm{NC},(0)}_{\mathrm{B},3,1,6} = -\frac{8\sqrt{(x-16)(x-4)}}{(x-16)(x-4)x} \tag{B.15}$$

B.1.2 Transformation Entries

$$t^{\mathrm{NC},(-1)}_{\mathrm{B},3,1,1} = \frac{x\,(x^4-36x^3+408x^2-1216x+1536)}{256(x-16)(x-4)}\,, \tag{B.16}$$

$$t^{\mathrm{NC},(-1)}_{\mathrm{B},3,1,1} = \frac{1}{256}x\left(x^3-44x^2+464x-1024\right)\,, \tag{B.17}$$

$$t^{\mathrm{NC},(0)}_{\mathrm{B},2,1,1} = \frac{x^2-40x+192}{8\sqrt{(x-16)(x-4)}}\,, \tag{B.18}$$

$$t^{\mathrm{NC},(0)}_{\mathrm{B},3,2,1} = \frac{x^3-40x^2+304x-256}{32\sqrt{(x-16)(x-4)}}\,, \tag{B.19}$$

$$t^{\mathrm{NC},(0)}_{\mathrm{B},3,1,1} = \frac{x^5-34x^4+512x^3-2688x^2+8192x+8192}{256(x-16)(x-4)}\,, \tag{B.20}$$

$$t^{\mathrm{NC},(0)}_{\mathrm{B},3,1,2} = -\frac{1}{2}\,, \tag{B.21}$$

$$t^{\mathrm{NC},(0)}_{\mathrm{B},3,1,3} = -\frac{x^3-40x^2+304x-256}{32\sqrt{(x-16)(x-4)}} \tag{B.22}$$

B.2 Two-Loop Banana

B.2.1 Ansatz Functions

$$a^{\mathrm{CC},(0)}_{\mathrm{B},2,1,1} = x-15 \tag{B.23}$$

$$a^{\mathrm{CC},(0)}_{\mathrm{B},2,1,2} = x^2-30x+45 \tag{B.24}$$

B.2.2 Transformation Entries

$$t^{\mathrm{CC},(0)}_{\mathrm{B},2,1,1} = \left\{\frac{1}{2}\left(x^2-30x+45\right)\right\} \tag{B.25}$$

Appendix C

More Mellin Moments

C.1 Axial–Axial

$$c^{2,(0,0)}_{2,\mathrm{g,aa}} = 0 \tag{C.1}$$

$$\begin{aligned}
c^{2,(1,0)}_{2,\mathrm{g,aa}} &= -T_F\langle \mathrm{l}_{\{\,\mathrm{a,a}\,\}}\rangle^{\mathrm{g}} n_\mathrm{l} + T_F\langle \mathrm{h}_{\{\,\mathrm{a,a}\,\}}\rangle^{\mathrm{g}} n_\mathrm{h}\Big[-1+14\mathrm{d}_1-30\mathrm{d}_1^2+32\mathrm{d}_1^3-16\mathrm{d}_1^4\\
&\quad +\mathrm{H}_0\Big(\frac{4}{3}-\frac{3}{2}\mathrm{d}_{-1}-\frac{21}{2}\mathrm{d}_1+27\mathrm{d}_1^2-\frac{134}{3}\mathrm{d}_1^3+40\mathrm{d}_1^4-16\,\mathrm{d}_1^5\Big)\Big]
\end{aligned} \tag{C.2}$$

$$\begin{aligned}
c^{2,(2,0)}_{2,\mathrm{g,aa}} &= C_A T_F\langle \mathrm{l}_{\{\,\mathrm{a,a}\,\}}\rangle^{\mathrm{g}} n_\mathrm{l}\Big[\frac{115}{162}-4\zeta_3\Big] + C_F T_F\langle \mathrm{l}_{\{\,\mathrm{a,a}\,\}}\rangle^{\mathrm{g}} n_\mathrm{l}\Big[-\frac{4799}{405}+\frac{32}{5}\zeta_3\Big]\\
&\quad +10T_F^2\langle \mathrm{l}_{\{\,\mathrm{a}\,\}}\mathrm{l}_{\{\,\mathrm{a}\,\}}\rangle^{\mathrm{g}} n_\mathrm{l}^2 + T_F^2\langle \mathrm{l}_{\{\,\mathrm{a}\,\}}\mathrm{h}_{\{\,\mathrm{a}\,\}}\rangle^{\mathrm{g}} n_\mathrm{h} n_\mathrm{l}\Big[20+\mathrm{H}_0\Big(-20\mathrm{d}_{-1}-20\mathrm{d}_1\Big)\Big]\\
&\quad +T_F^2\langle \mathrm{h}_{\{\,\mathrm{a}\,\}}\mathrm{h}_{\{\,\mathrm{a}\,\}}\rangle^{\mathrm{g}} n_\mathrm{h}^2\Big[10+\mathrm{H}_0\Big(-20\mathrm{d}_{-1}-20\mathrm{d}_1\Big)\\
&\quad +\mathrm{H}_{0,0}\Big(20\mathrm{d}_{-1}+20\mathrm{d}_{-1}^2-20\mathrm{d}_1+20\mathrm{d}_1^2\Big)\Big]\\
&\quad +C_F T_F\langle \mathrm{h}_{\{\,\mathrm{a,a}\,\}}\rangle^{\mathrm{g}} n_\mathrm{h}\Big[\frac{1855}{9}-\frac{1179}{10}\upsilon-\frac{62}{45}\upsilon^2-\frac{288}{5}\mathrm{d}_{-1}-\frac{288}{5}\mathrm{d}_{-1}^2-\frac{1179}{10}\mathrm{d}_0\\
&\quad -\frac{62}{45}\mathrm{d}_0^2+\frac{2924}{45}\mathrm{d}_1-\frac{7724}{45}\mathrm{d}_1^2+\frac{640}{3}\mathrm{d}_1^3-\frac{320}{3}\mathrm{d}_1^4\\
&\quad +\mathrm{H}_0\Big(\frac{13684}{45}-\frac{1753}{15}\upsilon-\frac{62}{45}\upsilon^2+\frac{1228}{15}\mathrm{d}_{-1}+\frac{864}{5}\mathrm{d}_{-1}^2+\frac{576}{5}\mathrm{d}_{-1}^3+\frac{1753}{15}\mathrm{d}_0\\
&\quad +\frac{62}{45}\mathrm{d}_0^2-\frac{7340}{9}\mathrm{d}_1+\frac{6648}{5}\mathrm{d}_1^2-\frac{152008}{45}\mathrm{d}_1^3+\frac{13864}{3}\mathrm{d}_1^4-\frac{9856}{3}\mathrm{d}_1^5+960\mathrm{d}_1^6\Big)\\
&\quad +\mathrm{H}_1\Big(16-344\mathrm{d}_1+1800\mathrm{d}_1^2-4832\mathrm{d}_1^3+7216\mathrm{d}_1^4-5760\mathrm{d}_1^5+1920\mathrm{d}_1^6\Big)\\
&\quad +\mathrm{H}_{-1,0}\Big(\frac{9392}{45}-\frac{2020}{9}\upsilon+\frac{3568}{15}\upsilon^2+\frac{124}{45}\upsilon^3+\frac{1088}{15}\mathrm{d}_{-1}+\frac{2020}{9}\mathrm{d}_0-\frac{3568}{15}\mathrm{d}_0^2\\
&\quad -\frac{124}{45}\mathrm{d}_0^3-\frac{3488}{9}\mathrm{d}_1+128\mathrm{d}_1^2-\frac{256}{3}\mathrm{d}_1^3\Big)
\end{aligned}$$

$$
\begin{aligned}
&+ \mathrm{H}_{0,0}\Big(- \frac{14248}{45} + \frac{1010}{3}\upsilon - \frac{1784}{5}\upsilon^2 - \frac{62}{15}\upsilon^3 - \frac{657}{5}\mathrm{d}_{-1} - \frac{1006}{5}\mathrm{d}_{-1}^2 - \frac{1152}{5}\mathrm{d}_{-1}^3 \\
&\quad - \frac{576}{5}\mathrm{d}_{-1}^4 + \frac{7543}{15}\mathrm{d}_1 - \frac{74692}{45}\mathrm{d}_1^2 + \frac{242396}{45}\mathrm{d}_1^3 - \frac{463168}{45}\mathrm{d}_1^4 + 11728\mathrm{d}_1^5 \\
&\quad - \frac{21952}{3}\mathrm{d}_1^6 + 1920\mathrm{d}_1^7\Big) \\
&+ \mathrm{H}_{0,1}\Big(9\mathrm{d}_{-1} + 135\mathrm{d}_1 - 1026\mathrm{d}_1^2 + 3804\mathrm{d}_1^3 - 8040\mathrm{d}_1^4 + 9936\mathrm{d}_1^5 - 6720\mathrm{d}_1^6 \\
&\quad + 1920\mathrm{d}_1^7\Big) \\
&+ \mathrm{H}_{1,0}\Big(- \frac{4696}{45} + \frac{1010}{9}\upsilon - \frac{1784}{15}\upsilon^2 - \frac{62}{45}\upsilon^3 - \frac{409}{15}\mathrm{d}_{-1} - \frac{1010}{9}\mathrm{d}_0 + \frac{1784}{15}\mathrm{d}_0^2 \\
&\quad + \frac{62}{45}\mathrm{d}_0^3 + \frac{2959}{9}\mathrm{d}_1 - 1090\mathrm{d}_1^2 + \frac{11540}{3}\mathrm{d}_1^3 - 8040\mathrm{d}_1^4 + 9936\mathrm{d}_1^5 - 6720\mathrm{d}_1^6 \\
&\quad + 1920\mathrm{d}_1^7\Big) \\
&+ \mathrm{H}_{-1,0,0}\Big(- \frac{128}{15} + \frac{1088}{15}\mathrm{d}_{-1} + \frac{1088}{15}\mathrm{d}_{-1}^2\Big) \\
&+ \mathrm{H}_{0,-1,0}\Big(\frac{128}{15} - \frac{1088}{15}\mathrm{d}_{-1} - \frac{1088}{15}\mathrm{d}_{-1}^2\Big) \\
&+ \mathrm{H}_{0,1,0}\Big(- \frac{64}{15} + \frac{544}{15}\mathrm{d}_{-1} + \frac{544}{15}\mathrm{d}_{-1}^2\Big) \\
&+ \mathrm{H}_{1,0,0}\Big(\frac{64}{15} - \frac{544}{15}\mathrm{d}_{-1} - \frac{544}{15}\mathrm{d}_{-1}^2\Big) \\
&+ \zeta_3\Big(\frac{32}{5} - \frac{272}{5}\mathrm{d}_{-1} - \frac{272}{5}\mathrm{d}_{-1}^2\Big)\Big] \\
+ C_A T_F \langle \mathrm{h}_{\{\mathrm{a,a}\}}\rangle^{\mathrm{g}} n_{\mathrm{h}} &\Big[\frac{18131}{90} - \frac{3467}{30}\upsilon - \frac{58}{45}\upsilon^2 + \frac{96}{5}\mathrm{d}_{-1} + \frac{96}{5}\mathrm{d}_{-1}^2 - \frac{3467}{30}\mathrm{d}_0 - \frac{58}{45}\mathrm{d}_0^2 \\
&- \frac{2489}{15}\mathrm{d}_1 + \frac{8947}{45}\mathrm{d}_1^2 - \frac{592}{9}\mathrm{d}_1^3 + \frac{296}{9}\mathrm{d}_1^4 \\
&+ \mathrm{H}_0\Big(\frac{40306}{135} - \frac{573}{5}\upsilon - \frac{58}{45}\upsilon^2 + \frac{67}{4}\mathrm{d}_{-1} - \frac{288}{5}\mathrm{d}_{-1}^2 - \frac{192}{5}\mathrm{d}_{-1}^3 + \frac{573}{5}\mathrm{d}_0 + \frac{58}{45}\mathrm{d}_0^2 \\
&\quad - \frac{37949}{60}\mathrm{d}_1 + \frac{25633}{90}\mathrm{d}_1^2 - \frac{73373}{135}\mathrm{d}_1^3 + \frac{4708}{9}\mathrm{d}_1^4 - \frac{1672}{9}\mathrm{d}_1^5\Big) \\
&+ \mathrm{H}_1\Big(\frac{22}{3} - \frac{308}{3}\mathrm{d}_1 + 220\mathrm{d}_1^2 - \frac{704}{3}\mathrm{d}_1^3 + \frac{352}{3}\mathrm{d}_1^4\Big) \\
&+ \mathrm{H}_{-1,0}\Big(\frac{13592}{45} - \frac{3428}{15}\upsilon + \frac{3496}{15}\upsilon^2 + \frac{116}{45}\upsilon^3 + \frac{1018}{15}\mathrm{d}_{-1} + \frac{3428}{15}\mathrm{d}_0 - \frac{3496}{15}\mathrm{d}_0^2 \\
&\quad - \frac{116}{45}\mathrm{d}_0^3 - \frac{1282}{3}\mathrm{d}_1 - 444\mathrm{d}_1^2 + \frac{6184}{9}\mathrm{d}_1^3 - \frac{1760}{3}\mathrm{d}_1^4 + \frac{704}{3}\mathrm{d}_1^5\Big) \\
&+ \mathrm{H}_{0,0}\Big(- \frac{7016}{15} + \frac{1714}{5}\upsilon - \frac{1748}{5}\upsilon^2 - \frac{58}{15}\upsilon^3 - \frac{817}{30}\mathrm{d}_{-1} + \frac{766}{15}\mathrm{d}_{-1}^2 + \frac{384}{5}\mathrm{d}_{-1}^3
\end{aligned}
$$

$$+\frac{192}{5}\mathrm{d}_{-1}^4+\frac{3883}{10}\mathrm{d}_1+\frac{2731}{15}\mathrm{d}_1^2-\frac{13298}{45}\mathrm{d}_1^3+\frac{4208}{15}\mathrm{d}_1^4-\frac{464}{3}\mathrm{d}_1^5+32\mathrm{d}_1^6\Big)$$
$$+\mathrm{H}_{0,1}\Big(-\frac{88}{9}+11\mathrm{d}_{-1}+77\mathrm{d}_1-198\mathrm{d}_1^2+\frac{2948}{9}\mathrm{d}_1^3-\frac{880}{3}\mathrm{d}_1^4+\frac{352}{3}\mathrm{d}_1^5\Big)$$
$$+\mathrm{H}_{1,0}\Big(-\frac{804}{5}+\frac{1714}{15}\upsilon-\frac{1748}{15}\upsilon^2-\frac{58}{45}\upsilon^3-\frac{344}{15}\mathrm{d}_{-1}-\frac{1714}{15}\mathrm{d}_0+\frac{1748}{15}\mathrm{d}_0^2$$
$$+\frac{58}{45}\mathrm{d}_0^3+\frac{872}{3}\mathrm{d}_1+24\mathrm{d}_1^2-16\mathrm{d}_1^3\Big)$$
$$+\mathrm{H}_{-1,0,0}\Big(\frac{16}{3}-\frac{32}{15}\mathrm{d}_{-1}-\frac{32}{15}\mathrm{d}_{-1}^2\Big)$$
$$+\mathrm{H}_{0,-1,0}\Big(-\frac{16}{3}+\frac{32}{15}\mathrm{d}_{-1}+\frac{32}{15}\mathrm{d}_{-1}^2\Big)$$
$$+\mathrm{H}_{0,1,0}\Big(\frac{8}{3}-\frac{16}{15}\mathrm{d}_{-1}-\frac{16}{15}\mathrm{d}_{-1}^2\Big)$$
$$+\mathrm{H}_{1,0,0}\Big(-\frac{8}{3}+\frac{16}{15}\mathrm{d}_{-1}+\frac{16}{15}\mathrm{d}_{-1}^2\Big)$$
$$+\zeta_3\Big(-4+\frac{8}{5}\mathrm{d}_{-1}+\frac{8}{5}\mathrm{d}_{-1}^2\Big)\Big] \tag{C.3}$$

$$c_{L,\mathrm{g,aa}}^{2,(0,0)}=0 \tag{C.4}$$

$$c_{L,\mathrm{g,aa}}^{2,(1,0)}=\frac{4}{3}T_F\langle \mathrm{l}_{\{\mathrm{a,a}\}}\rangle^{\mathrm{g}}n_\mathrm{l}+T_F\langle \mathrm{h}_{\{\mathrm{a,a}\}}\rangle^{\mathrm{g}}n_\mathrm{h}\Big[\frac{4}{3}+\frac{20}{3}\mathrm{d}_1-\frac{44}{3}\mathrm{d}_1^2+16\mathrm{d}_1^3-8\mathrm{d}_1^4$$
$$+\mathrm{H}_0\Big(-\frac{5}{2}\mathrm{d}_{-1}-\frac{11}{2}\mathrm{d}_1+13\mathrm{d}_1^2-22\mathrm{d}_1^3+20\mathrm{d}_1^4-8\mathrm{d}_1^5\Big)\Big] \tag{C.5}$$

$$c_{L,\mathrm{g,aa}}^{2,(2,0)}=\frac{346}{27}C_AT_F\langle \mathrm{l}_{\{\mathrm{a,a}\}}\rangle^{\mathrm{g}}n_\mathrm{l}+C_FT_F\langle \mathrm{l}_{\{\mathrm{a,a}\}}\rangle^{\mathrm{g}}n_\mathrm{l}\Big[-\frac{232}{135}-\frac{32}{5}\zeta_3\Big]$$
$$+4T_F^2\langle \mathrm{l}_{\{\mathrm{a}\}}\mathrm{l}_{\{\mathrm{a}\}}\rangle^{\mathrm{g}}n_\mathrm{l}^2+T_F^2\langle \mathrm{l}_{\{\mathrm{a}\}}\mathrm{h}_{\{\mathrm{a}\}}\rangle^{\mathrm{g}}n_\mathrm{h}n_\mathrm{l}\Big[8+\mathrm{H}_0\Big(-8\mathrm{d}_{-1}-8\mathrm{d}_1\Big)\Big]$$
$$+T_F^2\langle \mathrm{h}_{\{\mathrm{a}\}}\mathrm{h}_{\{\mathrm{a}\}}\rangle^{\mathrm{g}}n_\mathrm{h}^2\Big[4+\mathrm{H}_0\Big(-8\mathrm{d}_{-1}-8\mathrm{d}_1\Big)$$
$$+\mathrm{H}_{0,0}\Big(8\mathrm{d}_{-1}+8\mathrm{d}_{-1}^2-8\mathrm{d}_1+8\,\mathrm{d}_1^2\Big)\Big]$$
$$+C_AT_F\langle \mathrm{h}_{\{\mathrm{a,a}\}}\rangle^{\mathrm{g}}n_\mathrm{h}\Big[\frac{15436}{135}-\frac{293}{5}\upsilon+\frac{116}{15}\upsilon^2+\frac{64}{5}\mathrm{d}_{-1}+\frac{64}{5}\mathrm{d}_{-1}^2-\frac{293}{5}\mathrm{d}_0$$
$$+\frac{116}{15}\mathrm{d}_0^2-\frac{9154}{135}\mathrm{d}_1+\frac{11374}{135}\mathrm{d}_1^2-\frac{296}{9}\mathrm{d}_1^3+\frac{148}{9}\mathrm{d}_1^4$$
$$+\mathrm{H}_0\Big(\frac{1996}{15}-\frac{322}{5}\upsilon+\frac{116}{15}\upsilon^2-\frac{77}{4}\mathrm{d}_{-1}-\frac{192}{5}\mathrm{d}_{-1}^2-\frac{128}{5}\mathrm{d}_{-1}^3+\frac{322}{5}\mathrm{d}_0$$
$$-\frac{116}{15}\mathrm{d}_0^2-\frac{57143}{180}\mathrm{d}_1+\frac{11897}{90}\mathrm{d}_1^2-\frac{11959}{45}\mathrm{d}_1^3+\frac{2354}{9}\mathrm{d}_1^4-\frac{836}{9}\mathrm{d}_1^5\Big)$$

$$
\begin{aligned}
&+\mathrm{H}_1\bigg(-\frac{88}{9}-\frac{440}{9}\mathrm{d}_1+\frac{968}{9}\mathrm{d}_1^2-\frac{352}{3}\mathrm{d}_1^3+\frac{176}{3}\mathrm{d}_1^4\bigg)\\
&+\mathrm{H}_{-1,0}\bigg(\frac{2176}{15}-\frac{1832}{15}\upsilon+\frac{528}{5}\upsilon^2-\frac{232}{15}\upsilon^3+\frac{742}{15}\mathrm{d}_{-1}+\frac{1832}{15}\mathrm{d}_0-\frac{528}{5}\mathrm{d}_0^2\\
&\quad+\frac{232}{15}\mathrm{d}_0^3-\frac{590}{3}\mathrm{d}_1-\frac{572}{3}\mathrm{d}_1^2+\frac{968}{3}\mathrm{d}_1^3-\frac{880}{3}\mathrm{d}_1^4+\frac{352}{3}\mathrm{d}_1^5\bigg)\\
&+\mathrm{H}_{0,0}\bigg(-\frac{1088}{5}+\frac{916}{5}\upsilon-\frac{792}{5}\upsilon^2+\frac{116}{5}\upsilon^3-\frac{391}{10}\mathrm{d}_{-1}+\frac{79}{15}\mathrm{d}_{-1}^2+\frac{256}{5}\mathrm{d}_{-1}^3\\
&\quad+\frac{128}{5}\mathrm{d}_{-1}^4+\frac{1767}{10}\mathrm{d}_1+\frac{1174}{15}\mathrm{d}_1^2-\frac{678}{5}\mathrm{d}_1^3+\frac{704}{5}\mathrm{d}_1^4-\frac{232}{3}\mathrm{d}_1^5+16\mathrm{d}_1^6\bigg)\\
&+\mathrm{H}_{0,1}\bigg(\frac{55}{3}\mathrm{d}_{-1}+\frac{121}{3}\mathrm{d}_1-\frac{286}{3}\mathrm{d}_1^2+\frac{484}{3}\mathrm{d}_1^3-\frac{440}{3}\mathrm{d}_1^4+\frac{176}{3}\mathrm{d}_1^5\bigg)\\
&+\mathrm{H}_{1,0}\bigg(-\frac{1088}{15}+\frac{916}{15}\upsilon-\frac{264}{5}\upsilon^2+\frac{116}{15}\upsilon^3-\frac{32}{5}\mathrm{d}_{-1}-\frac{916}{15}\mathrm{d}_0+\frac{264}{5}\mathrm{d}_0^2-\frac{116}{15}\mathrm{d}_0^3\\
&\quad+\frac{416}{3}\mathrm{d}_1\bigg)\\
&+\mathrm{H}_{-1,0,0}\bigg(\frac{64}{5}\mathrm{d}_{-1}+\frac{64}{5}\mathrm{d}_{-1}^2\bigg)\\
&+\mathrm{H}_{0,-1,0}\bigg(-\frac{64}{5}\mathrm{d}_{-1}-\frac{64}{5}\mathrm{d}_{-1}^2\bigg)\\
&+\mathrm{H}_{0,1,0}\bigg(\frac{32}{5}\mathrm{d}_{-1}+\frac{32}{5}\mathrm{d}_{-1}^2\bigg)\\
&+\mathrm{H}_{1,0,0}\bigg(-\frac{32}{5}\mathrm{d}_{-1}-\frac{32}{5}\mathrm{d}_{-1}^2\bigg)\\
&+\zeta_3\bigg(-\frac{48}{5}\mathrm{d}_{-1}-\frac{48}{5}\mathrm{d}_{-1}^2\bigg)\bigg]\\
+&C_FT_F\langle\mathrm{h}_{\{\mathrm{a,a}\}}\rangle^{\mathrm{g}}n_{\mathrm{h}}\bigg[90-\frac{869}{15}\upsilon+\frac{124}{15}\upsilon^2-\frac{192}{5}\mathrm{d}_{-1}-\frac{192}{5}\mathrm{d}_{-1}^2-\frac{869}{15}\mathrm{d}_0+\frac{124}{15}\mathrm{d}_0^2\\
&+\frac{632}{15}\mathrm{d}_1-\frac{1432}{15}\mathrm{d}_1^2+\frac{320}{3}\mathrm{d}_1^3-\frac{160}{3}\mathrm{d}_1^4\\
&+\mathrm{H}_0\bigg(\frac{2012}{15}-\frac{962}{15}\upsilon+\frac{124}{15}\upsilon^2+\frac{682}{15}\mathrm{d}_{-1}+\frac{576}{5}\mathrm{d}_{-1}^2+\frac{384}{5}\mathrm{d}_{-1}^3+\frac{962}{15}\mathrm{d}_0-\frac{124}{15}\mathrm{d}_0^2\\
&\quad-\frac{1186}{3}\mathrm{d}_1+\frac{10196}{15}\mathrm{d}_1^2-\frac{8408}{5}\mathrm{d}_1^3+\frac{6896}{3}\mathrm{d}_1^4-\frac{4928}{3}\mathrm{d}_1^5+480\mathrm{d}_1^6\bigg)\\
&+\mathrm{H}_1\bigg(-176\mathrm{d}_1+880\mathrm{d}_1^2-2368\mathrm{d}_1^3+3584\mathrm{d}_1^4-2880\mathrm{d}_1^5+960\mathrm{d}_1^6\bigg)\\
&+\mathrm{H}_{-1,0}\bigg(\frac{512}{5}-104\upsilon+\frac{1552}{15}\upsilon^2-\frac{248}{15}\upsilon^3+\frac{384}{5}\mathrm{d}_{-1}+104\mathrm{d}_0-\frac{1552}{15}\mathrm{d}_0^2\\
&\quad+\frac{248}{15}\mathrm{d}_0^3-\frac{448}{3}\mathrm{d}_1+64\mathrm{d}_1^2-\frac{128}{3}\mathrm{d}_1^3\bigg)\\
&+\mathrm{H}_{0,0}\bigg(-\frac{768}{5}+156\upsilon-\frac{776}{5}\upsilon^2+\frac{124}{5}\upsilon^3-\frac{1939}{15}\mathrm{d}_{-1}-\frac{2452}{15}\mathrm{d}_{-1}^2-\frac{768}{5}\mathrm{d}_{-1}^3
\end{aligned}
$$

$$
\begin{aligned}
&\quad - \frac{384}{5}\mathrm{d}_{-1}^4 + \frac{3707}{15}\mathrm{d}_1 - \frac{4282}{5}\mathrm{d}_1^2 + \frac{13396}{5}\mathrm{d}_1^3 - \frac{76504}{15}\mathrm{d}_1^4 + 5840\mathrm{d}_1^5 - \frac{10976}{3}\mathrm{d}_1^6 \\
&\quad + 960\mathrm{d}_1^7\Big) \\
&+ \mathrm{H}_{0,1}\Big(15\mathrm{d}_{-1} + 81\mathrm{d}_1 - 510\mathrm{d}_1^2 + 1860\mathrm{d}_1^3 - 3960\mathrm{d}_1^4 + 4944\mathrm{d}_1^5 - 3360\mathrm{d}_1^6 + 960\mathrm{d}_1^7\Big) \\
&+ \mathrm{H}_{1,0}\Big(- \frac{256}{5} + 52\upsilon - \frac{776}{15}\upsilon^2 + \frac{124}{15}\upsilon^3 - \frac{117}{5}\mathrm{d}_{-1} - 52\mathrm{d}_0 + \frac{776}{15}\mathrm{d}_0^2 - \frac{124}{15}\mathrm{d}_0^3 \\
&\quad + \frac{467}{3}\mathrm{d}_1 - 542\mathrm{d}_1^2 + \frac{5644}{3}\mathrm{d}_1^3 - 3960\mathrm{d}_1^4 + 4944\mathrm{d}_1^5 - 3360\mathrm{d}_1^6 + 960\mathrm{d}_1^7\Big) \\
&+ \mathrm{H}_{-1,0,0}\Big(\frac{128}{15} + \frac{384}{5}\mathrm{d}_{-1} + \frac{384}{5}\mathrm{d}_{-1}^2\Big) \\
&+ \mathrm{H}_{0,-1,0}\Big(- \frac{128}{15} - \frac{384}{5}\mathrm{d}_{-1} - \frac{384}{5}\mathrm{d}_{-1}^2\Big) \\
&+ \mathrm{H}_{0,1,0}\Big(\frac{64}{15} + \frac{192}{5}\mathrm{d}_{-1} + \frac{192}{5}\mathrm{d}_{-1}^2\Big) \\
&+ \mathrm{H}_{1,0,0}\Big(- \frac{64}{15} - \frac{192}{5}\mathrm{d}_{-1} - \frac{192}{5}\mathrm{d}_{-1}^2\Big) \\
&+ \zeta_3\Big(- \frac{32}{5} - \frac{288}{5}\mathrm{d}_{-1} - \frac{288}{5}\mathrm{d}_{-1}^2\Big)\Big]
\end{aligned} \tag{C.6}
$$

$$
c_{2,\mathrm{q,aa}}^{2,(0,0)} = \langle\bar{\mathrm{l}}_{\{\,\mathrm{a,a}\,\}}\rangle^{\mathrm{q}} \tag{C.7}
$$

$$
c_{2,\mathrm{q,aa}}^{2,(1,0)} = \frac{1}{3}C_F\langle\bar{\mathrm{l}}_{\{\,\mathrm{a,a}\,\}}\rangle^{\mathrm{q}} \tag{C.8}
$$

$$
\begin{aligned}
c_{2,\mathrm{q,aa}}^{2,(2,0)} &= -\frac{266}{81}C_F T_F\langle\mathrm{l}_{\{\,\mathrm{a,a}\,\}}\rangle^{\mathrm{q}} n_\mathrm{l} - 8C_F T_F\langle\bar{\mathrm{l}}_{\{\,\mathrm{a,a}\,\}}\rangle^{\mathrm{q}} n_\mathrm{l} + C_A C_F\langle\bar{\mathrm{l}}_{\{\,\mathrm{a,a}\,\}}\rangle^{\mathrm{q}}\Big[\frac{3677}{135} - \frac{128}{5}\zeta_3\Big] \\
&\quad + C_F^2\langle\bar{\mathrm{l}}_{\{\,\mathrm{a,a}\,\}}\rangle^{\mathrm{q}}\Big[- \frac{4189}{810} + \frac{96}{5}\zeta_3\Big] + C_F T_F\langle\bar{\mathrm{l}}_{\{\,\mathrm{a}\,\}}\mathrm{l}_{\{\,\mathrm{a}\,\}}\rangle^{\mathrm{q}} n_\mathrm{l}\Big[- \frac{658}{15} - \frac{32}{5}\zeta_3\Big] \\
&\quad + C_F T_F\langle\bar{\mathrm{l}}_{\{\,\mathrm{a}\,\}}\mathrm{h}_{\{\,\mathrm{a}\,\}}\rangle^{\mathrm{q}} n_\mathrm{h}\Big[- \frac{1328}{45} + \frac{752}{15}\mathrm{d}_{-1} + \frac{752}{15}\mathrm{d}_{-1}^2 \\
&\quad\quad + \mathrm{H}_0\Big(- \frac{424}{45} - \frac{106}{45}\upsilon - \frac{428}{9}\mathrm{d}_{-1} - \frac{752}{5}\mathrm{d}_{-1}^2 - \frac{1504}{15}\mathrm{d}_{-1}^3\Big) \\
&\quad\quad + \mathrm{H}_1\Big(- \frac{964}{45} - \frac{106}{45}\upsilon - \frac{106}{45}\mathrm{d}_0\Big) \\
&\quad\quad + \mathrm{H}_{-1,0}\Big(48 - 24\upsilon + 96\mathrm{d}_{-1} + 24\mathrm{d}_0\Big) \\
&\quad\quad + \mathrm{H}_{0,0}\Big(- \frac{72}{5} + 36\upsilon - \frac{1036}{15}\mathrm{d}_{-1} + \frac{228}{5}\mathrm{d}_{-1}^2 + \frac{3008}{15}\mathrm{d}_{-1}^3 + \frac{1504}{15}\mathrm{d}_{-1}^4\Big) \\
&\quad\quad + \mathrm{H}_{0,1}\Big(\frac{144}{5} + \frac{288}{5}\mathrm{d}_{-1}\Big)
\end{aligned}
$$

$$
\begin{aligned}
&+ \mathrm{H}_{1,0}\left(\frac{24}{5} + 12\upsilon + \frac{48}{5}\mathrm{d}_{-1} - 12\mathrm{d}_0\right)\\
&+ \mathrm{H}_{0,0,1}\left(-\frac{32}{15} + \frac{496}{15}\mathrm{d}_{-1} + \frac{496}{15}\mathrm{d}_{-1}^2\right)\\
&+ \mathrm{H}_{0,1,0}\left(-\frac{32}{15} + \frac{496}{15}\mathrm{d}_{-1} + \frac{496}{15}\mathrm{d}_{-1}^2\right)\\
&+ \mathrm{H}_{1,0,0}\left(\frac{64}{15} - \frac{992}{15}\mathrm{d}_{-1} - \frac{992}{15}\mathrm{d}_{-1}^2\right)\\
&+ \zeta_3\left(-\frac{32}{5} + \frac{496}{5}\mathrm{d}_{-1} + \frac{496}{5}\mathrm{d}_{-1}^2\right)\Bigg]\\
+ C_F T_F \langle \bar{\mathrm{l}}_{\{\mathrm{a,a}\}}\rangle^{\mathrm{q}} n_{\mathrm{h}}&\Bigg[-\frac{509317}{42525} - \frac{26}{2025}\upsilon - \frac{16}{14175}\upsilon^2 + \frac{6484}{2835}\mathrm{d}_{-1} + \frac{6484}{2835}\mathrm{d}_{-1}^2\\
&- \frac{26}{2025}\mathrm{d}_0 - \frac{16}{14175}\mathrm{d}_0^2\\
&+ \mathrm{H}_0\Bigg(\frac{18992}{2835} - \frac{104}{135}\upsilon + \frac{58}{4725}\upsilon^2 + \frac{16}{14175}\upsilon^3 + \frac{1576}{135}\mathrm{d}_{-1} - \frac{596}{945}\mathrm{d}_{-1}^2\\
&\quad - \frac{1192}{2835}\mathrm{d}_{-1}^3\Bigg)\\
&+ \mathrm{H}_1\left(\frac{4292}{2835} - \frac{104}{135}\upsilon + \frac{58}{4725}\upsilon^2 + \frac{16}{14175}\upsilon^3 - \frac{104}{135}\mathrm{d}_0 + \frac{58}{4725}\mathrm{d}_0^2 + \frac{16}{14175}\mathrm{d}_0^3\right)\\
&+ \mathrm{H}_{0,0}\left(-\frac{32}{9} - \frac{56}{15}\mathrm{d}_{-1}^2 - \frac{112}{15}\mathrm{d}_{-1}^3 - \frac{56}{15}\mathrm{d}_{-1}^4\right)\Bigg]\\
+ C_F T_F \langle \mathrm{h}_{\{\mathrm{a,a}\}}\rangle^{\mathrm{q}} n_{\mathrm{h}}&\Bigg[\frac{8054}{45} - \frac{1762}{15}\upsilon - \frac{56}{45}\upsilon^2 + \frac{192}{5}\mathrm{d}_{-1} + \frac{192}{5}\mathrm{d}_{-1}^2 - \frac{1762}{15}\mathrm{d}_0\\
&- \frac{56}{45}\mathrm{d}_0^2 + \frac{176}{3}\mathrm{d}_1 - \frac{1712}{9}\mathrm{d}_1^2 + \frac{2368}{9}\mathrm{d}_1^3 - \frac{1184}{9}\mathrm{d}_1^4\\
&+ \mathrm{H}_0\Bigg(\frac{36776}{135} - \frac{1748}{15}\upsilon - \frac{56}{45}\upsilon^2 + \frac{112}{3}\mathrm{d}_{-1} - \frac{576}{5}\mathrm{d}_{-1}^2 - \frac{384}{5}\mathrm{d}_{-1}^3 + \frac{1748}{15}\mathrm{d}_0\\
&\quad + \frac{56}{45}\mathrm{d}_0^2 - \frac{2044}{5}\mathrm{d}_1 - \frac{1660}{9}\mathrm{d}_1^2 + \frac{5944}{27}\mathrm{d}_1^3 - \frac{1264}{9}\mathrm{d}_1^4 + \frac{352}{9}\mathrm{d}_1^5\Bigg)\\
&+ \mathrm{H}_1\left(-\frac{16}{3} + \frac{224}{3}\mathrm{d}_1 - 160\mathrm{d}_1^2 + \frac{512}{3}\mathrm{d}_1^3 - \frac{256}{3}\mathrm{d}_1^4\right)\\
&+ \mathrm{H}_{-1,0}\Bigg(\frac{1664}{9} - \frac{976}{5}\upsilon + \frac{1184}{5}\upsilon^2 + \frac{112}{45}\upsilon^3 - 16\mathrm{d}_{-1} + \frac{976}{5}\mathrm{d}_0 - \frac{1184}{5}\mathrm{d}_0^2 - \frac{112}{45}\mathrm{d}_0^3\\
&\quad - \frac{1360}{3}\mathrm{d}_1 + 288\mathrm{d}_1^2 - \frac{4288}{9}\mathrm{d}_1^3 + \frac{1280}{3}\mathrm{d}_1^4 - \frac{512}{3}\mathrm{d}_1^5\Bigg)\\
&+ \mathrm{H}_{0,0}\Bigg(-\frac{800}{3} + \frac{1464}{5}\upsilon - \frac{1776}{5}\upsilon^2 - \frac{56}{15}\upsilon^3 - \frac{124}{15}\mathrm{d}_{-1} + \frac{968}{15}\mathrm{d}_{-1}^2 + \frac{768}{5}\mathrm{d}_{-1}^3\\
&\quad + \frac{384}{5}\mathrm{d}_{-1}^4 + \frac{4852}{15}\mathrm{d}_1 - \frac{984}{5}\mathrm{d}_1^2 + \frac{2608}{9}\mathrm{d}_1^3 - 192\mathrm{d}_1^4 + \frac{128}{3}\mathrm{d}_1^5\Bigg)\\
&+ \mathrm{H}_{0,1}\left(\frac{64}{9} - 8\mathrm{d}_{-1} - 56\mathrm{d}_1 + 144\mathrm{d}_1^2 - \frac{2144}{9}\mathrm{d}_1^3 + \frac{640}{3}\mathrm{d}_1^4 - \frac{256}{3}\mathrm{d}_1^5\right)
\end{aligned}
$$

$$+ \mathrm{H}_{1,0}\bigg(-\frac{256}{3} + \frac{488}{5}\upsilon - \frac{592}{5}\upsilon^2 - \frac{56}{45}\upsilon^3 - \frac{488}{5}\mathrm{d}_0 + \frac{592}{5}\mathrm{d}_0^2 + \frac{56}{45}\mathrm{d}_0^3 + \frac{512}{3}\mathrm{d}_1\bigg)\bigg] \tag{C.9}$$

$$c^{2,(0,0)}_{L,\mathrm{q,aa}} = 0 \tag{C.10}$$

$$c^{2,(1,0)}_{L,\mathrm{q,aa}} = \frac{4}{3}C_F\langle\bar{\mathrm{l}}_{\{\,\mathrm{a,a}\,\}}\rangle^{\mathrm{q}} \tag{C.11}$$

$$\begin{aligned}
c^{2,(2,0)}_{L,\mathrm{q,aa}} = {} & -\frac{160}{27}C_FT_F\langle\mathrm{l}_{\{\,\mathrm{a,a}\,\}}\rangle^{\mathrm{q}}n_{\mathrm{l}} - \frac{184}{9}C_FT_F\langle\bar{\mathrm{l}}_{\{\,\mathrm{a,a}\,\}}\rangle^{\mathrm{q}}n_{\mathrm{l}} + C_AC_F\langle\bar{\mathrm{l}}_{\{\,\mathrm{a,a}\,\}}\rangle^{\mathrm{q}}\bigg[\frac{2878}{135} - \frac{32}{5}\zeta_3\bigg] \\
& + C_F^2\langle\bar{\mathrm{l}}_{\{\,\mathrm{a,a}\,\}}\rangle^{\mathrm{q}}\bigg[-\frac{1906}{135} + \frac{64}{5}\zeta_3\bigg] + C_FT_F\langle\bar{\mathrm{l}}_{\{\,\mathrm{a}\,\}}\mathrm{l}_{\{\,\mathrm{a}\,\}}\rangle^{\mathrm{q}}n_{\mathrm{l}}\bigg[\frac{368}{15} - \frac{128}{5}\zeta_3\bigg] \\
& + C_FT_F\langle\bar{\mathrm{l}}_{\{\,\mathrm{a}\,\}}\mathrm{h}_{\{\,\mathrm{a}\,\}}\rangle^{\mathrm{q}}n_{\mathrm{h}}\bigg[\frac{476}{15} + \frac{256}{5}\mathrm{d}_{-1} + \frac{256}{5}\mathrm{d}_{-1}^2 \\
& \quad + \mathrm{H}_0\bigg(-\frac{144}{5} + \frac{4}{5}\upsilon - 72\mathrm{d}_{-1} - \frac{768}{5}\mathrm{d}_{-1}^2 - \frac{512}{5}\mathrm{d}_{-1}^3\bigg) \\
& \quad + \mathrm{H}_1\bigg(-\frac{184}{5} + \frac{4}{5}\upsilon + \frac{4}{5}\mathrm{d}_0\bigg) \\
& \quad + \mathrm{H}_{-1,0}\bigg(32 - 16\upsilon + 64\mathrm{d}_{-1} + 16\mathrm{d}_0\bigg) \\
& \quad + \mathrm{H}_{0,0}\bigg(-\frac{48}{5} + 24\upsilon - \frac{904}{15}\mathrm{d}_{-1} + \frac{776}{15}\mathrm{d}_{-1}^2 + \frac{1024}{5}\mathrm{d}_{-1}^3 + \frac{512}{5}\mathrm{d}_{-1}^4\bigg) \\
& \quad + \mathrm{H}_{0,1}\bigg(\frac{96}{5} + \frac{192}{5}\mathrm{d}_{-1}\bigg) \\
& \quad + \mathrm{H}_{1,0}\bigg(\frac{16}{5} + 8\upsilon + \frac{32}{5}\mathrm{d}_{-1} - 8\mathrm{d}_0\bigg) \\
& \quad + \mathrm{H}_{0,0,1}\bigg(-\frac{128}{15} - \frac{32}{5}\mathrm{d}_{-1} - \frac{32}{5}\mathrm{d}_{-1}^2\bigg) \\
& \quad + \mathrm{H}_{0,1,0}\bigg(-\frac{128}{15} - \frac{32}{5}\mathrm{d}_{-1} - \frac{32}{5}\mathrm{d}_{-1}^2\bigg) \\
& \quad + \mathrm{H}_{1,0,0}\bigg(\frac{256}{15} + \frac{64}{5}\mathrm{d}_{-1} + \frac{64}{5}\mathrm{d}_{-1}^2\bigg) \\
& \quad + \zeta_3\bigg(-\frac{128}{5} - \frac{96}{5}\mathrm{d}_{-1} - \frac{96}{5}\mathrm{d}_{-1}^2\bigg)\bigg] \\
& + C_FT_F\langle\bar{\mathrm{l}}_{\{\,\mathrm{a,a}\,\}}\rangle^{\mathrm{q}}n_{\mathrm{h}}\bigg[-\frac{95416}{14175} - \frac{176}{4725}\upsilon + \frac{32}{4725}\upsilon^2 - \frac{10208}{135}\mathrm{d}_{-1} \\
& \quad - \frac{10208}{135}\mathrm{d}_{-1}^2 - \frac{176}{4725}\mathrm{d}_0 + \frac{32}{4725}\mathrm{d}_0^2 \\
& \quad + \mathrm{H}_0\bigg(\frac{1808}{945} - \frac{32}{315}\upsilon + \frac{64}{1575}\upsilon^2 - \frac{32}{4725}\upsilon^3 + \frac{10048}{315}\mathrm{d}_{-1} + \frac{3808}{45}\mathrm{d}_{-1}^2 + \frac{7616}{135}\mathrm{d}_{-1}^3\bigg)
\end{aligned}$$

$$
\begin{aligned}
&+ \mathrm{H}_1\Big(\frac{128}{945} - \frac{32}{315}\upsilon + \frac{64}{1575}\upsilon^2 - \frac{32}{4725}\upsilon^3 - \frac{32}{315}\mathrm{d}_0 + \frac{64}{1575}\mathrm{d}_0^2 - \frac{32}{4725}\mathrm{d}_0^3\Big) \\
&+ \mathrm{H}_{0,0}\Big(\frac{192}{5}\mathrm{d}_{-1}^2 + \frac{384}{5}\mathrm{d}_{-1}^3 + \frac{192}{5}\mathrm{d}_{-1}^4\Big)\Big] \\
&+ C_F T_F \langle \mathrm{h}_{\{\mathrm{a,a}\}}\rangle^{\mathrm{q}} n_{\mathrm{h}}\Big[\frac{12488}{135} - \frac{316}{5}\upsilon + \frac{112}{15}\upsilon^2 + \frac{128}{5}\mathrm{d}_{-1} + \frac{128}{5}\mathrm{d}_{-1}^2 - \frac{316}{5}\mathrm{d}_0 \\
&+ \frac{112}{15}\mathrm{d}_0^2 + \frac{800}{27}\mathrm{d}_1 - \frac{2576}{27}\mathrm{d}_1^2 + \frac{1184}{9}\mathrm{d}_1^3 - \frac{592}{9}\mathrm{d}_1^4 \\
&+ \mathrm{H}_0\Big(\frac{752}{5} - \frac{344}{5}\upsilon + \frac{112}{15}\upsilon^2 + \frac{47}{3}\mathrm{d}_{-1} - \frac{384}{5}\mathrm{d}_{-1}^2 - \frac{256}{5}\mathrm{d}_{-1}^3 + \frac{344}{5}\mathrm{d}_0 - \frac{112}{15}\mathrm{d}_0^2 \\
&- \frac{10009}{45}\mathrm{d}_1 - \frac{770}{9}\mathrm{d}_1^2 + \frac{956}{9}\mathrm{d}_1^3 - \frac{632}{9}\mathrm{d}_1^4 + \frac{176}{9}\mathrm{d}_1^5\Big) \\
&+ \mathrm{H}_1\Big(\frac{64}{9} + \frac{320}{9}\mathrm{d}_1 - \frac{704}{9}\mathrm{d}_1^2 + \frac{256}{3}\mathrm{d}_1^3 - \frac{128}{3}\mathrm{d}_1^4\Big) \\
&+ \mathrm{H}_{-1,0}\Big(\frac{256}{3} - \frac{544}{5}\upsilon + \frac{576}{5}\upsilon^2 - \frac{224}{15}\upsilon^3 - \frac{80}{3}\mathrm{d}_{-1} + \frac{544}{5}\mathrm{d}_0 - \frac{576}{5}\mathrm{d}_0^2 + \frac{224}{15}\mathrm{d}_0^3 \\
&- \frac{688}{3}\mathrm{d}_1 + \frac{416}{3}\mathrm{d}_1^2 - \frac{704}{3}\mathrm{d}_1^3 + \frac{640}{3}\mathrm{d}_1^4 - \frac{256}{3}\mathrm{d}_1^5\Big) \\
&+ \mathrm{H}_{0,0}\Big(- 128 + \frac{816}{5}\upsilon - \frac{864}{5}\upsilon^2 + \frac{112}{5}\upsilon^3 - \frac{76}{15}\mathrm{d}_{-1} + \frac{592}{15}\mathrm{d}_{-1}^2 + \frac{512}{5}\mathrm{d}_{-1}^3 \\
&+ \frac{256}{5}\mathrm{d}_{-1}^4 + \frac{2428}{15}\mathrm{d}_1 - \frac{1448}{15}\mathrm{d}_1^2 + 144\mathrm{d}_1^3 - 96\mathrm{d}_1^4 + \frac{64}{3}\mathrm{d}_1^5\Big) \\
&+ \mathrm{H}_{0,1}\Big(- (\frac{40}{3}\mathrm{d}_{-1}) - \frac{88}{3}\mathrm{d}_1 + \frac{208}{3}\mathrm{d}_1^2 - \frac{352}{3}\mathrm{d}_1^3 + \frac{320}{3}\mathrm{d}_1^4 - \frac{128}{3}\mathrm{d}_1^5\Big) \\
&+ \mathrm{H}_{1,0}\Big(- \frac{128}{3} + \frac{272}{5}\upsilon - \frac{288}{5}\upsilon^2 + \frac{112}{15}\upsilon^3 - \frac{272}{5}\mathrm{d}_0 + \frac{288}{5}\mathrm{d}_0^2 - \frac{112}{15}\mathrm{d}_0^3 \\
&+ \frac{256}{3}\mathrm{d}_1\Big)\Big] \qquad \text{(C.12)}
\end{aligned}
$$

C.2 Axial–Vector

$$c_{3,\mathrm{q,va}}^{1,(0,0)} = \langle \bar{\mathrm{l}}_{\{\mathrm{v,a}\}}\rangle^{\mathrm{q}} \qquad \text{(C.13)}$$

$$c_{3,\mathrm{q,va}}^{1,(1,0)} = -3C_F\langle \bar{\mathrm{l}}_{\{\mathrm{v,a}\}}\rangle^{\mathrm{q}} \qquad \text{(C.14)}$$

$$
\begin{aligned}
c_{3,\mathrm{q,va}}^{1,(2,0)} &= -23C_A C_F\langle \bar{\mathrm{l}}_{\{\mathrm{v,a}\}}\rangle^{\mathrm{q}} + \frac{21}{2}C_F^2\langle \bar{\mathrm{l}}_{\{\mathrm{v,a}\}}\rangle^{\mathrm{q}} + 8C_F T_F\langle \bar{\mathrm{l}}_{\{\mathrm{v,a}\}}\rangle^{\mathrm{q}} n_{\mathrm{l}} \\
&+ C_F T_F\langle \bar{\mathrm{l}}_{\{\mathrm{v}\}}\mathrm{l}_{\{\mathrm{a}\}} n_{\mathrm{l}}\Big[- \frac{97}{3} + 16\zeta_3\Big] \\
&+ C_F T_F\langle \bar{\mathrm{l}}_{\{\mathrm{v,a}\}}\rangle^{\mathrm{q}} n_{\mathrm{h}}\Big[\frac{389}{45} + \frac{2}{105}\upsilon + \frac{3908}{105}\mathrm{d}_{-1} + \frac{3908}{105}\mathrm{d}_{-1}^2 + \frac{2}{105}\mathrm{d}_0
\end{aligned}
$$

$$
\begin{aligned}
&+ \mathrm{H}_0\Big(- \frac{848}{315} - \frac{40}{63}\upsilon - \frac{2}{105}\upsilon^2 - \frac{1384}{63}\mathrm{d}_{-1} - \frac{1604}{35}\mathrm{d}_{-1}^2 - \frac{3208}{105}\mathrm{d}_{-1}^3\Big) \\
&+ \mathrm{H}_1\Big(\frac{412}{315} - \frac{40}{63}\upsilon - \frac{2}{105}\upsilon^2 - \frac{40}{63}\mathrm{d}_0 - \frac{2}{105}\mathrm{d}_0^2\Big) \\
&+ \mathrm{H}_{0,0}\Big(- (\frac{40}{3}\mathrm{d}_{-1}^2) - \frac{80}{3}\mathrm{d}_{-1}^3 - \frac{40}{3}\mathrm{d}_{-1}^4\Big)\Big] \\
+ {} & C_F T_F \langle \bar{\mathrm{l}}_{\{\mathrm{v}\}}\mathrm{h}_{\{\mathrm{a}\}}\rangle^{\mathrm{q}} n_\mathrm{h}\Big[- \frac{97}{3} - \frac{8}{3}\mathrm{d}_{-1} - \frac{8}{3}\mathrm{d}_{-1}^2 \\
&+ \mathrm{H}_0\Big(\frac{40}{3} + 16\mathrm{d}_{-1} + 8\mathrm{d}_{-1}^2 + \frac{16}{3}\mathrm{d}_{-1}^3\Big) \\
&+ \mathrm{H}_1\Big(\frac{40}{3}\Big) \\
&+ \mathrm{H}_{0,0}\Big(\frac{32}{3}\mathrm{d}_{-1} + \frac{16}{3}\mathrm{d}_{-1}^2 - \frac{32}{3}\mathrm{d}_{-1}^3 - \frac{16}{3}\mathrm{d}_{-1}^4\Big) \\
&+ \mathrm{H}_{0,0,1}\Big(\frac{16}{3} + \frac{64}{3}\mathrm{d}_{-1} + \frac{64}{3}\mathrm{d}_{-1}^2\Big) \\
&+ \mathrm{H}_{0,1,0}\Big(\frac{16}{3} + \frac{64}{3}\mathrm{d}_{-1} + \frac{64}{3}\mathrm{d}_{-1}^2\Big) \\
&+ \mathrm{H}_{1,0,0}\Big(- \frac{32}{3} - \frac{128}{3}\mathrm{d}_{-1} - \frac{128}{3}\mathrm{d}_{-1}^2\Big) \\
&+ \zeta_3\Big(16 + 64\mathrm{d}_{-1} + 64\mathrm{d}_{-1}^2\Big)\Big]
\end{aligned}
\tag{C.15}
$$

C.3 Scalar–Scalar

$$
c_{S,\mathrm{g}}^{2,(0,0)} = 1 \tag{C.16}
$$

$$
\begin{aligned}
c_{S,\mathrm{g}}^{2,(1,0)} = {} & -\frac{20}{9}T_F n_\mathrm{l} + \frac{203}{18}C_A + T_F n_\mathrm{h}\Big[- \frac{20}{9} + \frac{16}{3}\mathrm{d}_{-1} + \frac{16}{3}\mathrm{d}_{-1}^2 \\
&+ \mathrm{H}_0\Big(4 - 8\mathrm{d}_{-1}^2 - \frac{16}{3}\mathrm{d}_{-1}^3\Big) \\
&+ \mathrm{H}_1\Big(\frac{16}{3}\Big)\Big]
\end{aligned}
\tag{C.17}
$$

$$
\begin{aligned}
c_{S,\mathrm{g}}^{2,(2,0)} = {} & \frac{400}{81}T_F^2 n_\mathrm{l}^2 + C_A^2\Big[\frac{23473}{108} - 66\zeta_3\Big] + C_A T_F n_\mathrm{l}\Big[- \frac{8215}{81} - 24\zeta_3\Big] \\
&+ C_F T_F n_\mathrm{l}\Big[- \frac{3452}{81} + 48\zeta_3\Big] \\
&+ T_F^2 n_\mathrm{h} n_\mathrm{l}\Big[\frac{800}{81} - \frac{640}{27}\mathrm{d}_{-1} - \frac{640}{27}\mathrm{d}_{-1}^2 \\
&+ \mathrm{H}_0\Big(- \frac{320}{27} + \frac{320}{9}\mathrm{d}_{-1}^2 + \frac{640}{27}\mathrm{d}_{-1}^3\Big) \\
&+ \mathrm{H}_1\Big(- \frac{320}{27}\Big)\Big]
\end{aligned}
$$

$$
\begin{aligned}
&+ T_F^2 n_{\mathrm{h}}^2 \Bigg[\frac{400}{81} - \frac{640}{27}\mathrm{d}_{-1} + \frac{128}{27}\mathrm{d}_{-1}^2 + \frac{512}{9}\mathrm{d}_{-1}^3 + \frac{256}{9}\mathrm{d}_{-1}^4 \\
&\quad + \mathrm{H}_0 \bigg(-\frac{320}{27} + \frac{256}{9}\mathrm{d}_{-1} + 64\mathrm{d}_{-1}^2 - \frac{1664}{27}\mathrm{d}_{-1}^3 - \frac{1280}{9}\mathrm{d}_{-1}^4 - \frac{512}{9}\mathrm{d}_{-1}^5 \bigg) \\
&\quad + \mathrm{H}_1 \bigg(-\frac{320}{27} + \frac{256}{9}\mathrm{d}_{-1} + \frac{256}{9}\mathrm{d}_{-1}^2 \bigg) \\
&\quad + \mathrm{H}_{0,0} \bigg(\frac{128}{9} - \frac{256}{3}\mathrm{d}_{-1}^2 - \frac{512}{9}\mathrm{d}_{-1}^3 + 128\mathrm{d}_{-1}^4 + \frac{512}{3}\mathrm{d}_{-1}^5 + \frac{512}{9}\mathrm{d}_{-1}^6 \bigg) \\
&\quad + \mathrm{H}_{0,1} \bigg(\frac{128}{9} - \frac{128}{3}\mathrm{d}_{-1}^2 - \frac{256}{9}\mathrm{d}_{-1}^3 \bigg) \\
&\quad + \mathrm{H}_{1,0} \bigg(\frac{128}{9} - \frac{128}{3}\mathrm{d}_{-1}^2 - \frac{256}{9}\mathrm{d}_{-1}^3 \bigg) \\
&\quad + \mathrm{H}_{1,1} \bigg(\frac{128}{9} \bigg) \Bigg] \\
&+ C_A T_F n_{\mathrm{h}} \Bigg[-\frac{869228}{8505} - \frac{23}{5670}y - \frac{47}{2835}y^2 + \frac{156292}{2835}\mathrm{d}_{-1} + \frac{156292}{2835}\mathrm{d}_{-1}^2 - \frac{23}{5670}\mathrm{d}_0 \\
&\quad - \frac{47}{2835}\mathrm{d}_0^2 \\
&\quad + \mathrm{H}_0 \bigg(\frac{347894}{2835} + \frac{211}{945}y - \frac{4}{945}y^2 + \frac{47}{2835}y^3 + \frac{48616}{945}\mathrm{d}_{-1} - \frac{153956}{945}\mathrm{d}_{-1}^2 \\
&\quad - \frac{270952}{2835}\mathrm{d}_{-1}^3 \bigg) \\
&\quad + \mathrm{H}_1 \bigg(\frac{359024}{2835} + \frac{211}{945}y - \frac{4}{945}y^2 + \frac{47}{2835}y^3 - \frac{352}{9}\mathrm{d}_{-1} - \frac{352}{9}\mathrm{d}_{-1}^2 + \frac{211}{945}\mathrm{d}_0 \\
&\quad - \frac{4}{945}\mathrm{d}_0^2 + \frac{47}{2835}\mathrm{d}_0^3 \bigg) \\
&\quad + \mathrm{H}_{-1,0} \bigg(\frac{16}{9} + \frac{8}{3}y + \frac{64}{3}\mathrm{d}_{-1} + \frac{160}{3}\mathrm{d}_{-1}^2 + \frac{320}{9}\mathrm{d}_{-1}^3 - \frac{8}{3}\mathrm{d}_0 \bigg) \\
&\quad + \mathrm{H}_{0,0} \bigg(-\frac{292}{9} - 4y - \frac{128}{3}\mathrm{d}_{-1} + 32\mathrm{d}_{-1}^2 + \frac{736}{9}\mathrm{d}_{-1}^3 + \frac{104}{3}\mathrm{d}_{-1}^4 \bigg) \\
&\quad + \mathrm{H}_{0,1} \bigg(-\frac{112}{9} - \frac{16}{3}\mathrm{d}_{-1} + \frac{176}{3}\mathrm{d}_{-1}^2 + \frac{352}{9}\mathrm{d}_{-1}^3 \bigg) \\
&\quad + \mathrm{H}_{1,0} \bigg(-\frac{40}{3} - \frac{4}{3}y - 16\mathrm{d}_{-1} + 32\mathrm{d}_{-1}^2 + \frac{64}{3}\mathrm{d}_{-1}^3 + \frac{4}{3}\mathrm{d}_0 \bigg) \\
&\quad + \mathrm{H}_{-1,0,0} \bigg(\frac{32}{3} - \frac{128}{3}\mathrm{d}_{-1}^2 - \frac{256}{3}\mathrm{d}_{-1}^3 - \frac{128}{3}\mathrm{d}_{-1}^4 \bigg) \\
&\quad + \mathrm{H}_{0,-1,0} \bigg(-\frac{32}{3} + \frac{128}{3}\mathrm{d}_{-1}^2 + \frac{256}{3}\mathrm{d}_{-1}^3 + \frac{128}{3}\mathrm{d}_{-1}^4 \bigg) \\
&\quad + \mathrm{H}_{0,0,1} \bigg(-\frac{16}{3} + 16\mathrm{d}_{-1} + 16\mathrm{d}_{-1}^2 \bigg) \\
&\quad + \mathrm{H}_{0,1,0} \bigg(16\mathrm{d}_{-1} - \frac{16}{3}\mathrm{d}_{-1}^2 - \frac{128}{3}\mathrm{d}_{-1}^3 - \frac{64}{3}\mathrm{d}_{-1}^4 \bigg)
\end{aligned}
$$

$$
\begin{aligned}
&+ \mathrm{H}_{1,0,0}\Big(\frac{16}{3} - 32\mathrm{d}_{-1} - \frac{32}{3}\mathrm{d}_{-1}^2 + \frac{128}{3}\mathrm{d}_{-1}^3 + \frac{64}{3}\mathrm{d}_{-1}^4\Big)\\
&+ \zeta_3\Big(- 24 + 48\mathrm{d}_{-1} + 80\mathrm{d}_{-1}^2 + 64\mathrm{d}_{-1}^3 + 32\mathrm{d}_{-1}^4\Big)\Big]\\
+ C_F T_F n_\mathrm{h}\Big[&- \frac{15277}{315} + \frac{11}{189}y + \frac{74}{945}y^2 - \frac{220}{3}\mathrm{d}_{-1} - \frac{220}{3}\mathrm{d}_{-1}^2 + \frac{11}{189}\mathrm{d}_0 + \frac{74}{945}\mathrm{d}_0^2\\
&+ \mathrm{H}_0\Big(\frac{28808}{945} - \frac{34}{315}y - \frac{2}{105}y^2 - \frac{74}{945}y^3 + \frac{43856}{315}\mathrm{d}_{-1} + 204\mathrm{d}_{-1}^2 + 104\mathrm{d}_{-1}^3\\
&\quad + 16\mathrm{d}_1\Big)\\
&+ \mathrm{H}_1\Big(\frac{35668}{945} - \frac{34}{315}y - \frac{2}{105}y^2 - \frac{74}{945}y^3 + 96\mathrm{d}_{-1} + 96\mathrm{d}_{-1}^2 - \frac{34}{315}\mathrm{d}_0 - \frac{2}{105}\mathrm{d}_0^2\\
&\quad - \frac{74}{945}\mathrm{d}_0^3\Big)\\
&+ \mathrm{H}_{-1,0}\Big(- \frac{64}{3} + 128\mathrm{d}_{-1}^2 + \frac{256}{3}\mathrm{d}_{-1}^3\Big)\\
&+ \mathrm{H}_{0,0}\Big(\frac{128}{9} - 128\mathrm{d}_{-1} - 416\mathrm{d}_{-1}^2 - \frac{1232}{3}\mathrm{d}_{-1}^3 - \frac{376}{3}\mathrm{d}_{-1}^4 - 8\mathrm{d}_1\Big)\\
&+ \mathrm{H}_{0,1}\Big(- \frac{32}{3} - \frac{232}{3}\mathrm{d}_{-1} - 144\mathrm{d}_{-1}^2 - 96\mathrm{d}_{-1}^3 - 8\mathrm{d}_1\Big)\\
&+ \mathrm{H}_{1,0}\Big(- (\frac{232}{3}\mathrm{d}_{-1}) - 208\mathrm{d}_{-1}^2 - \frac{416}{3}\mathrm{d}_{-1}^3 - 8\mathrm{d}_1\Big)\\
&+ \mathrm{H}_{-1,0,0}\Big(- \frac{64}{3} + \frac{256}{3}\mathrm{d}_{-1}^2 + \frac{512}{3}\mathrm{d}_{-1}^3 + \frac{256}{3}\mathrm{d}_{-1}^4\Big)\\
&+ \mathrm{H}_{0,-1,0}\Big(\frac{64}{3} - \frac{256}{3}\mathrm{d}_{-1}^2 - \frac{512}{3}\mathrm{d}_{-1}^3 - \frac{256}{3}\mathrm{d}_{-1}^4\Big)\\
&+ \mathrm{H}_{0,0,1}\Big(\frac{32}{3}\Big)\\
&+ \mathrm{H}_{0,1,0}\Big(\frac{128}{3}\mathrm{d}_{-1}^2 + \frac{256}{3}\mathrm{d}_{-1}^3 + \frac{128}{3}\mathrm{d}_{-1}^4\Big)\\
&+ \mathrm{H}_{1,0,0}\Big(- \frac{32}{3} - \frac{128}{3}\mathrm{d}_{-1}^2 - \frac{256}{3}\mathrm{d}_{-1}^3 - \frac{128}{3}\mathrm{d}_{-1}^4\Big)\\
&+ \zeta_3\Big(48 - 64\mathrm{d}_{-1}^2 - 128\mathrm{d}_{-1}^3 - 64\mathrm{d}_{-1}^4\Big)\Big]
\end{aligned}
\tag{C.18}
$$

$$
c_{S,\mathrm{q}}^{2,(0,0)} = 0 \tag{C.19}
$$

$$
c_{S,\mathrm{q}}^{2,(1,0)} = -\frac{4}{3}C_F \tag{C.20}
$$

$$
\begin{aligned}
c_{S,\mathrm{q}}^{2,(2,0)} = {}& \frac{88}{3}C_F T_F n_\mathrm{l} + C_A C_F\Big[- \frac{6224}{81} + 32\zeta_3\Big] + C_F^2\Big[\frac{1237}{81} - 32\zeta_3\Big]\\
&+ C_F T_F n_\mathrm{h}\Big[\frac{305248}{8505} - \frac{472}{2835}y - \frac{32}{2835}y^2 + \frac{120256}{2835}\mathrm{d}_{-1} + \frac{120256}{2835}\mathrm{d}_{-1}^2 - \frac{472}{2835}\mathrm{d}_0
\end{aligned}
$$

$$
\begin{aligned}
&- \frac{32}{2835}\mathrm{d}_0^2 \\
&+ \mathrm{H}_0\Bigg(- \frac{2672}{81} + \frac{1984}{945}y + \frac{152}{945}y^2 + \frac{32}{2835}y^3 - \frac{28256}{945}\mathrm{d}_{-1} + \frac{8752}{945}\mathrm{d}_{-1}^2 \\
&- \frac{9376}{2835}\mathrm{d}_{-1}^3\Bigg) \\
&+ \mathrm{H}_1\Bigg(- \frac{1904}{81} + \frac{1984}{945}y + \frac{152}{945}y^2 + \frac{32}{2835}y^3 + \frac{256}{9}\mathrm{d}_{-1} + \frac{256}{9}\mathrm{d}_{-1}^2 + \frac{1984}{945}\mathrm{d}_0 \\
&+ \frac{152}{945}\mathrm{d}_0^2 + \frac{32}{2835}\mathrm{d}_0^3\Bigg) \\
&+ \mathrm{H}_{-1,0}\Bigg(\frac{128}{9} - \frac{256}{3}\mathrm{d}_{-1}^2 - \frac{512}{9}\mathrm{d}_{-1}^3\Bigg) \\
&+ \mathrm{H}_{0,0}\Bigg(- (\frac{256}{9}\mathrm{d}_{-1}^3) - \frac{64}{3}\mathrm{d}_{-1}^4\Bigg) \\
&+ \mathrm{H}_{0,1}\Bigg(\frac{64}{9} - \frac{128}{3}\mathrm{d}_{-1}^2 - \frac{256}{9}\mathrm{d}_{-1}^3\Bigg)\Bigg] \qquad \text{(C.21)}
\end{aligned}
$$

Appendix D

Feynman Rules

In this section we collect the Feynman rules used throughout this work. Colour indices in the fundamental representation, as well as Dirac indices, are suppressed throughout, and the Einstein summation convention is assumed unless stated otherwise. Here T^a denotes the generators of the fundamental representation of the $\mathrm{SU}(N_F)$ gauge group and f^{abc} its structure constants, where N_F is the dimension of the fundamental representation. Conventions for the colour algebra are chosen to agree with those of `color.h` [207], such that

$$N_A = N_F^2 - 1\,, \tag{D.1}$$

$$C_F = \frac{T_F(N_F^2-1)}{N_F}\,, \tag{D.2}$$

$$C_A = 2T_F N_F\,, \tag{D.3}$$

$$d^{abc}d_{abc} = \frac{(N_F^2-1)(N_F^2-4)}{N_F}\,. \tag{D.4}$$

All propagators are expressed in terms of the Feynman propagator D_F (see Subsec. 3.1.1). The gluon propagator is given in a general covariant gauge with gauge parameter α, such that $\alpha = 0$ corresponds to Feynman gauge. Explicitly, the propagators read:

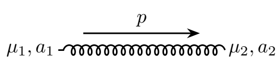

$$= -i\,\delta^{a_1a_2} D_\mathrm{F}(p)\left(g_{\mu_1\mu_2} - \alpha\,\frac{p_{\mu_1}p_{\mu_2}}{p^2}\right)\,, \tag{D.5}$$

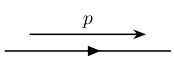

$$= i\,\not{p}\,D_\mathrm{F}(p)\,, \tag{D.6}$$

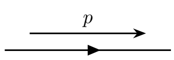

$$= i\left(\not{p} + m\right) D_\mathrm{F}(p)\,, \tag{D.7}$$

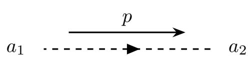

$$= i\,\delta^{a_1a_2} D_\mathrm{F}(p)\,. \tag{D.8}$$

The vertices below retain their full colour structure; the colour factors are stripped off later. Couplings of the vector boson to quarks are decomposed into vector and axial parts, which are encoded in the charge matrices Q_v and Q_a, where the second subscript indicates the flavour content of the current: l (h) for a light–light (heavy–heavy) quark pair, and [hl], [lh] for the flavour-changing combinations (see Sec. 2.3). For the scalar, the coupling constant is set to unity, while the strong coupling constant is denoted by g_s. All momenta are taken as incoming, as indicated in the graphs. With these conventions, the vertices read:

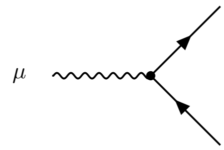

$$= i\left(Q_{\mathrm{v,l}} V^\mu_{\mathrm{vq}} + Q_{\mathrm{a,l}} V^\mu_{\mathrm{aq}}\right)\,, \tag{D.9}$$

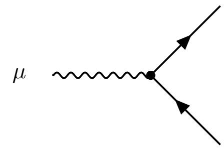

$$= i\left(Q_{\mathrm{v,h}} V^\mu_{\mathrm{vq}} + Q_{\mathrm{a,h}} V^\mu_{\mathrm{aq}}\right)\,, \tag{D.10}$$

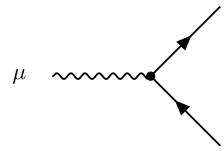

$$= i\left(Q_{\mathrm{v,[hl]}} V^\mu_{\mathrm{vq}} + Q_{\mathrm{a,[hl]}} V^\mu_{\mathrm{aq}}\right)\,, \tag{D.11}$$

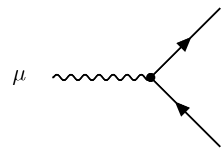

$$= i\left(Q_{\mathrm{v,[lh]}} V^\mu_{\mathrm{vq}} + Q_{\mathrm{a,[lh]}} V^\mu_{\mathrm{aq}}\right)\,, \tag{D.12}$$

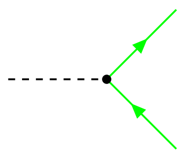

$$= -im\, V_{\mathrm{sq}}\,, \tag{D.13}$$

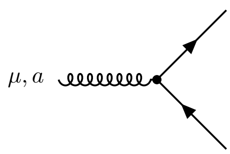

$$= ig_s T^a V^\mu_{\mathrm{vq}}\,, \tag{D.14}$$

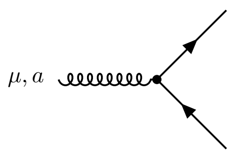

$$= ig_s T^a V^\mu_{\mathrm{vq}}\,, \tag{D.15}$$

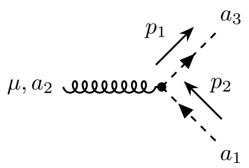

$$= ig_s f^{a_1 a_2 a_3} V_{\mathrm{gc}}^{\mu}(p_2)\,, \tag{D.16}$$

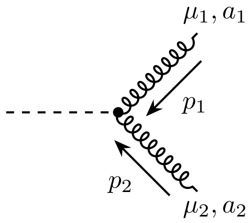

$$= -i\,\delta^{a_1 a_2} V_{\mathrm{g}^2}^{\mu_1 \mu_2}(p_1, p_2)\,, \tag{D.17}$$

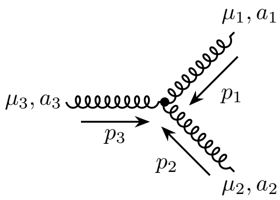

$$\begin{aligned} = ig_s\Big(& f^{a_1 a_2 a_3} V_{\mathrm{g}^3}^{\mu_1}(p_2, p_3) \\ & + f^{a_3 a_1 a_2} V_{\mathrm{g}^3}^{\mu_2}(p_3, p_1) \\ & + f^{a_2 a_3 a_1} V_{\mathrm{g}^3}^{\mu_3}(p_1, p_2)\Big)\,, \end{aligned} \tag{D.18}$$

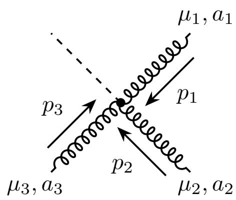

$$\begin{aligned} = ig_s\Big(& f^{a_1 a_2 a_3} V_{\mathrm{g}^3}^{\mu_1}(p_2, p_3) \\ & + f^{a_3 a_1 a_2} V_{\mathrm{g}^3}^{\mu_2}(p_3, p_1) \\ & + f^{a_2 a_3 a_1} V_{\mathrm{g}^3}^{\mu_3}(p_1, p_2)\Big)\,, \end{aligned} \tag{D.19}$$

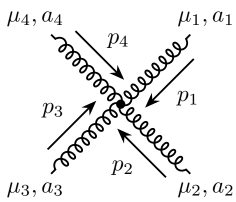

$$\begin{aligned} = -g_s^2\Big(& f^{a_1 a_2 c} f^{a_3 a_4 c}\, V_{\mathrm{g}^4}^{\mu_1 \mu_2 \mu_3 \mu_4} \\ & + f^{a_1 a_3 c} f^{a_2 a_4 c}\, V_{\mathrm{g}^4}^{\mu_1 \mu_3 \mu_2 \mu_4} \\ & + f^{a_1 a_4 c} f^{a_2 a_3 c}\, V_{\mathrm{g}^4}^{\mu_1 \mu_4 \mu_2 \mu_3}\Big)\,, \end{aligned} \tag{D.20}$$

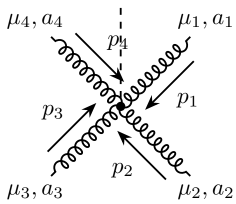

$$\begin{aligned} = -g_s^2\Big(& f^{a_1 a_2 c} f^{a_3 a_4 c}\, V_{\mathrm{g}^4}^{\mu_1 \mu_2 \mu_3 \mu_4} \\ & + f^{a_1 a_3 c} f^{a_2 a_4 c}\, V_{\mathrm{g}^4}^{\mu_1 \mu_3 \mu_2 \mu_4} \\ & + f^{a_1 a_4 c} f^{a_2 a_3 c}\, V_{\mathrm{g}^4}^{\mu_1 \mu_4 \mu_2 \mu_3}\Big)\,. \end{aligned} \tag{D.21}$$

In the expressions above we introduced a set of colour- and flavour-stripped vertex structures, which carry the Lorentz and Dirac content of each vertex. They are defined as follows:

$$V_{\mathrm{vq}}^{\mu} = \gamma^{\mu}\,, \tag{D.22}$$

$$V_{\mathrm{aq}}^{\mu} = \gamma^{\mu}\gamma_5\,, \tag{D.23}$$

$$V_{\mathrm{gc}}^{\mu}(p) = p^{\mu}\,, \tag{D.24}$$

$$V_{\mathrm{sq}} = 1\,, \tag{D.25}$$

$$V_{\mathrm{g}^2}^{\mu_1\mu_2}(p_1, p_2) = g^{\mu_1\mu_2}(p_1 \cdot p_2) - p_1^{\mu_2} p_2^{\mu_1}\,, \tag{D.26}$$

$$V_{\mathrm{g}^3}^{\mu}(p_1, p_2) = (p_1 - p_2)^{\mu}\,, \tag{D.27}$$

$$V_{\mathrm{g}^4}^{\mu_1\mu_2\mu_3\mu_4} = g^{\mu_1\mu_3} g^{\mu_2\mu_4} - g^{\mu_1\mu_4} g^{\mu_2\mu_3}\,. \tag{D.28}$$

It should be noted that the three- and four-gluon vertices with and without an attached scalar are structurally identical. They differ, however, in that momentum conservation takes a different form, since the scalar injects an additional momentum into the vertex. Simplifications that use momentum conservation implicitly to reduce gluonic structures, such as the procedures implemented in `Mincer` [172,173], therefore do not extend to the vertices involving the scalar.

Appendix E

Data Availability

This appendix describes the ancillary files accompanying the thesis. All results are supplied as MATHEMATICA packages (`.m`), accompanied by an overview notebook (`.nb`), and are available at

`https://github.com/mnklann/data-heavy-quark-production/`

The repository contains the master integrals of the neutral and charged currents (see Tabs. A.1 and A.2) as ε-expansions, together with their numerical values, the expansions of the associated periods, special functions, and integral kernels, as well as the Mellin moments at NLO and NNLO, including those presented in Ch. 5. The notation closely follows Sec. 4.5; the file structure and conventions are documented in the accompanying `README`. More intermediate results are available upon request to the author.

(This page is intentionally left blank.)

Bibliography

[1] E. D. Bloom et al. High-Energy Inelastic e–p Scattering at 6-Degrees and 10-Degrees. *Phys. Rev. Lett.*, 23:930–934, 1969.

[2] M. Breidenbach et al. Observed Behavior of Highly Inelastic Electron-Proton Scattering. *Phys. Rev. Lett.*, 23:935–939, 1969.

[3] J. D. Bjorken. Asymptotic Sum Rules at Infinite Momentum. *Phys. Rev.*, 179: 1547–1553, 1969.

[4] R. P. Feynman. Very High-Energy Collisions of Hadrons. *Phys. Rev. Lett.*, 23: 1415–1417, 1969.

[5] C. G. Callan, Jr. and D. J. Gross. High-energy Electroproduction and the Constitution of the Electric Current. *Phys. Rev. Lett.*, 22:156–159, 1969.

[6] D. J. Gross and F. Wilczek. Ultraviolet Behavior of Nonabelian Gauge Theories. *Phys. Rev. Lett.*, 30:1343–1346, 1973.

[7] H. D. Politzer. Reliable Perturbative Results for Strong Interactions? *Phys. Rev. Lett.*, 30:1346–1349, 1973.

[8] S. Alekhin, J. Blümlein, S. Moch, and R. Plačakytė. Parton Distribution Functions, α_s, and Heavy-Quark Masses for LHC Run II. *Phys. Rev. D*, 96(1):014011, 2017.

[9] T.-J. Hou et al. New CTEQ Global Analysis of Quantum Chromodynamics with High-Precision Data from the LHC. *Phys. Rev. D*, 103(1):014013, 2021.

[10] S. Bailey, T. Cridge, L. A. Harland-Lang, A. D. Martin, and R. S. Thorne. Parton Distributions from LHC, HERA, Tevatron and Fixed Target Data: MSHT20 PDFs. *Eur. Phys. J. C*, 81(4):341, 2021.

[11] R. D. Ball et al. The Path to Proton Structure at 1% Accuracy. *Eur. Phys. J. C*, 82(5):428, 2022.

[12] Particle Data Group. Review of Particle Physics. *Int. J. Mod. Phys. A*, 41: 2630011, 2026.

[13] V. N. Gribov and L. N. Lipatov. Deep Inelastic e–p Scattering in Perturbation Theory. *Sov. J. Nucl. Phys.*, 15:438–450, 1972.

[14] G. Altarelli and G. Parisi. Asymptotic Freedom in Parton Language. *Nucl. Phys. B*, 126:298–318, 1977.

[15] Y. L. Dokshitzer. Calculation of the Structure Functions for Deep Inelastic Scattering and $e^+ e^-$ Annihilation by Perturbation Theory in Quantum Chromodynamics. *Sov. Phys. JETP*, 46:641–653, 1977.

[16] J. C. Collins, D. E. Soper, and G. Sterman. Factorization of Hard Processes in QCD. In *Perturbative QCD*. World Scientific, 1989.

[17] W. A. Bardeen, A. J. Buras, D. W. Duke, and T. Muta. Deep Inelastic Scattering Beyond the Leading Order in Asymptotically Free Gauge Theories. *Phys. Rev. D*, 18:3998, 1978.

[18] A. J. Buras. Asymptotic Freedom in Deep Inelastic Processes in the Leading Order and Beyond. *Rev. Mod. Phys.*, 52:199, 1980.

[19] M. A. G. Aivazis, J. C. Collins, F. I. Olness, and W.-K. Tung. Leptoproduction of Heavy Quarks II – A Unified QCD Formulation of Charged and Neutral Current Processes from Fixed Target to Collider Energies. *Phys. Rev. D*, 50: 3102–3118, 1994a.

[20] M. A. G. Aivazis, F. I. Olness, and W.-K. Tung. Leptoproduction of Heavy Quarks I – General Formalism and Kinematics of Charged Current and Neutral Current Production Processes. *Phys. Rev. D*, 50:3085–3101, 1994b.

[21] R. S. Thorne and R. G. Roberts. An Ordered analysis of Heavy Flavor Production in Deep Inelastic Scattering. *Phys. Rev. D*, 57:6871–6898, 1998.

[22] R. S. Thorne. A Variable-Flavor Number Scheme for NNLO. *Phys. Rev. D*, 73: 054019, 2006.

[23] S. Forte, E. Laenen, P. Nason, and J. Rojo. Heavy Quarks in Deep-Inelastic Scattering. *Nucl. Phys. B*, 834:116–162, 2010.

[24] H. Abramowicz et al. Combination of Measurements of Inclusive Deep Inelastic $e^{\pm}p$ Scattering Cross Sections and QCD Analysis of HERA Data. *Eur. Phys. J. C*, 75(12):580, 2015.

[25] H. Abramowicz et al. Combination and QCD Analysis of Charm and Beauty Production Cross-Section Measurements in Deep Inelastic ep Scattering at HERA. *Eur. Phys. J. C*, 78(6):473, 2018.

[26] A. Accardi et al. Electron Ion Collider: The Next QCD Frontier: Understanding the Glue that Binds Us All. *Eur. Phys. J. A*, 52(9):268, 2016.

[27] R. Abdul Khalek et al. Science Requirements and Detector Concepts for the Electron-Ion Collider: EIC Yellow Report. *Nucl. Phys. A*, 1026:122447, 2022.

[28] SHiP Collaboration. A Facility to Search for Hidden Particles (SHiP) at the CERN SPS: Addendum to Technical Proposal. Technical report, CERN, 2015a.

[29] S. Alekhin et al. A Facility to Search for Hidden Particles at the CERN SPS: the SHiP Physics Case. *Rept. Prog. Phys.*, 79(12):124201, 2016.

[30] J. L. Feng et al. The Forward Physics Facility at the High-Luminosity LHC. *J. Phys. G*, 50(3):030501, 2023.

[31] E. B. Zijlstra and W. L. van Neerven. Order α_s^2 QCD Corrections to the Deep Inelastic Proton Structure Functions F_2 and F_L. *Nucl. Phys. B*, 383:525–574, 1992.

[32] S. Moch, J. A. M. Vermaseren, and A. Vogt. The Three Loop Splitting Functions in QCD: The Nonsinglet Case. *Nucl. Phys. B*, 688:101–134, 2004.

[33] A. Vogt, S. Moch, and J. A. M. Vermaseren. The Three-Loop Splitting Functions in QCD: The Singlet Case. *Nucl. Phys. B*, 691:129–181, 2004.

[34] S. Moch, J. A. M. Vermaseren, and A. Vogt. The Longitudinal Structure Function at the Third Order. *Phys. Lett. B*, 606:123–129, 2005.

[35] J. A. M. Vermaseren, A. Vogt, and S. Moch. The Third-Order QCD Corrections to Deep-Inelastic Scattering by Photon Exchange. *Nucl. Phys. B*, 724:3–182, 2005.

[36] S. A. Larin, T. van Ritbergen, and J. A. M. Vermaseren. The Next Next-to-Leading QCD Approximation for Nonsinglet Moments of Deep Inelastic Structure Functions. *Nucl. Phys. B*, 427:41–52, 1994.

[37] S. A. Larin, P. Nogueira, T. van Ritbergen, and J. A. M. Vermaseren. The Three-Loop QCD Calculation of the Moments of Deep Inelastic Structure Functions. *Nucl. Phys. B*, 492:338–378, 1997.

[38] S. Moch and J. A. M. Vermaseren. Deep Inelastic Structure Functions at Two Loops. *Nucl. Phys. B*, 573:853–907, 2000.

[39] M. Buza, Y. Matiounine, J. Smith, R. Migneron, and W. L. van Neerven. Heavy Quark Coefficient Functions at Asymptotic Values $Q^2 \gg m^2$. *Nucl. Phys. B*, 472:611–658, 1996.

[40] M. Buza, Y. Matiounine, J. Smith, and W. L. van Neerven. Charm Electroproduction Viewed in the Variable Flavor Number Scheme Versus Fixed Order Perturbation Theory. *Eur. Phys. J. C*, 1:301–320, 1998.

[41] J. Blümlein, A. De Freitas, C. Schneider, and K. Schönwald. The Variable Flavor Number Scheme at Next-to-Leading Order. *Phys. Lett. B*, 782:362–366, 2018.

[42] I. Bierenbaum, J. Blümlein, and S. Klein. Calculation of Massive 2-Loop Operator Matrix Elements with Outer Gluon Lines. *Phys. Lett. B*, 648:195–200, 2007a.

[43] I. Bierenbaum, J. Blümlein, and S. Klein. Two-Loop Massive Operator Matrix Elements and Unpolarized Heavy Flavor Production at Asymptotic Values $Q^2 \gg m^2$. *Nucl. Phys. B*, 780:40–75, 2007b.

[44] I. Bierenbaum, J. Blümlein, S. Klein, and C. Schneider. Two-Loop Massive Operator Matrix Elements for Unpolarized Heavy Flavor Production to $O(\epsilon)$. *Nucl. Phys. B*, 803:1–41, 2008.

[45] I. Bierenbaum, J. Blümlein, and S. Klein. The Gluonic Operator Matrix Elements at $O(\alpha_s^2)$ for DIS Heavy Flavor Production. *Phys. Lett. B*, 672:401–406, 2009a.

[46] I. Bierenbaum, J. Blümlein, and S. Klein. Mellin Moments of the $O(\alpha_s^3)$ Heavy Flavor Contributions to Unpolarized Deep-Inelastic Scattering at $Q^2 \gg m^2$ and Anomalous Dimensions. *Nucl. Phys. B*, 820:417–482, 2009b.

[47] J. Blümlein, A. De Freitas, W. L. van Neerven, and S. Klein. The Longitudinal Heavy Quark Structure Function $F_L^{Q\overline{Q}}$ in the Region $Q^2 \gg m^2$ at $O(\alpha_s^3)$. *Nucl. Phys. B*, 755:272–285, 2006.

[48] J. Ablinger, J. Blümlein, S. Klein, C. Schneider, and F. Wißbrock. The $O(\alpha_s^3)$ Massive Operator Matrix Elements of $O(n_f)$ for the Structure Function $F_2(x, Q^2)$ and Transversity. *Nucl. Phys. B*, 844:26–54, 2011.

[49] J. Blümlein, A. Hasselhuhn, S. Klein, and C. Schneider. The $O(\alpha_s^3 n_f T_F^2 C_{A,F})$ Contributions to the Gluonic Massive Operator Matrix Elements. *Nucl. Phys. B*, 866:196–211, 2013.

[50] A. Behring, I. Bierenbaum, J. Blümlein, A. De Freitas, S. Klein, and F. Wißbrock. The Logarithmic Contributions to the $O(\alpha_s^3)$ Asymptotic Massive Wilson Coefficients and Operator Matrix Elements in Deeply Inelastic Scattering. *Eur. Phys. J. C*, 74(9):3033, 2014.

[51] J. Ablinger et al. The Transition Matrix Element $A_{gq}(N)$ of the Variable Flavor Number Scheme at $O(\alpha_s^3)$. *Nucl. Phys. B*, 882:263–288, 2014a.

[52] J. Ablinger et al. The 3-Loop Non-Singlet Heavy Flavor Contributions and Anomalous Dimensions for the Structure Function $F_2(x, Q^2)$ and Transversity. *Nucl. Phys. B*, 886:733–823, 2014b.

[53] J. Ablinger, A. Behring, J. Blümlein, A. De Freitas, A. von Manteuffel, and C. Schneider. The 3-loop Pure Singlet Heavy Flavor Contributions to the Structure Function $F_2(x, Q^2)$ and the Anomalous Dimension. *Nucl. Phys. B*, 890: 48–151, 2014c.

[54] J. Ablinger et al. The Unpolarized and Polarized Single-Mass Three-Loop Heavy Flavor Operator Matrix Elements $A_{gg,Q}$ and $\Delta A_{gg,Q}$. *JHEP*, 12:134, 2022.

[55] J. Ablinger et al. The First–Order Factorizable Contributions to the Three–Loop Massive Operator Matrix Elements $A_{Qg}^{(3)}$ and $\Delta A_{Qg}^{(3)}$. *Nucl. Phys. B*, 999:116427, 2024a.

[56] J. Ablinger et al. The Non-First-Order-Factorizable Contributions to the Three-Loop Single-Mass Operator Matrix Elements $A_{Qg}^{(3)}$ and $\Delta A_{Qg}^{(3)}$. *Phys. Lett. B*, 854: 138713, 2024b.

[57] J. Ablinger et al. The Three-Loop Single-Mass Heavy-Flavor Corrections to the Structure Functions $F_2(x, Q^2)$ and $g_1(x, Q^2)$. *Phys. Lett. B*, 878:140540, 2026a.

[58] J. Ablinger et al. The Single-Mass Variable Flavor Number Scheme at Three-Loop Order. *JHEP*, 03:248, 2026b.

[59] M. Buza, Y. Matiounine, J. Smith, and W. L. van Neerven. $O(\alpha_s^2)$ Corrections to Polarized Heavy Flavor Production at $Q^2 \gg m^2$. *Nucl. Phys. B*, 485:420–456, 1997.

[60] I. Bierenbaum, J. Blümlein, A. De Freitas, A. Goedicke, S. Klein, and K. Schönwald. $O(\alpha_s^2)$ Polarized Heavy Flavor Corrections to Deep-Inelastic Scattering at $Q^2 \gg m^2$. *Nucl. Phys. B*, 988:116114, 2023.

[61] J. Ablinger et al. The Three-Loop Single Mass Polarized Pure Singlet Operator Matrix Element. *Nucl. Phys. B*, 953:114945, 2020a.

[62] J. Blümlein, A. De Freitas, M. Saragnese, C. Schneider, and K. Schönwald. Logarithmic Contributions to the Polarized $O({\alpha_s}^3)$ Asymptotic Massive Wilson Coefficients and Operator Matrix Elements in Deeply Inelastic Scattering. *Phys. Rev. D*, 104(3):034030, 2021.

[63] A. Behring, J. Blümlein, A. De Freitas, A. von Manteuffel, K. Schönwald, and C. Schneider. The Polarized Transition Matrix Element $A_{gq}(N)$ of the Variable Flavor Number Scheme at $O(\alpha_s^3)$. *Nucl. Phys. B*, 964:115331, 2021.

[64] J. Ablinger, J. Blümlein, A. De Freitas, A. Hasselhuhn, C. Schneider, and F. Wißbrock. Three Loop Massive Operator Matrix Elements and Asymptotic Wilson Coefficients with Two Different Masses. *Nucl. Phys. B*, 921:585–688, 2017.

[65] J. Ablinger, J. Blümlein, A. De Freitas, C. Schneider, and K. Schönwald. The Two-Mass Contribution to the Three-Loop Pure Singlet Operator Matrix Element. *Nucl. Phys. B*, 927:339–367, 2018a.

[66] J. Ablinger, J. Blümlein, A. De Freitas, A. Goedicke, C. Schneider, and K. Schönwald. The Two-mass Contribution to the Three-Loop Gluonic Operator Matrix Element $A_{gg,Q}^{(3)}$. *Nucl. Phys. B*, 932:129–240, 2018b.

[67] J. Ablinger, J. Blümlein, A. De Freitas, M. Saragnese, C. Schneider, and K. Schönwald. The Three-Loop Polarized Pure Singlet Operator Matrix Element with Two Different Masses. *Nucl. Phys. B*, 952:114916, 2020b.

[68] J. Ablinger et al. The Two-Mass Contribution to the Three-Loop Polarized Gluonic Operator Matrix Element $A_{gg,Q}^{(3)}$. *Nucl. Phys. B*, 955:115059, 2020c.

[69] E. Laenen and S.-O. Moch. Soft Gluon Resummation for Heavy Quark Electroproduction. *Phys. Rev. D*, 59:034027, 1999.

[70] S. Catani, M. Ciafaloni, and F. Hautmann. Gluon Contributions to Small x Heavy Flavor Production. *Phys. Lett. B*, 242:97–102, 1990.

[71] S. Catani, M. Ciafaloni, and F. Hautmann. High-energy Factorization and Small x Heavy Flavor Production. *Nucl. Phys. B*, 366:135–188, 1991.

[72] F. Caola, G. Gambuti, and M. Link. Analytic Results for Heavy-Quark Contributions to Charged-Current DIS at NNLO, 2026. arXiv:2606.21702 [hep-ph].

[73] E. Laenen, S. Riemersma, J. Smith, and W. L. van Neerven. Complete $O(\alpha_s)$ Corrections to Heavy Flavor Structure Functions in Electroproduction. *Nucl. Phys. B*, 392:162–228, 1993.

[74] E. Laenen, S. Riemersma, J. Smith, and W. L. van Neerven. On the Heavy Quark Content of the Nucleon. *Phys. Lett. B*, 291:325–328, 1992.

[75] B. W. Harris and J. Smith. Heavy Quark Correlations in Deep Inelastic Electroproduction. *Nucl. Phys. B*, 452:109–160, 1995.

[76] S. Riemersma, J. Smith, and W. L. van Neerven. Rates for Inclusive Deep Inelastic Electroproduction of Charm Quarks at HERA. *Phys. Lett. B*, 347: 143–151, 1995.

[77] F. Hekhorn and M. Stratmann. Next-to-Leading Order QCD Corrections to Inclusive Heavy-Flavor Production in Polarized Deep-Inelastic Scattering. *Phys. Rev. D*, 98(1):014018, 2018.

[78] J. Blümlein, G. Falcioni, and A. De Freitas. The Complete $O(\alpha_s^2)$ Non-Singlet Heavy Flavor Corrections to the Structure Functions $g_{1,2}^{ep}(x,Q^2)$, $F_{1,2,L}^{ep}(x,Q^2)$, $F_{1,2,3}^{\nu(\bar{\nu})}(x,Q^2)$ and the Associated Sum Rules. *Nucl. Phys. B*, 910:568–617, 2016.

[79] J. Blümlein, A. De Freitas, C. G. Raab, and K. Schönwald. The Unpolarized Two-Loop Massive Pure Singlet Wilson Coefficients for Deep-Inelastic Scattering. *Nucl. Phys. B*, 945:114659, 2019.

[80] E. Witten. Heavy Quark Contributions to Deep Inelastic Scattering. *Nucl. Phys. B*, 104:445–476, 1976.

[81] J. Babcock and D. W. Sivers. The Role of Gluons in the Neutrino Production of Charm. *Phys. Rev. D*, 18:2301, 1978.

[82] M. A. Shifman, A. I. Vainshtein, and V. I. Zakharov. Remarks on Charm Electroproduction in QCD. *Nucl. Phys. B*, 136:157, 1978.

[83] J. P. Leveille and T. J. Weiler. Characteristics of Heavy Quark Leptoproduction in QCD. *Nucl. Phys. B*, 147:147–173, 1979.

[84] M. Glück and E. Reya. Deep Inelastic Quantum Chromodynamic Charm Leptoproduction. *Phys. Lett. B*, 83:98–102, 1979.

[85] M. Glück, R. M. Godbole, and E. Reya. Heavy Flavour Production at High-Energy e–p Colliders. *Z. Phys. C*, 38:441, 1988.

[86] H. Kawamura, N. A. Lo Presti, S. Moch, and A. Vogt. On the Next-to-Next-to-Leading Order QCD Corrections to Heavy-Quark Production in Deep-Inelastic Scattering. *Nucl. Phys. B*, 864:399–468, 2012.

[87] A. Barontini, M. Bonvini, and N. Laurenti. Implementation of DIS at N^{3}LO for PDF Determination, 2026. arXiv:2606.25498 [hep-ph].

[88] J. McGowan, T. Cridge, L. A. Harland-Lang, and R. S. Thorne. Approximate N^{3}LO Parton Distribution Functions with Theoretical Uncertainties: MSHT20aN^{3}LO PDFs. *Eur. Phys. J. C*, 83(3):185, 2023.

[89] J. Collins. *Foundations of Perturbative QCD.* Cambridge University Press, 2011. doi: 10.1017/CBO9780511975592.

[90] C. Bogner and S. Weinzierl. Feynman Graph Polynomials. *Int. J. Mod. Phys. A*, 25:2585–2618, 2010.

[91] N. Nakanishi. *Graph Theory and Feynman Integrals.* Gordon and Breach, 1971.

[92] G. 't Hooft and M. J. G. Veltman. Regularization and Renormalization of Gauge Fields. *Nucl. Phys. B*, 44:189–213, 1972.

[93] C. G. Bollini and J. J. Giambiagi. Dimensional Renormalization: The Number of Dimensions as a Regularizing Parameter. *Nuovo Cim. B*, 12:20–26, 1972.

[94] K. G. Chetyrkin and F. V. Tkachov. Integration by Parts: The Algorithm to Calculate β-functions in 4 Loops. *Nucl. Phys. B*, 192:159–204, 1981.

[95] F. V. Tkachov. A Theorem on Analytical Calculability of 4-Loop Renormalization Group Functions. *Phys. Lett. B*, 100:65–68, 1981.

[96] A. N. Vasiliev, Y. M. Pismak, and Y. R. Khonkonen. $1/N$ Expansion: Calculation of the Exponents η and ν in the Order $1/N^2$ for Arbitrary Number of Dimensions. *Theor. Math. Phys.*, 47:465–475, 1981.

[97] A. V. Kotikov. Differential Equations Method: New Technique for Massive Feynman Diagrams Calculation. *Phys. Lett. B*, 254:158–164, 1991a.

[98] A. V. Kotikov. Differential Equation Method: The Calculation of N point Feynman Diagrams. *Phys. Lett. B*, 267:123–127, 1991b.

[99] E. Remiddi. Differential Equations for Feynman Graph Amplitudes. *Nuovo Cim. A*, 110:1435–1452, 1997.

[100] J. M. Henn. Multiloop Integrals in Dimensional Regularization Made Simple. *Phys. Rev. Lett.*, 110:251601, 2013.

[101] V. A. Smirnov. Asymptotic Expansions in Limits of Large Momenta and Masses. *Commun. Math. Phys.*, 134:109–137, 1990.

[102] V. A. Smirnov. Asymptotic Expansions in momenta and Masses and Calculation of Feynman Diagrams. *Mod. Phys. Lett. A*, 10:1485–1500, 1995.

[103] K.-T. Chen. Iterated Path Integrals. *Bull. Am. Math. Soc.*, 83:831–879, 1977.

[104] C. Itzykson and J. B. Zuber. *Quantum Field Theory.* McGraw-Hill, 1980.

[105] M. E. Peskin and D. V. Schroeder. *An Introduction to Quantum Field Theory.* Addison-Wesley, 1995. doi: 10.1201/9780429503559.

[106] M. D. Schwartz. *Quantum Field Theory and the Standard Model.* Cambridge University Press, 2014.

[107] G. F. Sterman. *An Introduction to Quantum Field Theory.* Cambridge University Press, 1993. doi: 10.1017/CBO9780511622618.

[108] S. Weinberg. *The Quantum Theory of Fields. Vol. 1: Foundations.* Cambridge University Press, 1995. doi: 10.1017/CBO9781139644167.

[109] S. Weinberg. *The Quantum Theory of Fields. Vol. 2: Modern Applications.* Cambridge University Press, 1996. doi: 10.1017/CBO9781139644174.

[110] V. A. Smirnov. *Analytic Tools for Feynman Integrals.* Springer, 2012. doi: 10.1007/978-3-642-34886-0.

[111] J. M. Henn and J. C. Plefka. *Scattering Amplitudes in Gauge Theories.* Springer, 2014. doi: 10.1007/978-3-642-54022-6.

[112] S. Weinzierl. *Feynman Integrals. A Comprehensive Treatment for Students and Researchers.* Springer, 2022. doi: 10.1007/978-3-030-99558-4.

[113] I. Dubovyk, J. Gluza, and G. Somogyi. *Mellin-Barnes Integrals: A Primer on Particle Physics Applications.* Springer, 2022. doi: 10.1007/978-3-031-14272-7.

[114] K. G. Chetyrkin, B. A. Kniehl, and M. Steinhauser. Decoupling Relations to $\mathcal{O}(\alpha_s^3)$ and their Connection to Low-Energy Theorems. *Nucl. Phys. B*, 510: 61–87, 1998.

[115] J. C. Collins. *Renormalization : An Introduction to Renormalization, the Renormalization Group and the Operator-Product Expansion.* Cambridge University Press, 1984. doi: 10.1017/CBO9780511622656.

[116] K. Fujikawa and H. Suzuki. *Path Integrals and Quantum Anomalies.* Oxford University Press, 2004. doi: 10.1093/acprof:oso/9780198529132.001.0001.

[117] W. Rudin. *Real and Complex Analysis.* McGraw-Hill, 1987.

[118] Y. Frishman. Light Cone and Short Distances. *Phys. Rept.*, 13:1, 1974.

[119] H. Georgi and H. D. Politzer. Electroproduction Scaling in an Asymptotically Free Theory of Strong Interactions. *Phys. Rev. D*, 9:416–420, 1974.

[120] D. J. Gross and F. Wilczek. Asymptotically Free Gauge Theories 2. *Phys. Rev. D*, 9:980–993, 1974.

[121] J. Bros, H. Epstein, and V. Glaser. A Proof of the Crossing Property for Two-Particle Amplitudes in General Quantum Field Theory. *Commun. Math. Phys.*, 1(3):240–264, 1965.

[122] S. Weinberg. New Approach to the Renormalization Group. *Phys. Rev. D*, 8: 3497–3509, 1973.

[123] E. G. Floratos, D. A. Ross, and C. T. Sachrajda. Higher Order Effects in Asymptotically Free Gauge Theories: The Anomalous Dimensions of Wilson Operators. *Nucl. Phys. B*, 129:66–88, 1977.

[124] D. R. T. Jones. Two Loop Diagrams in Yang-Mills Theory. *Nucl. Phys. B*, 75: 531, 1974.

[125] W. E. Caswell. Asymptotic Behavior of Nonabelian Gauge Theories to Two Loop Order. *Phys. Rev. Lett.*, 33:244, 1974.

[126] E. Egorian and O. V. Tarasov. Two Loop Renormalization of the QCD in an Arbitrary Gauge. *Theor. Math. Phys.*, 41:26–32, 1979.

[127] P. A. Baikov, K. G. Chetyrkin, and J. H. Kühn. Five-Loop Running of the QCD Coupling Constant. *Phys. Rev. Lett.*, 118(8):082002, 2017.

[128] F. Herzog, B. Ruijl, T. Ueda, J. A. M. Vermaseren, and A. Vogt. The Five-Loop Beta Function of Yang-Mills Theory with Fermions. *JHEP*, 02:090, 2017.

[129] T. Luthe, A. Maier, P. Marquard, and Y. Schröder. The Five-Loop Beta Function for a General Gauge Group and Anomalous Dimensions beyond Feynman Gauge. *JHEP*, 10:166, 2017.

[130] K. G. Chetyrkin, G. Falcioni, F. Herzog, and J. A. M. Vermaseren. Five-Loop Renormalisation of QCD in Covariant Gauges. *JHEP*, 10:179, 2017.

[131] Y. Schröder and M. Steinhauser. Four-Loop Decoupling Relations for the Strong Coupling. *JHEP*, 01:051, 2006.

[132] L. Chen, Z. Li, and M. Niggetiedt. On-shell Matrix Elements of the EMT Trace in Gauge Theories and Heavy Quark Masses. *Phys. Lett. B*, 871:139935, 2025.

[133] F. Forner, M. Klann, S.-O. Moch, K. Schönwald, and L. Tancredi. On QCD Propagators with Heavy Quarks. In Preparation, 2026a.

[134] M. Fael, K. Schönwald, and M. Steinhauser. Exact Results for Z_m^{OS} and Z_2^{OS} with two Mass Scales and up to Three Loops. *JHEP*, 10:087, 2020.

[135] S. A. Larin. The Renormalization of the Axial Anomaly in Dimensional Regularization. *Phys. Lett. B*, 303:113–118, 1993.

[136] B. J. G. Ruijl. *Advances in Computational Methods for Quantum Field Theory Calculations*. PhD thesis, Leiden U., 2017.

[137] S. Moch, J. A. M. Vermaseren, and A. Vogt. On γ_5 in Higher-Order QCD Calculations and the NNLO Evolution of the Polarized Valence Distribution. *Phys. Lett. B*, 748:432–438, 2015.

[138] B. Ruijl, T. Ueda, and J. Vermaseren. `FORM` Version 4.2, 2017. arXiv:1707.06453 [hep-ph].

[139] J. Davies, T. Kaneko, C. Marinissen, T. Ueda, and J. A. M. Vermaseren. `FORM` Version 5.0, 2026. arXiv:2601.19982 [hep-ph].

[140] N. Cabibbo. Unitary Symmetry and Leptonic Decays. *Phys. Rev. Lett.*, 10: 531–533, 1963.

[141] M. Kobayashi and T. Maskawa. CP Violation in the Renormalizable Theory of Weak Interaction. *Prog. Theor. Phys.*, 49:652–657, 1973.

[142] S. Weinberg. A Model of Leptons. *Phys. Rev. Lett.*, 19:1264–1266, 1967.

[143] S. L. Glashow. Partial Symmetries of Weak Interactions. *Nucl. Phys.*, 22:579–588, 1961.

[144] G. Passarino and M. J. G. Veltman. One Loop Corrections for e^+e^- Annihilation Into $\mu^+\mu^-$ in the Weinberg Model. *Nucl. Phys. B*, 160:151–207, 1979.

[145] A. Pak. The Toolbox of Modern Multi-Loop Calculations: Novel Analytic and Semi-Analytic Techniques. *J. Phys. Conf. Ser.*, 368:012049, 2012.

[146] E. K. Leĭnartas. Factorization of Rational Functions of Several Variables Into Partial Fractions. *Sov. Math. (Iz. VUZ)*, 22(10):35–38, 1978.

[147] D. Bendle et al. pfd-parallel, a Singular/GPI-Space Package for Massively Parallel Multivariate Partial Fractioning. *Comput. Phys. Commun.*, 294:108942, 2024.

[148] L. Schwartz. *Théorie des Distributions*. Hermann, 1950.

[149] H. Epstein and V. Glaser. The Role of Locality in Perturbation Theory. *Ann. Inst. Henri Poincaré A*, 19(3):211–295, 1973.

[150] N. N. Bogoliubov and O. S. Parasiuk. On the Multiplication of the Causal Function in the Quantum Theory of Fields. *Acta Math.*, 97:227–266, 1957.

[151] J. S. Schwinger. On Gauge Invariance and Vacuum Polarization. *Phys. Rev.*, 82:664–679, 1951.

[152] R. Durrett. *Probability: Theory and Examples*. Cambridge University Press, 5th edition, 2019. doi: 10.1017/9781108591034.

[153] F. Brown and K. Yeats. Spanning Forest Polynomials and the Transcendental Weight of Feynman Graphs. *Commun. Math. Phys.*, 301:357–382, 2011.

[154] R. N. Lee and A. A. Pomeransky. Critical Points and Number of Master Integrals. *JHEP*, 11:165, 2013.

[155] R. N. Lee. Group Structure of the Integration-by-Part Identities and its Application to the Reduction of Multiloop Integrals. *JHEP*, 07:031, 2008.

[156] R. N. Lee. LiteRed 1.4: a Powerful Tool for Reduction of Multiloop Integrals. *J. Phys. Conf. Ser.*, 523:012059, 2014.

[157] V. Maheria. *Semi- and Fully-Inclusive Phase-Space Integrals at Four Loops*. PhD thesis, Hamburg U., 2022.

[158] OEIS Foundation Inc. Entry A001353 in The On-Line Encyclopedia of Integer Sequences, 2026a. URL `https://oeis.org/A001353`.

[159] OEIS Foundation Inc. Entry A317405 in The On-Line Encyclopedia of Integer Sequences, 2026b. URL `https://oeis.org/A317405`.

[160] B. D. McKay and A. Piperno. Practical Graph Isomorphism, II. *J. Symbolic Comput.*, 60:94–112, 2014.

[161] W. Zimmermann. Convergence of Bogolyubov's Method of Renormalization in Momentum Space. *Commun. Math. Phys.*, 15:208–234, 1969.

[162] K. Hepp. Proof of the Bogolyubov-Parasiuk Theorem on Renormalization. *Commun. Math. Phys.*, 2:301–326, 1966.

[163] S. Weinberg. High-Energy Behavior in Quantum Field Theory. *Phys. Rev.*, 118: 838–849, 1960.

[164] F. Brown and D. Kreimer. Angles, Scales and Parametric Renormalization. *Lett. Math. Phys.*, 103:933–1007, 2013.

[165] A. Connes and M. Marcolli. *Noncommutative Geometry, Quantum Fields and Motives*. American Mathematical Soc., 2019. doi: 10.1090/coll/055.

[166] M. Marcolli. *Feynman Motives*. World Scientific, 2010.

[167] A. V. Smirnov and A. V. Petukhov. The Number of Master Integrals is Finite. *Lett. Math. Phys.*, 97:37–44, 2011.

[168] E. Casali, S. Mizera, and P. Tourkine. Monodromy Relations from Twisted Homology. *JHEP*, 12:087, 2019.

[169] S. Caron-Huot and A. Pokraka. Duals of Feynman integrals. Part I. Differential Equations. *JHEP*, 12:045, 2021.

[170] S. Caron-Huot and A. Pokraka. Duals of Feynman Integrals. Part II. Generalized Unitarity. *JHEP*, 04:078, 2022.

[171] B. Ruijl, T. Ueda, and J. A. M. Vermaseren. Forcer, a FORM Program for the Parametric Reduction of Four-Loop Massless Propagator Diagrams. *Comput. Phys. Commun.*, 253:107198, 2020.

[172] S. A. Larin, F. V. Tkachov, and J. A. M. Vermaseren. The `FORM` Version of `MINCER`. `https://lib-extopc.kek.jp/preprints/PDF/1991/9111/9111169.pdf`, 1991.

[173] S. G. Gorishnii, S. A. Larin, L. R. Surguladze, and F. V. Tkachov. Mincer: Program for Multiloop Calculations in Quantum Field Theory for the Schoonschip System. *Comput. Phys. Commun.*, 55:381–408, 1989.

[174] M. Steinhauser. MATAD: A Program Package for the Computation of MAssive TADpoles. *Comput. Phys. Commun.*, 134:335–364, 2001.

[175] J. Kuipers, T. Ueda, J. A. M. Vermaseren, and J. Vollinga. FORM Version 4.0. *Comput. Phys. Commun.*, 184:1453–1467, 2013.

[176] S. Laporta. High-Precision Calculation of Multiloop Feynman Integrals by Difference Equations. *Int. J. Mod. Phys. A*, 15:5087–5159, 2000.

[177] P. Maierhöfer, J. Usovitsch, and P. Uwer. Kira—A Feynman Integral Reduction Program. *Comput. Phys. Commun.*, 230:99–112, 2018.

[178] J. Klappert, F. Lange, P. Maierhöfer, and J. Usovitsch. Integral Reduction with Kira 2.0 and Finite Field Methods. *Comput. Phys. Commun.*, 266:108024, 2021a.

[179] F. Lange, J. Usovitsch, and Z. Wu. `Kira 3`: Integral Reduction with Efficient Seeding and Optimized Equation Selection. *Comput. Phys. Commun.*, 322: 109999, 2026.

[180] A. V. Smirnov and F. S. Chukharev. FIRE6: Feynman Integral REduction with Modular Arithmetic. *Comput. Phys. Commun.*, 247:106877, 2020.

[181] A. V. Smirnov and M. Zeng. `FIRE 6.5`: Feynman Integral Reduction with New Simplification Library. *Comput. Phys. Commun.*, 302:109261, 2024.

[182] A. V. Smirnov and M. Zeng. FIRE 7: Automatic Reduction with Modular Approach. *Comput. Phys. Commun.*, 325:110200, 2026.

[183] C. Studerus. Reduze – Feynman Integral Reduction in C++. *Comput. Phys. Commun.*, 181:1293–1300, 2010.

[184] A. von Manteuffel and C. Studerus. Reduze 2 - Distributed Feynman Integral Reduction, 2012. arXiv:1201.4330 [hep-ph].

[185] A. V. Smirnov and V. A. Smirnov. How to Choose Master Integrals. *Nucl. Phys. B*, 960:115213, 2020.

[186] J. Usovitsch. Factorization of Denominators in Integration-by-Parts Reductions, 2020. arXiv:2002.08173 [hep-ph].

[187] O. V. Tarasov. Connection between Feynman Integrals having Different Values of the Space-Time Dimension. *Phys. Rev. D*, 54:6479–6490, 1996.

[188] O. V. Tarasov. Generalized Recurrence Relations for Two Loop Propagator Integrals with Arbitrary Masses. *Nucl. Phys. B*, 502:455–482, 1997.

[189] T. Gehrmann and E. Remiddi. Differential Equations for Two-Loop Four-Point Functions. *Nucl. Phys. B*, 580:485–518, 2000.

[190] J. M. Henn. Lectures on Differential Equations for Feynman Integrals. *J. Phys. A*, 48:153001, 2015.

[191] M. Argeri et al. Magnus and Dyson Series for Master Integrals. *JHEP*, 03:082, 2014.

[192] V. A. Smirnov. *Applied Asymptotic Expansions in Momenta and Masses.* Springer, 2002. doi: 10.1007/3-540-44574-9.

[193] M. Chakraborty and F. Herzog. The Asymptotic Hopf Algebra of Feynman Integrals. *JHEP*, 01:006, 2025.

[194] C. Duhr. Hopf Algebras, Coproducts and Symbols: an Application to Higgs Boson Amplitudes. *JHEP*, 08:043, 2012.

[195] A. B. Goncharov. Galois Symmetries of Fundamental Groupoids and Noncommutative Geometry. *Duke Math. J.*, 128(2):209–284, 2005.

[196] A. B. Goncharov. Multiple polylogarithms, cyclotomy and modular complexes. *Math. Res. Lett.*, 5(4):497–516, 1998.

[197] F. Brown. Multiple Modular Values and the Relative Completion of the Fundamental Group of $M_{1,1}$, 2014. arXiv:1407.5167 [math.NT].

[198] E. Remiddi and J. A. M. Vermaseren. Harmonic Polylogarithms. *Int. J. Mod. Phys. A*, 15:725–754, 2000.

[199] M. Besier, P. Wasser, and S. Weinzierl. RationalizeRoots: Software Package for the Rationalization of Square Roots. *Comput. Phys. Commun.*, 253:107197, 2020.

[200] G. Papathanasiou, S. Weinzierl, K. Wu, and Y. Zhang. Rationalisation of Multiple Square Roots in Feynman integrals. *JHEP*, 05:078, 2025.

[201] J. Vollinga and S. Weinzierl. Numerical Evaluation of multiple Polylogarithms. *Comput. Phys. Commun.*, 167:177, 2005.

[202] G. Baur and C. Duhr. IterInt: Evaluating Iterated Integrals via Differential Equations, 2026. arXiv:2606.02744 [hep-ph].

[203] J. Jackson. *Classical Electrodynamics.* Wiley, 2012.

[204] K. S. Thorne. Multipole expansions of gravitational radiation. *Rev. Mod. Phys.*, 52:299, 1980.

[205] R. Stanley. *Enumerative Combinatorics: Volume 1.* Cambridge University Press, 1997. doi: 10.1017/CBO9780511805967.

[206] T. Kaneko. A Feynman Graph Generator for any Order of Coupling Constants. *Comput. Phys. Commun.*, 92:127–152, 1995.

[207] T. van Ritbergen, A. N. Schellekens, and J. A. M. Vermaseren. Group Theory Factors for Feynman Diagrams. *Int. J. Mod. Phys. A*, 14:41–96, 1999.

[208] OEIS Foundation Inc. Entry A029858 in The On-Line Encyclopedia of Integer Sequences, 2026c. URL `https://oeis.org/A029858`.

[209] P. A. Baikov and K. G. Chetyrkin. Four Loop Massless Propagators: An Algebraic Evaluation of All Master Integrals. *Nucl. Phys. B*, 837:186–220, 2010.

[210] A. Georgoudis, V. Gonçalves, E. Panzer, R. Pereira, A. V. Smirnov, and V. A. Smirnov. Glue-and-Cut at Five Loops. *JHEP*, 09:098, 2021.

[211] M. Klann, S.-O. Moch, and K. Schönwald. Heavy-Quark Production in Deep-Inelastic Scattering Mellin Moments of Structure Functions. *Nucl. Phys. B*, page 117572, 2026.

[212] J. Klappert and F. Lange. Reconstructing Rational Functions with `FireFly`. *Comput. Phys. Commun.*, 247:106951, 2020.

[213] J. Klappert, S. Y. Klein, and F. Lange. Interpolation of Dense and Sparse Rational Functions and Other Improvements in `FireFly`. *Comput. Phys. Commun.*, 264:107968, 2021b.

[214] C. Meyer. Algorithmic Transformation of Multi-Loop Master Integrals to a Canonical Basis with CANONICA. *Comput. Phys. Commun.*, 222:295–312, 2018.

[215] F. Forner, C. Nega, and L. Tancredi. On the Photon Self-Energy to Three Loops in QED. *JHEP*, 03:148, 2025.

[216] C. Nega. *Calabi-Yau Manifolds and Feynman Integral Computations: The Family of Banana Feynman Graphs*. PhD thesis, U. Bonn (main), 2022.

[217] J. Broedel, C. Duhr, and N. Matthes. Meromorphic Modular Forms and the Three-Loop Equal-Mass Banana Integral. *JHEP*, 02:184, 2022.

[218] A. Klemm, C. Nega, and R. Safari. The l-Loop Banana Amplitude from GKZ Systems and Relative Calabi-Yau Periods. *JHEP*, 04:088, 2020.

[219] K. Bönisch, C. Duhr, F. Fischbach, A. Klemm, and C. Nega. Feynman Integrals in Dimensional Regularization and Extensions of Calabi-Yau Motives. *JHEP*, 09:156, 2022.

[220] L. Görges, C. Nega, L. Tancredi, and F. J. Wagner. On a Procedure to Derive ϵ-Factorised Differential Equations beyond Polylogarithms. *JHEP*, 07:206, 2023.

[221] F. Forner, C. C. Mella, C. Nega, L. Tancredi, and F. J. Wagner. Integrand Analysis, Leading Singularities and Canonical Bases beyond Polylogarithms, 2026b. arXiv:2604.25270 [hep-th].

[222] A. Primo and L. Tancredi. Maximal Cuts and Differential Equations for Feynman Integrals. An application to the Three-Loop Massive Banana Graph. *Nucl. Phys. B*, 921:316–356, 2017a.

[223] A. Primo and L. Tancredi. On the Maximal Cut of Feynman integrals and the Solution of Their Differential Equations. *Nucl. Phys. B*, 916:94–116, 2017b.

[224] K. Bönisch, F. Fischbach, A. Klemm, C. Nega, and R. Safari. Analytic Structure of all Loop Banana Integrals. *JHEP*, 05:066, 2021.

[225] J. Broedel, C. Duhr, F. Dulat, R. Marzucca, B. Penante, and L. Tancredi. An Analytic Solution for the Equal-Mass Banana Graph. *JHEP*, 09:112, 2019a.

[226] P. A. Baikov. Explicit Solutions of the Multiloop Integral Recurrence Relations and its Application. *Nucl. Instrum. Meth. A*, 389:347–349, 1997.

[227] P. A. Baikov. Explicit Solutions of the Three Loop Vacuum Integral Recurrence Relations. *Phys. Lett. B*, 385:404–410, 1996.

[228] H. Frellesvig and C. G. Papadopoulos. Cuts of Feynman Integrals in Baikov Representation. *JHEP*, 04:083, 2017.

[229] G. S. Joyce. On the Simple Cubic Lattice Green Function. *Phil. Trans. R. Soc. Lond. A*, 273(1236):583–610, 1973.

[230] S. Pögel, X. Wang, and S. Weinzierl. Bananas of Equal Mass: any Loop, any Order in the Dimensional Regularisation Parameter. *JHEP*, 04:117, 2023.

[231] J. Broedel, C. Duhr, F. Dulat, B. Penante, and L. Tancredi. Elliptic Polylogarithms and Feynman Parameter Integrals. *JHEP*, 05:120, 2019b.

[232] M. F. Singer. Solving Homogeneous Linear Differential Equations in Terms of Second Order Linear Differential Equations. *Bull. Am. Math. Soc*, 107(3): 663–696, 1985.

[233] A. Sabry. Fourth order spectral functions for the electron propagator. *Nucl. Phys.*, 33:401–430, 1962.

[234] S. Laporta and E. Remiddi. Analytic Treatment of the Two Loop Equal Mass Sunrise Graph. *Nucl. Phys. B*, 704:349–386, 2005.

[235] D. J. Broadhurst, J. Fleischer, and O. V. Tarasov. Two Loop Two Point Functions with Masses: Asymptotic Expansions and Taylor Series, in any Dimension. *Z. Phys. C*, 60:287–302, 1993.

[236] S. Müller-Stach, S. Weinzierl, and R. Zayadeh. A Second-Order Differential Equation for the Two-Loop Sunrise Graph with Arbitrary Masses. *Commun. Num. Theor. Phys.*, 6:203–222, 2012.

[237] S. Bloch and P. Vanhove. The Elliptic Dilogarithm for the Sunset Graph. *J. Number Theor.*, 148:328–364, 2015.

[238] C. Duhr, F. Gasparotto, C. Nega, L. Tancredi, and S. Weinzierl. On the Electron Self-Energy to Three Loops in QED. *JHEP*, 11:020, 2024.

[239] J. Goode, F. Herzog, and S. Teale. OPITeR: A Program for Tensor Reduction of Multi-Loop Feynman Integrals. *Comput. Phys. Commun.*, 312:109606, 2025.

[240] E. Panzer. Algorithms for the Symbolic Integration of Hyperlogarithms with Applications to Feynman Integrals. *Comput. Phys. Commun.*, 188:148–166, 2015a.

[241] E. Panzer. *Feynman Integrals and Hyperlogarithms.* PhD thesis, Humboldt U., 2015b. arXiv:1506.07243 [math-ph].

[242] A. Kardos, S.-O. Moch, and O. Schnetz. HyperFORM: a FORM Package for Parametric Integration with Hyperlogarithms. *Eur. Phys. J. C*, 86(6):659, 2026.

[243] B. A. Kniehl, A. F. Pikelner, and O. L. Veretin. Three-Loop Massive Tadpoles and Polylogarithms Through Weight Six. *JHEP*, 08:024, 2017.

[244] R. N. Lee and V. A. Smirnov. The Dimensional Recurrence and Analyticity Method for Multicomponent Master Integrals: Using Unitarity Cuts to Construct Homogeneous Solutions. *JHEP*, 12:104, 2012.

[245] R. N. Lee. Space-Time Dimensionality D as Complex Variable: Calculating Loop Integrals Using Dimensional Recurrence Relation and Analytical Properties with Respect to D. *Nucl. Phys. B*, 830:474–492, 2010.

[246] D. Bailey and H. Ferguson. A polynomial time, numerically stable integer relation algorithm. *NASA Technical Report RNR–91–032*, 1991.

[247] J. M. Henn, A. V. Smirnov, and V. A. Smirnov. Evaluating Multiple Polylogarithm Values at Sixth Roots of Unity up to Weight Six. *Nucl. Phys. B*, 919: 315–324, 2017.

[248] A. V. Smirnov, N. D. Shapurov, and L. I. Vysotsky. FIESTA5: Numerical High-Performance Feynman Integral Evaluation. *Comput. Phys. Commun.*, 277: 108386, 2022.

[249] X. Liu and Y.-Q. Ma. AMFlow: A Mathematica Package for Feynman Integrals Computation via Auxiliary Mass Flow. *Comput. Phys. Commun.*, 283:108565, 2023.

[250] A. Chuvakin, J. Smith, and W. L. van Neerven. Comparison between Variable Flavor Number Schemes for Charm Quark Electroproduction. *Phys. Rev. D*, 61:096004, 2000.

[251] J. A. M. Vermaseren. Harmonic Sums, Mellin Transforms and Integrals. *Int. J. Mod. Phys. A*, 14:2037–2076, 1999.

[252] J. Blümlein and S. Kurth. Harmonic Sums and Mellin Transforms up to Two-Loop Order. *Phys. Rev. D*, 60:014018, 1999.

[253] D. Maitre. HPL, a Mathematica Implementation of the Harmonic Plylogarithms. *Comput. Phys. Commun.*, 174:222–240, 2006.

[254] T. Huber and D. Maître. HypExp, a Mathematica Package for Expanding Hypergeometric Functions around Integer-Valued Parameters. *Comput. Phys. Commun.*, 175:122–144, 2006.

[255] E. B. Zijlstra and W. L. van Neerven. Order-α_s^2 Corrections to the Polarized Structure Function $g_1(x, Q^2)$. *Nucl. Phys. B*, 417:61–100, 1994.

[256] H. S. Hannesdottir, A. J. McLeod, M. D. Schwartz, and C. Vergu. Applications of the Landau Bootstrap. *Phys. Rev. D*, 111(8):085003, 2025.

[257] SHiP Collaboration. A Facility to Search for Hidden Particles (SHiP) at the CERN SPS. Technical report, CERN, 2015b. arXiv:1504.04956 [physics.ins-det].

[258] S. L. Adler. Axial Vector Vertex in Spinor Electrodynamics. *Phys. Rev.*, 177: 2426–2438, 1969.

[259] J. S. Bell and R. Jackiw. A PCAC Puzzle: $\pi^0 \to \gamma\gamma$ in the σ model. *Nuovo Cim. A*, 60:47–61, 1969.

[260] N. Laurenti. Construction of a Next-to-Next-to-Next-to-Leading Order Approximation for Heavy Flavour Production in Deep Inelastic Scattering with Quark Masses. Master's thesis, Rome U., 2021. arXiv:2401.12139 [hep-ph].

[261] J. Ablinger, J. Blümlein, A. De Freitas, A. von Manteuffel, C. Schneider, and K. Schönwald. The Two-Mass Contributions to the Three-Loop Massive Operator Matrix Elements $\widetilde{A}_{Qg}^{(3)}$ and $\Delta\widetilde{A}_{Qg}^{(3)}$. *JHEP*, 01:111, 2026c.

(This page is intentionally left blank.)

Declaration on Oath

I hereby declare and affirm that this doctoral dissertation is my own work and that I have not used any aids and sources other than those indicated. If electronic resources based on generative artificial intelligence (gAI) were used in the course of writing this dissertation, I confirm that my own work was the main and value-adding contribution and that complete documentation of all resources used is available in accordance with good scientific practice. I am responsible for any erroneous or distorted content, incorrect references, violations of data protection and copyright law or plagiarism that may have been generated by the gAI.

M. Klann

Hamburg, July 7, 2026
Place, date

Marco Klann
Signature